



UNIVERSITY OF
BIRMINGHAM

**PROGRESS TOWARDS THE TOTAL SYNTHESIS OF
HERQULINE A AND B**

by

He Yang

A thesis submitted to the University of Birmingham for the degree of
DOCTOR OF PHILOSOPHY

School of Chemistry
University of Birmingham

August 2015

UNIVERSITY OF
BIRMINGHAM

University of Birmingham Research Archive

e-theses repository

This unpublished thesis/dissertation is copyright of the author and/or third parties. The intellectual property rights of the author or third parties in respect of this work are as defined by The Copyright Designs and Patents Act 1988 or as modified by any successor legislation.

Any use made of information contained in this thesis/dissertation must be in accordance with that legislation and must be properly acknowledged. Further distribution or reproduction in any format is prohibited without the permission of the copyright holder.

Abstract

Herquline A and B were isolated from the fungal strain *Penicillium herquei* Fg-372 and have been shown to exhibit potent platelet aggregation inhibitory activities. The unusual and strained structure of herquline A makes it a highly attractive and challenging synthetic target. Herquline B is conceived to be an analogue of herquline A, even though its absolute structure has not been elucidated.

A biomimetic approach was initially investigated in Chapter 2, featuring an intramolecular direct oxidative phenol coupling strategy. While extensive experimentation failed to afford the desired coupling products, an advanced piperazine intermediate possessing a similar fused tricyclic ring system to that in herquline A was accessed *via* an intramolecular *aza*-Michael addition reaction.

Chapter 3 describes the transition metal-mediated intramolecular aryl coupling strategy. Small amounts of biaryl coupling products were fashioned *via* a Pd-catalysed Suzuki-Miyaura coupling protocol. The conformational analysis of diketopiperazines and piperazines is also introduced.

The intramolecular oxidative coupling of enolates or enol silanes approach is presented in Chapter 4. While the intramolecular coupling at the piperazine stage was found to be challenging, trace coupling product with a 1,4-dicarbonyl moiety was detected by mass spectrometry and was conceived to share close structural resemblance to herquline B.

Acknowledgements

First and foremost, I would like to thank my supervisor Professor Nigel Simpkins for kindling my interest in organic synthesis and his support, inspiration and encouragement over the past few years. I have been very grateful for being given the opportunity to work in his group, where I not only enhanced and broadened my knowledge in organic chemistry, but also gained the positive and passionate attitude toward scientific research. The PhD study will certainly be one of the most valuable and rewarding experiences for me. Next I offer my gratitude to my second supervisor Dr. John Fossey for his guidance and advice.

Thanks also go to the past and present members of the Simpkins research group. I would like to thank Matt, François and Mike for their advice and help with the thesis, Alex, Gary, Peter, Jennifer, Mark and Cynthia for their help and friendship. I would also like to thank Edgar and Ryan in the Butterworth group.

I would like to acknowledge the analytical services in the School of Chemistry, in particular Dr. Neil Spencer and Dr. Allen Bowden for their kind help in carrying out valuable NMR experiments within this thesis, Dr. Louise Male for X-ray crystallography, Dr. Chi Tsang and Peter Ashton for mass spectrometry. I would also like to acknowledge Dr. Ian Shannon for providing the high pressure reactor for part of the research in this thesis.

I am grateful for the financial support from the School of Chemistry at the University of Birmingham and the China Scholarship Council.

I cannot express enough gratitude to my beloved family who has been caring about my research and life at Birmingham. Special thanks must also go to Ruiqin, for always being there for me no matter the distance and her love and understanding.

Table of Contents

List of Figures	vii
List of Tables.....	ix
Abbreviations	x
CHAPTER 1 INTRODUCTION TO HERQULINE A AND B.....	1
1.1 The Herquelines: Isolation and Structure Elucidation	1
1.2 Biological Activity: New Platelet Aggregation Inhibitors	3
1.3 Proposed Biosynthesis of the Herquiline Alkaloids	6
1.4 Previous Synthesis Towards the Herquelines and Relevant Structures.....	8
1.4.1 Synthetic Studies Towards the Herquelines.....	8
1.4.2 Progress in the Synthesis of Relevant Structures	10
CHAPTER 2 STUDIES ON DIRECT OXIDATIVE PHENOL COUPLING –A	
BIOMIMETIC APPROACH	15
2.1 Initial Considerations and Retrosynthetic Analysis.....	15
2.2 Introduction to Phenolic Oxidative Coupling	17
2.2.1 Oxidative Phenol Coupling in Nature.....	17
2.2.2 Oxidative Phenol Coupling in Organic Synthesis	22
2.3 Efforts on Intramolecular Oxidative Coupling of Piperazine Substrates	31
2.3.1 Initial Forward Synthesis Towards Piperazine Intermediates	31
2.3.2 Vanadium(V) Species as Coupling Oxidants.....	40
2.3.3 Hypervalent Iodine(III) Reagents as Coupling Oxidants	44

2.3.4 Oxidative Coupling with Silver(I) Oxide, Fe(III) and Pb(IV) Reagents	46
2.4 Tricyclic Ring Formation <i>via</i> an Intramolecular <i>Aza</i> -Michael Addition Reaction	51
2.5 Summary	56

CHAPTER 3 TRANSITION METAL-MEDIATED ARYL COUPLING APPROACH

TOWARD HERQULINE A AND B58

3.1 Oxidative Coupling of Organocuprates.....	58
3.1.1 Introduction	58
3.1.2 Synthesis and Conformational Analysis of Piperazine Derivatives.....	63
3.1.3 Attempted Intramolecular Oxidative Coupling of Diarylcuprates	69
3.2 Palladium-Catalysed Coupling Reactions.....	82
3.2.1 Introduction to Intramolecular Suzuki-Miyaura and Stille-Kelly Couplings	83
3.2.2 Other Palladium-Catalysed Coupling Methods	87
3.2.3 Application to the Synthesis of the Herqulines	89
3.3 C–C Bond Formation from Organochalcogenides	98
3.3.1 Introduction	99
3.3.2 Application to the Intramolecular Coupling of Piperazine Substrates	103
3.4 Comparison of the Conformation of DKPs and Piperazines.....	110
3.5 Attempted Transformations with Biaryl Coupling Products.....	114
3.6 Summary	116

CHAPTER 4 OXIDATIVE ENOL SILANES OR ENOLATES COUPLING

APPROACH118

4.1 Initial Considerations and Retrosynthetic Analysis of Herquline A	118
4.2 Introduction to the Oxidative Coupling of Enol Silanes and Enolates	124

4.2.1 1,4-Dicarbonyl Formation <i>via</i> Enol Silane Oxidative Coupling	124
4.2.2 Advances in Oxidative Enolate Coupling	127
4.3 Initial Forward Synthesis	130
4.4 Revised Retrosynthesis.....	138
4.5 Formation of the 1,4-Dicarbonyl Functionality	140
4.6 Summary	146
CHAPTER 5 CONCLUSIONS	147
CHAPTER 6 EXPERIMENTAL.....	151
6.1 Materials and Methods	151
6.2 Preparative Procedures for Chapter 2.....	152
6.3 Preparative Procedures for Chapter 3.....	181
6.4 Preparative Procedures for Chapter 4.....	218
APPENDICES	239
A X-ray Crystal Structure Data for Compound 108	239
B X-ray Crystal Structure Data for Compound 102	241
C X-ray Crystal Structure Data for Compound 160	243
D Selected NMR Spectra.....	245
REFERENCES	257

List of Figures

- Figure 1.1:** Herquline A and its X-ray crystal structure.
- Figure 1.2:** Structure comparison between herquline A and B.
- Figure 1.3:** Structure of PAF (**3**).
- Figure 1.4:** (A) Structure of the P2Y₁ receptor and BPTU complex.
(B) Top view of the extracellular side of P2Y₁ receptor.
(C) Structure of BPTU (**4**), a P2Y₁ receptor antagonist.
- Figure 1.5:** Structure of piperazinomycin (**21**).
- Figure 2.1:** Structures of vancomycin and balhimycin.
- Figure 2.2:** Structure of cyclodityrosine-bound CYP121.
- Figure 2.3:** Examples of cyclic biaryl natural products.
- Figure 2.4:** Partial ¹H NMR spectrum of DKP **99** (300 MHz, CDCl₃, 298 K).
- Figure 2.5:** Partial ¹H NMR spectrum of DKP **89** (300 MHz, CDCl₃, 298 K).
- Figure 2.6:** X-ray crystal structure of *trans*-DKP **108**.
- Figure 2.7:** NOE NMR of the major component for **130**.
- Figure 3.1:** Crystal structure of **102**.
- Figure 3.2:** Possible conformations of bis-sulfonamide, bis-amide and bis-carbamate.
- Figure 3.3:** (A) Vicinal coupling constants between the protons on the piperazine ring of **160** (CDCl₃, 400 MHz).
(B) X-ray crystal structure of **160**.
- Figure 3.4:** Vicinal coupling constants between the protons on the piperazine ring of **161**.
- Figure 3.5:** Structures of piperazines.
- Figure 3.6:** Structures of piperazine **101** and **111**.
- Figure 3.7:** Partial ¹H NMR spectrum of piperazine **216** (300 MHz, CDCl₃, 298 K).

Figure 3.8: The proposed catalytic cycle for Pd-catalysed homocoupling of tellurides.

Figure 3.9: Possible conformations of 2,5-diketopiperazines.

Figure 3.10: Crystal structure of DKP **34**.

Figure 3.11: Different piperazine structures.

Figure 3.12: Piperazinomycin and its X-ray crystal structure.

Figure 4.1: X-ray crystal structure of herquline A (**1**).

List of Tables

Table 2.1: Condition screening for phenolic oxidative coupling.

Table 2.2: Oxidative coupling conditions with PIDA or PIFA.

Table 2.3: Attempted oxidative coupling conditions.

Table 3.1: Condition screening for the direct lithiation of piperazine **159**.

Table 3.2: Cuprate formation (transmetallation) and oxidation conditions.

Table 3.3: Pd-catalysed intramolecular coupling reactions.

Table 3.4: Attempted Suzuki-Miyaura couplings with piperazine and DKP substrates.

Table 3.5: Attempted Stille-Kelly coupling reactions.

Table 4.1: Condition screening for the synthesis of bis-silyl enol ethers.

Abbreviations

acac	acetylacetonate
ADP	adenosine diphosphate
Boc	<i>tert</i> -butoxycarbonyl
Bn	benzyl
CAN	diammonium cerium(IV) nitrate
Cbz	carboxybenzyl
DCM	dichloromethane
<i>de</i>	diastereomeric excess
DIPEA	diisopropylethylamine
DKP	diketopiperazine
DMF	<i>N, N'</i> -dimethylformamide
DMP	Dess-Martin periodinane
DMPU	1,3-dimethyl-3,4,5,6-tetrahydro-2(1 <i>H</i>)-pyrimidinone
DMSO	dimethyl sulfoxide
dppf	1,1'-bis(diphenylphosphino)ferrocene
ee	enantiomeric excess
eq.	equivalent
ESI	electrospray ionisation
g	gramme (s)
h	hour (s)
HATU	<i>O</i> -(7-azabenzotriazol-1-yl)- <i>N, N, N', N'</i> -tetramethyluronium hexafluorophosphate

HCl	hydrochloric acid
HOBt	hydroxybenzotriazole
HRMS	high-resolution mass spectrometry
IC ₅₀	half maximal inhibitory concentration
IR	infrared spectroscopy
<i>J</i>	coupling constant (in nuclear magnetic resonance spectroscopy)
LAH	lithium aluminium hydride
LDA	lithium diisopropylamide
LHMDS	lithium hexamethyldisilazide
m.p.	melting point
MS	mass spectrometry
NaHMDS	sodium hexamethyldisilazide
NMR	nuclear magnetic resonance spectroscopy
NOE	nuclear Overhauser effect
Tf	trifluoromethanesulfonyl
PAF	platelet activating factor
Ph	phenyl
PIDA	phenyliodine diacetate
PIFA	phenyliodine bis(trifluoroacetate)
ppm	parts per million
RNA	ribonucleic acid
rt	room temperature
TBS	<i>tert</i> -butyldimethylsilyl
TEA	triethylamine

TFA	trifluoroacetic acid
TFAA	trifluoroacetic anhydride
THF	tetrahydrofuran
TLC	thin layer chromatography
TMEDA	tetramethylethylenediamine
TMP	2,2,6,6-tetramethylpiperidine
TMS	trimethylsilyl

CHAPTER 1 INTRODUCTION TO HERQUILINE A AND B

1.1 The Herquelines: Isolation and Structure Elucidation

Herquiline A (**1**) was isolated from the culture broth of *Penicillium herquei* Fg-372 by Ōmura and co-workers in 1979.¹ The terrestrial fungal strain, Fg-372 was obtained from a soil sample collected at Saitama Prefecture, Japan and was identified as *Penicillium herquei* according to its growth characteristics. Later on herquiline A was also isolated from the marine-derived fungus *Penicillium* species separated from the Okinawan bivalve *Mytilus coruscus*.² This natural product was purified by solvent extraction and silica gel chromatography and the molecular formula was determined as C₁₉H₂₆N₂O₂ on the basis of elemental analysis and high resolution mass spectrometry. In 1980, Ōmura and co-workers reported the X-ray crystal structure of this alkaloid, which unambiguously determined its absolute structure (Figure 1.1).³

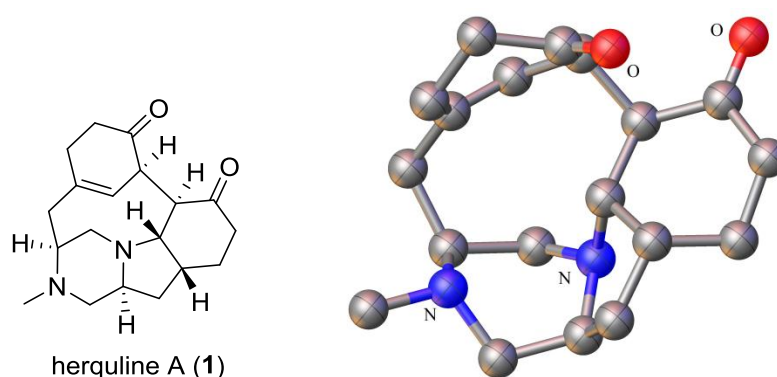


Figure 1.1: Herquiline A and its X-ray crystal structure (Reproduced using data requested from the Cambridge Crystallographic Data Centre).

Herquiline A is a piperazine derivative possessing a novel structural skeleton. The structure features a 1,4-dicarbonyl moiety, six stereogenic centres and a nitrogen bridgehead fused

tricyclic system consisting of piperazine, pyrrolidine and cyclohexanone functionalities. The two ketone rings are tethered together at the α -positions of their carbonyl groups to form a nine-membered ring. As exemplified by its crystal structure, the piperazine ring adopts a boat-like conformation and the cyclohexenone ring is distorted and forced to bend towards the tricycle to render herquline A a very strained molecule. Addressing these intriguing and unprecedented structural features of this natural product is without doubt a real challenge in total synthesis.

In 1995, the Ōmura research group reported the isolation of another nitrogen-containing natural product, named herquline B (**2**), from the same fungal strain Fg-372.⁴ Herquline B was shown to have the same molecular formula to that of herquline A by mass spectrometry and its structure was elucidated based on NMR spectral analysis (Figure 1.2).

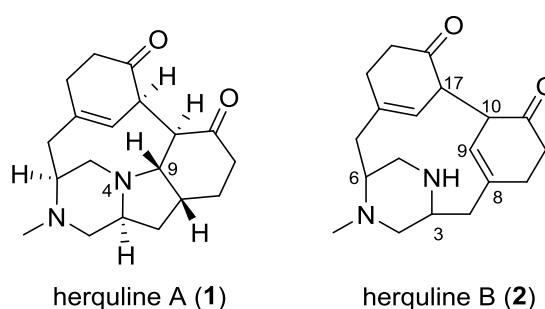


Figure 1.2: Structure comparison between herquline A and B.

Different from herquline A as a pentacycle, an extra double bond is present between C₈ and C₉ in herquline B with the absence of a pyrrolidine ring. Although it has the same structural constitution as herquline A, the absolute structure of herquline B has not been confirmed, since the stereochemistry at C₃, C₆, C₁₀ and C₁₇ remains unassigned. Considering the fact that both herquline A and B were isolated from the same origin and were shown to bear a high degree of structural homology, they possibly share the same configuration at some of the asymmetric centres. According to the proposed biosynthesis, tyrosine was presumed to be the

precursor of the two natural products. Therefore, it seems reasonable to deduce that herquiline B has the same stereochemistry to herquiline A at C₃ and C₆ positions, which derives from the chirality of L-tyrosine, leaving the configuration at C₁₀ and C₁₇ positions waiting for further confirmation.

1.2 Biological Activity: New Platelet Aggregation Inhibitors

During the isolation process conducted by Ōmura and co-workers, antimicrobial activities of herquiline A and B were assayed using several organisms. However, neither of them was active against the tested organisms at 1 mg/mL concentration.^{1,4}

Ōmura and co-workers also reported the platelet aggregation inhibitory properties of herquiline A and B. According to their preliminary biological data, herquiline A showed weak inhibitory activity (IC₅₀ values of 240 and 180 μM respectively) against platelet aggregation induced by PAF (platelet activating factor) and ADP (adenosine diphosphate) using the platelet rich plasma (PRP) from rabbit blood. Surprisingly, with only a little change in structure, herquiline B exhibited more potent inhibition against PAF and ADP induced platelet aggregation, with IC₅₀ values of 5.0 and 1.6 μM, respectively.

It is known that blood platelets are small anuclear cells and play one of the most important roles in physiological haemostatic process. Under normal conditions, platelets circulate in the blood freely without adhering to each other. Upon vessel wall injury, platelets can then interact with subendothelial adhesive proteins, leading to platelet adhesion and activation.^{5,6} Platelet activation includes several rapid positive feedback loops such as release of the contents of intraplatelet granules or cell shape change. All together, these events amplify the

activation signals for platelet aggregation and lead to haemostatic plug formation and subsequent arrest of bleeding. In contrast to normal platelet response, platelet hyperactivity can result in arterial thrombosis.⁷

PAF is an endogenous synthesised phospholipid product with the name of 1-alkyl-2-acetyl-*sn*-glycero-3-phosphocholine (Figure 1.3). It is a biologically active mediator responsible for many physiological functions including platelet aggregation. A variety of natural products and synthetic entities with PAF inhibitory activities have been reported.⁸

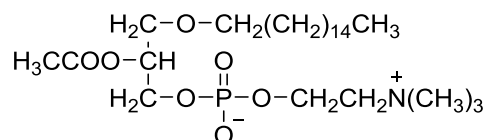


Figure 1.3: Structure of PAF (3).

ADP is an important mediator of haemostasis and thrombosis. Although it is regarded as a weak agonist of circulating blood platelets, ADP plays a vital role in platelet activation induced by other activators (such as thrombin and collagen) which promote ADP release from intraplatelet storage pools.⁹ This results in a positive feedback that enhances platelet aggregation and proliferation of platelet plug. Additionally, ADP acts synergistically with other platelet agonists.¹⁰

Two purinergic P2Y receptors, designated P2Y₁ and P2Y₁₂ have been reported to be responsible for the effect of ADP on platelets.^{11,12} Upon activated by ADP, the G_q-coupled P2Y₁ receptor mediates the first, reversible phase of platelet aggregation by changing platelet shape and initiating platelet response to ADP. The other receptor, G_i-coupled P2Y₁₂ can enhance the activating signal and platelet secretion to amplify the platelet aggregation. Both of these two receptors belong to the most prominent clinical drug targets for inhibition of platelet aggregation. The P2Y₁ receptor consists of a canonical seven-transmembrane helical

bundle architecture. Figure 1.4 (A) shows the structure of the complex between P2Y₁ receptor and BPTU (4), a urea derivative acting as the P2Y₁ receptor antagonist.¹³

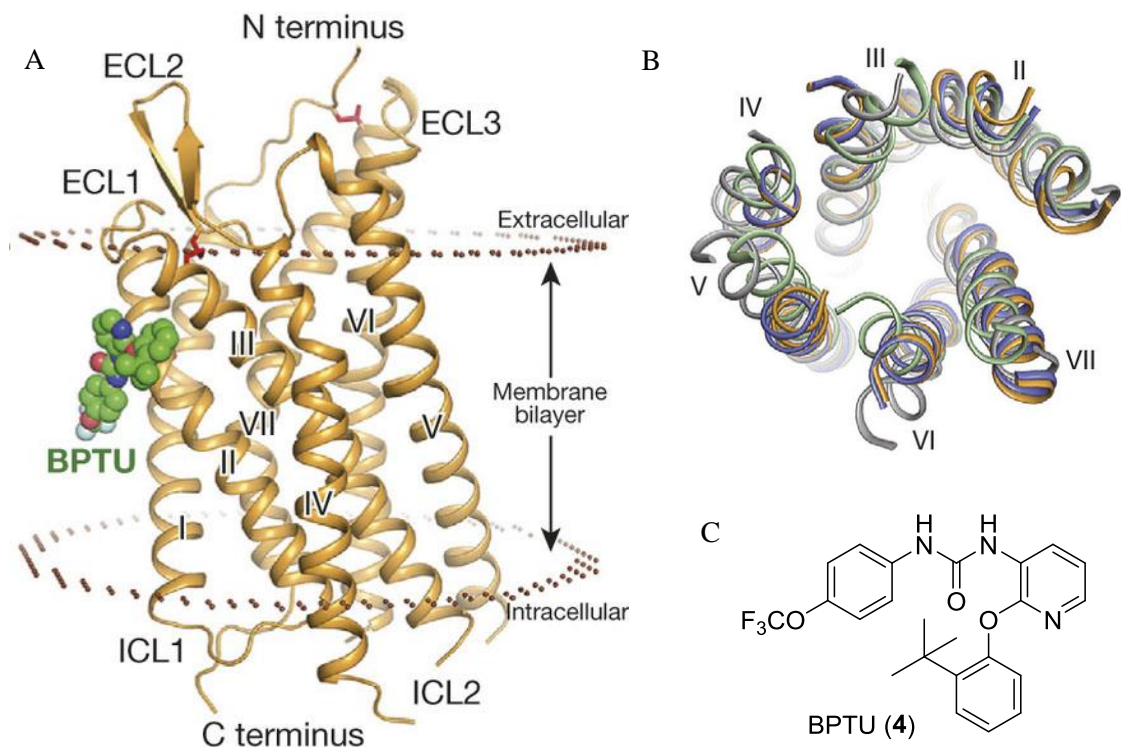


Figure 1.4: (A) Structure of the P2Y₁ receptor and BPTU complex. (B) Top view of the extracellular side of P2Y₁ receptor. (C) Structure of BPTU (4), a P2Y₁ receptor antagonist. (Reproduced from *Nature*).¹³

While the mode of inhibitory action of the herquelines is still not clear, Ōmura and co-workers postulated that it could be related to subcellular reaction concerning their non-selective inhibition against PAF- and ADP-induced aggregation.⁴ Due to the prominent activities, the herquiline alkaloids and their analogues might have great potential for the treatment of diseases related to platelet aggregation and thrombosis, such as stroke, myocardial infarction and pulmonary embolism.

Apart from antimicrobial and platelet aggregation inhibitory activities, no other biological properties of herquiline A and B have been investigated and reported. While more material of the herquelines might be possibly obtained from the microorganism *Penicillium herquei* Fg-

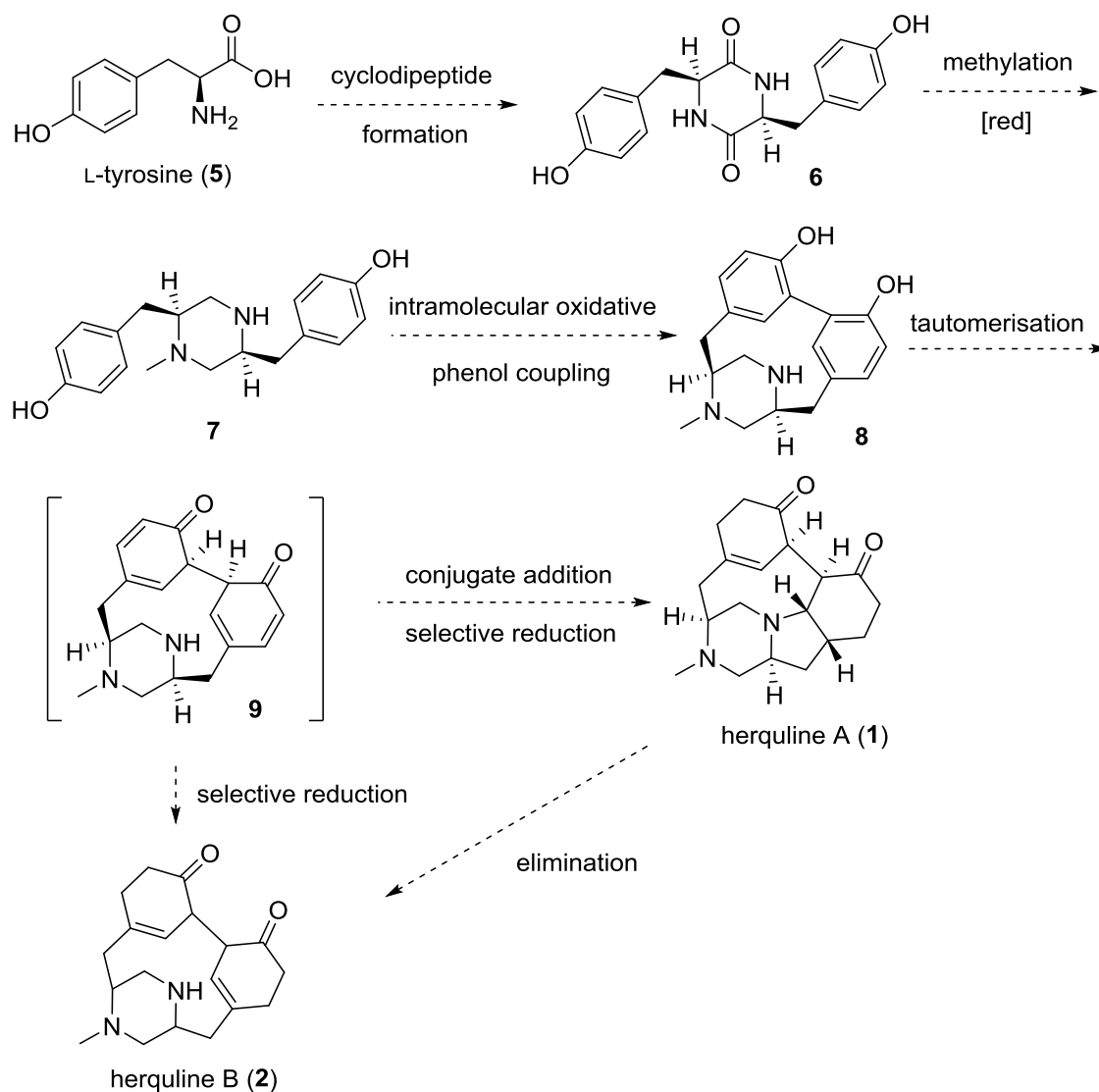
372 for further biological study, chemical synthesis of these two natural products will no doubt provide an avenue for adequate material supplies and procure a chance to diversify the molecular architectures of herquline derivatives.

1.3 Proposed Biosynthesis of the Herquline Alkaloids

During the course of screening herquline-producing media, Ōmura and co-workers found that the production of herquline A was enhanced when tyrosine was added to the culture broth.⁴ Though no further biosynthesis study has been conducted since then, it seems conceivable to suggest tyrosine to be the biosynthetic precursor of the herqulines based on this clue.

Actually after close scrutiny, it is clear that the chirality within the piperazine moiety of herquline A matches that in the naturally occurring amino acid, L-tyrosine. The cyclohexenone or cyclohexanone ring can derive from the phenol group of tyrosine. With this hypothesis, a possible route for the biogenesis of the herquline alkaloids was proposed, as shown in Scheme 1.1.

Diketopiperazine **6** is considered to be initially assembled from two molecules of L-tyrosine through cyclodipeptide formation process. After selective methylation and reduction, piperazine intermediate **7** could be produced. At this stage, an intramolecular oxidative phenol coupling process is conceived to take place to afford the coupling product bis-phenol **8**. Since dearomatisation is necessary for further functionalisation, the keto-tautomer **9** might be involved in the biosynthesis to allow an *aza*-Michael addition to occur, forming the pyrrolidine ring and herein the fused tricycle in herquline A (**1**).



Scheme 1.1: Postulated biosynthesis of the herquines.

Herquiline B (2) could arise from either the selective reduction of keto-tautomer 9, or an E₂-type elimination of herquiline A.

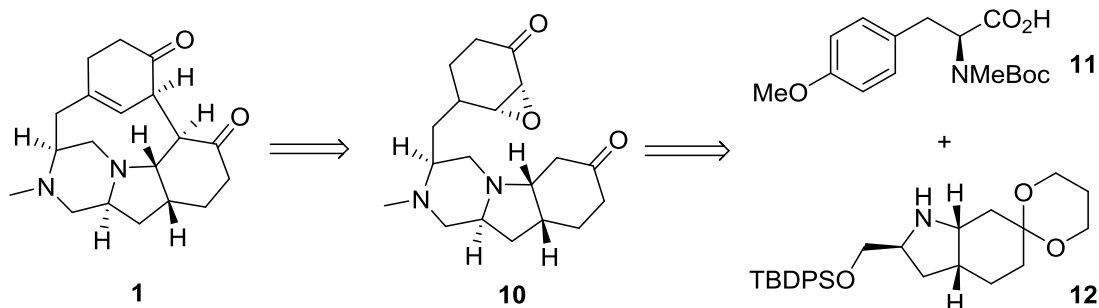
It is still not clear at which oxidation state (either diketopiperazine or piperazine) the phenol coupling reaction occurs, but one could argue that once the coupling product (either bis-phenol 8 or bis-ketone 9) formed in the first place, with the assistance of certain enzymes, the addition of the amino group within the piperazine ring to the conjugated dienone in 9 would be a straightforward process to generate the pyrrolidine ring within herquiline A.

1.4 Previous Synthesis Towards the Herquelines and Relevant Structures

1.4.1 Synthetic Studies Towards the Herquelines

Even though the structures of herquelines have been identified for a long time, no total synthesis has been published so far. Synthetic efforts towards these two natural products have been made from several research groups worldwide, with research results mainly being unveiled in PhD theses.

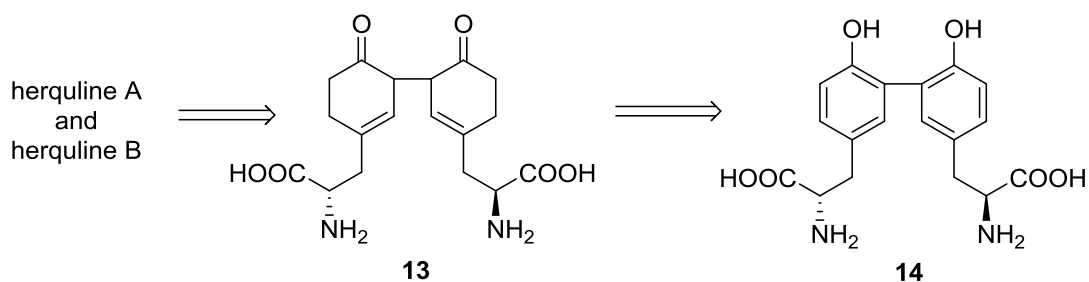
In 1997, Kim disclosed studies towards the synthesis of herquiline A.¹⁴ The retrosynthesis was based on an epoxide opening reaction of **10** as a key step to form the C–C bond within the 1,4-dicarbonyl moiety (Scheme 1.2). During their synthesis, the assembly of acid **11** and amine **12** was not successful with various coupling reagents and the synthetic work was not carried on following their synthetic plan.



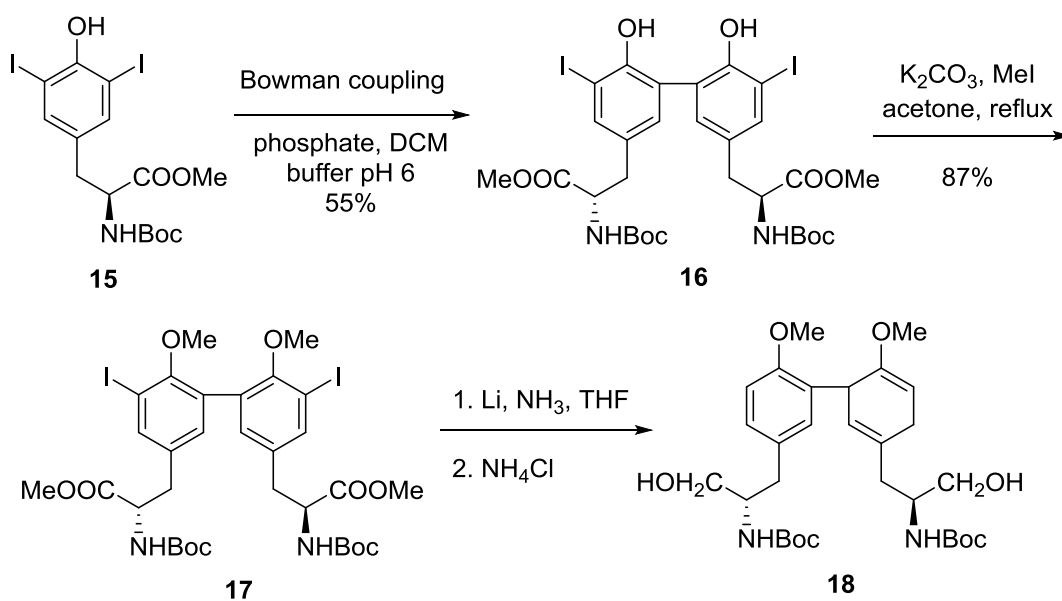
Scheme 1.2: Kim's retrosynthetic analysis of herquiline A.¹⁴

Hart from the University of Leeds focused on the formation and reduction of dityrosine derivatives, which were considered to be the precursors of the herquelines according to their retrosynthetic analysis (Scheme 1.3).^{15*}

*During the course of our project, an electronic copy of the thesis digitised from paper original was obtained upon request from the British Library.

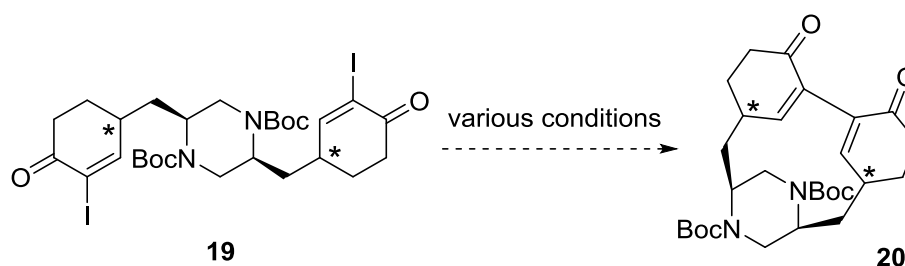
Scheme 1.3: Hart's retrosynthetic analysis of the herquelines.¹⁵

For the formation of dityrosine products such as **16** (Scheme 1.4), while direct oxidative phenol coupling or transition metal-catalysed Ullmann coupling methods did not give any promising results, the homo-coupling of tyrosine derivative **15** proceeded in moderate yield under Bowman coupling conditions.

Scheme 1.4: Hart's synthetic efforts towards the herquelines.¹⁵

When the fully protected dityrosine **17** was subjected to Birch reduction conditions, the partially reduced product **18** was the main one in all cases, even though no yield was mentioned in the thesis. Since the two aromatic rings within **17** could not be reduced successively, the synthesis towards the herquelines was not progressed.

During the course of our research project, the synthetic efforts from Stawski within the Trauner research group were disclosed in 2012, focusing on the intramolecular coupling of bis-ketone **19**, in order to obtain piperazine derivative **20** for further operations (Scheme 1.5).¹⁶



Scheme 1.5: Synthetic efforts from Stawski in 2012.¹⁶

Several metal-catalysed coupling conditions (Ni, Cu and Pd) were screened without generating the desired coupling product. Some of the reactions only gave dimers or trimers that derived from **19**.

1.4.2 Progress in the Synthesis of Relevant Structures

Piperazinomycin (**21**) is a piperazine-possessing natural product which shares structural resemblance with herquiline A and B (Figure 1.5). It was isolated as a minor metabolite from *Streptoverticillium olivoreticuli* subsp. *Neoenacticus* and has been found to exhibit inhibitory activity against fungi and yeasts.^{17,18}

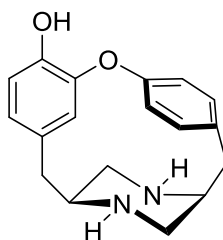
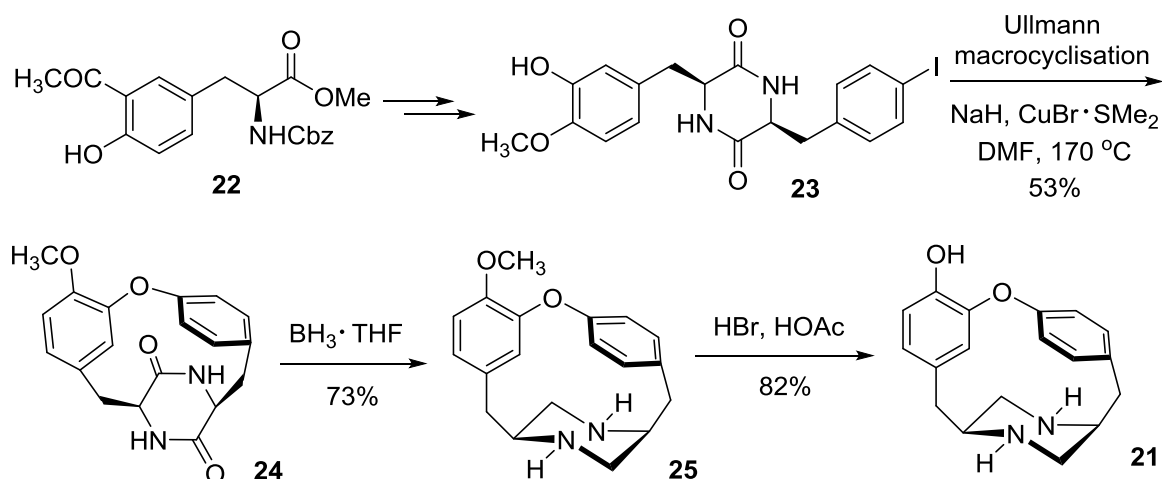


Figure 1.5: Structure of piperazinomycin (**21**).

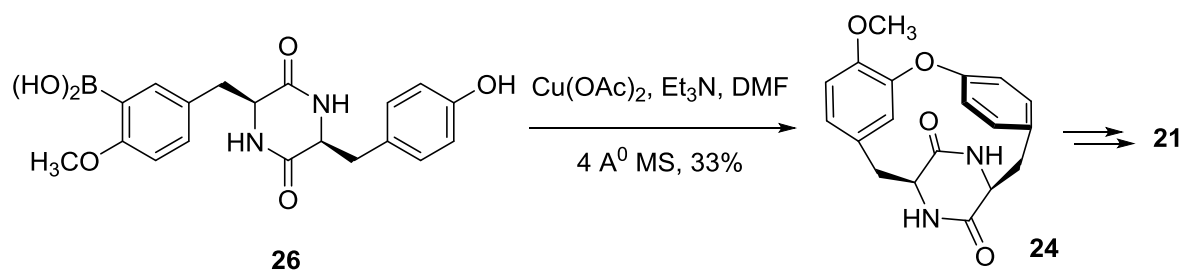
This natural product bears a 14-membered ring system that is composed of a piperazine moiety and a diaryl ether linkage. Similar to herquelines, it has been presumed to arise from L-tyrosine in Nature. Several total syntheses of this piperazine natural product have been reported, most of which selected the optically pure amino acid, L-tyrosine or its derivatives as starting materials.¹⁹⁻²¹

The synthetic work from the Boger research group is depicted in Scheme 1.6.¹⁹ Firstly, two molecules of amino acid derivatives were coupled to form a dipeptide, which cyclised to give DKP derivative **23**. After an intramolecular Ullmann reaction, the 14-membered diaryl ether derivative **24** was provided. Reduction of the DKP moiety with borane-THF complex followed by demethylation completed the total synthesis.



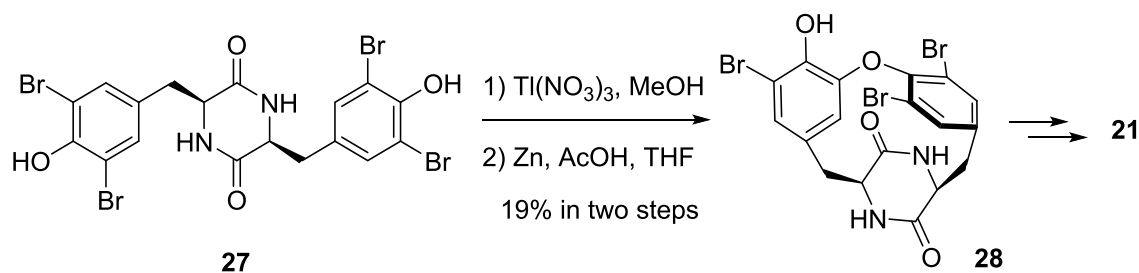
Scheme 1.6: Boger's total synthesis of piperazinomycin.¹⁹

Sundararajan and co-workers reported a formal synthesis of piperazinomycin in 2009 featuring a copper-mediated intramolecular *O*-arylation reaction between the arylboronic acid unit and the phenol moiety in **26** to form the macrocyclic biaryl ether **24** (Scheme 1.7).²⁰ With diketopiperazine **24** in hand, the formal synthesis finally afforded the natural product after several previously reported operations.



Scheme 1.7: Formal synthesis of piperazinomycin by Sundararajan and co-workers.²⁰

In Yamamura's total synthesis of piperazinomycin, a thallium trinitrate-promoted oxidative phenol coupling method was employed, followed by reduction with zinc to afford the key intermediate **28** in 19% yield (Scheme 1.8).²¹ Although the material return for this reaction was not efficient, the coupling product **28** was subjected to the next manipulation and the final product was synthesised after seven further steps.

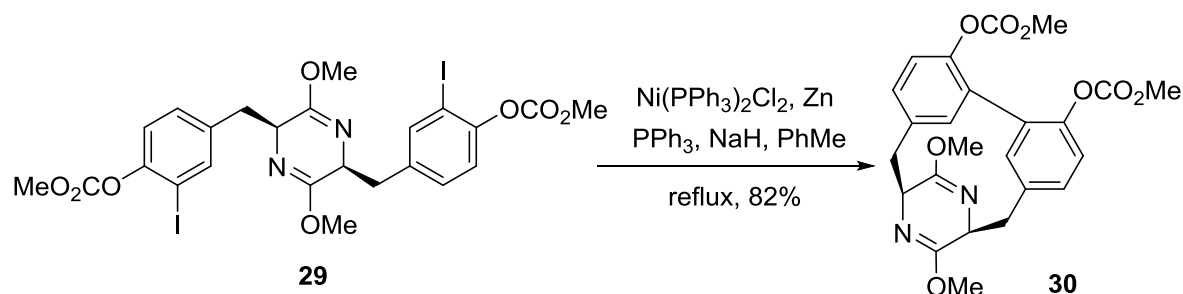


Scheme 1.8: Tl-mediated oxidative coupling in Yamamura's total synthesis of piperazinomycin.²¹

Even though the herquelines and piperazinomycin could all be traced back to tyrosine biosynthetically, the structural difference between these two types of alkaloids is that the phenol rings in piperazinomycin are not reduced to the cyclohexanone and cyclohexenone which exist in the former. In addition, the two aryl rings in piperazinomycin are tethered together by an ether linkage, while the cyclohexanone and cyclohexenone rings in herquiline A are connected *via* a C–C bond. Nevertheless, the accomplishment of the cyclisation to generate the diaryl ether linkage within piperazinomycin might provide an instructive strategy that could be applied in the total synthesis of herquiline A and B.

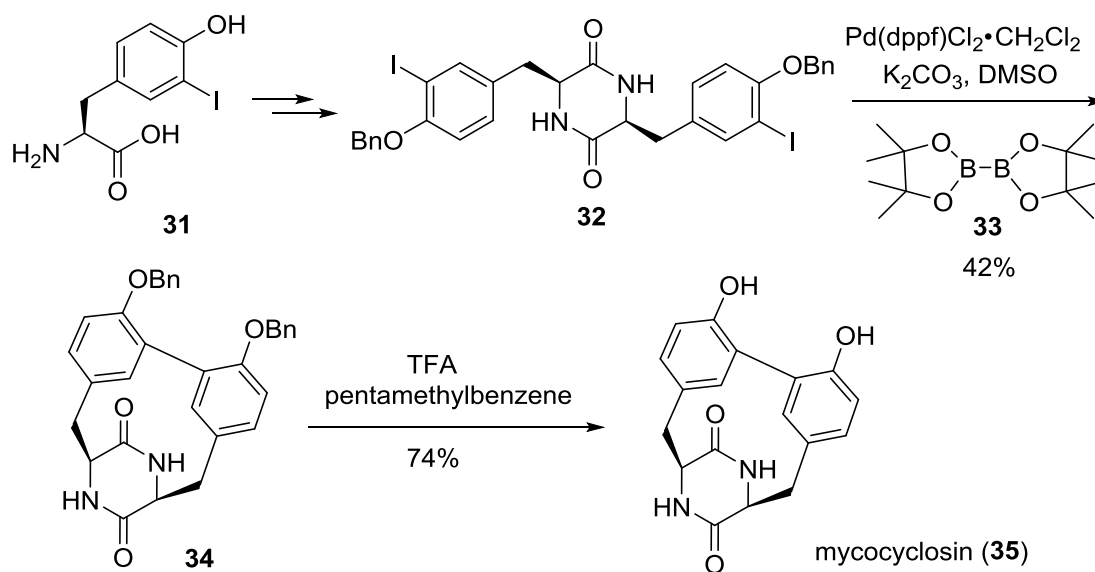
Besides the intramolecular diaryl ether synthesis, efforts have also been made in C–C bond formation to generate macrocyclic biaryl linkages. Some of the products also bear close structural similarity to herquelines.

In 2003, Atsumi and Noriyoshi reported the synthesis of cyclic biaryl product **30** through a Ni-catalysed aryl iodide coupling reaction (Scheme 1.9).²² Treating bis(carboximidate) **29** with nickel complex, the intramolecular coupling process proceeded smoothly to afford biaryl **30** in 82% yield, with the formation of a new C–C bond.



Scheme 1.9: Ni-catalysed intramolecular aryl iodide coupling.²²

Another relevant work is the total synthesis of mycocyclosin (**35**), published by the Hutton research group in 2012 (Scheme 1.10).²³ Mycocyclosin is a diketopiperazine derivative produced by *Mycobacterium tuberculosis* as a secondary metabolite.^{24,25} Starting from tyrosine derivative **31**, diketopiperazine intermediate **32** was initially synthesised. The cyclisation was performed with a Pd-catalysed domino Suzuki-Miyaura coupling method to afford **34** in moderate yield. The final product **35** was obtained after benzyl group cleavage with trifluoroacetic acid (TFA) and pentamethylbenzene. According to the crystal structure of **34**, it was confirmed that this cyclised product is a highly strained molecule with a significantly distorted biaryl linkage.

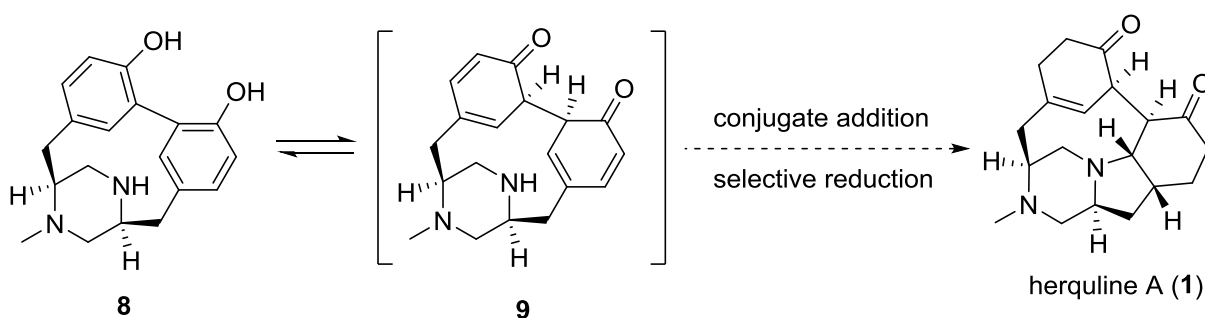
Scheme 1.10: Hutton's total synthesis of mycocyclosin.²³

There has been no evidence to show the biosynthetic relationship between mycocyclosin and herquelines, since they were isolated from different sources. However, these natural products are all considered to originate from tyrosine in Nature and from a chemical synthesis perspective, they can all be traced back to tyrosine-derived building blocks.

CHAPTER 2 STUDIES ON DIRECT OXIDATIVE PHENOL COUPLING – A BIOMIMETIC APPROACH

2.1 Initial Considerations and Retrosynthetic Analysis

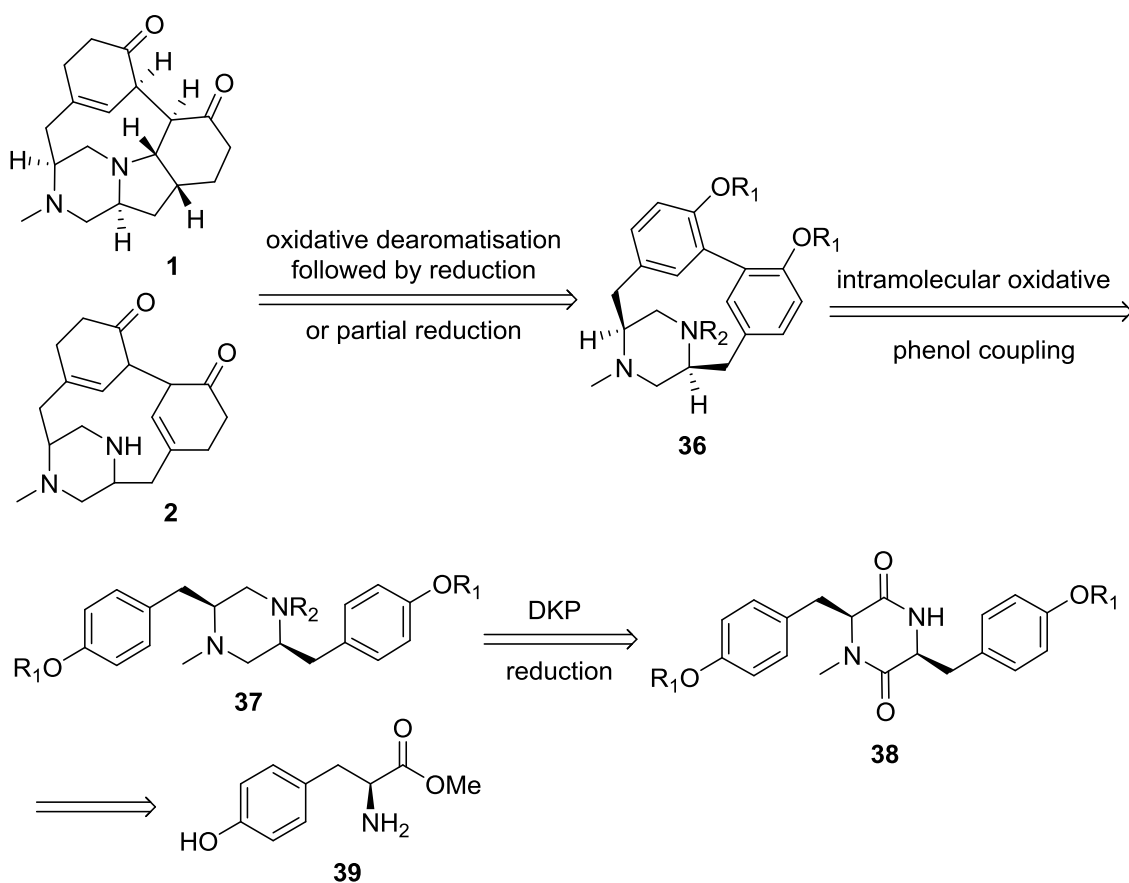
Attracted by the combination of the novel structural features of the herquelines and their promising biological activities, we decided to take up the challenge to explore the total synthesis of herquiline A and B. Before embarking on the retrosynthesis of the two natural products with logical disconnections, it was valuable to have a close analysis of the putative biosynthesis, which might suggest a potentially efficient synthetic avenue.



Scheme 2.1: Plausible biosynthetic pathway leading to the formation of the pyrrolidine ring in herquiline A.

As depicted in Scheme 2.1, the formation of the pyrrolidine ring was conceived to proceed after the generation of the 1,4-dicarbonyl moiety in the organism. Since the two ketone rings were tethered together within intermediate **9**, rendering the secondary amine and the adjacent dienone moiety in close proximity, the intramolecular *aza*-Michael addition was indeed facilitated at this stage. Presumably, within an enzymatic environment, this transformation would be a regio- and stereoselective one to form the 5-membered pyrrolidine ring in the final natural product **1**.

While Nature can find a way to convert **8** to herquiline A precisely, from a synthetic point of view, reductive or oxidative dearomatisation of the biaryl unit within **36** would give an advanced intermediate, which could be further manipulated towards the herquelines (Scheme 2.2). The dearomatisation transformations could be a Birch reduction of the phenol ether moieties followed by hydrolysis of the resultant cyclohexadiene to enone functionality, or oxidative conversion of phenol to enone derivative, which would facilitate a subsequent intramolecular *aza*-Michael addition.



Scheme 2.2: Retrosynthetic analysis of the herquelines.

Even though the outcome of the proposed dearomatisation remained to be negotiated during the late stage synthesis, having piperazine intermediate **36** as a sub-target rendered the

synthesis more manageable and might provide a quick access to the core skeleton of the herqulines.

For the synthesis of biaryl structure **36**, Nature's oxidative phenolic coupling strategy seems to be appealing and inspirational. Actually, a variety of methods have been developed to effect phenol oxidative coupling in the laboratory. Herein we envisioned an intramolecular version of this transformation on piperazine **37** to afford **36**. Piperazine substrate **37** would be furnished from the reduction of diketopiperazine **38**, which could be assembled from two molecules of tyrosine derivatives.

According to the above analysis, the primary goal was the synthesis of the cyclised piperazine derivatives, such as **36**, starting from tyrosine or tyrosine derivatives.

Before introducing our attempts in this biomimetic approach, it is valuable to have an overview of phenol oxidative coupling processes that happen in Nature and that have been developed in the laboratory.

2.2 Introduction to Phenolic Oxidative Coupling

2.2.1 Oxidative Phenol Coupling in Nature

It is known that oxidative phenol coupling is an essential transformation during the biosynthesis of a large number of biaryllic or related natural products. Biosynthetic pathways of several natural products have been investigated and some studies also identified the enzymes involved in the phenol coupling steps. A famous example of this kind is the biosynthetic studies of vancomycin-type glycopeptides, a group of clinically important

antibiotics that can inhibit the biosynthesis of bacterial peptidoglycan. As exemplified in Figure 2.1, there are two diaryl ether linkages and one biaryl moiety within the molecule of vancomycin (**40**) or balhimycin (**41**).

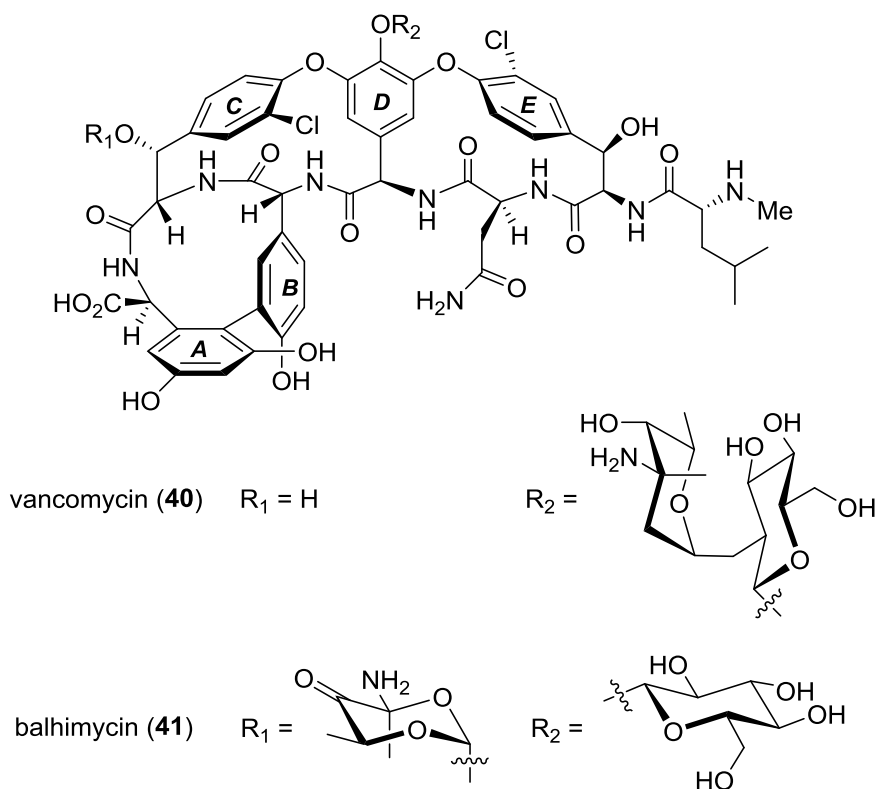
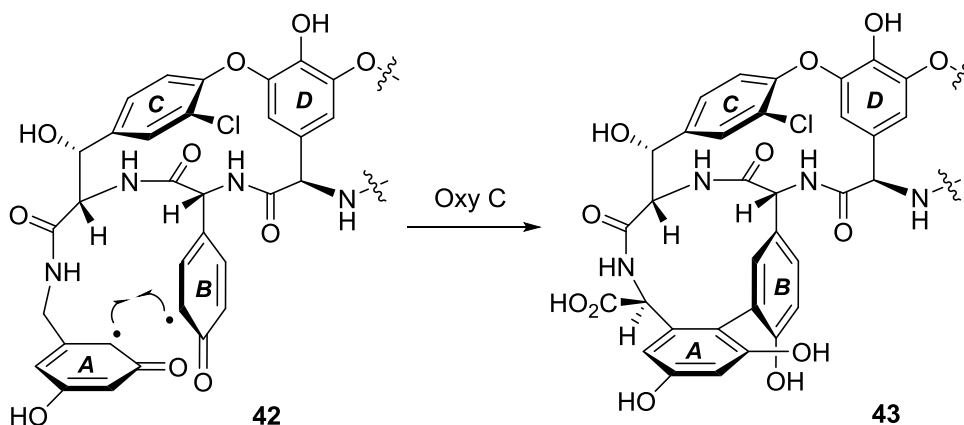


Figure 2.1: Structures of vancomycin and balhimycin.

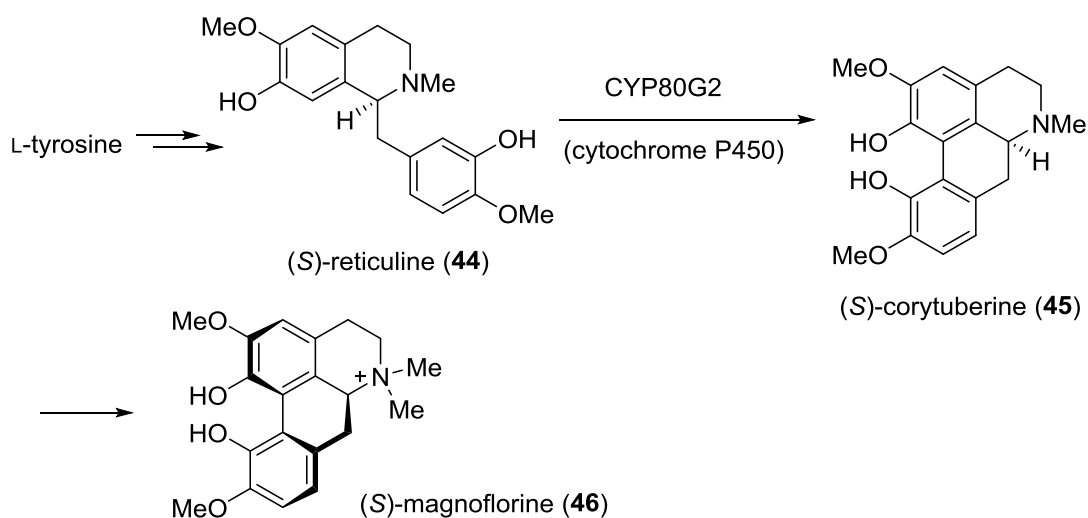
It has been reported that these linkages are formed in three separate oxidative cross-linking steps, catalysed by different cytochrome P450 enzymes.²⁶⁻²⁸ Presumably, the C-O-D system is produced as the first phenol coupling process, catalysed by oxygenase OxyB, followed by OxyA mediated carbon-oxygen coupling to generate the D-O-E linkage. The biaryl unit is synthesised in the last oxidative phenol coupling reaction, which is a carbon-carbon coupling transformation catalysed by OxyC enzyme. For the last phenol coupling reaction, a biradical mechanism has been suggested, oxidised by $\text{Cys}_4\text{Fe}_2\text{S}_2$ ferredoxin (Scheme 2.3). It is not known yet whether these cross-coupling transformations occur on a free heptapeptide precursor or before the formation of the linear peptide, but Nature's way of synthesising these

bis-aryl linkages is very efficient and precise, with all these units being generated atroposelectively.



Scheme 2.3: Oxidative phenol coupling reaction in the biosynthesis of the vancomycin-type glycopeptide antibiotics.²⁷

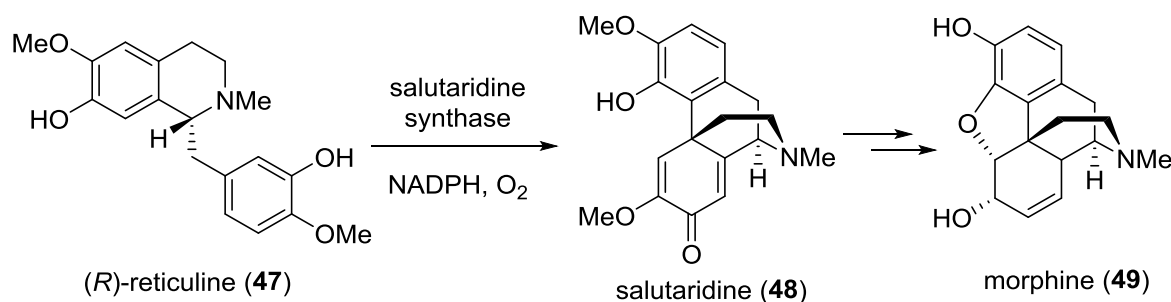
In isoquinoline alkaloid biosynthesis, several oxidative phenol coupling reactions involving cytochrome P450 enzymes have been reported. As delineated in Scheme 2.4, (*S*)-reticuline (**44**) is an alkaloid isolated from the Japanese goldthread *Coptis japonica* and is proposed to derive from L-tyrosine.²⁹



Scheme 2.4: Oxidative phenol coupling involved in the biosynthesis of isoquinoline alkaloids.²⁹

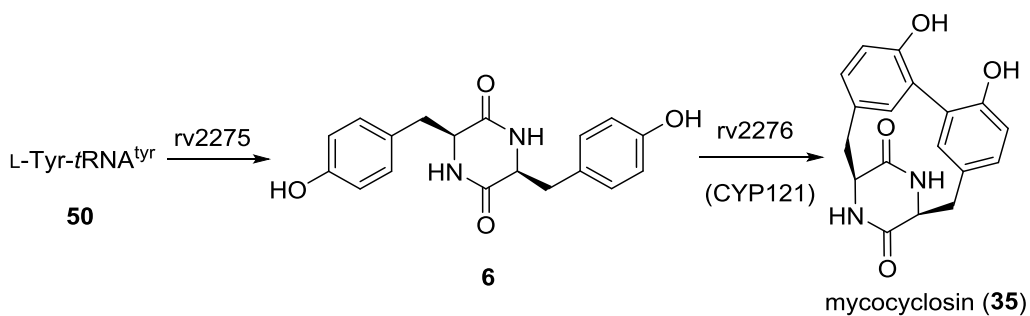
Within the plant, (*S*)-reticuline can be converted to (*S*)-corytuberine (**45**) via the CYP80G2 (a P450 enzyme) catalysed oxidative phenol coupling reaction. After a methylation process, another naturally occurring entity, (*S*)-magnoflorine (**46**) can be synthesised from (*S*)-corytuberine.

Interestingly, (*R*)-reticuline (**47**) is considered to be the biosynthetic precursor for morphine (**49**).^{29,30} Catalysed by salutaridine synthase, a P450-dependent monooxygenase, (*R*)-reticuline undergoes an *ortho-para* oxidative phenol coupling to give salutaridine (**48**) which is further functionalised to afford morphine (**49**) (Scheme 2.5).



Scheme 2.5: Key step in the biosynthesis of morphine.²⁹

Another example of oxidative phenol coupling in Nature is the biosynthesis of the previously introduced mycocyclosin (**35**), a diketopiperazine natural product produced by *Mycobacterium tuberculosis*. It is believed that this secondary metabolite derives from cyclo(L-Tyr-L-Tyr) which is formed from two molecules of tyrosyl-*t*-RNA (**50**) catalysed by rv2275, a cyclodityrosine synthetase (Scheme 2.6).^{24,25} Subsequent oxidative phenol coupling is catalysed by the cytochrome P450 enzyme rv2276 (also called CYP121).²⁵ Recently, it has been shown that the gene encoding the P450 enzyme (CYP121) is essential for the viability of *M. tuberculosis*,³¹ which indicates that this enzyme might be a potential target for *M. tuberculosis* inhibitor discovery.



Scheme 2.6: Biosynthetic sequence for mycrocyclosin.^{24,25}

Based on the crystal structure of cyclodityrosine-bound CYP121 obtained by Belin and co-workers (Figure 2.2),²⁵ the diketopiperazine ring adopts a flattened-boat conformation with a dihedral angle of 15° between the two peptide bonds. One tyrosine side chain points between helices F and G and the other tyrosine side chain faces the DKP ring and approaches the iron.

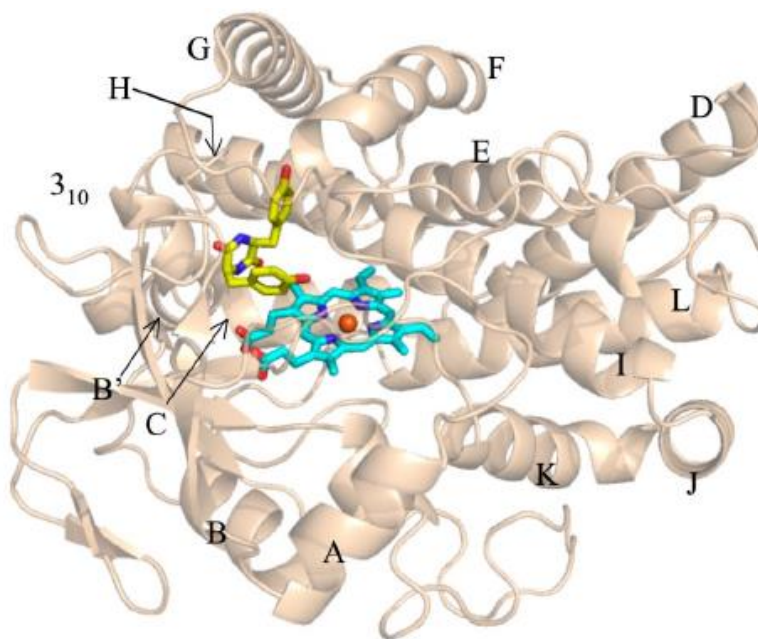


Figure 2.2: Structure of cyclodityrosine-bound CYP121 (the heme in cyan, the iron in orange, and the cyclodityrosine in yellow with nitrogen atoms in blue and oxygen atoms in red, reproduced from *PNAS*).²⁵

This conformation does not seem to allow a sufficient proximity of the two tyrosyl groups for the C–C coupling reaction. Belin and co-workers explained that the two tyrosyl side chains can rotate around their C_α – C_β bond during the catalysis due to the existence of a large water-

filled pocket around the molecule. These movements would guarantee the two tyrosyl side chains are sufficiently close together and in appropriate orientation to form the biaryl linkage.

2.2.2 Oxidative Phenol Coupling in Organic Synthesis

Complementary to Nature's enzymatic synthesis of bis-aryl products, the construction of bioactive cyclic biaryl molecules also represents a fascinating and challenging goal in organic synthesis.

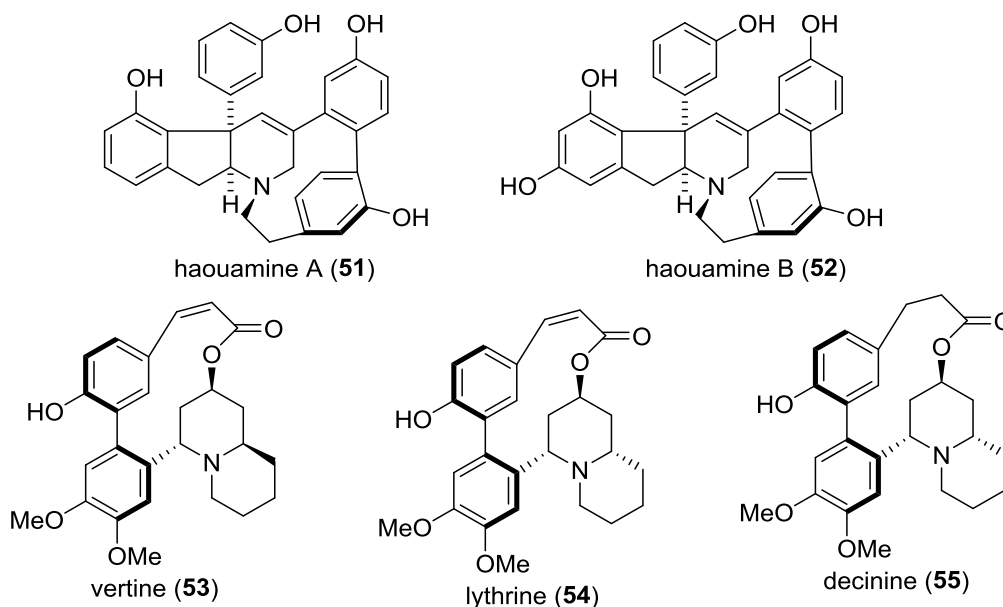
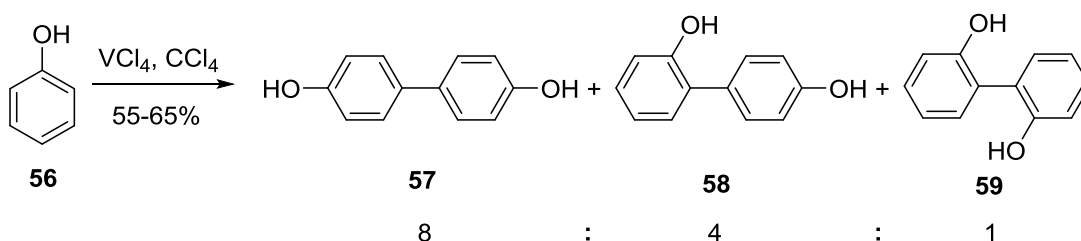


Figure 2.3: Examples of cyclic biaryl natural products.

A wide range of biarylic natural products, such as haouamine A (**51**) and B (**52**) and the Lythraceae family alkaloids vertine (**53**), lythrine (**54**) and decinine (**55**) (Figure 2.3), have attracted significant synthetic interest.³²⁻³⁶ In some of the studies, intramolecular oxidative phenol couplings have been tested or even employed as the key steps during the syntheses. A variety of oxidising reagents have been discovered and developed to effect phenolic coupling reactions.

Vanadium Oxidants as the Coupling Agents

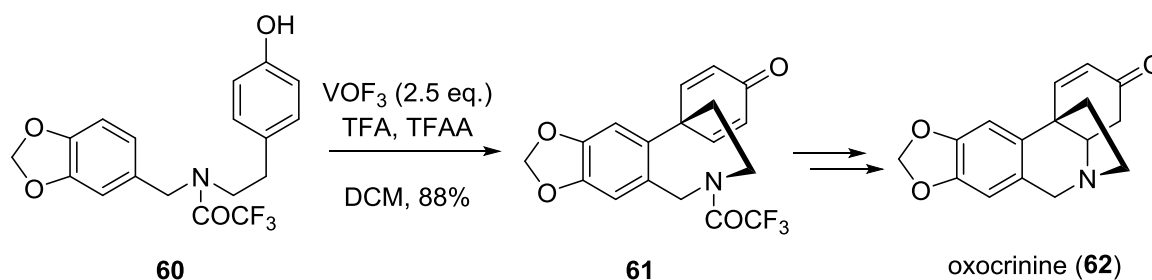
Vanadium species belong to the most common oxidants for oxidative phenol coupling. The earliest example can be traced back to the oxidative coupling of simple phenol substrates reported by Carrick and co-workers in 1968.³⁷ It was found that dimeric products were obtained through a C–C coupling reaction upon treating simple phenols with VCl_4 . Using unsubstituted phenol as the substrate, three biphenols were isolated, favouring the *para-para* coupling product **57** (Scheme 2.7).



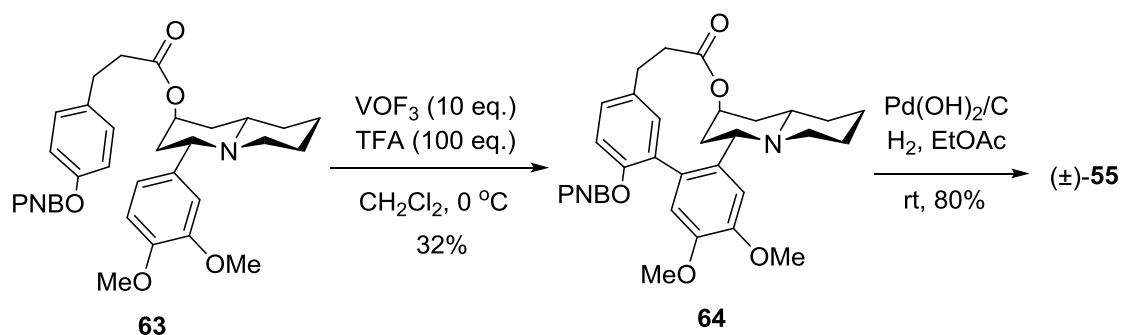
Scheme 2.7: VCl_4 -promoted phenol coupling.³⁷

Although the mechanism has not been completely elucidated, Carrick and co-workers pointed out that the hydroxy group might play an important role during the course of the reaction by coordinating to the metal center to form a complex. Shift of electrons occurred within the complex to fashion a subsequent coupling reaction.

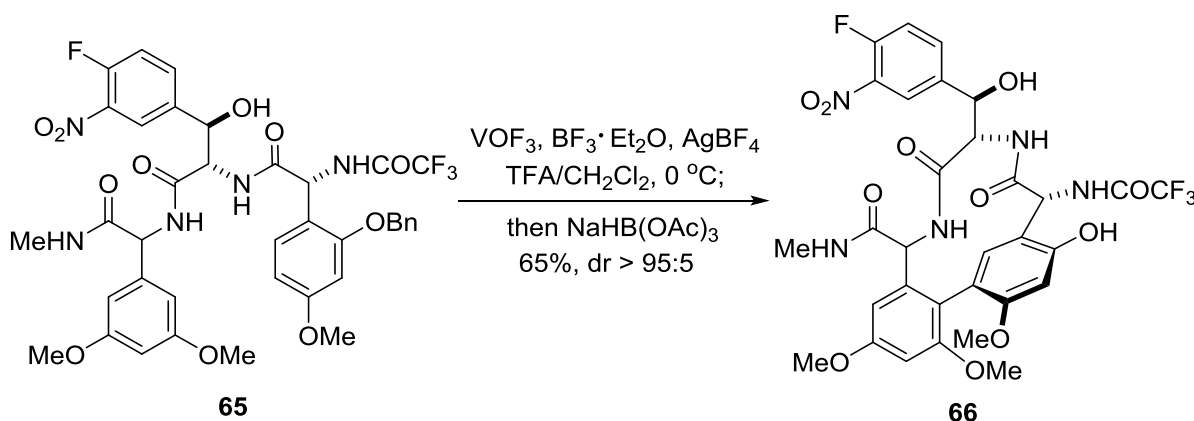
Remarkable success has been achieved in alkaloid syntheses. Dienone **61**, a synthetic precursor of the amaryllidaceae alkaloid (\pm)-oxocrinine (**62**), was synthesised by treating mono-phenolic amide **60** with VOF_3 in dichloromethane in the presence of trifluoroacetic acid and trifluoroacetic anhydride (Scheme 2.8).³⁸ In one step, linear amide **60** was converted to a compact and rigid structure, which demonstrated that oxidative phenolic coupling is an efficient tool in organic synthesis.

Scheme 2.8: Intramolecular oxidative coupling with VOF_3 .³⁸

Another application of vanadium-mediated oxidative coupling towards alkaloid natural products is exemplified in the total synthesis of (\pm)-decinine (**55**), published by Yang and co-workers in 2012.³⁶ After attempting the VOF_3 -promoted oxidative coupling with several different substrates, they finally managed to construct the 12-membered ring of decinine from *p*-nitrobenzyl (PNB) protected phenol ether **63** (Scheme 2.9). The cyclised product **64** was delivered in 32% yield and converted to (\pm)-decinine (**55**) after removal of the PNB group.

Scheme 2.9: Key steps in the total synthesis of decinine.³⁶

In Evans' synthesis of vancomycin aglycon, a biomimetic approach towards the macrocyclic subunit containing a biaryl moiety was employed.^{39,40} Tripeptide **65** was subjected to VOF_3 -mediated oxidative coupling conditions followed by reductive quench with $\text{NaBH}(\text{OAc})_3$ to give cyclic product **66** in 65% yield (Scheme 2.10). Although the unnatural *R* atropisomer was obtained predominately (d.r. > 95:5), this atropisomerism issue was corrected completely in one of the following steps through a thermal equilibration.



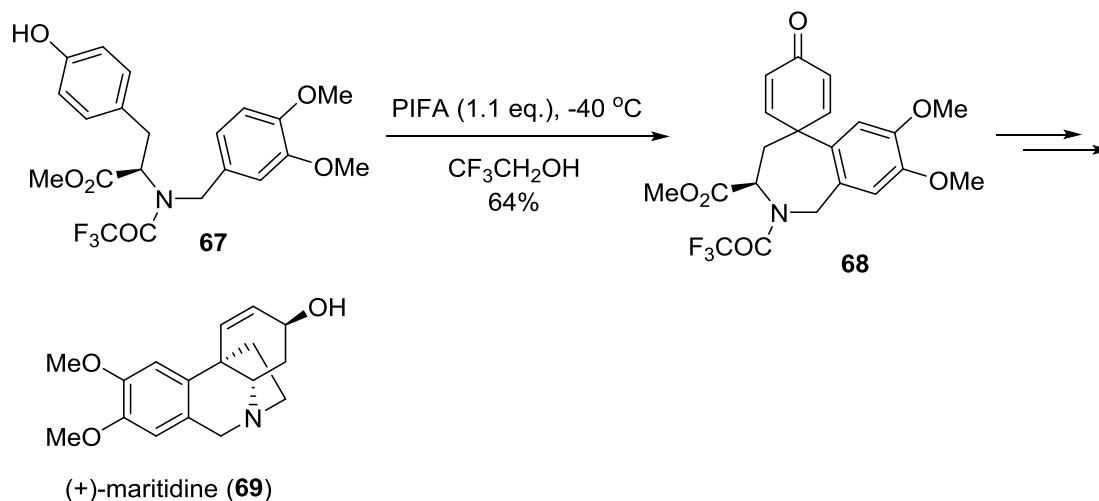
Scheme 2.10: VOF_3 -mediated oxidative coupling in Evans' synthesis of vancomycin aglycon.^{39,40}

It is noted that the addition of a reducing agent, either $\text{NaBH}(\text{OAc})_3$ or zinc, is necessary to quench the radical cation derived from the biaryl linkage in the product, which is prone to nucleophilic attack.

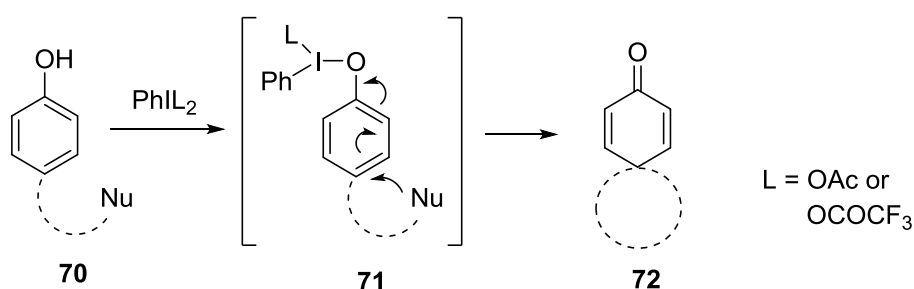
Hypervalent Iodine Induced Oxidative Phenol Coupling

Organic hypervalent iodine derivatives have been used routinely for various oxidative transformations and are classified as environmentally friendly oxidants because of their lower toxicity than heavy metal-containing reagents. It has been shown that oxidation of phenolic substrates in less or non-nucleophilic solvents (e.g. MeCN, $\text{CF}_3\text{CH}_2\text{OH}$ and DCM) can promote coupling reactions to proceed and lead to cyclisation if the reactions occur intramolecularly. PIDA (phenyliodine diacetate) and PIFA (phenyliodine bis(trifluoroacetate)) are two of the most popular reagents employed for these transformations.

As shown in Scheme 2.11, treating amide **67** with PIFA in trifluoroethanol at low temperature, cyclisation took place to afford dienone **68**, a key intermediate in Kita's total synthesis of (+)-maritidine (**69**).⁴¹

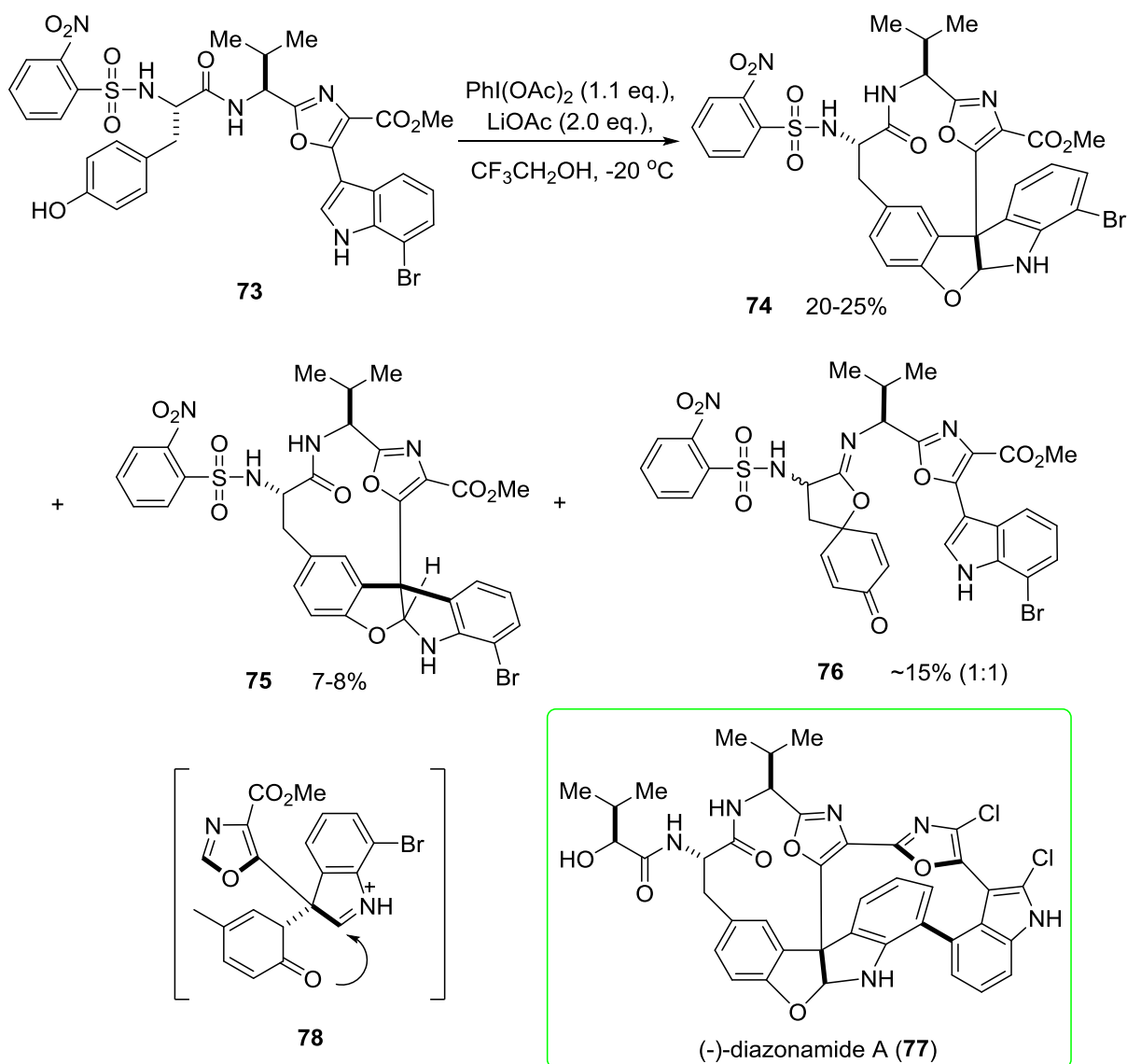
Scheme 2.11: PIFA promoted intramolecular coupling.⁴¹

In general, the mechanism for hypervalent iodine-mediated phenol coupling transformations involves the reaction between phenolic oxygen and the iodine centre of the oxidant, a process of exchanging one ligand on iodine(III) with a nucleophile (such as phenol or phenoxide anion) through an addition-elimination sequence (Scheme 2.12).⁴² After ligand exchange, the generated intermediate **71** is prone to nucleophilic attack by either an electron-rich aromatic ring or other nucleophile, to give cross-conjugated cyclohexadienone **72**. Therefore, the phenolic hydroxy group has an important role in the coupling process.

Scheme 2.12: Postulated mechanism of hypervalent iodine induced transformations of phenols.⁴²

Scheme 2.13 exemplified an intramolecular cross-coupling between a phenol and an indole moiety which belonged to one of the most efficient steps in the total synthesis of (-)-diazonamide A (**77**) accomplished by the Harran research group in 2003.⁴³ Under the

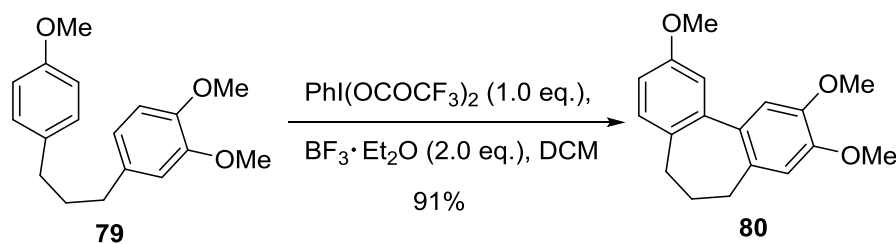
$\text{PhI}(\text{OAc})_2$ oxidation conditions, the desired aminal **74** was isolated as the main product, alongside its diastereoisomer **75** and the epimeric spirodienones **76**. The dihydrobenzofuro[2,3-b]indole subunit within **74** is supposed to form from **73** through a cyclohexadienone-linked indoleninium species **78**.



Scheme 2.13: $\text{PhI}(\text{OAc})_2$ -mediated cyclisation in Harran's total synthesis of **(-)-diazonamide A**.⁴³

Different from the oxidative coupling of phenol derivatives, the number of reactions with phenol ethers as the coupling substrates is limited, largely due to the preferred formation of iodonium salts when phenol ethers were treated with hypervalent iodine agents.⁴² However,

oxidative coupling of phenol ethers can occur in certain circumstances, especially with electron-rich ones, such as the example shown in Scheme 2.14. Treating the simple phenol ether **79** with PIFA in the presence of $\text{BF}_3 \cdot \text{Et}_2\text{O}$ in DCM gave **80** with a tricyclic [6-7-6] ring system in high yield.⁴⁴



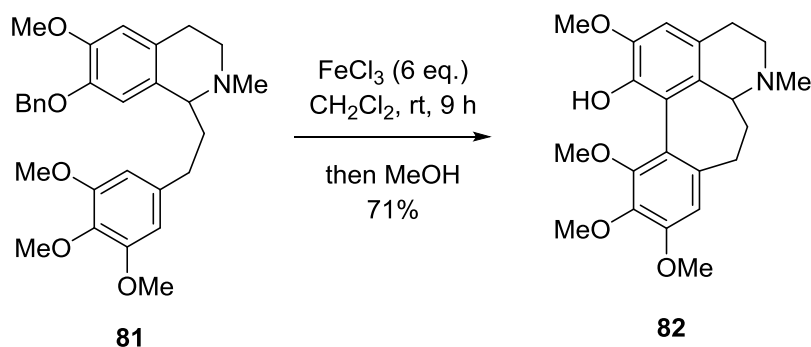
Scheme 2.14: Oxidative coupling of phenol ethers.⁴⁴

Mechanistically, without a hydroxy functionality, the coupling pathway might involve the reaction between hypervalent iodine reagent and phenol ether substrate to generate a cation radical intermediate *via* a single electron transfer process, which has been studied by UV-visible and ESR (electron spin resonance) spectroscopic methods.^{45,46} Subsequent nucleophilic attack of another phenol ether on the cation radical, or the coupling reaction between two radical intermediates would furnish the biaryl product. Thus it seems reasonable to infer that the more electron-rich aromatic ring tends to react with the oxidant more easily because of the lower oxidation potential.

Other Oxidants Used in Phenolic Coupling Reactions

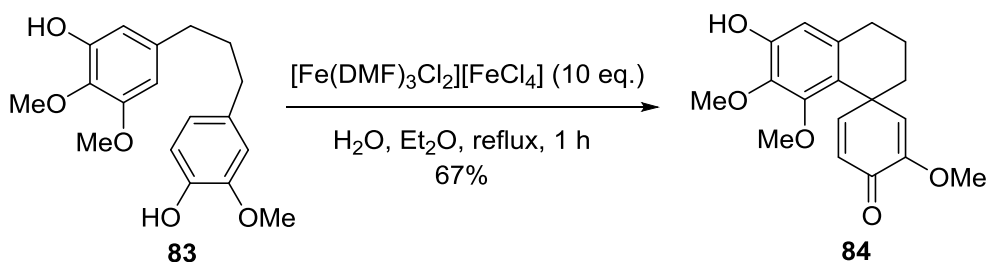
Dimerisations of phenol derivatives promoted by iron(III) species have been investigated extensively. Presumably the radical cation of the corresponding phenol substrate is involved during the coupling process. Among all the iron(III) oxidants, iron(III) chloride is a mild and inexpensive agent that has been employed in numerous C–C bond forming reactions.⁴⁷⁻⁴⁹

As demonstrated in Scheme 2.15, tetrahydroquinoline **81** was used as the substrate in an FeCl_3 -promoted intramolecular coupling reaction during the synthesis of alkaloid (\pm)-kreysigine (**82**).⁴⁸ After a reductive work-up with methanol, the natural product was obtained directly in 71% yield, with concomitant cleavage of the benzyl protecting group.



Scheme 2.15: FeCl_3 -mediated intramolecular coupling in the synthesis of (\pm)-kreysigine (**82**).⁴⁸

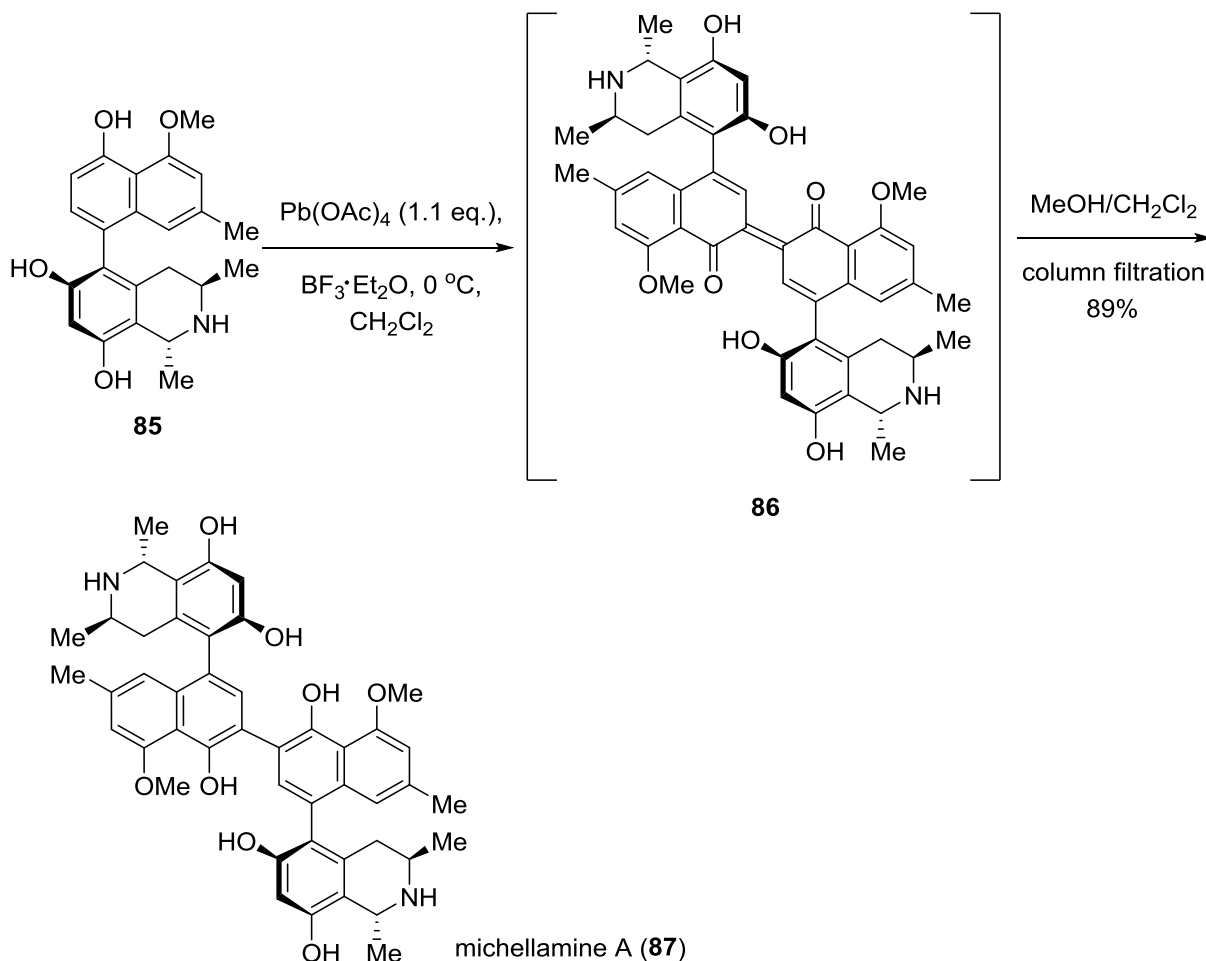
Another example of intramolecular oxidative aryl aryl coupling was reported by Tobinaga and Kotani.⁴⁹ They treated bis-phenolic substrate **83** with $[\text{Fe}(\text{DMF})_3\text{Cl}_2][\text{FeCl}_4]$, a complex prepared from ferric chloride and DMF (Scheme 2.16). Dienone product **84** was delivered in 67% yield. It was stated that the use of this specific iron complex as the oxidant improved the reaction yield and also avoided the formation of polymeric compounds.



Scheme 2.16: Intramolecular oxidative phenol coupling with Fe(III) complex.⁴⁹

The utility of lead(IV) and silver(I) oxidants has been revealed in the synthesis of dimeric arenes. Good to excellent results can be obtained when the substrate is a naphthol derivative.

Such an example can be found in the synthesis of the antiviral natural product michellamine A (**87**), reported by Bringmann and co-workers (Scheme 2.17).⁵⁰



Scheme 2.17: Oxidative dimerisation with $\text{Pb}(\text{IV})$.⁵⁰

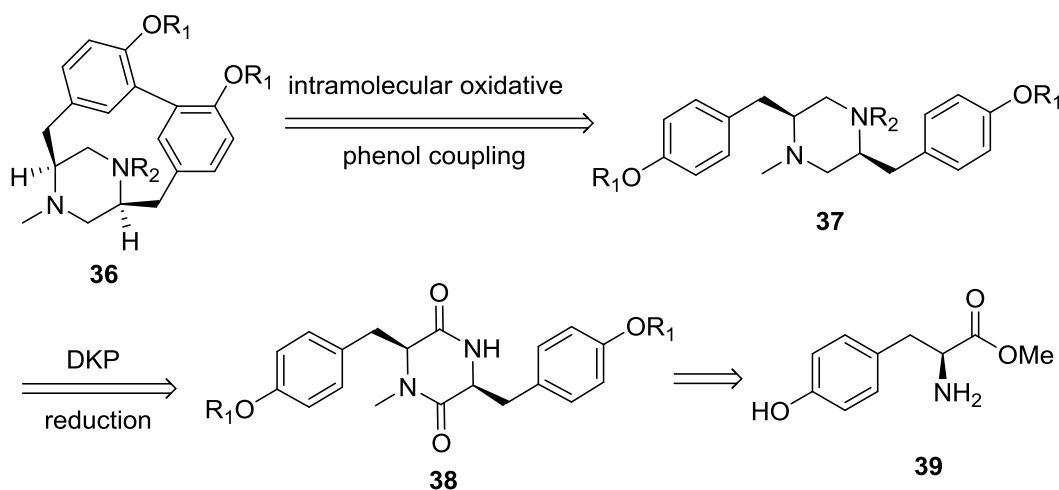
Treatment of isoquinoline alkaloid korupensamine A (**85**), the natural monomer of michellamine A, with lead tetraacetate in the presence of $\text{BF}_3 \cdot \text{Et}_2\text{O}$ led to diphenoquinone **86**. It was noteworthy that this intermediate was readily converted to the final product **87** during the purification process under incandescent light with MeOH as the reducing reagent. This essentially one-step homo-coupling reaction is the first non-enzymatic direct synthesis of michellamine A, without losing any axial chirality. It has been reported that similar dimerisation could also be fashioned with silver(I) oxide as the oxidant.⁵¹

Beyond the above mentioned agents, the oxidative coupling of phenol derivatives can also be effected in some cases by Cu(II)-amine complexes,⁵² Mo(V) and Tl(III) salts,^{53,54} or with different approaches including anodic oxidation and enzymatic conditions.^{55,56} These methods were not essentially explored in our project.

2.3 Efforts on Intramolecular Oxidative Coupling of Piperazine Substrates

2.3.1 Initial Forward Synthesis Towards Piperazine Intermediates

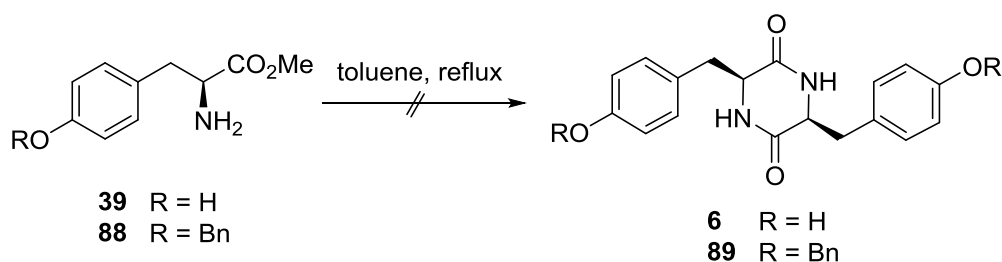
Based on the retrosynthetic plan, our initial goal in the biomimetic approach towards the herquelines was the synthesis of biaryl structure **36** through the intramolecular direct oxidative coupling of piperazine **37** which could be obtained from the reduction of DKP **38** (Scheme 2.18).



Scheme 2.18

For the synthesis of diketopiperazine derivative **38**, we first explored the dimerisation of tyrosine or its derivatives, which was considered to be an appealing approach and could also shorten the synthetic sequence.

It was reported that thermal dimerisation of phenylalanine methyl ester afforded the corresponding 2,5-diketopiperazine in high yield.⁵⁷ Following the reported procedure, heating tyrosine methyl ester **39** in toluene at reflux for 6 h, no reaction occurred (Scheme 2.19). With a longer reaction time or *O*-benzyl-protected tyrosine methyl ester **88** as the substrate, the cyclisation still failed to proceed and mainly starting material was recovered from the reaction mixture.

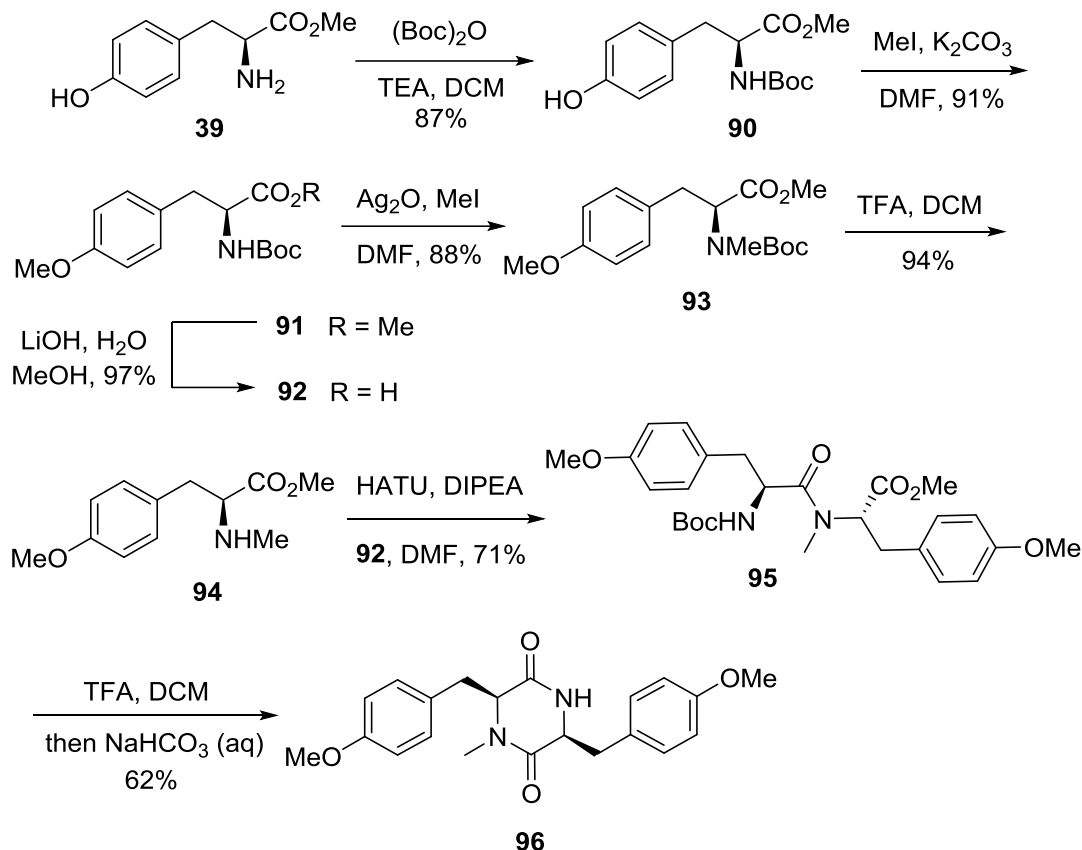


Scheme 2.19

Although the Lewis acid-catalysed or microwave-assisted condensation of free amino acids to cyclodipeptides had been reported to be successful,^{58,59} these conditions always led to epimerisation which was deleterious to the efficient synthesis of *cis*-DKP products in this study. We then abandoned this direct cyclisation approach and opted for a stepwise strategy.

The efforts started from the synthesis of dipeptide **95** following similar procedures reported in the literature (Scheme 2.20).^{60,61} Protection of the amine group of L-tyrosine methyl ester **39** with (Boc)₂O in the presence of Et₃N in DCM afforded the Boc-protected substrate **90** in 87% yield. Methylation of the phenol group was accomplished by treating **90** with MeI and K₂CO₃. With compound **91** in hand, *N*-methylation was performed using Ag₂O and MeI in DMF. Removal of the Boc protecting group of **93** with TFA in DCM delivered free amine **94**. Tyrosine methyl ester **91** could also be hydrolysed to acid **92**.

At this stage, amino acid coupling reaction was attempted and dipeptide **95** was successfully synthesised with coupling reagent HATU.

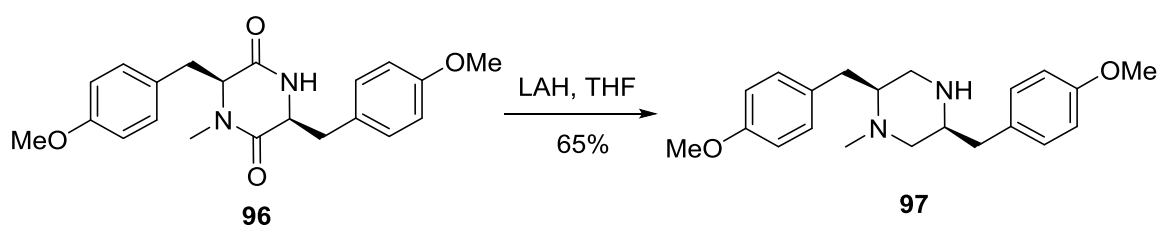


Scheme 2.20

To carry on the synthesis, dipeptide **95** was treated with TFA in DCM in order to remove the Boc protecting group. Surprisingly, diketopiperazine **96**, instead of the linear deprotected dipeptide, was isolated from the reaction mixture as the only product, which indicated that cyclisation occurred during the basic work-up process after Boc deprotection.

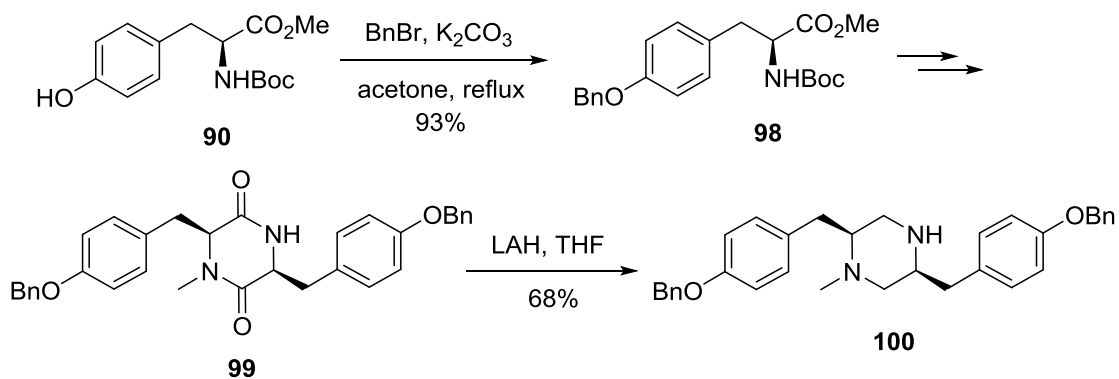
Having reached DKP derivative **96**, we then turned our attention to the reduction of **96** to piperazine **97** (Scheme 2.21). Several reducing reagents have been reported for the reduction of DKPs, including $\text{NaBH}_4/\text{BF}_3$,⁶² BH_3 ,^{63,64} lithium aluminium hydride,^{65,66} and $\text{NaBH}_4/\text{TiCl}_4$.⁶⁷ Among these reducing agents, LAH turned out to be the best choice for our

system because of the reasonable reaction time and low reaction temperature (0 °C to rt). While it was reported that the reduction of phenolic cyclo-dityrosine derivatives with LAH was problematic due to the poor solubility of their phenoxide conjugate bases in ethereal solvents,⁶³ the reduction of bis-phenol ether **96** proceeded smoothly to give unsymmetrical piperazine **97** in 65% yield.



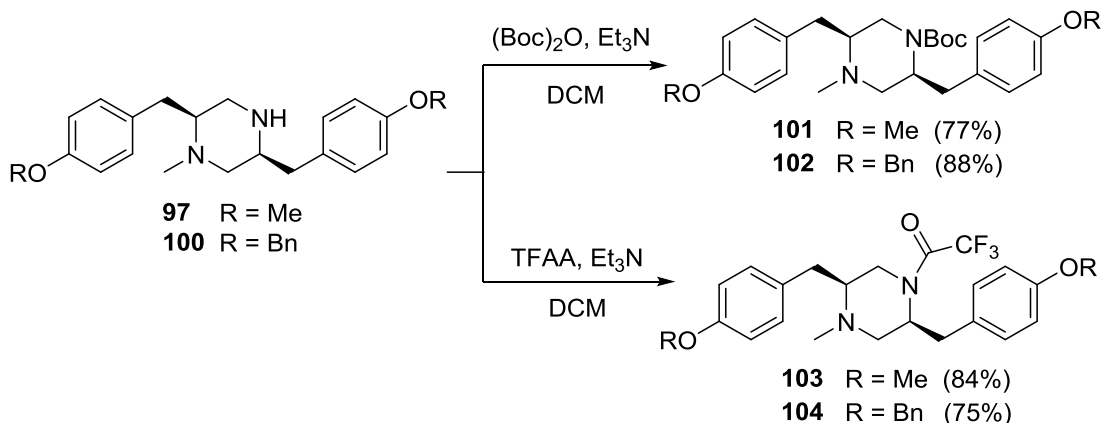
Scheme 2.21

O-Bn-protected piperazine **100** was also synthesised following a similar procedure from *O*-Bn tyrosine derivative **98** which was generated from the benzylation of **90** with benzyl bromide and potassium carbonate in refluxing acetone (Scheme 2.22).



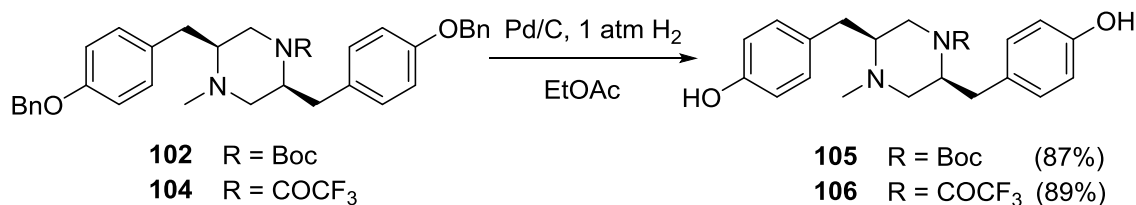
Scheme 2.22

Both of these piperazines were protected with either Boc or COCF₃ groups for further transformations (Scheme 2.23).



Scheme 2.23

The bis-phenol products **105** and **106** were obtained *via* the catalytic hydrogenolysis of **102** and **104**, respectively (Scheme 2.24).



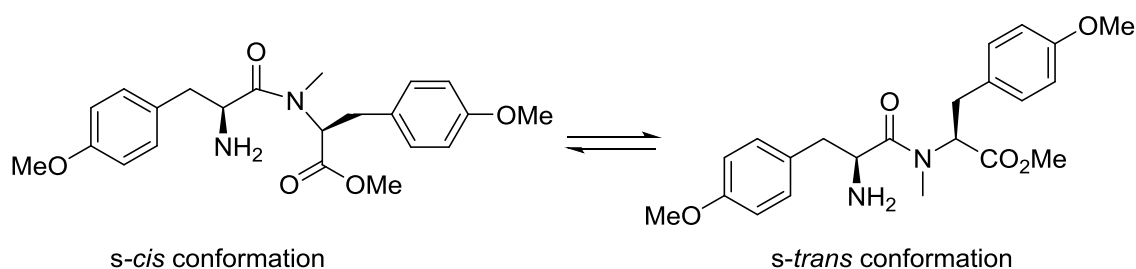
Scheme 2.24

Overall, the syntheses of these piperazines are straightforward processes, although several phenomena and chemistry issues during the course of the synthesis merit further discussion.

The *N*-methylation of tyrosine derivative **91** was initially performed with MeI and NaH. A degree of racemisation was observed during this process and was confirmed by the subsequent isolation of a small amount of *trans*-DKP product. According to several studies, racemisation has been observed during the methylations of chiral α -alkyl- α -amino acids using this method.^{68,69} Based on the amounts of the *cis* and *trans* DKP diastereoisomers, we

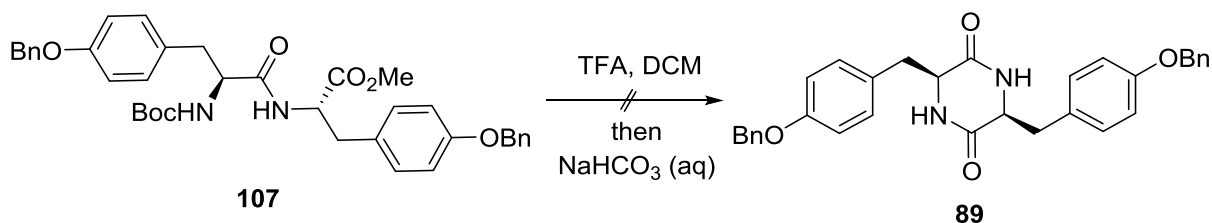
deduced that the ratio of L-**93** to D-**93** was about 4:1. The enantiopure **93** was obtained exclusively by treating substrate **91** with Ag₂O and MeI in DMF.

The ease of cyclisation of dipeptide **95** to DKP **96** is an interesting phenomenon. Similar results have been mentioned in several reports.^{70,71} It could be attributed to the *cis/trans* conformation equilibrium of the amide bond (Scheme 2.25).



Scheme 2.25: The *cis/trans* conformation equilibrium of *N*-methyl amide bond.

It has been reported that *N*-alkylated amide bond could affect the *cis/trans* isomerisation and drive the equilibrium to a significant extent of the *cis* form, which tended to cyclise easily.⁷² Actually, during the synthesis of symmetrical DKPs which will be introduced in Chapter 3, only removal of the Boc protecting group was observed when dipeptide **107** was subjected to the same conditions (Scheme 2.26). No further cyclisation took place to afford DKP **89**, which supports the above explanation.



Scheme 2.26

When the ¹H NMR spectrum of DKP **99** was interpreted, a doublet of doublets signal for one of the H-3 protons was found to show up at 0.82 ppm with CDCl₃ as the solvent (Figure 2.4).

The highfield shift with respect to the chemical shift of 2.85 ppm for the other β -proton in DKP **99**, indicates that one of the two β -protons is significantly shielded. The conformation of the DKP structure may play an important role in such a shielding effect.

Similar magnetic shielding effects for DKPs with a side chain containing an aromatic ring have also been observed from several studies.^{73,74} According to Kopple and Marr's analysis,⁷³ at ambient temperature cyclic dipeptides adopt a folded conformation, in which one side chain lies over the DKP ring while the other side chain orientates away from the peptide ring, as exemplified by DKP **99** in our case (Figure 2.4). They proposed that the preference for a folded conformation is largely due to the stabilisation from the interaction of two amide dipoles with the polarisable π electron system of the aromatic side chain, and this conformational bias is not significantly dependent on solvent.

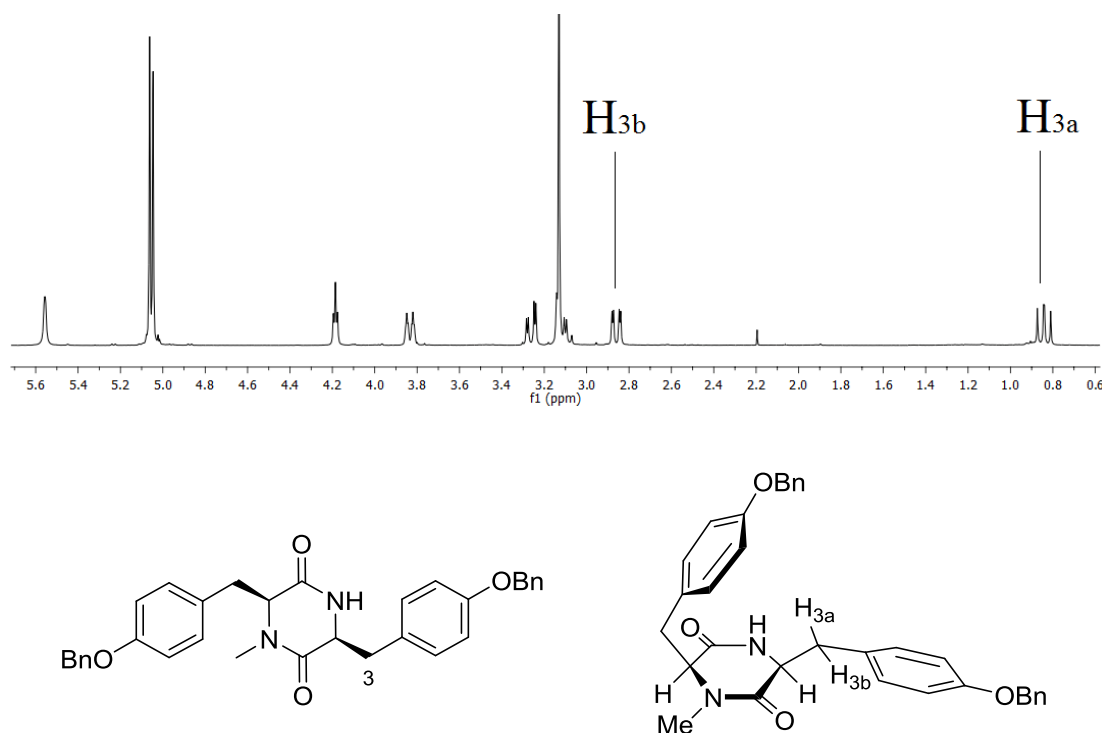


Figure 2.4: Partial ^1H NMR spectrum of DKP **99** (300 MHz, CDCl_3 , 298 K).

Since both DKPs **96** and **99** were isolated as oils, no crystals could be obtained. But based on the evidence from the literature, it appears that both of the two DKP derivatives would adopt folded conformations in solution at room temperature, with one aromatic residue facing the DKP ring and the other in an extended orientation.

Similar resonance patterns were observed from the ^1H NMR spectrum of symmetrical DKP **89**, with chemical shifts at 2.31 ppm and 3.06 ppm for the two chemically inequivalent β -protons (Figure 2.5).

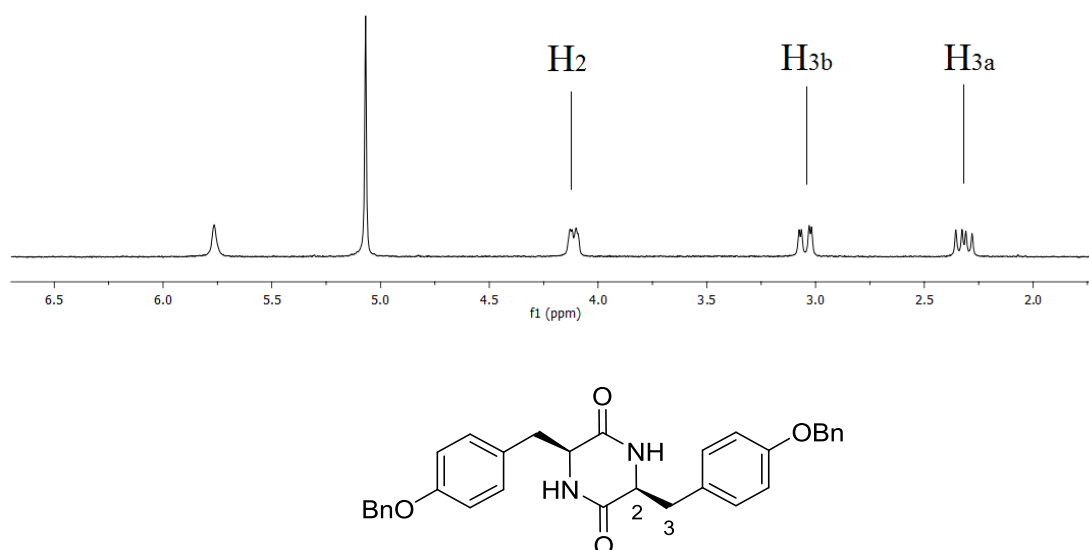


Figure 2.5: Partial ^1H NMR spectrum of DKP **89** (300 MHz, CDCl_3 , 298 K).

However, the shielding effect within **89** was not as distinct as that within unsymmetrical DKP **96** or **99**. On the one hand, the crystal structure of cyclo(L-phenylalanine-L-phenylalanine) published by Gdaniec and Liberek revealed that the folded form is adopted by this symmetrical DKP.⁷⁵ On the other hand, considering the interactions between aromatic ring and amide bond, Kopple and Marr proposed a likely conformation for symmetrical DKPs in solution that each aromatic ring might associate with one amide group to render the two β -methylene moieties in identical environments without distinct shielding effects.⁷³ While it

might be possible that symmetrical DKPs have a different conformation in solution from that in the solid state, another explanation could be that a fast equilibrium exists between the two equivalent folded conformers for symmetrical DKPs at room temperature.⁷⁶ In contrast, the conformation of DKP **99** (or **96**) in our case might be locked due to the presence of the NMe group which forced the adjacent aromatic residue facing the DKP ring to avoid the potential steric clash.

During the synthesis, we did obtain the crystal structure of DKP **108** (Figure 2.6), a side-product due to the racemisation of tyrosine derivative in the *N*-methylation step with NaH and MeI.

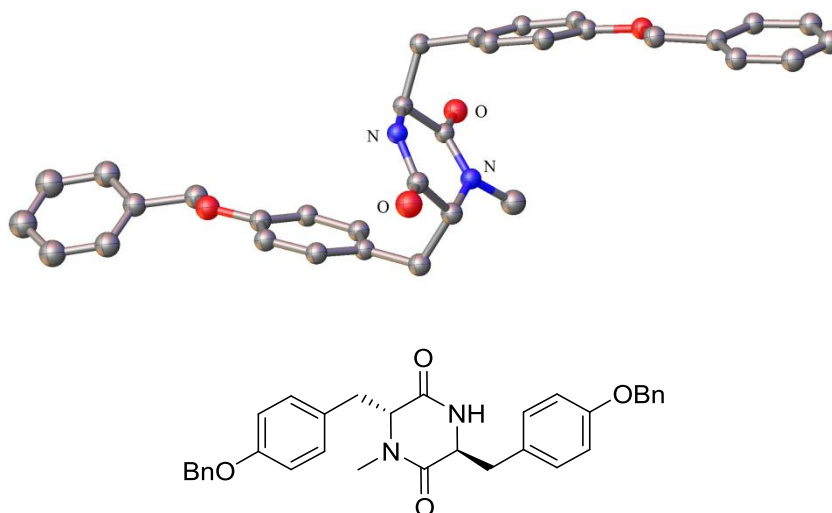


Figure 2.6: X-ray crystal structure of *trans*-DKP **108**.

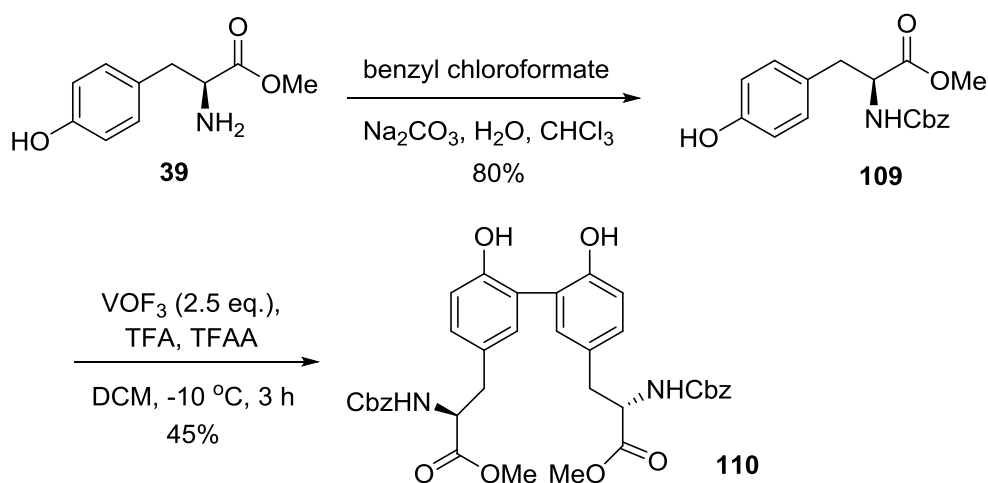
Even though this compound has a *trans*-configuration, it provides certain evidence about the potential interaction between aromatic rings and amide bonds, since both aromatic residues orientate to overlap with the 2,5-diketopiperazine ring.

2.3.2 Vanadium(V) Species as Coupling Oxidants

Model System: Formation of a Dityrosine Derivative

With several piperazine substrates in hand, the stage was set to investigate the intramolecular oxidative coupling, a key step in the biomimetic synthesis of herquiline A and B. Before attempting this approach with the real system, we performed a model reaction involving VOF₃-mediated oxidation of *N*-Cbz-L-tyrosine methyl ester **109** (Scheme 2.27). This intermolecular oxidative coupling reaction was first studied by Edwards and co-workers in 1990.⁷⁷

Substrate **109** was initially synthesised by vigorously stirring a mixture of tyrosine methyl ester **39**, benzyl chloroformate and Na₂CO₃ in CHCl₃/H₂O.⁷⁸



Scheme 2.27

Under the oxidative coupling conditions, dityrosine derivative **110** was successfully fashioned in a comparable yield to the one reported by Edwards and co-workers.

Intramolecular Oxidative Coupling of Piperazine Derivatives

With the success of reproducing the intermolecular phenol coupling of tyrosine derivative **109**, our attention was then turned to effecting the oxidative coupling in an intramolecular version. If the coupling reaction could occur, we presumed that the *ortho-ortho* coupling product should be the favourable one, rather than the *ortho-para* one which was predicted to be impossibly strained.

It is worthy of note that a large excess of TFA is usually needed when the substrate possesses an amino group, because the formation of the amine salt will reduce the oxidative tendency of the corresponding amine functionality.³⁶ Therefore the addition of TFA would play an important role in VOF₃-mediated phenolic couplings in our case since there is a tertiary amine moiety within the piperazine substrate.

The coupling reaction was initially performed with piperazine **106** (Entry 1, Table 2.1). Subjecting this bis-phenol substrate to the specific reaction conditions employed for the model reaction, there was still starting material in the reaction mixture after 3 h and no other distinct spot was observed by TLC. When the reaction mixture was warmed up slowly and maintained at room temperature, starting material was consumed gradually. However, the reaction gave no cyclised products detectable by mass spectrometry. According to the mass spectrum, peaks for traces of the corresponding dimeric compounds were observed, along with some undefined signals which might arise from decomposition of **106**.

In terms of the function of TFAA, it was pointed out by Dhingra and co-workers that a higher yield of coupling product was obtained in the presence of TFAA which could assure an anhydrous reaction medium.³⁸ Since anhydrous solvent was used in all of our vanadium-

mediated reactions, the oxidative coupling was also tested in the absence of TFAA (Entry 2, Table 2.1), but a similar result was obtained to Entry 1.

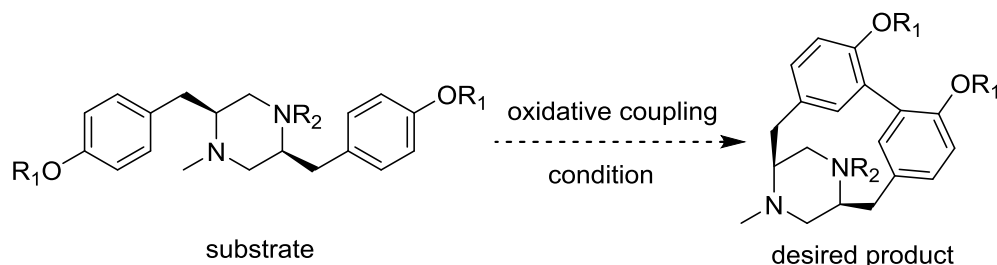


Table 2.1: Condition screening for phenolic oxidative coupling.

Entry	Substrate		Coupling conditions*	Reaction outcome
	R ₁	R ₂		
1 (106)	H	COCF ₃	VOF ₃ (2.5 eq.), TFA, TFAA, -10 °C to rt	Decomposition
2 (106)	H	COCF ₃	VOF ₃ (2.5 eq.), TFA, 0 °C to rt	Decomposition
3 (106)	H	COCF ₃	VOF ₃ (2.5 eq.), TFA, BF ₃ ·Et ₂ O, 0 °C	106 and partial decomposition
4 (106)	H	COCF ₃	VOCl ₃ (3.0 eq.), -10 °C to rt	106 and partial decomposition
5 (104)	Bn	COCF ₃	VOF ₃ (10.0 eq.), TFA, 0 °C to rt	104
6 (103)	Me	COCF ₃	VOF ₃ (10.0 eq.), TFA, 0 °C to rt	103

* All reactions were conducted in anhydrous dichloromethane.

We also tested the conditions with the addition of BF₃·Et₂O, which were employed in Evans' synthesis of a vancomycin segment as introduced in Section 2.2.2. Once again, no related cyclised products could be detected by mass spectrometry and part of the starting material was recovered (Entry 3, Table 2.1). The reaction of bis-phenol **106** with VOCl₃ mainly led to recycling of starting material with partial decomposition (Entry 4, Table 2.1).

Besides using bis-phenol substrate **106**, the oxidative coupling reactions were also attempted with phenol ether derivatives **104** and **103** (Entry 5 and 6, Table 2.1). Unfortunately, no reaction took place at room temperature with VOF_3 as the oxidant. When the systems were warmed up to reflux in DCM, side reactions occurred in both cases to give inseparable mixtures without producing any traces of the desired coupling products.

Based on our detailed experimentation, it was likely that the piperazine rings or the phenol groups within the substrates tended to decompose under the oxidation conditions we explored, even though an excess of TFA was added to convert the piperazine moieties into their amine salts. In most cases, vanadium oxidants played an undesired role in the decomposition of substrates and formation of intermolecular coupling products, other than effecting intramolecular phenolic coupling to generate the cyclised products.

In the cases of phenol ether oxidative coupling, while the poor results observed at high temperature (refluxing DCM) might be attributed to the vulnerability of the piperazine ring to VOF_3 , the inertness of the substrate to the oxidants at room temperature could be explained by the high oxidation potentials of aromatic rings. As discussed in Section 2.2.2, a cation radical generated from the aromatic ring might be involved in phenol ether oxidative coupling process. Therefore, the proneness of the phenol ether to oxidation would have a decisive role in the success of the coupling transformation. Referring to the literature, in most phenol ether coupling reactions, at least one of the two aromatic coupling partners bears two or more alkoxy groups besides an alkyl substituent. The existence of electron-donating groups would essentially reduce the oxidation potential of the whole aromatic ring. Since only one alkoxy group is possessed by each of the aromatic moiety in our substrates, the oxidation potential might not be low enough for the generation of the requisite cation radicals under the screened conditions.

Nevertheless, another possibility should not be ruled out entirely that the expected coupling products might be produced in some of the reactions. However, they might decompose *in situ* due to instability as one could imagine that the coupling products would represent a class of strained structures. With negative results being obtained from vanadium-mediated cyclisation, we then focused on hypervalent iodine species mediated oxidative couplings.

2.3.3 Hypervalent Iodine(III) Reagents as Coupling Oxidants

Hypervalent iodine agents are another class of versatile but mild oxidants, which have been used widely in intramolecular oxidative phenolic coupling reactions.

In our study, the attempted coupling reactions were carried out in non-nucleophilic solvents such as DCM, acetonitrile and 2,2,2-trifluoroethanol, with PIDA or PIFA as the oxidants. For bis-phenol substrates, one equivalent of oxidant was initially used, anticipating that one of the phenolic hydroxyl groups could coordinate to the positively charged iodine atom of the oxidant while the other phenol ring could act as a nucleophile to furnish the coupling product.

Following a similar procedure to the one employed by Kita and co-workers in Section 2.2.2, bis-phenol **105** was treated with PIDA in DCM at -40 °C (Entry 1, Table 2.2). However, no reaction was observed. When the reaction solution was warmed up to ambient temperature, starting material was still the main component that could be isolated. Subjecting the bis-phenol substrate to a slightly larger excess of PIDA did not change the situation. The reaction performed in MeCN followed a similar pattern (Entry 2, Table 2.2). When the reaction mixture was maintained at room temperature, the bis-phenol substrate was consumed slowly without any distinct production of new entities.

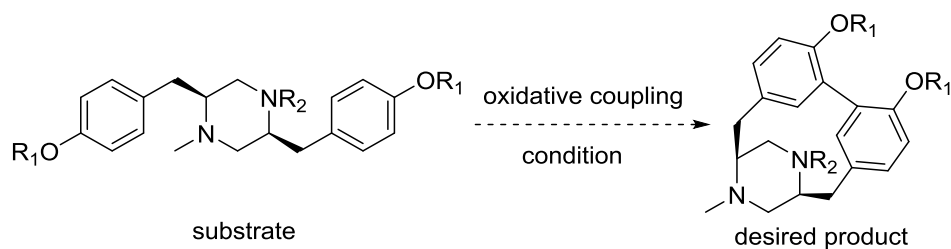


Table 2.2: Oxidative coupling conditions with PIDA or PIFA.

Entry	Substrate		Coupling conditions	Reaction outcome
	R ₁	R ₂		
1 (105)	H	Boc	PIDA, DCM, -40 °C to rt	105
2 (105)	H	Boc	PIDA, MeCN, -40 °C to rt	105 and partial decomposition
3 (105)	H	Boc	PIFA, CF ₃ CH ₂ OH, rt	105
4 (102)	Bn	Boc	PIFA, CF ₃ CH ₂ OH, rt	102
5 (102)	Bn	Boc	PIDA, MeCN, rt to 60 °C	Decomposition
6 (111)	Me	Me	PIFA, CF ₃ CH ₂ OH, rt	111
7 (101)	Me	Boc	PIDA, BF ₃ ·Et ₂ O, DCM, -40 °C to rt	101 at -40 °C; Boc cleavage at rt
8 (103)	Me	COCF ₃	PIDA, BF ₃ ·Et ₂ O, DCM, -40 °C to rt	103

Treating bis-phenol **105** with PIFA in trifluoroethanol mainly led to recovery of the piperazine starting material (Entry 3, Table 2.2). According to the mass spectrum, the existence of deprotected product without the Boc protecting group and the dienone products which derived from the nucleophilic addition of trifluoroethanol, were also identified.

The phenol ether substrate suffered similar fates to that of bis-phenol **105**. For example, both piperazine derivatives **102** and **111** resisted to the oxidation conditions (PIFA in CF₃CH₂OH) (Entry 4 and 6, Table 2.2). Decomposition was observed again when a solution of phenol

ether **102** and PIDA in MeCN was warmed to 60 °C, possibly due to oxidative reactions of the tertiary amine or phenol ether moieties (Entry 5, Table 2.2).

$\text{BF}_3 \cdot \text{Et}_2\text{O}$ has been reported to be an activator of PIDA or PIFA and the combination of the oxidant and $\text{BF}_3 \cdot \text{Et}_2\text{O}$ has been employed in several studies for successful phenol ether coupling reactions.³⁶⁻³⁸ This activating effect might arise from the coordination of BF_3 to the acetoxy or trifluoroacetoxy ligand, rendering the iodine centre more electropositive. Disappointingly, no coupling reactions were effected with our piperazine systems. Specifically, no transformation occurred with COCF_3 -protected piperazine **103** (Entry 8, Table 2.2). In the case of **101**, only removal of the Boc protecting group was observed (Entry 7, Table 2.2).

Since there is no general rule that can indicate the optimal oxidant for a specific coupling reaction and the success of oxidative phenol or phenol ether couplings reported in the literature usually based on extensive screening of different types of oxidising agents, we then turned our attention to other oxidative coupling methods.

2.3.4 Oxidative Coupling with Silver(I) Oxide, Fe(III) and Pb(IV) Reagents

Bis-phenol **106** was used as the substrate for Ag_2O -mediated coupling approach. Unfortunately, no reaction took place under the employed condition (Entry 1, Table 2.3). On the contrary, the phenol coupling reaction with $\text{Pb}(\text{OAc})_4$ as the oxidant led to complete decomposition of the starting material (Entry 2, Table 2.3).

FeCl_3 was also tested as the oxidant but no transformations were observed at ambient temperature. When the reaction system in DCM or MeOH was heated to reflux, slow

decomposition occurred to give an inseparable mixture, from which no new product could be defined according to the mass spectra (Entry 3, Table 2.3). In terms of phenol ether coupling, piperazine **104** was found to be inert to the FeCl_3 oxidation conditions and only starting material was recycled (Entry 4, Table 2.3).

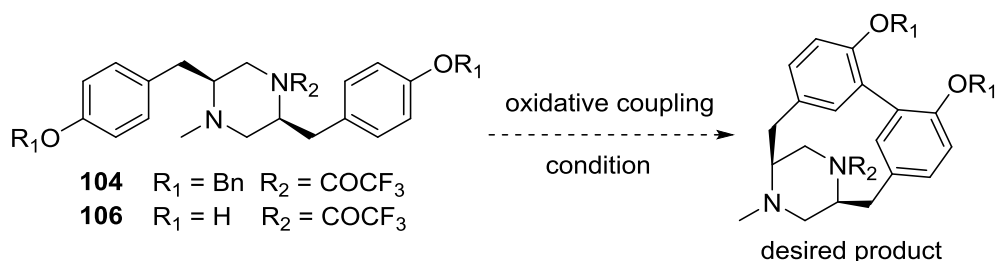


Table 2.3: Attempted oxidative coupling conditions.

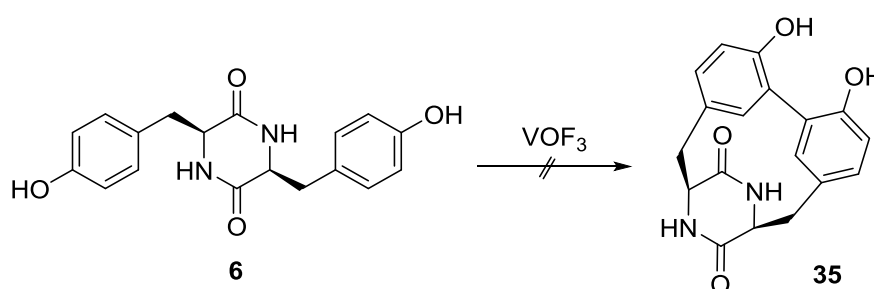
Entry & Substrate	Coupling conditions	Reaction outcome
1 (106)	Ag_2O (10.0 eq.), Et_3N , CHCl_3 , rt	106
2 (106)	$\text{Pb}(\text{OAc})_4$ (0.5 eq. to 1.0 eq.), $\text{BF}_3 \cdot \text{Et}_2\text{O}$, DCM, 0 °C	Decomposition
3 (106)	FeCl_3 (2.5 eq.), DCM or MeOH, rt to reflux	Decomposition
4 (104)	FeCl_3 (2.5 eq. to 5.0 eq.), DMF, rt or DCM, reflux	104

Overall, we were unable to identify any coupling products or related cyclised structures after extensive experimentation. To explain this, the mismatch between the oxidation potentials of the substrates and the redox potentials of the oxidants might be one reason. However, another possibility is worthy of consideration that the direct oxidative coupling reaction could be difficult, or even impossible to proceed with piperazine substrates.

Regarding the biosynthesis of herquiline A and B, the unsuccessful outcome of the biomimetic oxidative coupling at the piperazine oxidation state raises an interesting question of whether the oxidative phenol coupling takes place with piperazine intermediate as the substrate, or at

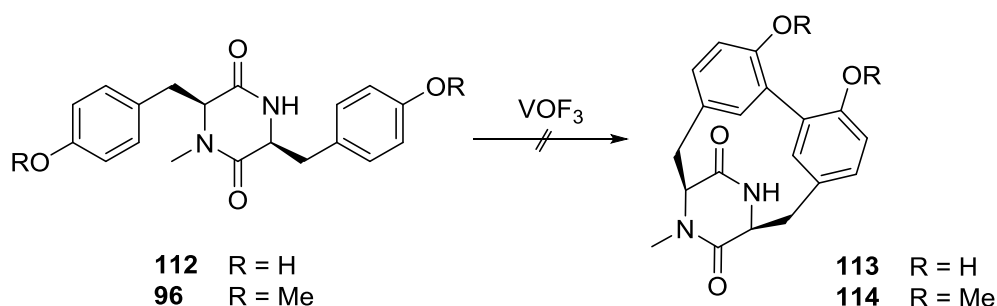
other stages, such as the diketopiperazine stage, since the DKP natural product mycocyclosin possessing the biphenol linkage has been isolated.

Actually, during the total synthesis of mycocyclosin by the Hutton research group, the direct oxidative coupling of diketopiperazine **6** was firstly attempted using VOF_3 as the oxidant.²³ Without success in generating the natural product **35**, only intermolecular coupling reactions occurred to give dimeric and trimeric products (Scheme 2.28).



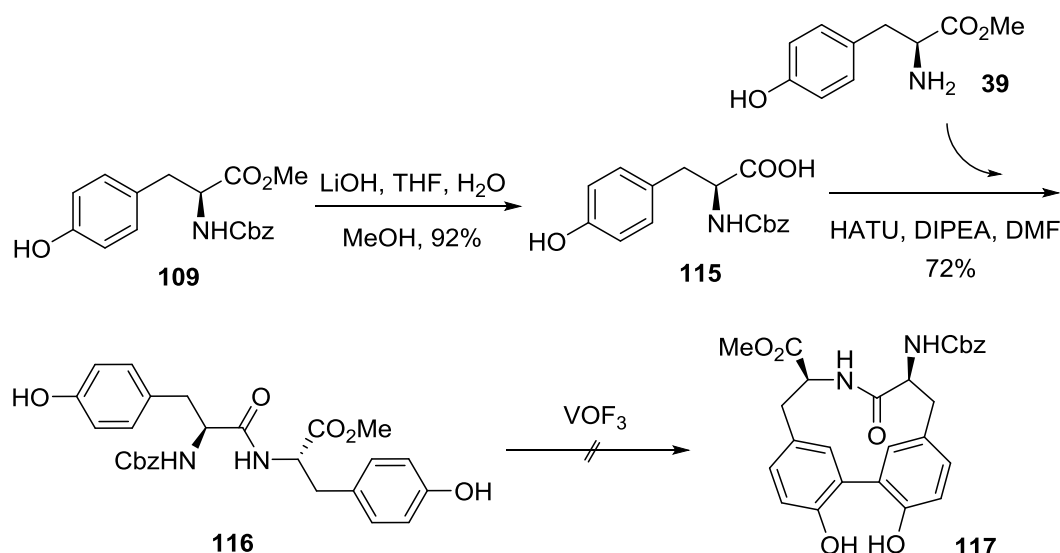
Scheme 2.28: Oxidative phenol coupling reaction attempted by Hutton and co-workers.²³

In our project, similar results were obtained from the oxidative coupling of DKP substrates (Scheme 2.29). The unsymmetrical bis-phenol **112** was initially afforded *via* the catalytic hydrogenolysis of **99**. On treating DKP **112** with VOF_3 , dimeric products were detected by mass spectrometry without the presence of the desired product **113**. In the case of phenol ether **96**, mainly starting material was isolated accompanied by debenzylated products.



Scheme 2.29

In addition, dipeptide **116** was also synthesised from the coupling reaction between acid **115** and amine **39**. When this bis-phenol was subjected to the VOF_3 oxidation conditions, decomposition occurred without any observation of intramolecular phenolic coupling to generate cyclic dipeptide derivative **117** (Scheme 2.30).

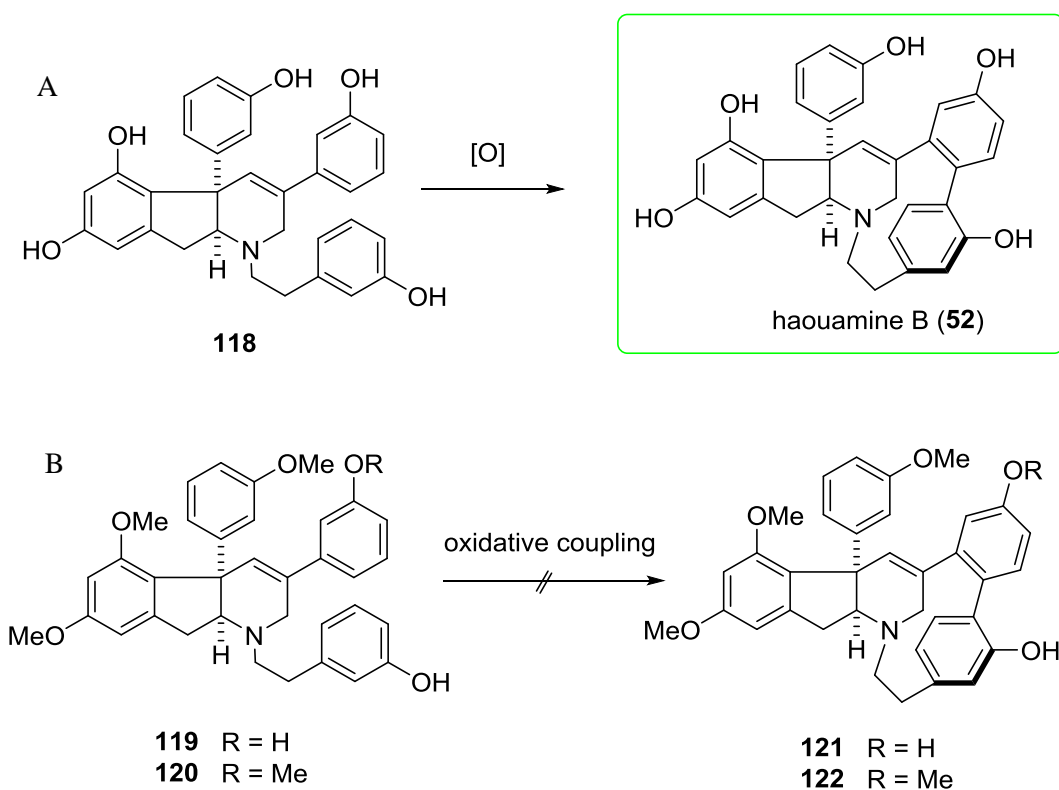


Scheme 2.30

While no success has been achieved in direct intramolecular oxidative couplings, it is plausible that under certain enzymatic assistance within the microorganism the piperazine substrate could adopt a favourable conformation for the formation of biphenol product.

Similarly, biphenyl or diphenyl ether linkages possessed by several natural products are proposed to derive from direct oxidative phenol coupling processes in Nature, but all the biomimetic approaches in the laboratory failed,^{33,79-81} such as the total synthesis of alkaloid haouamine B (**52**) reported by Trauner and co-workers in 2012.³³ The polyphenol intermediate **118** was proposed to be a possible biosynthetic precursor of haouamine B and could undergo a regio- and stereoselective oxidative phenolic coupling to afford the natural product in the producing organism (Scheme 2.31 A). Efforts were made to mimic this process

by subjecting substrates **119** or **120** to enzymatic conditions, anodic oxidation conditions or chemical oxidations with silver salts, hypervalent iodine reagents, vanadium oxyhalides as well as copper and iron reagents, but no desired coupling products were identified (Scheme 2.31 B). A different synthetic route was adopted finally.

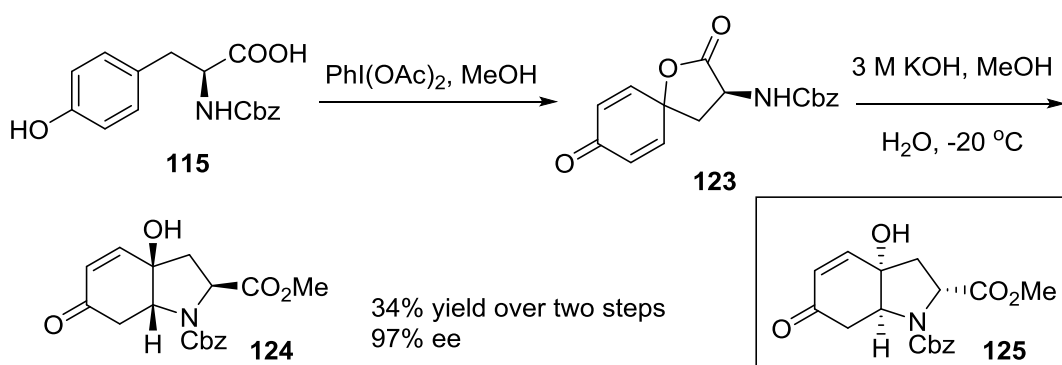


Scheme 2.31: (A) Proposed oxidative phenol coupling step in the biosynthesis of haouamine B. (B) Attempted biomimetic synthesis by Trauner and co-workers.³³

With the biomimetic approach towards herquiline A and B being precluded by difficulties in the direct oxidative coupling step, we resolved to employ several alternative aryl coupling strategies to fashion the desired biaryl sub-target.

2.4 Tricyclic Ring Formation *via* an Intramolecular *Aza*-Michael Addition Reaction

During the exploration of hypervalent iodine reagent-mediated phenol coupling reactions, our attention was attracted by an interesting transformation, that is, the oxidative dearomatisation of phenols.

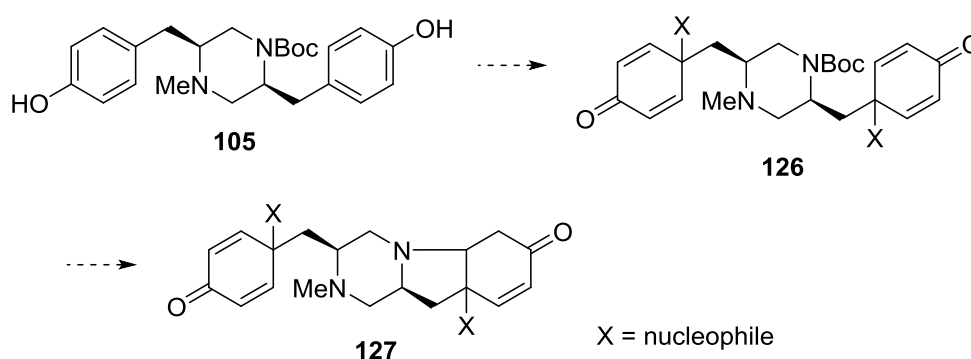


Scheme 2.32: $\text{PhI}(\text{OAc})_2$ -mediated transformations of tyrosine derivative reported by Wipf and co-workers.^{72,83}

It has been shown that phenols can react with hypervalent iodine species, such as PIDA or PIFA, to give cyclohexadienones in the presence of nucleophiles. As outlined in Scheme 2.32, Wipf and co-workers treated tyrosine derivative **115** with $\text{PhI}(\text{OAc})_2$ to obtain spiro lactone **123** with the carboxyl group acting as a nucleophile.^{72,83} Upon methanolysis, the lactone was cleaved and an intramolecular conjugate addition reaction took place to afford hydroxyhydroindole **124** in 34% overall yield with 97% ee due to the contamination from **125** which arose from partial racemisation likely occurring at the lactone stage prior to methanolysis. The diastereoselectivity for the formation of bicycle **124** might be due to the less steric interaction involved in the transition state of the cyclisation process.

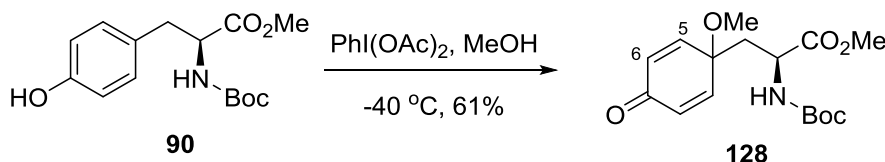
With bis-phenol piperazine **105** in hand, it was envisioned that oxidation of both phenol groups with $\text{PhI}(\text{OAc})_2$ in the presence of a nucleophile such as an alcohol or a halide anion, would afford bis-dienone intermediate **126** (Scheme 2.33). The formation of a tricyclic ring

system within **127** could then be rationalised by an intramolecular *aza*-Michael addition of the secondary amine to the adjacent dienone moiety upon removal of the Boc protecting group on the piperazine ring. It would be interesting to generate this tricycle since it shares a close structural resemblance to that in herquiline A.



Scheme 2.33: Proposed transformations of bis-phenol **105**.

Fascinated by this transformation, we carried out a model reaction with tyrosine methyl ester **90** (Scheme 2.34). Oxidation with $\text{PhI}(\text{OAc})_2$ in anhydrous methanol gave dienone **128** in 61% yield under optimised conditions. MeOH acted as the nucleophile in this case and no cyclisation was observed without the presence of a base, which was indicated by the presence of a doublet signal corresponding to the N–H at 5.21 ppm in the ^1H NMR spectrum, with a doublet at 6.83 ppm for vinyl protons H-5 and a multiplet at 6.40–6.35 ppm for H-6.

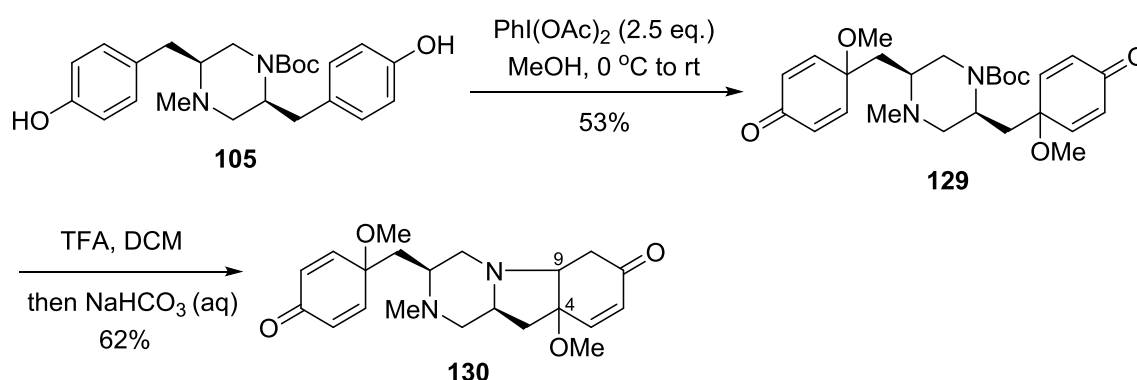


Scheme 2.34: Model reaction with tyrosine derivative.

The reaction was successfully applied to the bis-phenol system (Scheme 2.35). Subjecting piperazine derivative **105** to the oxidation conditions with a slight excess of $\text{PhI}(\text{OAc})_2$ in anhydrous methanol afforded bis-dienone **129** in 53% yield. Even though the yield was

moderate, possibly due to the side-reactions involving the tertiary amino group, it was gratifying to isolate a new product from the reaction mixture after treating piperazine **129** with TFA in DCM, followed by a basic work-up with NaHCO₃ aqueous solution.

At this stage, it was considered that the intramolecular conjugate addition should occur readily upon removal of the Boc protecting group in **129**. In terms of the regioselectivity of the *aza*-Michael reaction, it was envisaged that the addition of the secondary amine to the adjacent enone moiety to form the pyrrolidine ring within **130** should be the preferential pathway. And two diastereoisomers with H₉ and the adjacent methoxy group adopting a *cis*-configuration should be the most favourable products, because other structures would be too strained to form according to the constructed molecular models and relevant reported bicyclic structures.^{72,83}



The removal of the Boc protecting group was supported by the absence of a peak from *t*-butyl protons in the ¹H NMR spectrum. The occurrence of the *aza*-Michael addition was also confirmed by NMR spectroscopy that overall six vinylic protons from enone functionalities were identified. According to the mass spectrum, it showed a [M+H]⁺ peak at *m/z* 373.2130 (calculated: 373.2127), indicating a molecular formula C₂₁H₂₈N₂O₄ for the new entity obtained, which was in accord with structure **130**.

Actually, a small amount of another product was isolated from the reaction mixture. Although no NMR experiment was carried out due to the low material quantity, the corresponding mass spectrum revealed that this minor component had the same molecular formula to the main product and was presumed to be the other diastereoisomer generated from the intramolecular cyclisation reaction.

Since no structure could be found in the literature bearing close similarity to the tricyclic system in our product, it was difficult to gain any clue about the stereochemistry at C-4 and C-9 positions within piperazine **130** via NMR data comparison. Therefore, one-dimensional NOE experiments were performed to assist the assignment of the stereochemistry within **130** (Figure 2.7).

When the protons from one methoxy group (with chemical shift of 3.18 ppm) were irradiated, only interactions to vinyl protons were observed. We presumed that this methoxy group was possessed by the dienone ring. Upon saturation of the protons (H-10) from the other methoxy group (with chemical shift of 3.34 ppm), medium strength NOE interactions were observed to H₉, which indicated a *cis*-configuration between the methoxy group and H₉.

It seemed not obvious to differentiate between the two diastereoisomers **130a** and **130b** based on NOE experiments since no valuable stereochemical relationship between certain protons could be identified within the extended structures. However, one could argue that H-2 within **130b** should be close in space to H-9 or the methoxy group (H-10) and NOE enhancement would be detected accordingly if **130b** was the main product.

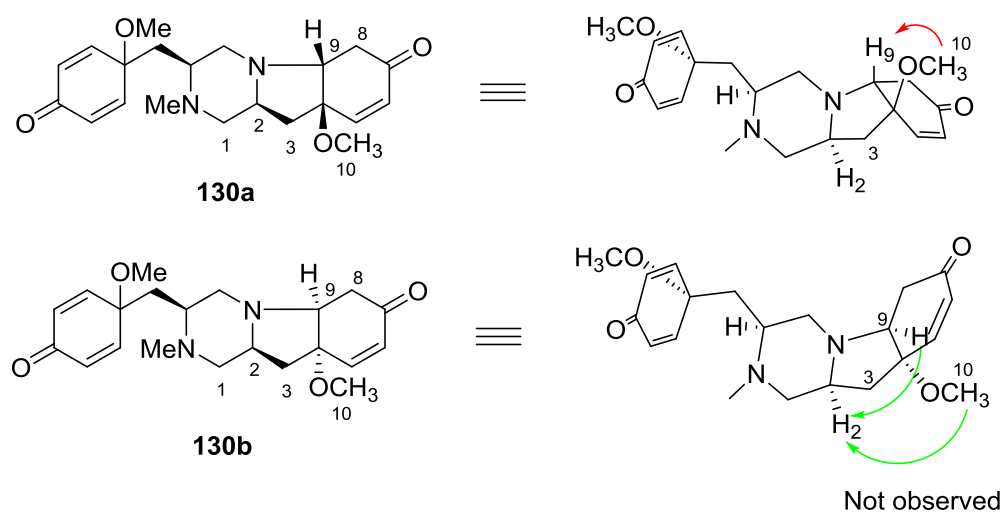
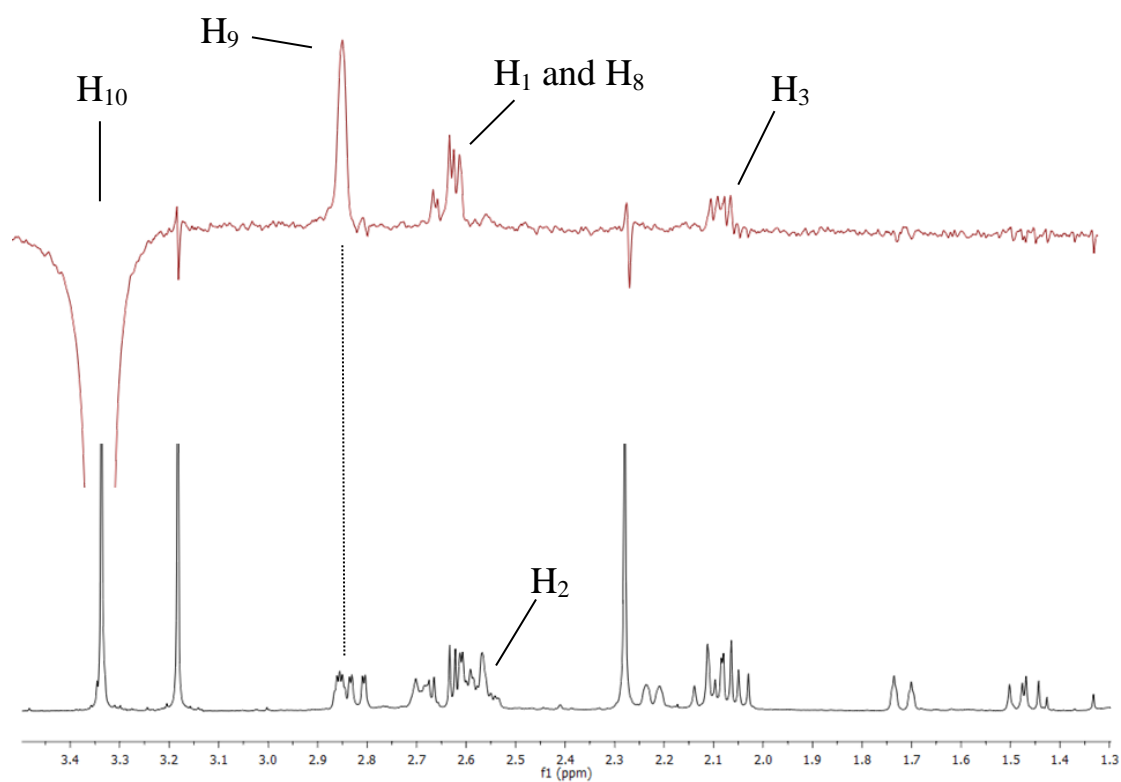
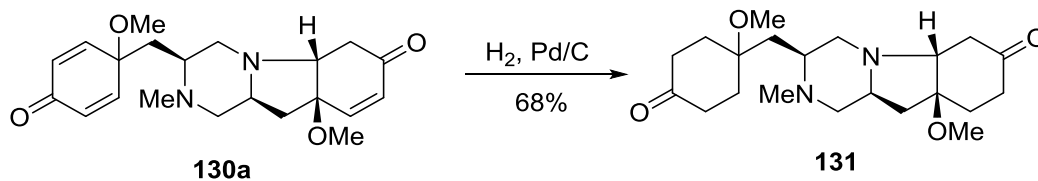


Figure 2.7

When either H-9 or the protons from the methoxy group (H-10) were irradiated, no NOE was observed to H-2. Therefore, it was presumed that **130a** was the main isomer that was generated from the intramolecular conjugate addition reaction.



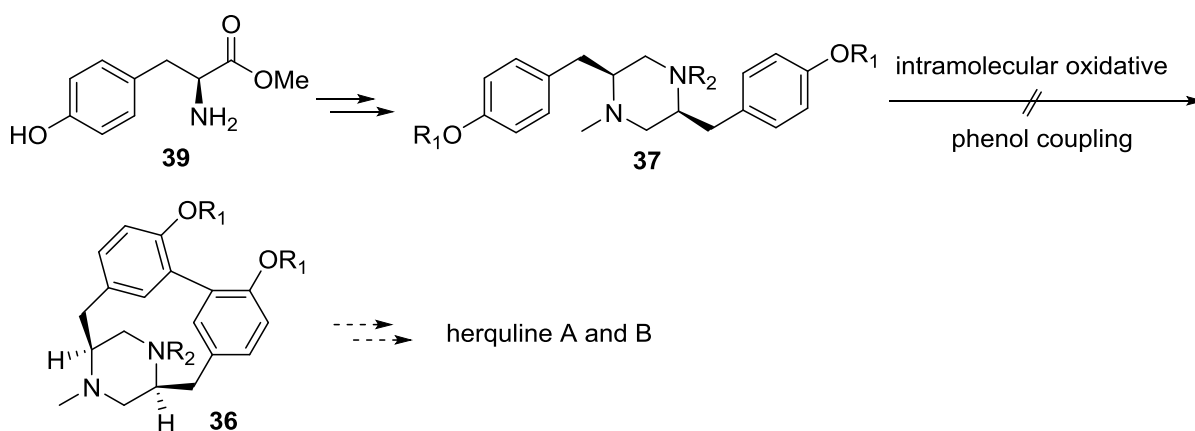
Scheme 2.36

Further global hydrogenation of **130a** delivered bis-ketone **131** in 68% yield (Scheme 2.36).

Piperazine **131** possesses a similar fused tricyclic ring system to that in herquiline A.

2.5 Summary

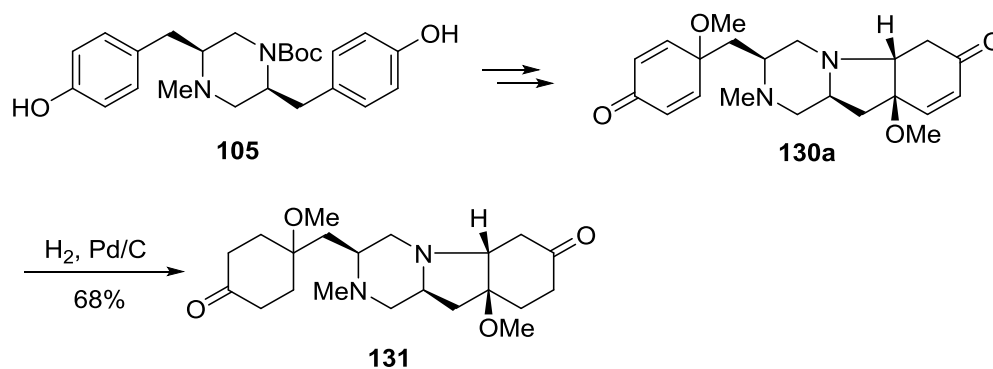
Inspired by the biosynthesis of the herquiline alkaloids, a biomimetic synthetic approach was explored in this Chapter.



Scheme 2.37

Having accomplished the synthesis of several piperazine intermediates from a tyrosine derivative, the intramolecular oxidative phenol or phenol ether coupling was attempted with a variety of oxidants including vanadium(V) species, hypervalent iodine reagents, FeCl_3 , Ag_2O and $\text{Pb}(\text{OAc})_4$. However, extensive experimentation failed to fashion the desired biaryl products.

Further investigation led to the synthesis of an advanced piperazine intermediate possessing a fused tricyclic ring system which consisted of piperazine, pyrrolidine and cyclohexanone moieties and showed close structural similarity to that in herquline A.



Scheme 2.38

Since the direct oxidative phenol coupling approach encountered difficulties in accessing the piperazine coupling products for further transformations towards herquline A and B, an alternative transition metal-mediated biaryl coupling strategy was employed and studied in detail in Chapter 3.

CHAPTER 3 TRANSITION METAL-MEDIATED ARYL COUPLING APPROACH TOWARD HERQULINE A AND B

Since no success had been achieved in the biomimetic synthesis of herquiline A and B, our focus was turned to the metal-mediated aryl coupling strategies. The primary consideration was based on the assumption that the two aromatic rings could be tethered together by certain metal species during the reaction processes. Presumably, this spatial proximity would facilitate the desired intramolecular C–C bond formation, which made this approach superior to the direct oxidative phenol coupling. Referring back to the literature, two types of efficient and well-established aryl coupling methods attracted our attention: the oxidative coupling of aryl cuprates and the palladium-catalysed aryl couplings, which are introduced herein.

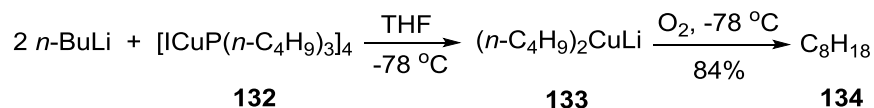
3.1 Oxidative Coupling of Organocuprates

3.1.1 Introduction

The oxidative coupling of the ligands in lithium organocuprates was observed as a common side reaction in organocopper chemistry and has been developed as a powerful tool for C–C bond formation.

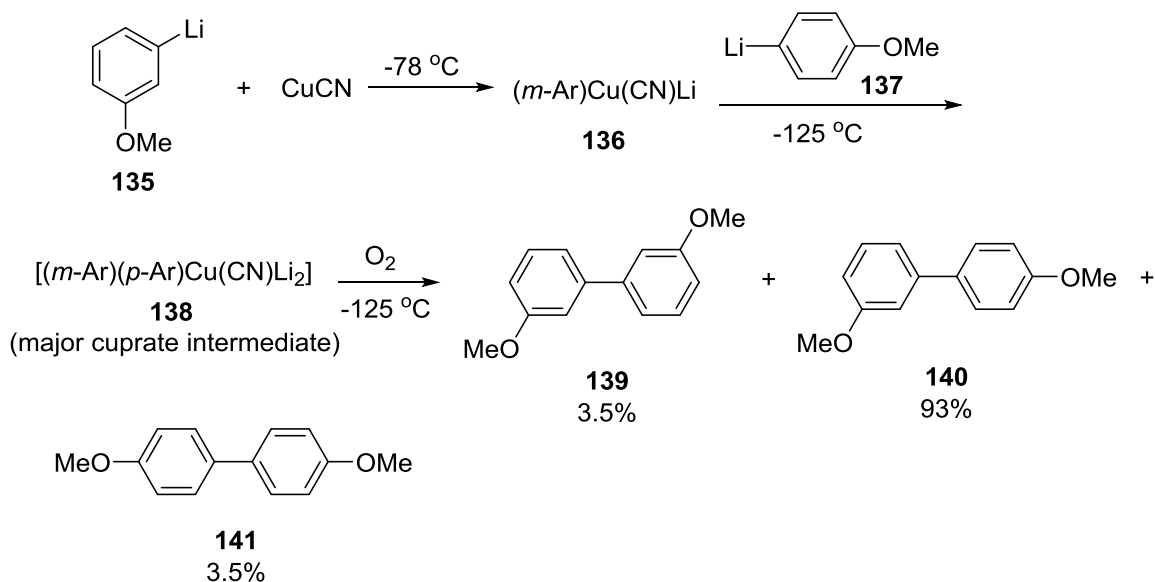
One of the earliest studies reported by Whitesides and co-workers focused on the oxidative coupling of cuprate complexes, such as **133** which was generated from the reaction between one equivalent of tetrakis[iodo(tri-*n*-butylphosphine)copper(I)] (**132**) and two equivalents of

organolithium reagent (Scheme 3.1).⁸⁴ They found that similar homo-coupling reactions could occur with organocuprates bearing vinyl, aryl, primary or secondary alkyl groups.



Scheme 3.1

While statistical ratios of products were usually obtained in terms of the oxidative coupling of heteroleptic cuprates, Lipshutz and co-workers revealed a new route to unsymmetrical biaryl products *via* the formation of the corresponding kinetic higher order cyanocuprates.⁸⁵ Specifically, by controlling the reaction temperature and the formation mode of the organocuprates, high levels of unsymmetrical ligands couplings were achieved. As shown in Scheme 3.2, the kinetic cuprate **138** was generated preferentially under properly controlled conditions.



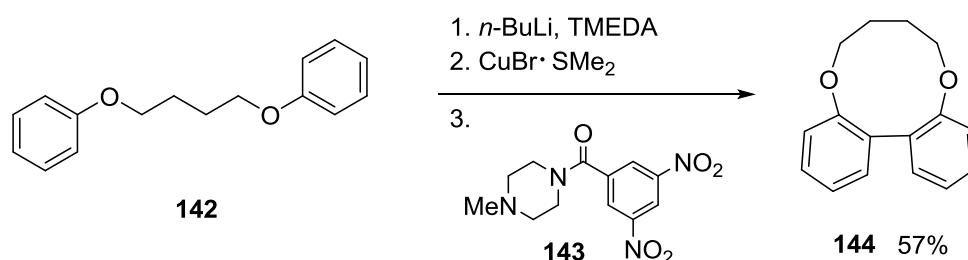
Scheme 3.2

It was noted that the ratio of hetero-coupling product **140** dropped to 50% when the reaction mixture with organocuprate **138** was warmed up to $-75\text{ }^\circ\text{C}$ for a few minutes prior to oxidation

at -125 °C, indicative of the equilibrium between **138** and other homoleptic cuprates at higher temperature.

The application of oxidative organocuprate coupling to intramolecular C–C biaryl bond formation makes this methodology more attractive. A wide diversity of biaryl-containing structures with medium rings has been constructed with this method.

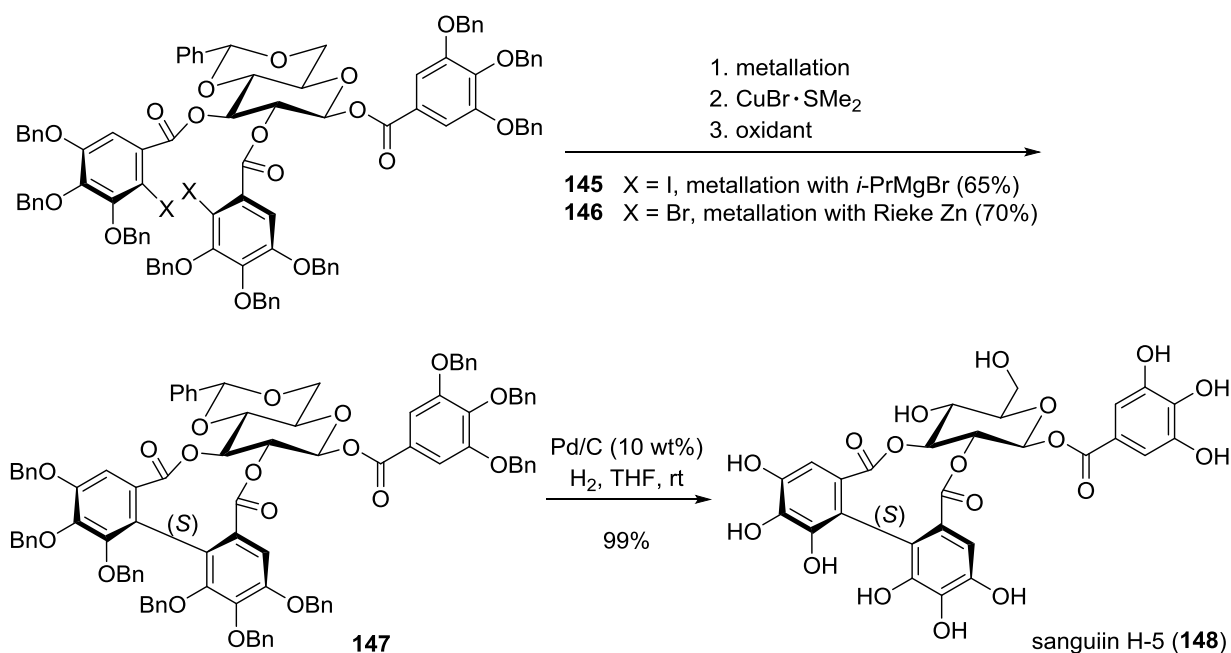
Scheme 3.3 demonstrated an example reported by Spring and co-workers.⁸⁶ Biaryl product **144** with a 10-membered ring was synthesised following a sequence consisting of the direct double lithiation of bis-phenol ether **142**, intramolecular cuprate formation and subsequent oxidative coupling using oxidant **143**. This cyclised product was fashioned from simple linear substrate **142** in 57% yield.



Scheme 3.3

An atropdiastereoselective oxidative biarylcuprate coupling was employed by Spring and co-workers as the key step in their total synthesis of sanguin H-5 (**148**),⁸⁷ a plant polyphenol natural product belonging to the ellagitannin class. As shown in Scheme 3.4, the benzyl-protected biaryl intermediate **147** was afforded in 65% yield after treating iodide **145** with isopropylmagnesium chloride, followed by transmetalation with copper(I) bromide dimethyl sulfide complex and oxidation with dinitroamide **143**. Alternatively, initial metallation could be fashioned by treatment of bromide **146** with Rieke zinc. Transmetalation and subsequent intramolecular cuprate oxidation gave access to sanguin H-5 precursor **147** in an optimised

70% yield. Both reactions gave rise to the specific (*S*)-atropisomer, which was attributed to the structural restraint imposed by the galloylated sugar ring according to Spring and co-workers' analysis. Hydrogenolytic global deprotection of **147** completed the total synthesis to afford the natural product in quantitative yield. The success of the oxidative coupling reaction in the presence of three ester groups revealed the high functional group tolerance of this transformation.

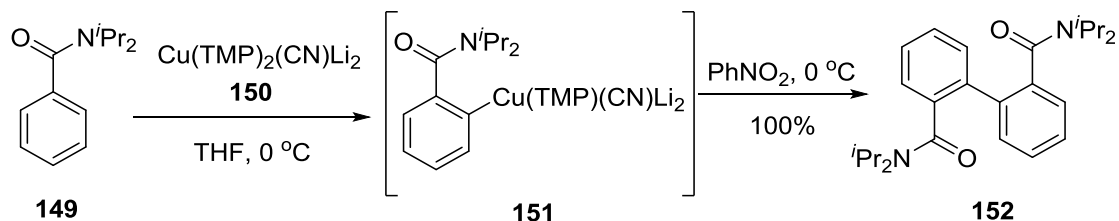


Scheme 3.4

Besides the two-step sequence mentioned above involving aryllithium formation and transmetallation for the generation of arylcuprates, another potential route is *via* the direct deprotonative cupration of functionalised aromatics.

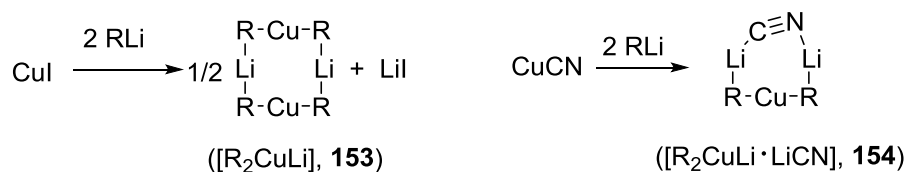
In 2007, Wheatley, Uchiyama and co-workers reported a diversity of chemical transformations that could be realised with functionalised phenyl cuprate intermediates, such as aryl cuprate **151** which was initially generated from the direct *ortho* cupration of amide **149** with Lipshutz-type amidocuprate **150** (Scheme 3.5).⁸⁸ Interestingly, homo-coupling product

152 was produced in quantitative yield upon oxidation of cuprate intermediate **151** with nitrobenzene, indicating this protocol as a potential aryl coupling method.



Scheme 3.5

It has been reported that the Gilman and the Lipshutz cuprates are two dominant types of structures in organocuprate(I) chemistry and that cuprates of the latter type show higher reactivity in most cases including direct *ortho* metallation.⁸⁹



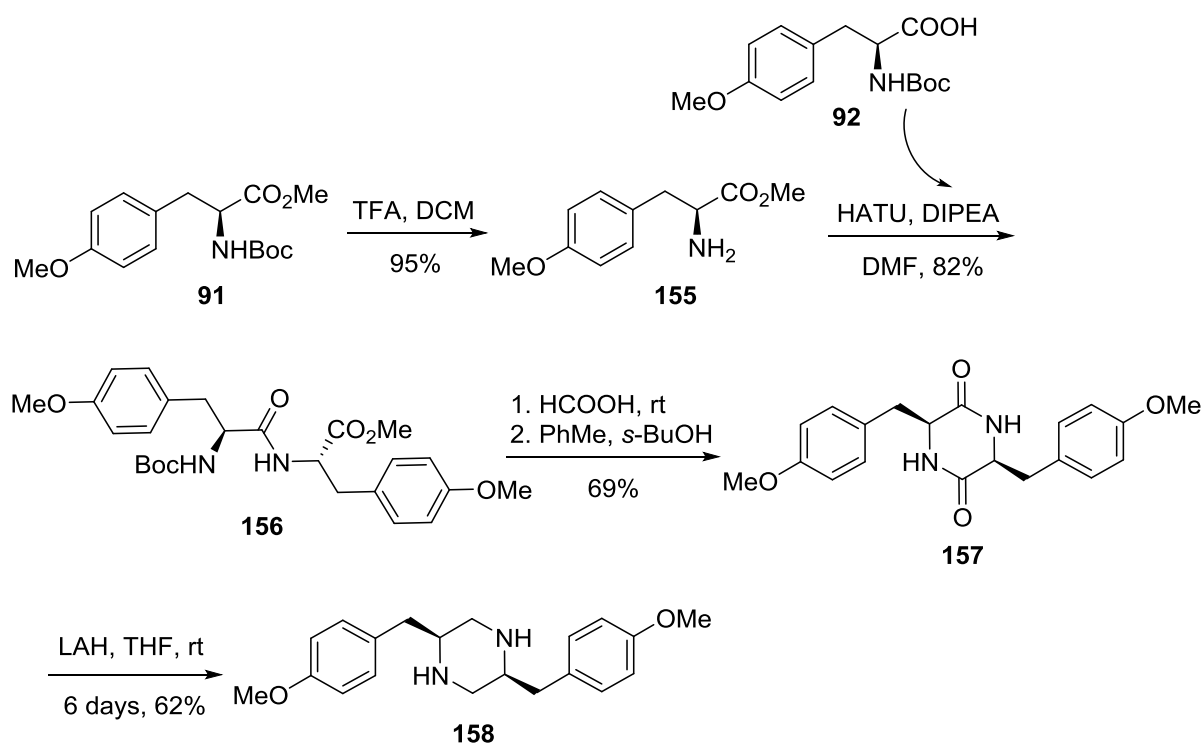
Scheme 3.6

The generation of either type of cuprate depends largely on preparation methods and reaction conditions. While the Gilman-type cuprates have homodimeric structures, such as **153** in Scheme 3.6, heteroaggregate structures are usually exhibited by the Lipshutz-type species in the presence of halides or *pseudo*-halides, as exemplified by **154**.⁹⁰ The higher order cyanocuprate formed in Scheme 3.2 was presumed to be the Lipshutz-type.

3.1.2 Synthesis and Conformational Analysis of Piperazine Derivatives

In order to simplify the NMR spectra of the piperazine substrates and the potential coupling products, symmetrical piperazine derivatives were synthesised initially.

The manipulation followed a similar route to the synthesis of the unsymmetrical piperazines (Scheme 3.7). The coupling reaction between acid **92** and amine **155** which was obtained from the deprotection of **91** with TFA gave rise to dipeptide **156**. After removal of the Boc protecting group, the resulting dipeptide intermediate was subjected to a thermal cyclisation step in toluene and *s*-BuOH to deliver DKP **157** in 69% yield.

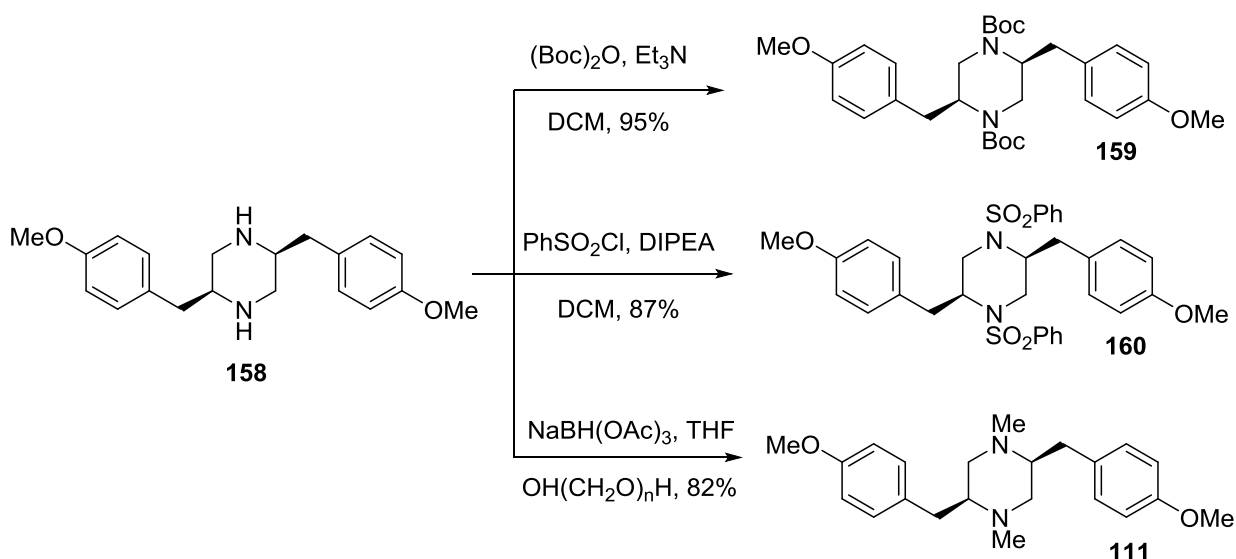


Scheme 3.7

Reduction using LAH was applied to the newly formed DKP **157**. However, the reaction was relatively slow at room temperature and a considerable amount of partially reduced intermediate was isolated with the same reaction time as previously employed. This

retardation might be due to solubility issues since this symmetrical DKP which was isolated as a solid has a poorer solubility in THF than unsymmetrical DKP **96** with an NMe group. When the reaction mixture was warmed up, a degree of isomerisation was observed. Therefore the original reduction conditions were adopted to perform the reaction at room temperature but with a longer reaction time.

Piperazine **158** was further protected with Boc or benzenesulfonyl groups to give **159** or **160**, respectively. The *N, N'*-dimethylpiperazine derivative **111** was also formed by reductive amination with paraformaldehyde and sodium triacetoxyborohydride, as depicted in Scheme 3.8.



Scheme 3.8

Before moving on to test the intramolecular coupling reactions with several different functionalised piperazines, it would be helpful to investigate the conformation of these structures, since the arrangement of the two aromatic residues in these piperazine substrates was conceived to have a substantial influence on the intramolecular coupling reactions.

It is known that in substituted piperazine or piperidine amides, the substituent at the vicinal position to the amide group prefers to reside in the axial position of the corresponding chair conformation due to the *pseudo* allylic strain between the bulky substituent and the essentially planar amide functionality. This phenomenon is exemplified by piperazine **102** in our synthesis. As demonstrated by the X-ray crystal structure of this piperazine that is shown in Figure 3.1, while the piperazine ring still adopts a normal chair conformation, the side chain adjacent to the *tert*-butyl carbamate moiety is forced to present in the axial position due to the potential A^{1,3} strain.

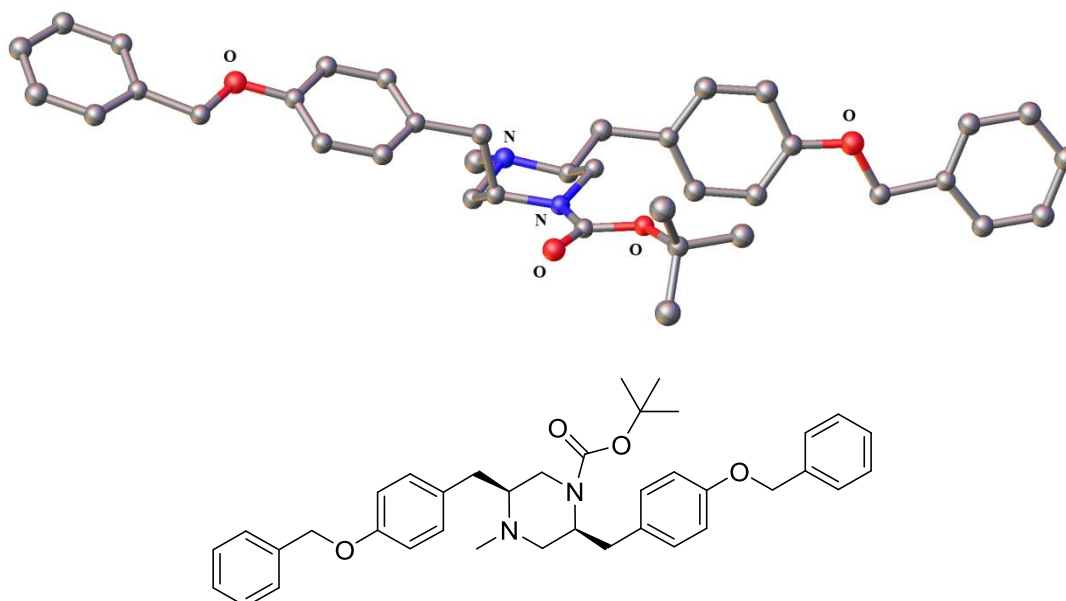


Figure 3.1: Crystal structure of **102**.

Inspired by this conformational behaviour of piperazine derivatives, it was presumed that the presence of two amide groups in our *cis*-2,5-disubstituted piperazine derivatives would not only result in biased orientations of substituents, but could also affect profoundly the conformations of piperazine rings. Specifically, if the methyl group within **102** was replaced by another Boc protecting group, the side chain adjacent to it would not be able to lie in the

equatorial position due to steric interaction. Instead, a low-energy conformation would be adopted by the piperazine ring with rearranged side chain orientations.

Ideally, a boat-like conformation with both substituents (R_1) in *pseudo*-axial positions would be possible, such as the boat form (A), (B) or (C) in Figure 3.2, which was also assumed to be beneficial for the intramolecular aryl coupling strategy. Since the two aromatic rings were proposed to be joined together by a metal species during the coupling reaction, the two side chains (R_1) within the boat conformation seemed to be close enough to each other to facilitate this process.

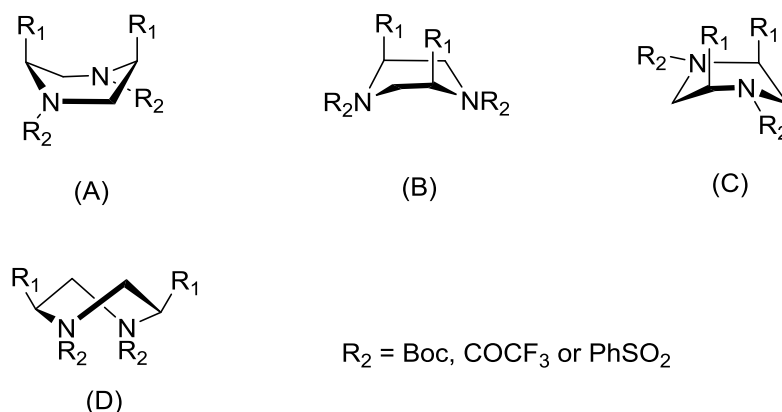


Figure 3.2: Possible conformations of bis-sulfonamide, bis-amide and bis-carbamate.

The ^1H NMR spectra were analysed in order to obtain sufficient evidence on the conformation of these piperazine substrates. In the case of piperazine **160**, it revealed that the vicinal coupling constants between the ring protons H_a and $H_b/H_{b'}$ were J_{ab} 4.8 Hz and $J_{ab'}$ 6.0 Hz respectively (Figure 3.3 (A)), which indicated that the molecule could not adopt a normal chair conformation. Since the *cis* coupling between H_a and H_b from Form (B) in Figure 3.2 was considered to be larger than the observed magnitude, piperazine **160** might adopt the boat form (A) or (C) in solution. The analysis was subsequently supported by the X-ray crystal structure of **160** (Figure 3.3 (B)). In the solid state the piperazine ring exists in the boat form

(C) in which the torsion angle of N–C–C–N is around 50° . The dihedral angles between H_a and $H_b/H_{b'}$ are 69° and 51° respectively in the solid state, which is in agreement with the corresponding coupling constants.

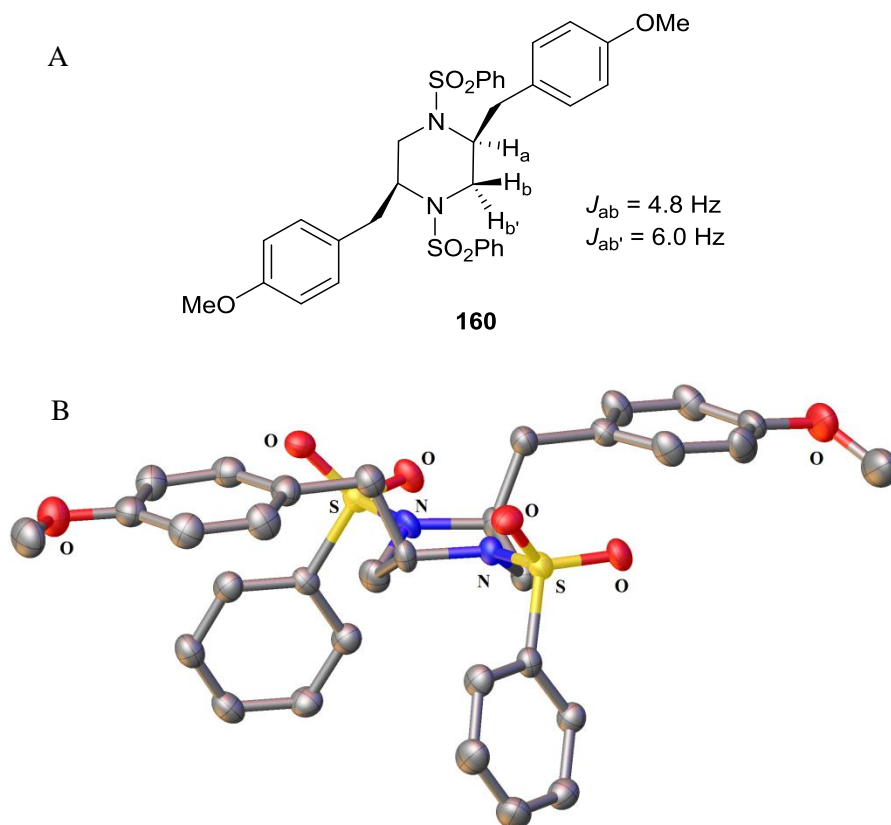


Figure 3.3: (A) Vicinal coupling constants between the protons on the piperazine ring of **160** (CDCl_3 , 400 MHz). (B) X-ray crystal structure of **160**.

It was noted that the NMR data of **160** showed strong temperature dependence. When the NMR experiments were conducted with $\text{DMSO-}d_6$ as the solvent, the signals from the two diastereotopic geminal protons H_b and $H_{b'}$ on the piperazine ring coalesced as the temperature was raised and emerged accidentally as one set of resonances at 90°C , indicating a fast equilibrium between different conformers.

In contrast, the coupling constants between protons H_a and $H_b/H_{b'}$ were observed as $J_{ab'}$ 5.2 Hz and J_{ab} 12.4 Hz respectively for piperazine **161** (Figure 3.4). According to the studies in the

literature, the *N, N'*-diacyl-protected *cis*-2,5-disubstituted piperazines tend to adopt a twist boat conformation such as the form (D) in Figure 3.2, which has been confirmed by relevant crystal structures.⁹¹ For the twist-boat conformation, the published coupling constants between H_a and H_b/H_{b'} from related compounds were around 11 Hz and 7 Hz,⁹² which were slightly different from those observed for piperazine **161**. Potentially the *N*-trifluoroacetyl-protected piperazine **161** and the Boc-protected piperazines could exist as equilibrium mixtures of different conformers in solution at room temperature, such as form (B) and (D) in Figure 3.2.

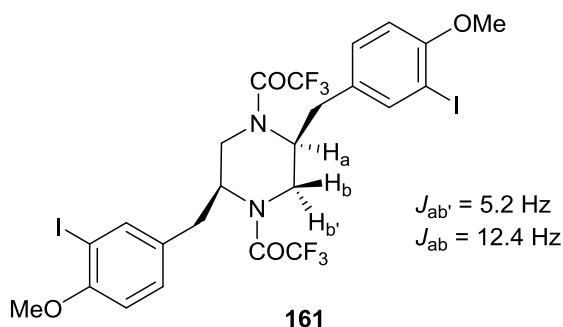


Figure 3.4: Vicinal coupling constants between the protons on the piperazine ring of **161** (CDCl₃, 400 MHz).

Based on the above analysis, a substantial proportion of boat conformers exist in solution for bis-amide structures such as **159**, **160** and **161**, in which the two side chains on the piperazine rings could reside in the *pseudo*-axial positions and be close in space (Figure 3.5).

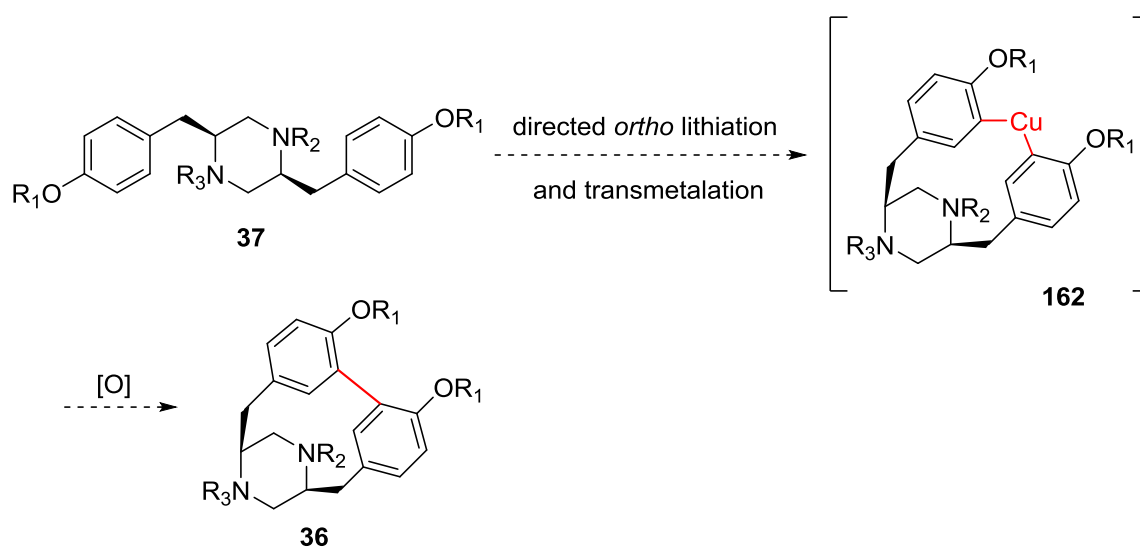


Figure 3.5

Therefore, structures like **159**, **160** and **161** were envisaged to be superior substrates for intramolecular aryl coupling reactions compared with **101** and **111**, which exist in normal chair conformations in solution at room temperature.

3.1.3 Attempted Intramolecular Oxidative Coupling of Diarylcuprates

As demonstrated in Section 3.1.1, the organocuprate involved in the oxidative coupling could be accessed through several different approaches. The method of direct lithiation followed by transmetalation seemed to be the most straightforward and reasonable sequence for our system because no pre-halogenation of piperazine substrates was required (Scheme 3.9).



Scheme 3.9

In addition, it was envisioned that the copper species would serve as a template to tether the two aromatic rings together during the transmetalation process to give a cyclic cuprate **162**. This reduced flexibility of the metal-bridged intermediate should be beneficial for the subsequent oxidative coupling reaction.

Attempts started from the double lithiation of piperazine substrates **159**, with methoxy functionalities as the directing metalation groups. Since TMEDA is a commonly used additive to essentially break down the alkyllithium aggregates, hence increasing their basicity and effectively accelerating the reaction rate,^{93,94} this bidentate ligand was employed in all of our direct lithiation reactions.

Initial treatment of piperazine **159** with *n*-butyllithium at -20 °C or 0 °C, followed by quenching with TMSCl gave no product, with only starting material being recovered (Entry 1 and 2, Table 3.1). Since the substrate possessed two *tert*-butyl carbamate moieties which could coordinate with butyllithium, we proposed that an excess of lithium base might be required. Increasing the amount of lithium base seemed to be beneficial since a small amount of piperazine **163** which derived from mono-lithiation was isolated, but the conversion of **159** was still low (Entry 3, Table 3.1).

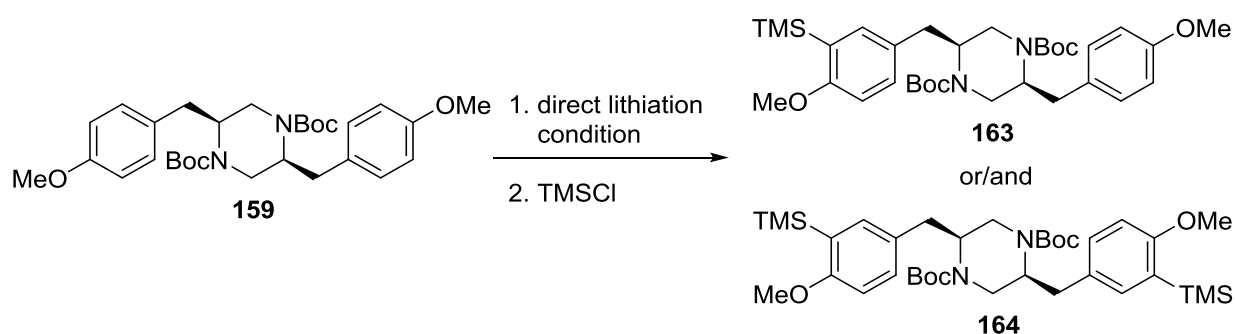


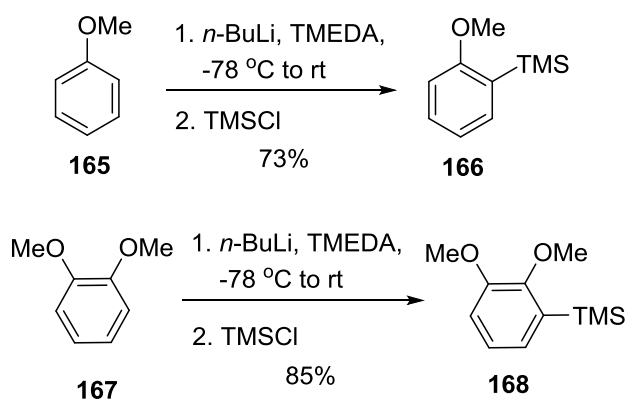
Table 3.1

Entry	Lithiation conditions*	Reaction time with TMSCl	Reaction outcome
1	<i>n</i> -BuLi (2.2 eq.), THF, -78 °C to -20 °C	30 min at -78 °C; 5 h at -20 °C	159
2	<i>n</i> -BuLi (2.2 eq.), THF, -78 °C to 0 °C	15 min at -78 °C; 3 h at 0 °C	159
3	<i>n</i> -BuLi (4.0 eq.), THF, -78 °C to 0 °C	15 min at -78 °C; 3 h at 0 °C	159 and 163 (12%)
4	<i>n</i> -BuLi (4.0 eq.), THF, -78 °C to rt	15 min at -78 °C; 3 h at rt	159 , 163 (15%) and 164 (9%)
5	<i>n</i> -BuLi (3.0 eq.), Et ₂ O, -78 °C to rt	15 min at -78 °C; 2 h at rt	159 , 163 (18%), 164 (13%) and by-products

*Equal moles of TMEDA and *n*-BuLi were used.

It was conceived that temperature should be a decisive parameter for this process. Referring to previous studies in the literature, direct lithiation of alkyl anisoles with *n*-butyllithium was usually performed at room temperature,^{86,95} such as the reaction shown in Scheme 3.3 in Section 3.1.1. In our case, the double lithiation of bis-anisole derivative **159** should be more challenging.

At this stage, two model reactions were carried out with anisole and 1,2-dimethoxybenzene (Scheme 3.10). For both reactions, good results were obtained when the substrates were treated with *n*-butyllithium at room temperature before trapping the aryllithium species with TMSCl. Decreasing the temperature of the lithiation process resulted in lower yields in both cases.

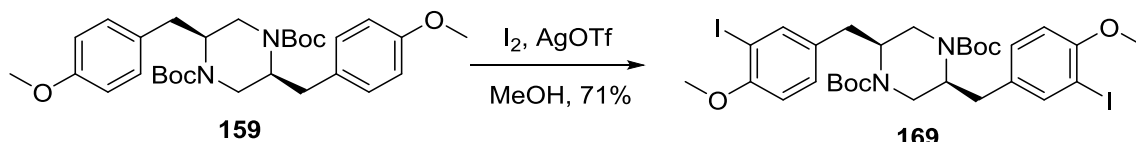


Scheme 3.10

Accordingly, conducting the lithiation reaction at room temperature for the piperazine system, mainly starting material and mono-silylated product **163** were isolated, accompanied by the desired product **164** only as a minor component (Entry 4, Table 3.1). A similar result was obtained when the reaction was performed in diethyl ether (Entry 5, Table 3.1). Extending the reaction time or increasing the temperature led to side-reactions, giving several irrelevant products according to the mass spectra. Considering that the methoxy moiety is only a

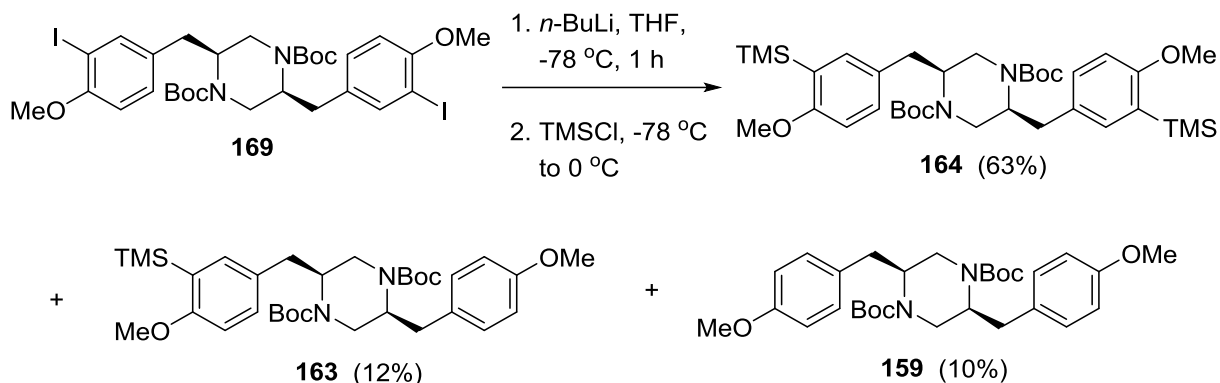
moderate metalation directing group, deprotonation at the benzylic position or side-reactions from the Boc-protected piperazine ring might be competing processes during the *ortho*-metalation of **159** above room temperature.⁹⁶

Without fashioning an efficient double lithiation, we resolved to adopt the lithium-halogen exchange strategy, hoping the dilithio species could be generated readily from halogenated piperazine substrates. For this alternative protocol, iodinated or brominated piperazines would be the ideal substrates. Scrutinising the synthetic sequence, any substrates bearing aryl halide functionalities prior to the DKP reduction step would face the risk of losing halogen atoms upon treatment with LAH. Therefore, the direct halogenation of piperazine **159** seemed to be a potential solution to the synthesis of piperazine substrates for the lithium-halogen exchange approach. Fortunately, treating piperazine **159** with iodine and silver triflate in methanol gave the desired bis-iodide **169** in 71% yield, accompanied by a small amount of mono-iodinated product which could be removed by careful column chromatography (Scheme 3.11).



Scheme 3.11

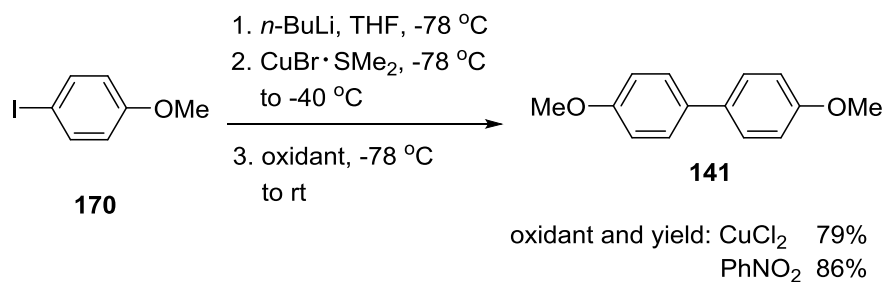
With piperazine **169** in hand, the efficacy of lithium-iodine exchange was initially studied. The aryllithium species generated under various conditions were trapped with TMSCl for further analysis. Extensive experimentation led to the optimal conditions for the current piperazine system, as shown in Scheme 3.12.



Scheme 3.12

Efforts were made to improve the yield of **164** by using TMSOTf as the electrophile or warming up the silylation reaction system to room temperature, but a considerable amount of by-products were obtained, due to the removal of the Boc protecting group and other side reactions. Treating piperazine **169** with *n*-BuLi at a higher temperature gave a similar result to the one shown in Scheme 3.12. Even though increasing the amount of butyllithium (from 2.2 eq. to 3.0 eq.) resulted in a slightly higher isolation yield of **164**, this modification was not employed in the subsequent experiments. It appeared that the Li-I exchange process was complete under the optimised condition (2.2 eq. of *n*-BuLi) since no iodine atom presented in any of the products isolated from the reaction mixture. Theoretically, two equivalents of butyllithium would be the ideal amount of base for double lithium-iodine exchange and be beneficial for the subsequent oxidative cuprate coupling process, because excess *n*-BuLi would inevitably compete with the newly generated aryllithium in the cuprate formation step.

Before progressing towards the intramolecular oxidative cuprate coupling, model reactions were conducted with 4-iodoanisole (Scheme 3.13). On treating iodoanisole with *n*-BuLi, followed by transmetalation in the presence of copper(I) bromide dimethyl sulfide complex, the generated diaryl cuprate was oxidised with either CuCl₂ or nitrobenzene to give 4,4'-dimethoxybiphenyl **141** in high yield.



Scheme 3.13

For the piperazine system, a similar procedure for Li-I exchange was used as discussed above. In the literature, the conditions for transmetallation varied depending largely on the substrates. Therefore, our elaboration commenced from screening the optimal cuprate formation conditions as shown in Table 3.2, with nitrobenzene as the oxidant since it gave impressive results with the model system.

Initial treatment of the bis-aryllithium intermediate generated from **169** with copper(I) bromide dimethylsulfide at -78 °C under N₂, followed by oxidation resulted in complete deiodination (Entry 1, Table 3.2), possibly due to the failure of cupration. With a higher temperature for transmetallation (-40 °C), the reactions gave two new products which were found to be oxygenated products **174** and **175**, accompanied by a small amount of deiodinated product **159** (Entry 2, Table 3.2). Further increasing the temperature to -20 °C or 0 °C led to a lower combined yield of the three products (Entry 3, Table 3.2). It seemed that maintaining the transmetallation reaction system at -40 °C was more efficient for the hydroxylation process. When CuCN was employed as the Cu(I) source, a comparable result was obtained without any detection of coupling product by mass spectrometry (Entry 4, Table 3.2).

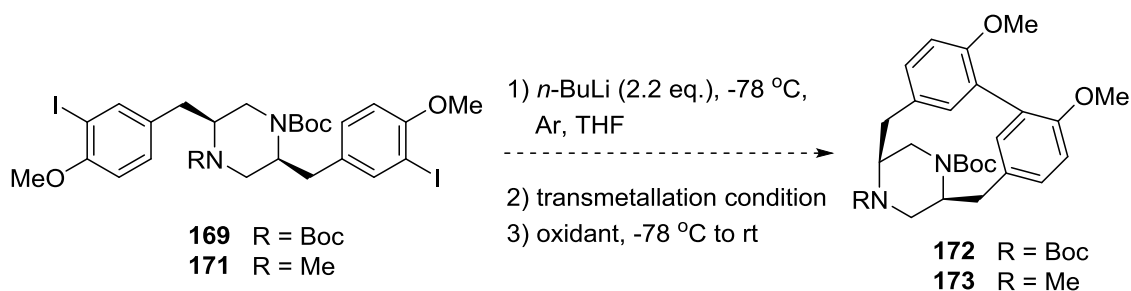
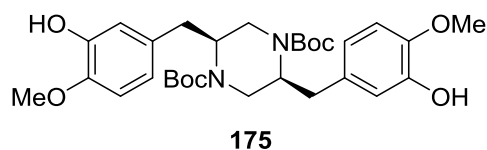
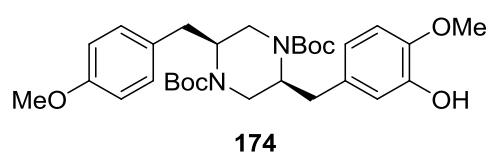
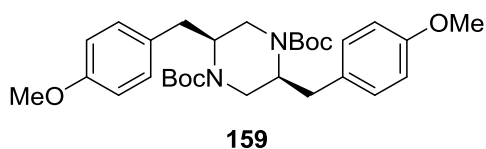


Table 3.2: Cuprate formation (transmetallation) and oxidation conditions.

Entry (& substrate)	Cu(I) reagent*	Transmetallation conditions	Oxidant	Reaction outcome
1 (169)	CuBr·SMe ₂	-78 °C, 1 h	PhNO ₂	159
2 (169)	CuBr·SMe ₂	-78 °C, 30 min; -40 °C, 1 h	PhNO ₂	175 (45%), 174 (25%) and 159
3 (169)	CuBr·SMe ₂	-78 °C, 30 min; -20 °C or 0 °C, 30min	PhNO ₂	175 (33%), 174 (20%) and 159
4 (169)	CuCN	-78 °C, 30 min; -40 °C, 1 h	PhNO ₂	175 (50%), 174 (20%) and 159
5 (169)	CuCN	-78 °C, 30 min; -40 °C, 1 h	O ₂	175 (53%), 174 (26%) and 159
6 (169)	CuCN	-78 °C, 30 min; -40 °C, 1 h	CuCl ₂	159
7 (171)	CuCN	-78 °C, 30 min; -40 °C, 1 h	PhNO ₂	Hydroxylation and deiodination

*Equal moles of piperazine substrate and Cu(I) reagent were used.



The use of molecular oxygen as the oxidant did not essentially change the reaction pattern, giving a similar result to the coupling reactions using PhNO₂ (Entry 5, Table 3.2). For the oxidation reaction using CuCl₂, the proto-deiodinated product **159** was predominantly isolated (Entry 6, Table 3.2), which was quite different from the result obtained from the model reaction.

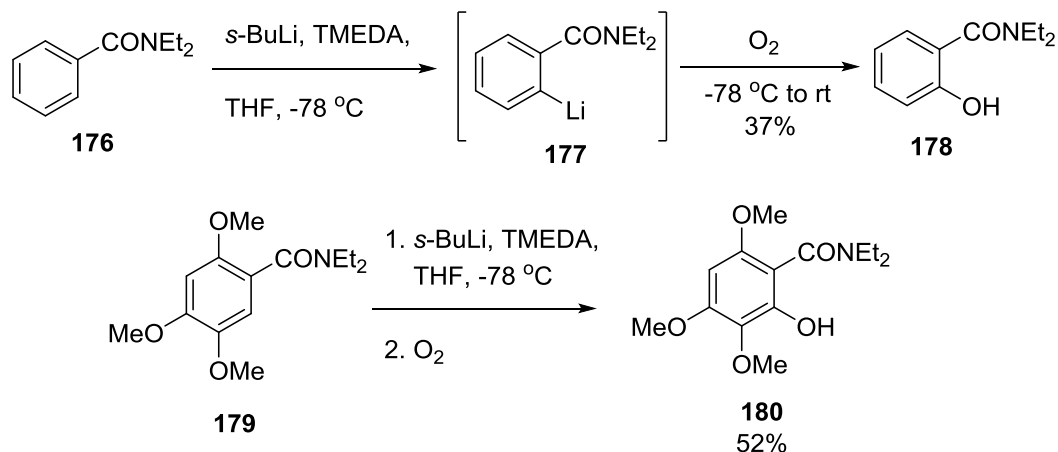
This sequence was also attempted with unsymmetrical piperazine **171**. Regrettably, oxygenation and deiodination were still the dominating processes (Entry 7, Table 3.2).

Referring to the mass spectra of the oxidative cuprate coupling reactions, some high molecular weight products were also detected accompanying the oxygenated piperazines, which indicated that intermolecular oxidative coupling took place and certain amounts of linear aryl cuprates rather than the bridged ones formed during the reaction processes.

In terms of the oxygenation process, it seems explainable when molecular oxygen was used as the oxidant because hydroxylation has been reported to be a competing process in some cases of oxidative coupling of organocuprates to generate phenol by-products.⁸⁶ However, it is not clear whether the oxidative coupling reaction using PhNO₂ would follow a similar pathway. It seems unlikely that oxygen from the atmosphere could intervene during the coupling process since all the reaction were carried out under argon and subsequent experiments using degassed solvent gave similar results to those shown in Table 3.2.

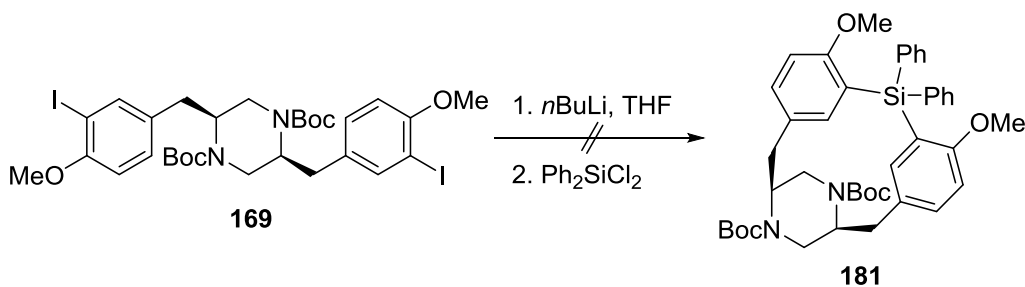
Another possibility also considered was that oxygenated piperazines could be the products from the reaction between aryllithium and O₂, if the dilithio intermediate failed to react with Cu(I) species. Parker and Koziski reported the directed oxygenation of aromatic compounds in 1987 (Scheme 3.14). In their study, a variety of aryllithium species prepared from

functional group-directed metalation were transformed to the hydroxylated products upon oxidation with O₂.⁹⁷



Scheme 3.14: Directed oxygenation of aromatic compounds reported by Parker and Koziski.⁹⁷

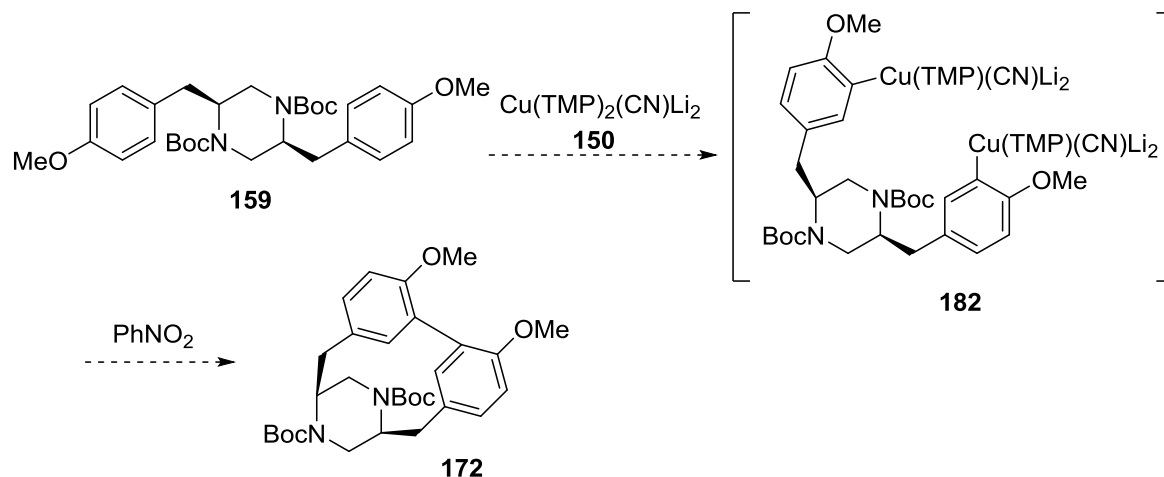
At this stage, another reaction was performed by treating the dilithiopiperazine derived from **169** with Ph₂SiCl₂, anticipating that silacycle **181** would be afforded if the piperazine substrate was prone to form the bridged structure (Scheme 3.15).



Scheme 3.15

However, only deiodination was observed to give piperazine **159** in 63% yield, without any detection of cyclised product **181**. Although it is not the same type of reaction to the cupration of aryllithium species, the failure in generating **181** may indicate that cyclic cuprate was also difficult to form under the previously employed conditions.

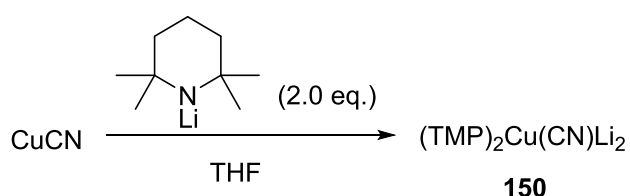
As an alternative approach, the direct *ortho* cupration strategy was then tested. Bis-aryl cuprate **182** was expected to be fashioned after the deprotonative cupration of piperazine **159** with an amidocuprate, such as **150** (Scheme 3.16).



Scheme 3.16

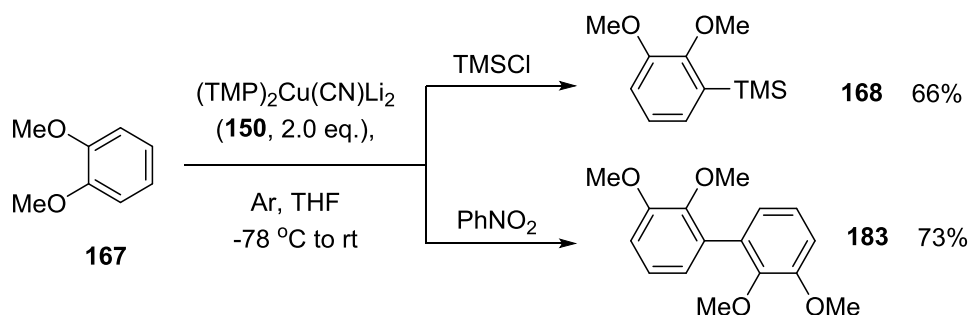
Intermediate **182** in this case was different from the cyclic cuprates in which the two phenol ethers were tethered together by copper species. Upon oxidation, the two aryl cuprate moieties within **182** were expected to undergo a coupling process to give cyclic product **172**.

Following the procedure reported by Uchiyama and co-workers,⁸⁸ amidocuprate **150** was prepared from the reaction between copper cyanide and LTMP that was generated from the deprotonation of 2,2,6,6-tetramethylpiperidine with *n*-BuLi (Scheme 3.17). Model reactions were also performed to test the efficiency of this amidocuprate base.



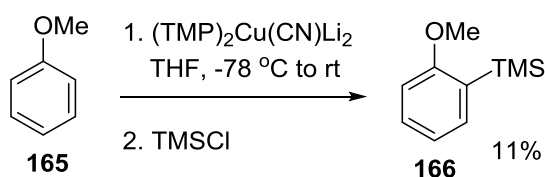
Scheme 3.17

As demonstrated in Scheme 3.18, treatment of 1,2-dimethoxybenzene with **150**, followed by trapping the resultant arylcuprate with TMSCl gave silylated product **168** in 66% yield. It should be noted that warming up the reaction mixture to room temperature during the deprotonative cupration step was crucial, since a lower yield was observed when the cupration process was carried out at 0 °C. This might be due to the absence of activating (electron-withdrawing) groups on the aromatic ring compared with the benzamide substrates that were employed in Uchiyama's study as shown in Scheme 3.5 in Section 3.1.1.⁸⁸ The oxidative coupling reaction of arylcuprates proceeded smoothly to afford biaryl product **183** in 73% yield.



Scheme 3.18

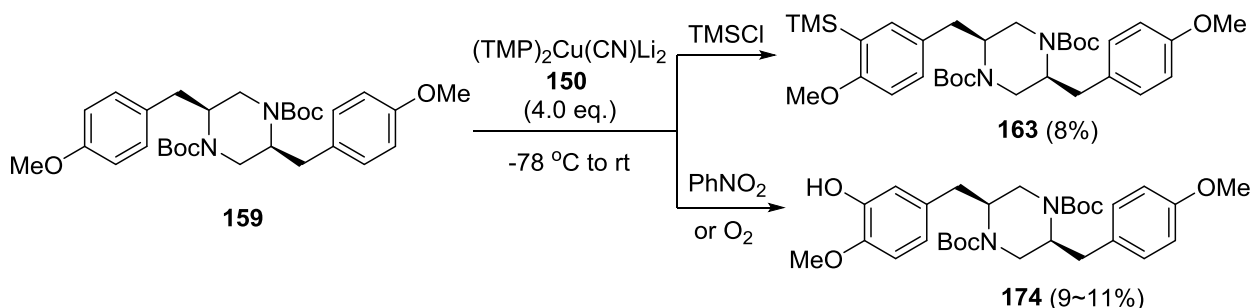
While the deprotonative cupration could be fashioned with 1,2-dimethoxybenzene using the specific amidocuprate **150**, the applicability of this method to anisole-type substrates still awaited examination. When the same procedure was followed with anisole as the substrate, reduced efficiency was observed as product **166** was only isolated in 11% yield, with starting material largely intact (Scheme 3.19).



Scheme 3.19

Poor yields in the deprotonation of anisole were also mentioned by Mongin and co-workers.⁹⁸ In their work, anisole was deprotonated with a similar lithium cuprate base followed by quenching with elemental iodine resulting in 20% isolation of 2-iodoanisole. Even though 2,2'-dimethoxybiphenyl was also isolated as a by-product, possibly derived from the I₂ oxidised cuprate coupling route, the combined yield of all the products was still low. For our piperazine system, it was then hoped that the alkylphenol ether within the substrate would behave differently from anisole.

Treatment of piperazine derivative **159** with **150**, followed by electrophilic trapping with TMSCl gave only 8% of the mono-silylated product **163**, leaving unreacted starting material as the main component (Scheme 3.20). Oxidation of the cupration system with either nitrobenzene or O₂ provided no C–C bond formation, but a small amount of the mono-hydroxylated piperazine **174**, with a large quantity of starting material being recovered.



Even though the cupration conditions were also tested with other piperazine substrates including **101** and **111** (Figure 3.6), no promising results were obtained.

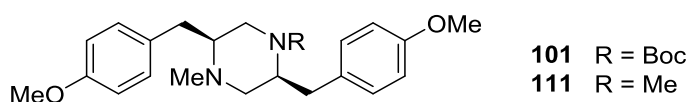
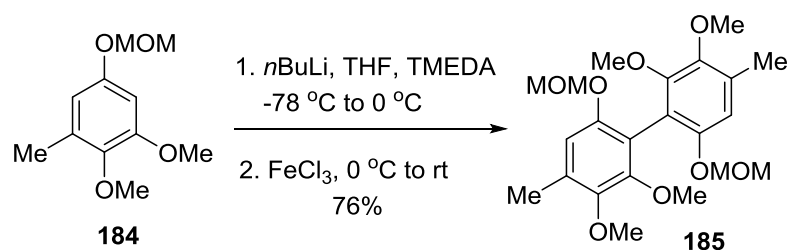


Figure 3.6

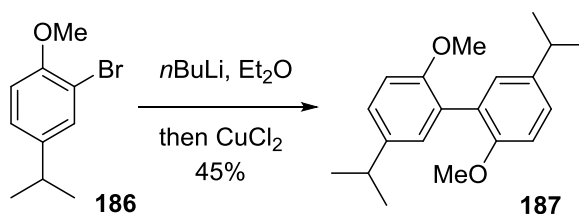
Compared with the Li-I exchange and transmetalation protocol, the direct *ortho* cupration seemed to be a less efficient method of generating aryl cuprate intermediate with our system.

Following thorough experimentation in intramolecular oxidative cuprate coupling, the last attempt was made on the oxidative coupling of aryllithium species. It is known that treating organolithium intermediates with an appropriate oxidant could lead to coupling products. Several studies have demonstrated the practical usefulness of this method in synthesising biaryl compounds.^{99,100} For example, Shair and co-workers employed this transformation at the early stage of the total syntheses of several polyketides.⁹⁹ In their study, FeCl₃-mediated oxidative dimerisation of aryllithium species generated from the regioselective *ortho* lithiation of **184** afforded biaryl **185** in 76% yield (Scheme 3.21).



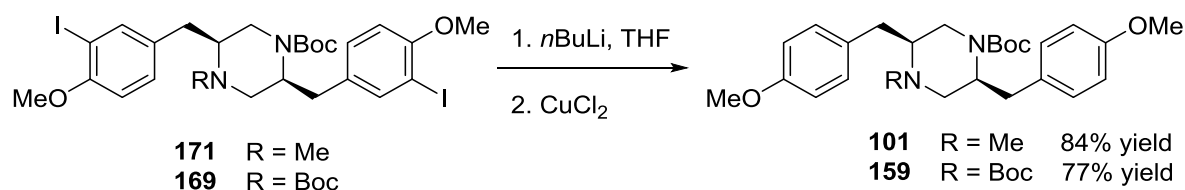
Scheme 3.21: Oxidative dimerisation of aryllithium reported by Shair and co-workers.⁹⁹

Other oxidants were also used for the oxidation of organolithium intermediate, such as the synthesis of biaryl **187**, which was produced from CuCl₂-mediated oxidative coupling of the aryllithium derived from bromide **186** (Scheme 3.22).¹⁰⁰



Scheme 3.22: Cu(II)-mediated homocoupling of aryllithium species.¹⁰⁰

Nevertheless, no intramolecular coupling reactions using this method have been reported and piperazines **169** and **171** were tested preliminarily. The Li-I exchange should be a straightforward process for the generation of the bis-aryllithium intermediates. However, oxidation with CuCl_2 failed to deliver any novel products apart from deiodinated piperazines (Scheme 3.23).



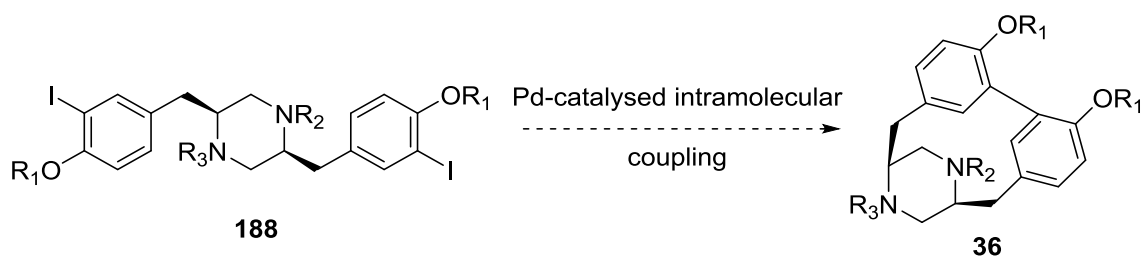
Scheme 3.23

Further efforts on this approach were not made since the lack of reactivity towards cyclisation might be due to a conformational issue of the piperazine substrates. Even though the side chains, specifically the two benzylic methylene groups, were proposed to reside in the *pseudo*-axial positions of the boat conformer of the Boc-protected piperazine **159** or **169**, the disposition of the two aromatic rings was not obvious concerning the rotation along the corresponding C–C bonds.

3.2 Palladium-Catalysed Coupling Reactions

Palladium-catalysed coupling methodology has gained widespread use for the formation of carbon–carbon and carbon–heteroatom bonds. It is also a well-developed and powerful tool to effect aryl coupling reactions, both inter- and intramolecularly. Focusing on generating the biaryl piperazine sub-target for the synthesis of herquiline A and B, two synthetic aspects were worthy of consideration at the starting point. Firstly, functionalisation of the phenol ether to

aryl halide was essentially needed because Pd-catalysed direct C(sp²)-H/C(sp²)-H coupling would be extremely difficult since the two aromatic rings were not in close proximity. Secondly, equal functionality would be possessed by the two phenol ethers in the piperazine substrate because selective functionalisation of the two aromatic moieties would be challenging at this stage. Ideally, biaryl piperazine product **36** could be delivered from the previously synthesised bis-iodide **188** *via* a palladium-catalysed intramolecular coupling reaction (Scheme 3.24).



Scheme 3.24

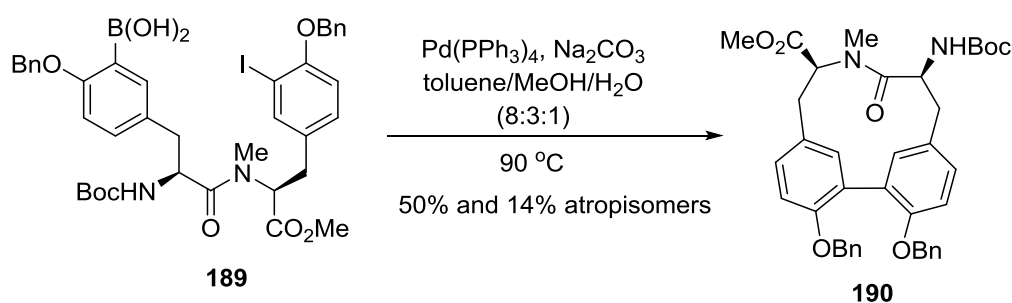
Biaryl formation from two aryl halides can be fashioned with several different Pd-catalysed transformations, among which the domino Suzuki-Miyaura and Stille-Kelly couplings have been demonstrated to be two productive ones, especially for intramolecular aryl couplings. Other methods have also been developed for intermolecular coupling of aryl halides, which could also be modified for an intramolecular version.

3.2.1 Introduction to Intramolecular Suzuki-Miyaura and Stille-Kelly Couplings

Both the Stille and Suzuki couplings are well-established methods that have been used for the formation of C-C bonds, with high tolerance of many different functional groups. Here we

mainly focused on Pd-catalysed intramolecular coupling reactions that gave cyclic biaryl structures.

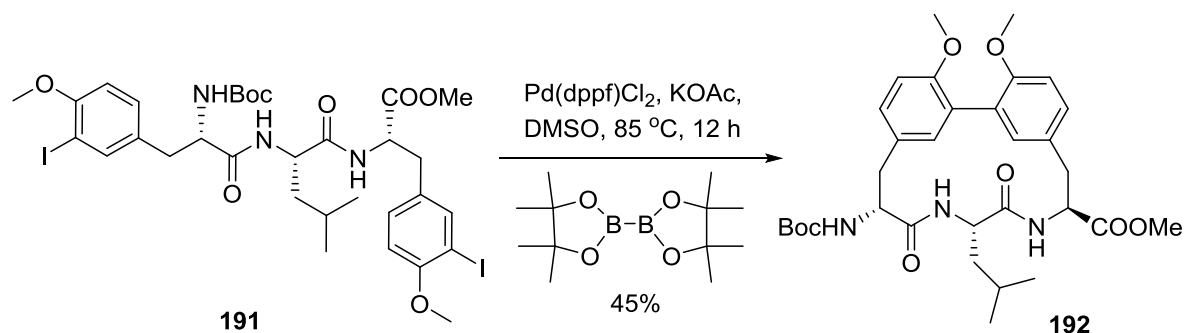
In a classic Suzuki coupling reaction, as reported by Takeya and co-workers, dipeptide **189** bearing a boronic acid and an iodide moiety was converted to the 12-membered ring structure **190** catalysed by Pd(PPh₃)₄ (Scheme 3.25).¹⁰¹ Two indistinguishable atropisomers were obtained in 64% combined yield. While the success of this cyclisation reaction demonstrated the efficiency of intramolecular Suzuki coupling, it indicated the requirement that both aryl halide moiety and its boronic acid (or equivalent functionality) coupling partner should be present within the substrate, which increased the complexity and challenge of the synthesis.



Scheme 3.25

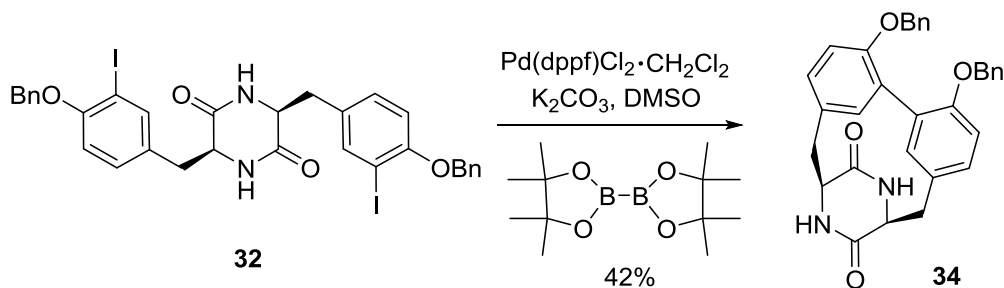
In 2000, Zhu and co-workers developed a domino macrocyclisation procedure for the synthesis of cyclic peptides with biaryl linkages, such as tripeptide **192** (Scheme 3.26).¹⁰² Specifically, diiodide **191** was treated with Pd(dppf)Cl₂ in the presence of KOAc and diboron ester to give the 15-membered cyclophane **192** in moderate yield. The aryl coupling process was proposed to consist of two ordered transformations, the Miyaura borylation of **191** and a subsequent intramolecular Suzuki coupling. This could be partially proved by controlled experiments in which Pd(dppf)Cl₂ or Pd(PPh₃)₄ alone failed to promote the coupling reaction and the diboron ester was found to be crucial for the cyclisation. Even though the existence of certain arylboronates were not detected during the reaction process, they were considered to

be the key intermediates during the process and could undergo a Suzuki coupling reaction to afford the cyclic product.



Scheme 3.26

During the course of our studies on the total synthesis of herquiline A and B, Hutton and co-workers reported the total synthesis of mycrocyclosin employing this deft Suzuki-Miyaura coupling manifold as a key step (Scheme 3.27).²³

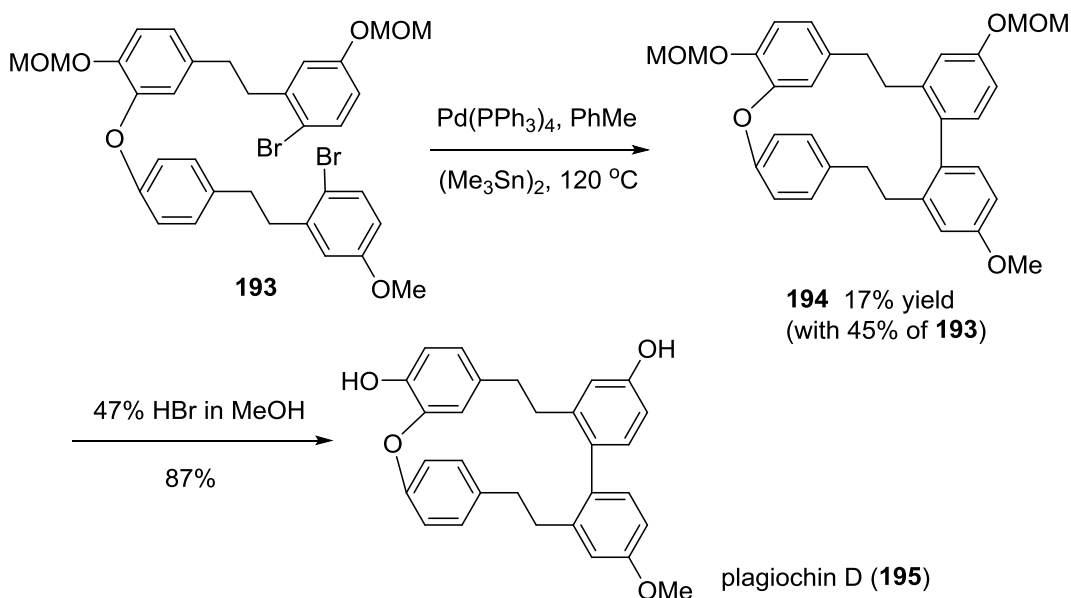


Scheme 3.27

The success of the intramolecular coupling of DKP **32** is particularly instructive, since the only difference between **32** and our substrates lies in the oxidation state of the piperazine rings. Application of the promising coupling conditions to our piperazine systems would provide a general view on the reactivity of these two kinds of structures.

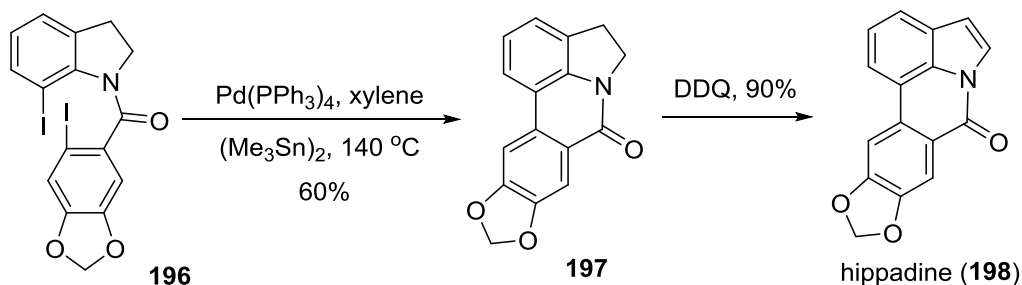
The intramolecular Stille-Kelly coupling of bis-aryl halides shares a similar concept. Such as the cyclisation of bis-bromide **193** catalysed by $\text{Pd(PPh}_3)_4$ in the presence of hexamethylditin (Scheme 3.28), the reaction gave biaryl macrocycle **194** in 17% yield.¹⁰³ Even though the

intramolecular cyclisation was not productive, the starting material could be recycled and cyclic product **194** served successfully as a synthetic precursor of the macrocyclic natural product plagiochin D (**195**). In contrast to the absence of mono-arylboronate intermediates in Suzuki-Miyaura coupling reactions, the arylstannane intermediates were isolated from the reaction mixture in this case.



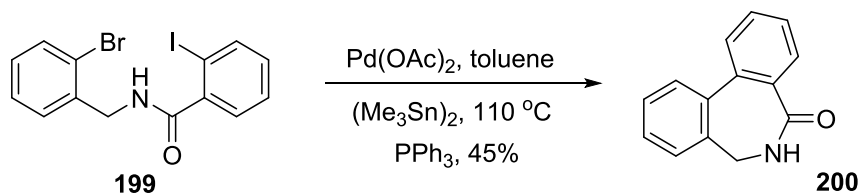
Scheme 3.28

Compared to macrocyclisation, this tandem stannylation-aryl coupling sequence exhibits enhanced efficiency in the formation of 5-, 6- and 7-membered rings. Grigg and co-workers used this tactic in their synthesis of alkaloid hippadine (**198**) (Scheme 3.29).¹⁰⁴



Scheme 3.29

The bis-aryl iodide **196** was subjected to the Stille-Kelly coupling conditions to give indoline **197** in 60% yield. Upon oxidation with DDQ, the final natural product was produced from **197** in high yield.



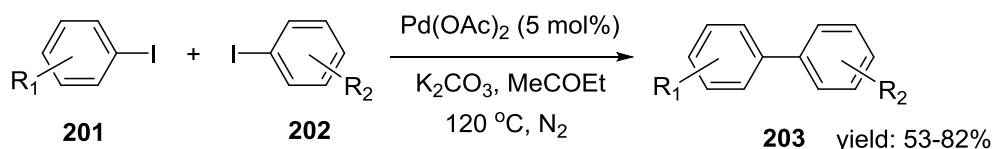
Scheme 3.30

The seven-membered lactam **200** could also be fashioned from the intramolecular coupling of amide **199** catalysed by Pd(OAc)_2 (Scheme 3.30).

3.2.2 Other Palladium-Catalysed Coupling Methods

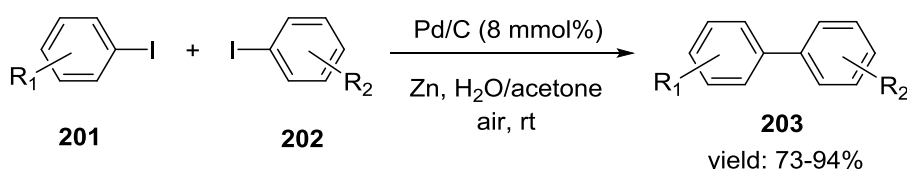
Besides the tandem coupling strategies, the Pd-catalysed direct biaryl formation from two aryl halides is another appealing method. A variety of palladium catalysts and conditions have been reported to effect the Ullmann-type reductive coupling reactions.

With the catalytic system developed by Lu and co-worker, biaryls could be synthesised in moderate to good yields by treating aryl iodides with Pd(OAc)_2 and K_2CO_3 in MeCOEt (Scheme 3.31).¹⁰⁵ While homo-couplings of aryl iodide proceeded smoothly, they pointed out that the reactivity difference between two iodide substrates and their ratios could affect the selectivity of cross-coupling reactions.



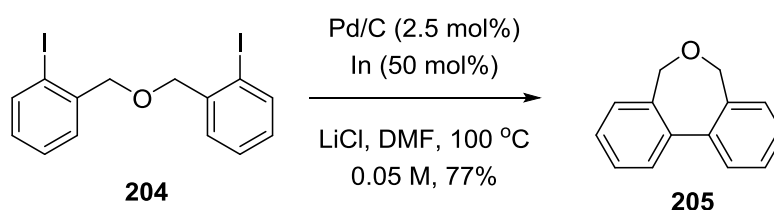
Scheme 3.31

Different from the Pd(II)-catalysed aryl iodide coupling, the Ullmann-type reaction using Pd/C as the catalyst also showed high efficiency in the homo-coupling of various aryl halides. According to Li and co-workers' study, subjecting aryl halides, especially aryl iodides to the conditions involving Pd/C and Zn in aqueous acetone, symmetrical biaryl products were afforded in high yields (Scheme 3.32).¹⁰⁶ In contrast to the general Pd catalytic cycle, this system was found to be air-tolerant since identical results were obtained when the reactions were performed under nitrogen, air or oxygen atmosphere. It was proposed that the palladium intermediate might be stabilised by coordinating to the carbonyl group of acetone during the course of the catalytic cycle.



Scheme 3.32

Lee and co-workers reported another Pd/C catalysed Csp²-Csp² bond formation method with aryl or vinyl halides as the substrates.¹⁰⁷



Scheme 3.33

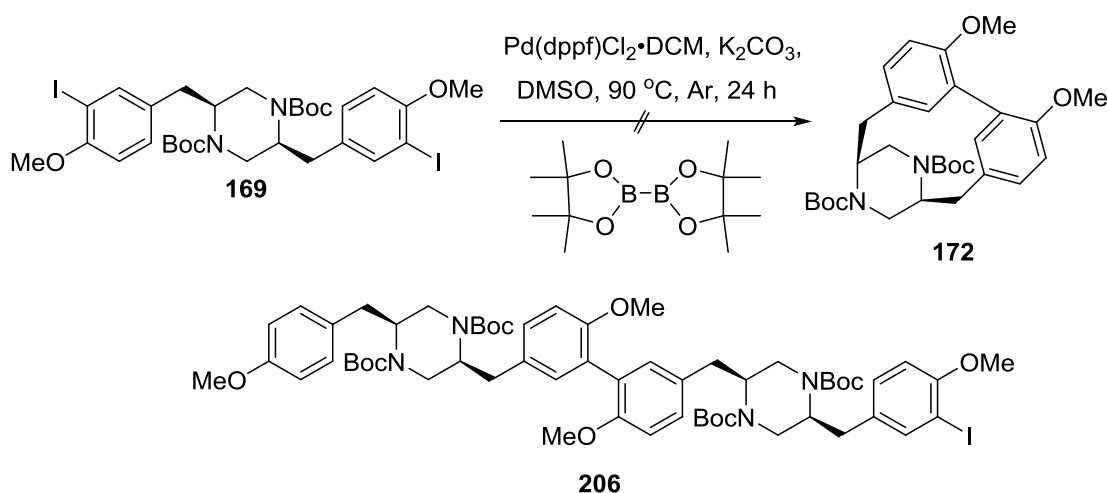
The combination of Pd/C, indium and LiCl in DMF effects the coupling of iodide or bromide substrates both inter- and intramolecularly. For example, the seven-membered biaryl product **205** was afforded in 77% yield from bis-aryl iodide **204** in dilute conditions (Scheme 3.33).

3.2.3 Application to the Synthesis of the Herquines

With several promising Pd-catalysed coupling methods available, our elaboration commenced with the synthesis of the advanced biaryl precursor of herquiline A and B. Since most of these Pd-catalysed reactions were carried out at relatively high temperature compared with the phenol or organocuprate oxidative coupling reactions, it was anticipated that the favourable conformer with a suitable aromatic side chain orientation would contribute to a sizable extent of the piperazine substrate *via* conformational equilibrium during the intramolecular coupling processes.

Suzuki-Miyaura Coupling Approach

The conditions adopted by Hutton and co-workers were employed primarily in our attempts. Initial treatment of symmetrical piperazine **169** with Pd(dppf)Cl₂·CH₂Cl₂, K₂CO₃ and diboron ester in DMSO did not deliver the desired coupling product **172** (Scheme 3.34).

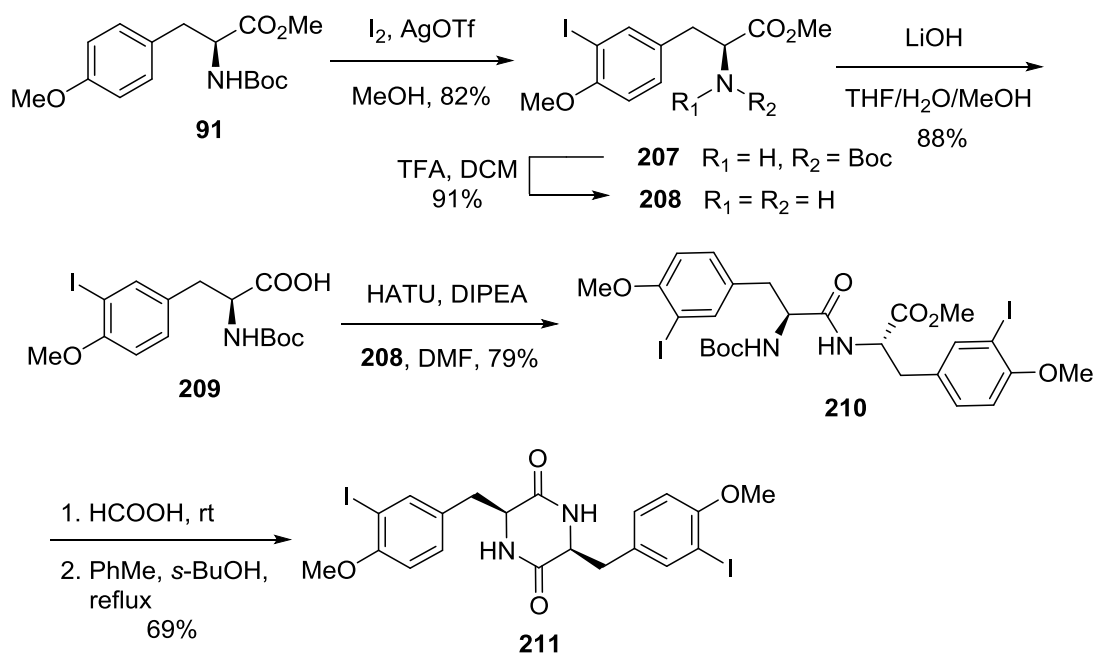


Scheme 3.34

Instead, dimeric by-products, such as **206**, deiodinated material and even trimeric structures were detected by mass spectrometry. After careful column chromatography, compound **206** was isolated. It was noted that further dilution of the reaction mixture failed to change this outcome. These preliminary results indicated that intermolecular coupling was a superior pathway to the desired intramolecular reaction with the Boc-protected piperazine substrate. In addition, proto-deiodination was a competing process during this transformation.

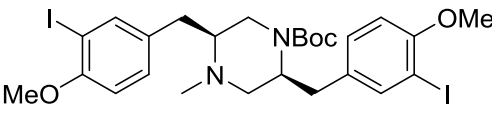
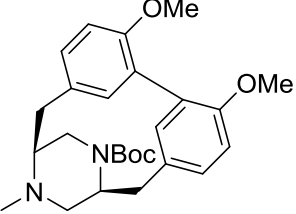
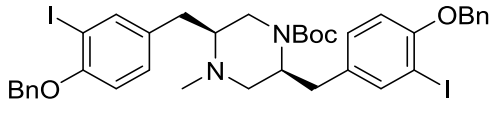
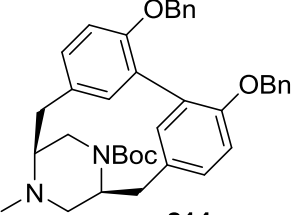
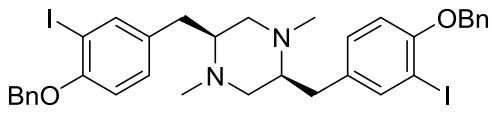
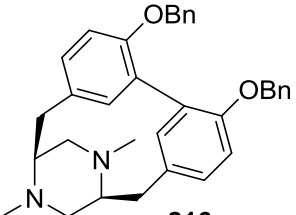
While the lack of reactivity in terms of piperazine substrate **169** for the coupling reactions awaited further investigation, we decided to reproduce the tandem reaction from the literature with a DKP substrate in order to confirm that the reaction conditions employed by Hutton and co-workers were replicated in our attempts.

To obtain substrate **211** for the coupling reaction, the direct iodination method failed due to the poor solubility of the corresponding symmetrical DKP precursor. Instead, a stepwise route was pursued, commencing from the iodination of tyrosine derivative **91** (Scheme 3.35).



Scheme 3.35

Table 3.3: Pd-catalysed intramolecular coupling reactions.

Substrate	Coupling product	Isolation yield
 <p style="text-align: center;">171</p>	 <p style="text-align: center;">173</p>	4%
 <p style="text-align: center;">213</p>	 <p style="text-align: center;">214</p>	6%
 <p style="text-align: center;">215</p>	 <p style="text-align: center;">216</p>	4%

The coupling of *N, N'*-dimethyl piperazine **215** gave a similar result to deliver biaryl piperazine **216** with C_2 symmetry. This was supported by HRMS spectrum which showed a $[M+H]^+$ peak at m/z 505.2844 ($C_{34}H_{37}N_2O_2$ requires 505.2855). In the 1H NMR spectrum of piperazine **216**, a doublet resonance for H_a was observed at 8.20 ppm (Figure 3.7). The downfield shift, compared with the chemical shift of 6.49 ppm for the protons H_a in DKP coupling product **212**, indicated that the H_a protons within **216** might be deshielded due to the magnetic anisotropy effect from both aromatic rings of the biphenyl moiety.

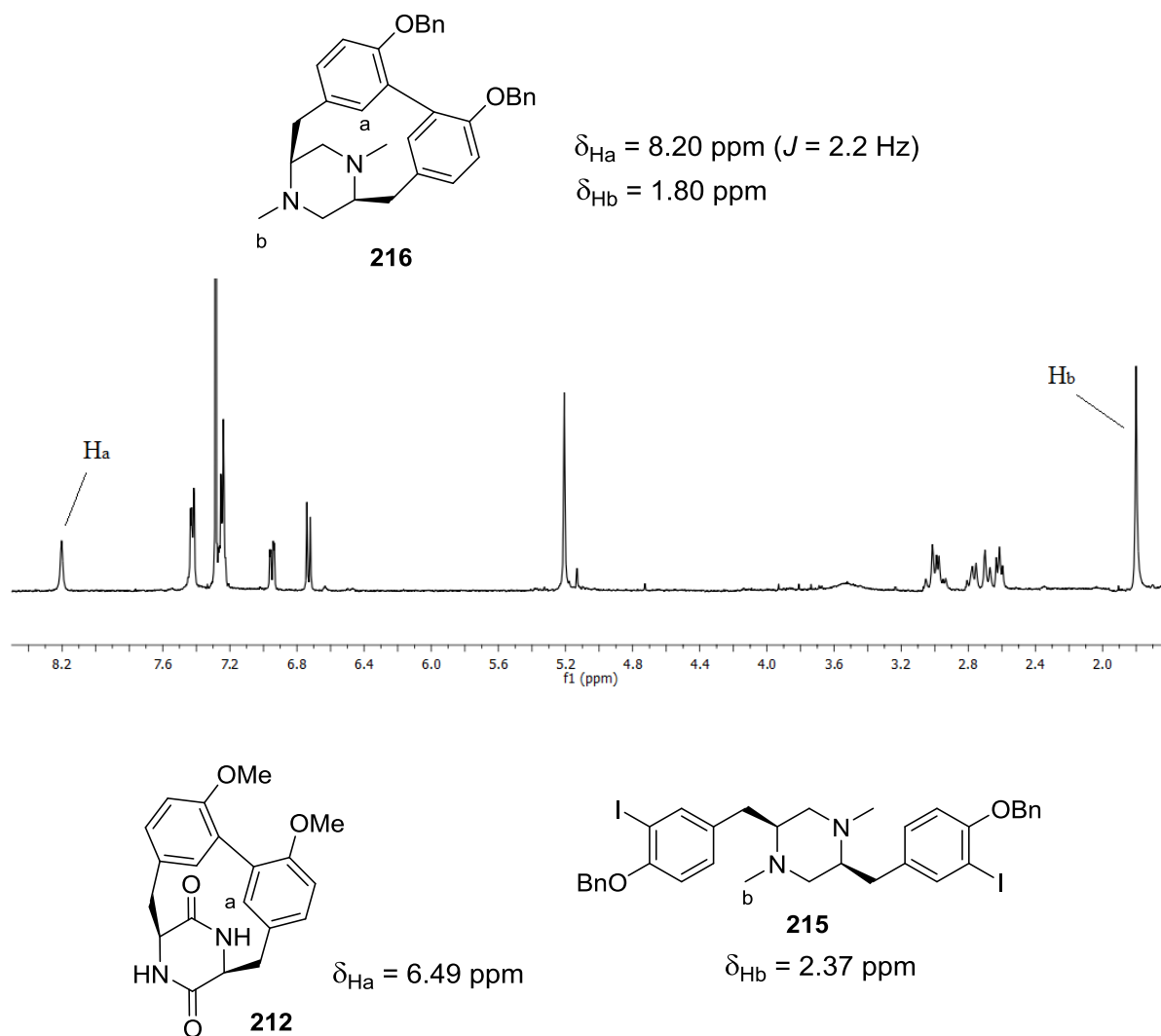


Figure 3.7: Partial ^1H NMR spectrum of piperazine **216** (400 MHz, CDCl_3 , 298 K).

On the contrary, the signals from protons H_b (NCH_3) in **216** were relatively highfield shifted to 1.80 ppm with respect to those from the methyl protons in precursor **215** ($\delta = 2.37$ ppm), indicating that the H_b protons in structure **216** were slightly shielded by corresponding aromatic rings.

At this stage, efforts had been made to optimise the reaction conditions, since the above conditions that gave satisfactory results with DKP substrates might not be suitable for the intramolecular coupling of piperazines. As introduced in Zhu and co-workers' study in

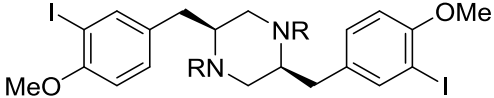
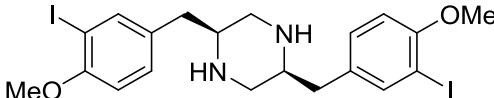
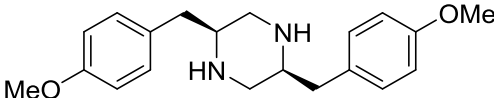
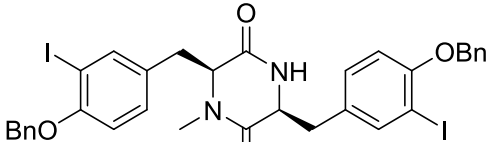
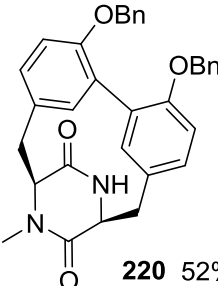
Section 3.2.1, this Pd-catalysed domino coupling reaction was proposed to consist of two steps: Miyaura borylation and Suzuki coupling. For the former step, Miyaura and co-workers screened various conditions and found that the combination of Pd(dppf)Cl₂/KOAc/DMSO was the optimal reaction condition for the cross-coupling of diboron ester and haloarenes to give arylboronic esters.¹⁰⁸ Interestingly, they found that the use of stronger base K₂CO₃ instead of KOAc in the borylation reaction could promote further Suzuki reaction between the newly generated arylboronic ester and haloarene to produce biaryl by-product, which was a highly desired process for our domino coupling sequence. Based on this analysis, it seems the conditions employed in our system (Pd(dppf)Cl₂/K₂CO₃/DMSO) were the most promising ones. However, the success of KOAc rather than K₂CO₃ in promoting the intramolecular coupling of linear dipeptide **191** in Scheme 3.26 in Section 3.2.1 reported by Zhu made the choice of base negotiable.

The use of KOAc as the base was tested with substrate **171** while other reaction parameters remained unchanged, but deiodination was found to be the dominating process and no coupling reaction was observed. Therefore, K₂CO₃ was used in subsequent coupling reactions. In terms of reaction temperature, performing the reaction at lower temperature than 80 °C or above 110 °C led to a considerable degree of deiodination and other side reactions.

Since intermolecular coupling reaction occurred under the current conditions with a substrate concentration of 0.005-0.01 M, further diluting the reaction mixture was attempted. Unfortunately, no improvement was achieved apart from resulting in a longer reaction time.

The results from the coupling reactions of **171** and **213** indicated that the methyl or benzyl groups on the phenol rings caused no reactivity difference. However, the functional groups on the piperazine rings played a decisive role in the cyclisation process (Table 3.4).

Table 3.4: Attempted Suzuki-Miyaura couplings with piperazine and DKP substrates.

Substrate	Reaction outcome*
 <p>R = Boc (169), SO₂Ph (217), or COCF₃ (161)</p>	Intermolecular coupling and deiodination
 <p>218</p>	 <p>158 69% yield</p>
 <p>219</p>	 <p>220 52% yield</p>

*The same reaction conditions as shown in Scheme 3.36 were employed.

When bis-carbamate **169**, bis-sulfonamide **217** and bis-amide **161** were employed as the substrates, only traces of coupling products were detected by mass spectrometry without successful isolation of any of the desired compounds due to low quantities. Instead, intermolecular coupling products were the main components isolated from the reaction mixtures. In the case of unprotected piperazine **218**, the secondary amino moieties seemed to be detrimental for the aryl coupling process since the system delivered exclusively the deiodinated material.

Attracted by the promising reactivity of DKP substrates, bis-aryl iodide **219** synthesised from the direct iodination of the corresponding DKP substrate in our project was subjected to the Pd-catalysed Suzuki-Miyaura reaction conditions. The biaryl coupling product **220** was

successfully obtained in 52% yield. The higher yield compared with that in the synthesis of symmetrical DKP **212** could possibly be attributed to the good solubility of **220**, which simplified the purification process.

Stille-Kelly and Other Palladium-Catalysed Coupling Approaches

According to our attempts on Suzuki-Miyaura coupling, reactions with piperazines **171** and **213** seemed to give promising results. Therefore, these two substrates were employed in the studies of Stille-Kelly coupling and direct aryl halide coupling approaches.

The Stille-Kelly reaction was initially carried out by treating **171** with Pd(PPh₃)₄ and *n*-Bu₆Sn₂ in refluxing toluene (Entry 1, Table 3.5). However, deiodination took place to give compound **101** accompanied by mono-iodide materials according to the mass spectrum. Interestingly, the signals corresponding to the arylstannane intermediates were also observed from the mass spectrum, which indicated the Pd-catalysed stannylation occurred during the process but the coupling reaction was precluded by the undesired deiodination pathway. Switching the solvent to DMF, a trace amount of coupling product was detected by mass spectrometry, but could not be isolated due to the low quantity (Entry 2, Table 3.5). The main products were piperazine **102** and dimeric compounds. The occurrence of intermolecular coupling reactions demonstrated that the conditions were effective for aryl coupling, even though not in an intramolecular manner.

Taking into the consideration that the bulky tributyltin group might have a negative effect on the intramolecular transmetallation step to give the transitory palladacycle, the use of

hexamethyldistannane was tested. However, a similar result was obtained without changing the reaction pattern (Entry 3, Table 3.5).

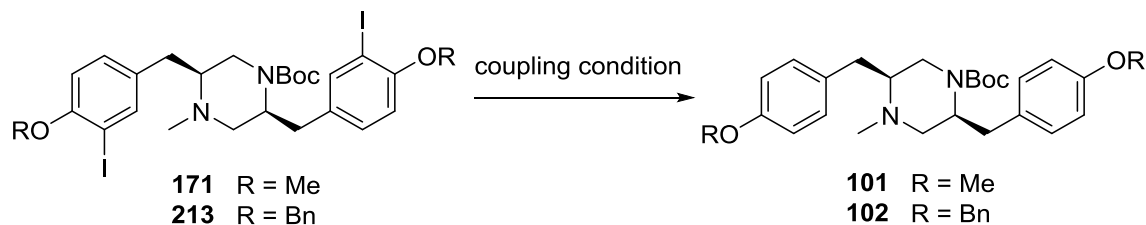
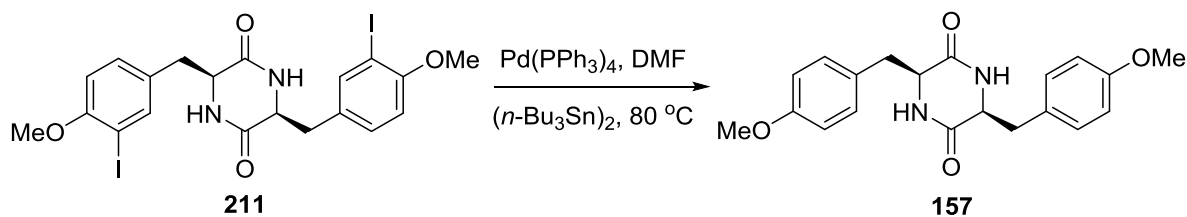


Table 3.5

Entry	Substrate	Coupling conditions*	Reaction outcome
1	171	Pd(PPh ₃) ₄ , <i>n</i> -Bu ₆ Sn ₂ , PhMe, 120 °C, 20 h	Deiodination and stannylation
2	213	Pd(PPh ₃) ₄ , <i>n</i> -Bu ₆ Sn ₂ , DMF, 80 °C, 12 h	Deiodination and intermolecular coupling
3	171	Pd(PPh ₃) ₄ , Me ₆ Sn ₂ , DMF, 80 °C, 12 h	Deiodination and intermolecular coupling
4	171	Pd(PPh ₃) ₄ , <i>n</i> -Bu ₆ Sn ₂ , DMF, MW, 80 °C, 1 h	Partial deiodination
5	171	Pd(PPh ₃) ₂ Cl ₂ , <i>n</i> -Bu ₆ Sn ₂ , DMF, 80 °C, 12 h	Deiodination

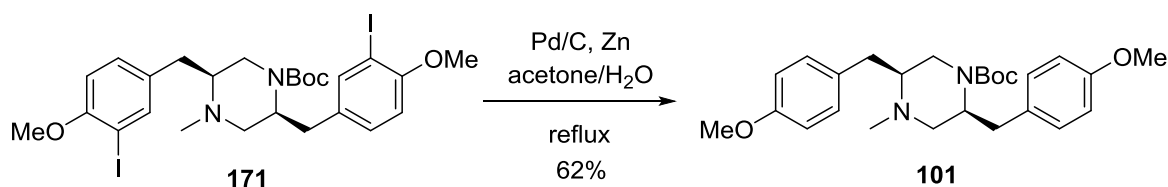
* All reactions were carried out with anhydrous solvents under Ar atmosphere.

Further efforts were made by using microwave irradiation or employing Pd(PPh₃)₂Cl₂ as the catalyst (Entry 4 and 5, Table 3.5). Unfortunately, piperazine **101** was the only compound that could be isolated from the reaction mixtures. At this stage, it seemed clear that Stille-Kelly coupling might not be the suitable method for the cyclisation of our piperazine substrates or even DKP derivatives, since the attempted coupling reaction with DKP **211** also failed to give the cyclised product (Scheme 3.37).



Scheme 3.37

The method developed by Li was also examined by treating bis-iodide **171** with Pd(0) and Zn in aqueous acetone.¹⁰⁶ However, the reaction did not proceed in the same manner as reported and only deiodinated material **101** was recovered (Scheme 3.38).



Scheme 3.38

Bearing in mind the difficulty with intramolecular coupling of piperazines, the Pd-catalysed direct coupling of aryl halides was not investigated in detail. Especially these methods are still at their infancies and the methodologies have been developed mainly with simple substrates.

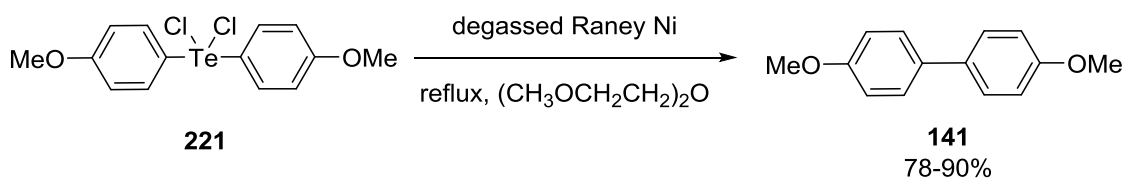
3.3 C–C Bond Formation from Organochalcogenides

In order to improve the yields of the cyclised piperazine products for further manipulations towards herquiline A and B, another C–C bond formation strategy was studied, that is, the extrusion reactions of organochalcogenides. Specifically, it has been reported that organotellurides (or organosulfides) could undergo detelluration (or sulfur expulsion) process to afford coupling products with the formation of new C–C bonds.¹⁰⁹⁻¹¹¹ The substrates employed in this kind of reactions include a diversity of organochalcogenides, such as diaryl,

dialkyl and dialkenyl ones. Relevant to our project, mainly the formation of Csp^2-Csp^2 bonds is introduced here.

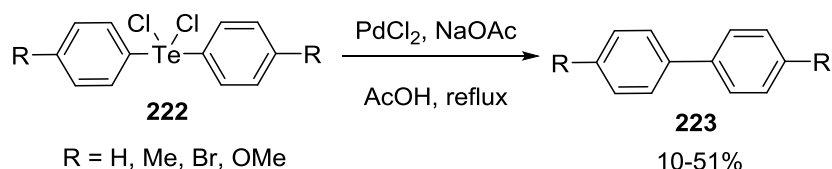
3.3.1 Introduction

The initial disclosure of C–C bond formation from organotellurium intermediates was reported by Bergman and co-workers in the 1970s.¹⁰⁹ Treatment of diaryltellurium dichloride **221** with degassed Raney nickel in refluxing bis(2-methoxyethyl) ether afforded 4,4'-dimethoxybiphenyl **141** in high yield (Scheme 3.39).



Scheme 3.39

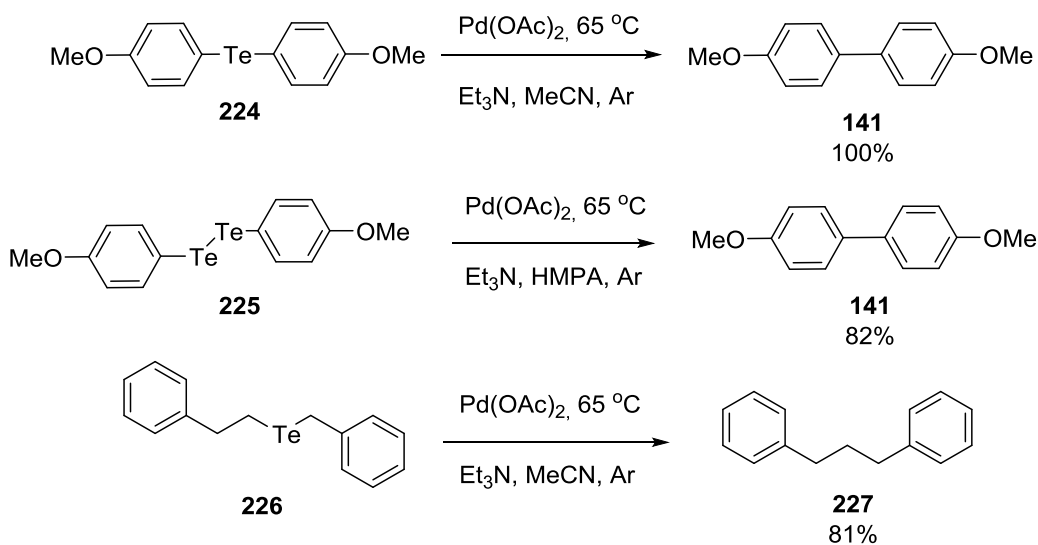
Milder conditions for similar transformations were later disclosed by Uemura and co-workers.¹¹² They carried out the reactions with PdCl₂ (2 eq.) and NaOAc (4 eq.) in refluxing acetic acid and obtained homo-coupling products in moderate yields (Scheme 3.40). Even though the palladium catalyst was used in superstoichiometric quantities and the reaction yields were not high, the potential synthetic utility of this method should not be ignored.



Scheme 3.40

The conversion of telluride R_1-Te-R_2 into the coupled product R_1-R_2 has made this transformation more appealing. Developed by Barton and co-workers, the Pd(0)-mediated C–

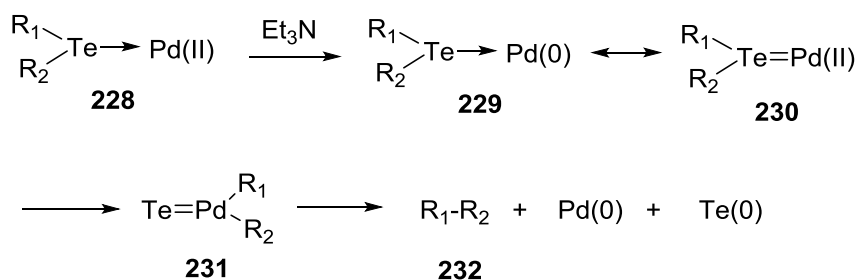
C bond formation could be fashioned with several types of tellurides, such as diaryl-, dialkyl- or aryl alkyl tellurides.¹¹⁰



Scheme 3.41

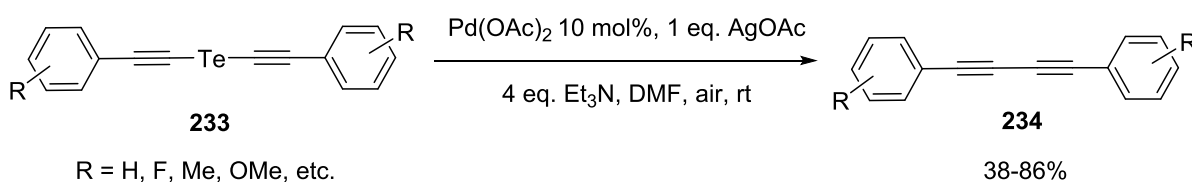
Upon treatment with a stoichiometric amount of Pd(OAc)_2 and an excess of triethylamine in acetonitrile, bis(4-methoxyphenyl)telluride **224** was successfully converted to dianisyl **141** quantitatively (Scheme 3.41). In the case of ditelluride **225**, which was much less reactive than **224**, the coupling reaction was performed in HMPA and **141** was delivered in 82% yield.

The reaction with dialkyltelluride, such as **226**, also proceeded smoothly to afford **227** in 81% yield. Interestingly, no intermolecular coupling was observed when this unsymmetrical telluride was employed as the substrate. Barton and co-workers postulated a working hypothesis that certain Pd–Te bonding during the process should be responsible for the success of these coupling reactions (Scheme 3.42). While this proposed pathway may not be necessarily correct and precise, it is very inspirational for further investigation on this interesting coupling method.



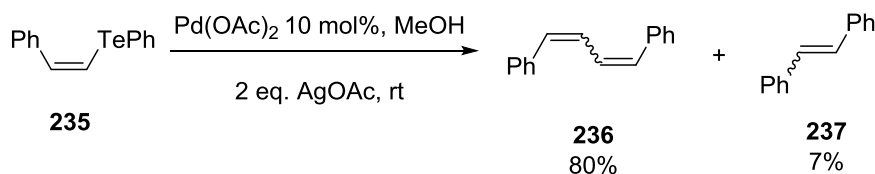
Scheme 3.42

The use of substoichiometric amounts of palladium catalyst for detelluration has been developed initially with dialkenyltellurides and dialkyltellurides. As shown in Scheme 3.43, upon treating symmetrical bis(arylethynyl)tellurides **233** with a catalytic amount of Pd(OAc)₂, triethylamine and AgOAc additive in DMF at room temperature, homo-coupling products were synthesised in moderate to high yields.¹¹³



Scheme 3.43

Uemura and co-workers found that complex products were usually observed during the Pd-catalysed detelluration of a series of unsymmetrical aryl styryl tellurides (Scheme 3.44).¹¹⁴



Scheme 3.44

When (*Z*)-phenyl styryl telluride **235** was subjected to the coupling conditions, the isomeric mixture of 1,3-dienes **236** were isolated in high overall yield, with the *Z, Z* isomer as the main component, indicative of largely retention of stereochemistry. Accompanied with the

formation of dienes, a small amount of stilbene **237** was also identified. This favourable formation of dienes **236** (R_1-R_1 or R_2-R_2) rather than **237** (R_1-R_2) from unsymmetrical telluride (R_1-Te-R_2) was in sharp contrast to the observation by Barton and co-workers (R_1-R_2 formation). It might be possible that the stoichiometry variations of palladium catalyst had an impact on the outcome of the reactions. In addition, the preferential formation of **236** to **237** indicated that the phenyl moiety might be less labile for this type of reaction than the vinyl moiety attached to the same Te atom. Therefore, the transmetalation of Te with Pd being more facile at the vinylic carbon than at the aryl carbon might be another explanation for the unmatched phenomena.

Uemura and co-workers also proposed a catalytic cycle of the coupling reaction in their study (Figure 3.8). According to this putative mechanism, an organic Te-Pd complex was formed initially (stage I) followed by transmetalation (stage II) to give an organopalladium intermediate. Upon reacting with another organotellurium species, a diorganopalladium was afforded (stage III). After reductive elimination (stage IV), the coupling product could be generated.

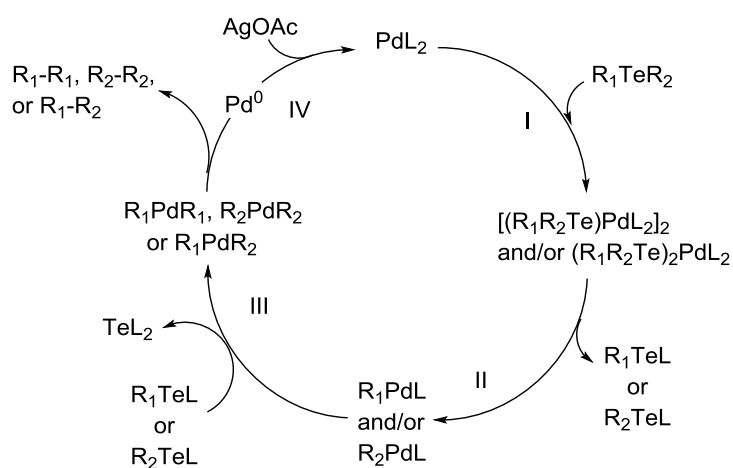
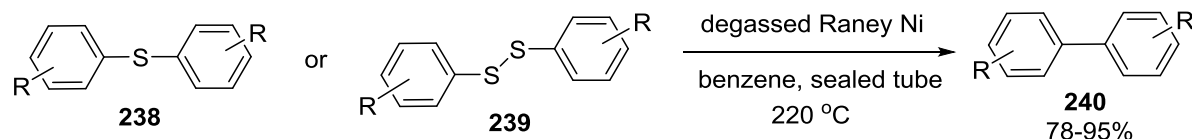


Figure 3.8

While detellurations could be furnished under mild conditions, the extrusion reactions with organosulfides were usually induced thermally.

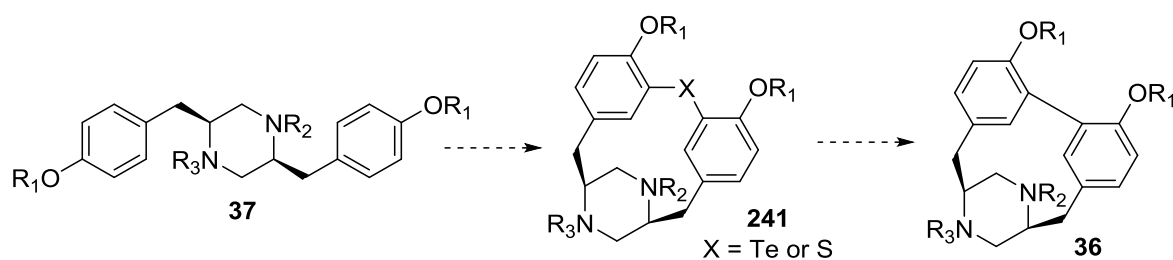


Scheme 3.45

Hauptmann and co-workers reported in 1958 that biphenyl derivatives could form in high yields after treating aromatic thioethers, disulfides or thioesters with Raney nickel at 220 °C (Scheme 3.45).¹¹¹ It was also pointed out that a mixture of products were usually isolated when unsymmetrical substrate was used.

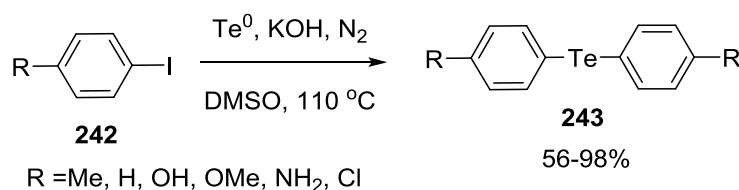
3.3.2 Application to the Intramolecular Coupling of Piperazine Substrates

Even though the extrusion reactions have been studied mainly with simple substrates in the literature, this appealing strategy provided reasonable blueprints for the synthesis of our cyclic biaryl intermediates for herquiline synthesis. Similar to the metal-mediated coupling methods, the two aromatic rings were also expected to be linked together *via* a tellurium or sulfur atom in this approach (Scheme 3.46). And the resultant tellurides or sulfides **241** were assumed to be isolable entities. At a practical level, the formation of these cyclic tellurides or sulfides should be addressed beforehand.



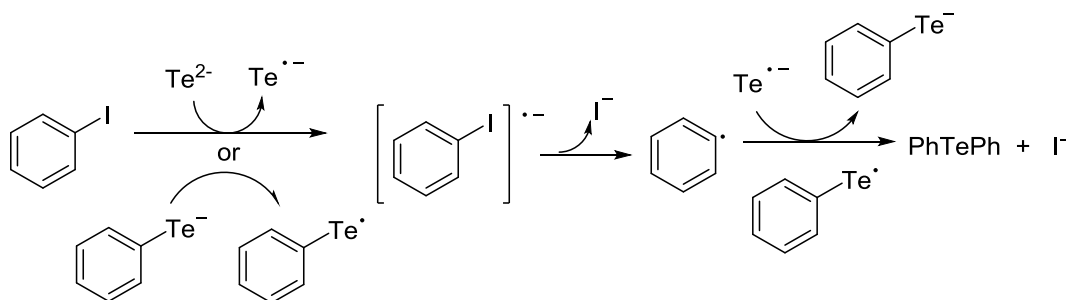
Scheme 3.46

Our efforts towards the synthesis of organotellurides commenced with several model reactions using 4-iodoanisole as the substrate. The efficient protocol reported by Jin and co-workers was initially tested. It was reported that the reaction of aryl iodide, elemental tellurium and KOH in DMSO at high temperature led to symmetrical diaryl telluride in good to excellent yields (Scheme 3.47).¹¹⁵ A variety of aryl iodides with either electron-withdrawing or electron-donating substituents were employed as the substrates.



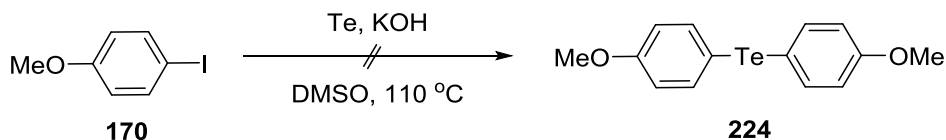
Scheme 3.47

According to the mechanism that was postulated by Jin and co-workers, the active tellurium species was K_2Te , which was generated from the disproportionation reaction between Te^0 and KOH. For the displacement of iodine by tellurium, a single electron transfer mechanism was proposed, which belonged to the $\text{S}_{\text{RN}}1$ type reaction (radical-nucleophilic aromatic substitution). As exemplified in Scheme 3.48, the electron transfer from Te^{2-} or ArTe^- to aryl iodide would generate an aryl iodide anion radical which could possibly collapse into an aryl radical and an iodine anion. The combination of radical ArTe^\bullet and radical Ar^\bullet would afford the diaryltelluride.



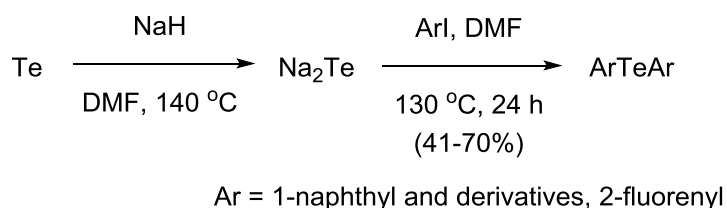
Scheme 3.48

Following the same procedure, the telluration reaction did not proceed at all with 4-iodoanisole in our case (Scheme 3.49). Only starting material was recovered after the reported or even longer reaction time.



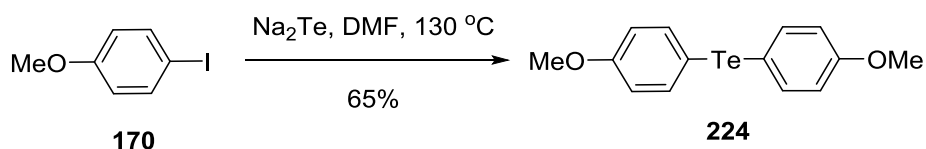
Scheme 3.49

An alternative method for the generation of Te^{2-} is by treating tellurium element with a reducing agent such as NaH (Scheme 3.50).¹¹⁶ A variety of symmetrical aromatic tellurides were synthesised by treating the corresponding aryl iodides with Na_2Te that was generated *in situ*.



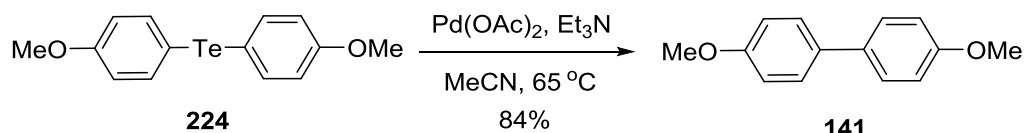
Scheme 3.50

Accordingly, another model reaction was performed by adding 4-iodoanisole to the newly prepared Na_2Te suspension in DMF. Gratifyingly, bis(4-methoxyphenyl)telluride **224** was obtained in 65% yield (Scheme 3.51).



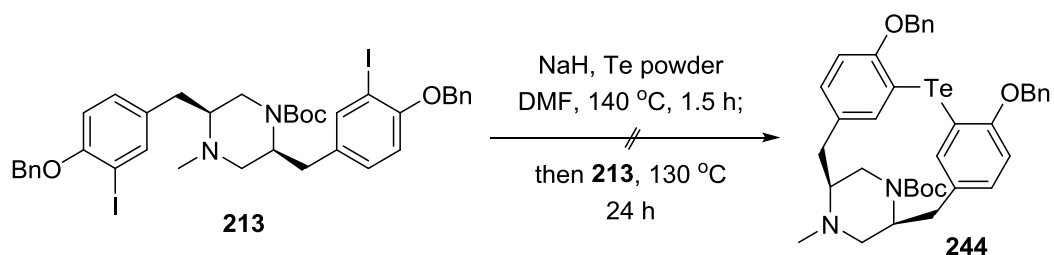
Scheme 3.51

With this symmetrical telluride in hand, the detelluration method developed by Barton and co-workers was initially tested. Upon exposure of **224** to a stoichiometric amount of Pd(OAc)₂ and two equivalents of triethylamine in acetonitrile, 4,4'-dimethoxybiphenyl **141** was obtained in 84% yield (Scheme 3.52).



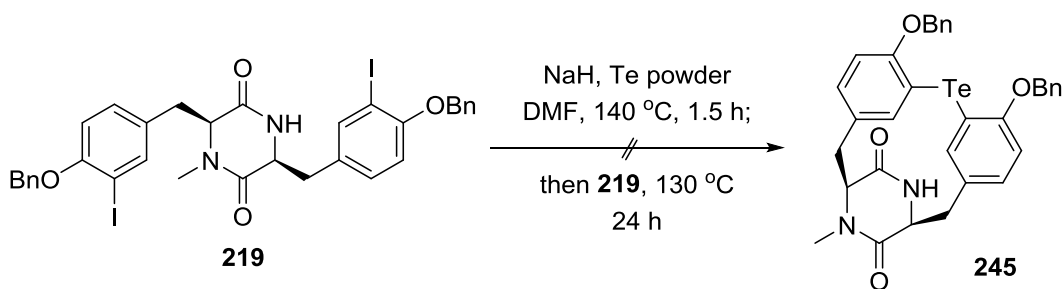
Scheme 3.52

Having achieved the biaryl telluride synthesis and the subsequent Pd-catalysed C–C bond formation in the model reactions, we then investigated the application of this two-step sequence to the piperazine system. The primary task was the synthesis of cyclic piperazine intermediate with a Te bridge. Initial subjecting of bis-aryl iodide **213** to the telluration conditions we adopted in the model reaction did not produce the desired product **244** (Scheme 3.53). From the reaction mixture only isolated deiodinated material. After close scrutiny of the mass spectrum, tellurium type isotope distributions were observed. However, no structures could be defined except the identification of certain dimeric products.



Scheme 3.53

The reaction with DKP substrate **219** suffered a similar fate. While the proto-deiodination was the dominating process, a degree of isomerisation also took place under the reaction conditions (Scheme 3.54).

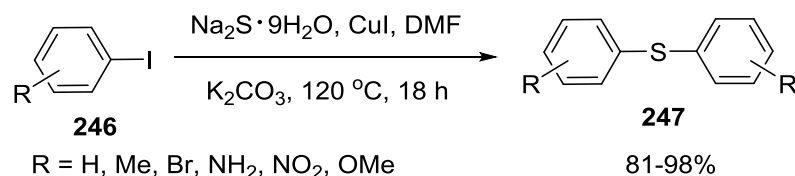


Scheme 3.54

It was difficult to draw any conclusions from the failure of the cyclic telluride formation. However, based on the mechanism depicted in Scheme 3.48, one could conceive that a diradical piperazine intermediate (piperazine with Ar• and ArTe• radical moieties) would need to be generated in order to fashion an intramolecular coupling reaction. While the ease of generation and the stability of such a diradical species were not clear, the desired reaction pathway might be challenging and unfavourable.

Besides the diaryl telluride synthesis, various methods have been developed towards C–S bond formations, which could serve as an alternative approach to the chalcogen atom-bridged piperazine target.

The copper-catalysed sulfuration of aryl iodide developed by Duan and Li employed the easily available Na_2S as the sulfur source (Scheme 3.55).¹¹⁷

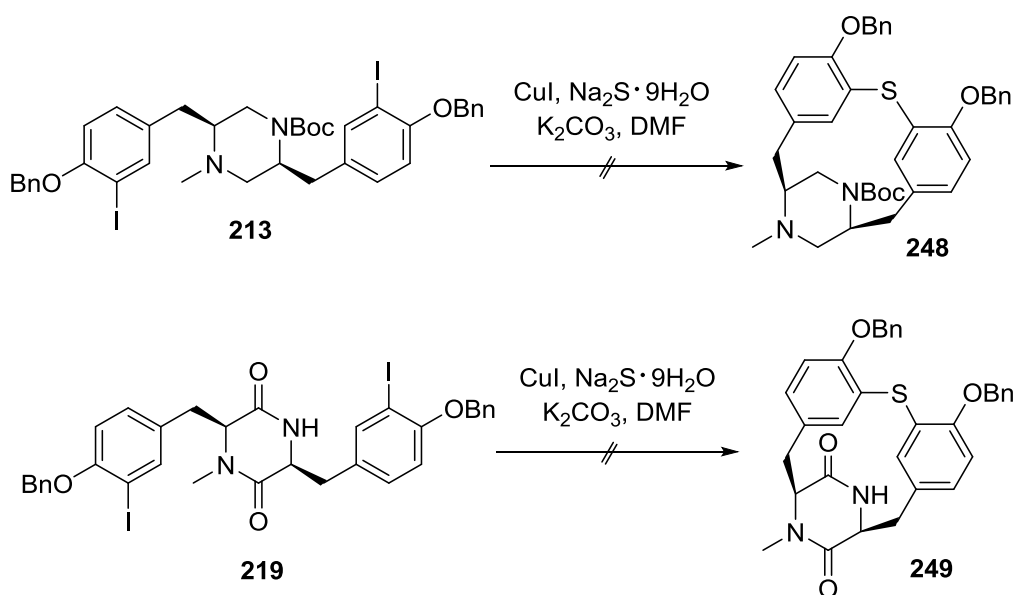


Scheme 3.55

Under optimised conditions, a wide range of symmetrical diaryl sulfides **247** were synthesised by treating the corresponding aryl iodides **246** with CuI, $\text{Na}_2\text{S}\cdot 9\text{H}_2\text{O}$ and K_2CO_3 in DMF.

Presumably, diaryl sulfide was formed in a stepwise fashion, with a thiophenolate anion as the intermediate.

Due to its experimental simplicity and a high level of functional group toleration, this sulfuration method was initially tested with both piperazine **213** and DKP derivative **219** (Scheme 3.56).

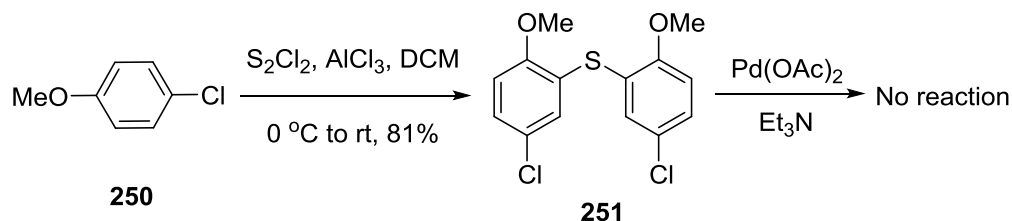


Scheme 3.56

However, no positive results were obtained after subjecting the two substrates to similar reaction conditions as reported. A large degree of deiodination was observed in both cases, along with recovery of part of the starting materials. In the case of the attempted cyclisation with **219**, isomeric products were also obtained due to the basic reaction conditions.

In contrast to Cu-catalysed C–S bond forming reactions, diaryl sulfides could be synthesised at lower temperature. It has been reported that benzene could react with S₂Cl₂ in the presence of AlCl₃ to give biphenyl sulfide.¹¹⁸ This potentially useful reaction might consist of two electrophilic aromatic substitution steps. Before applying this method to the piperazine system, the model reaction with 4-chloroanisole **250** was performed (Scheme 3.57). Upon exposure of

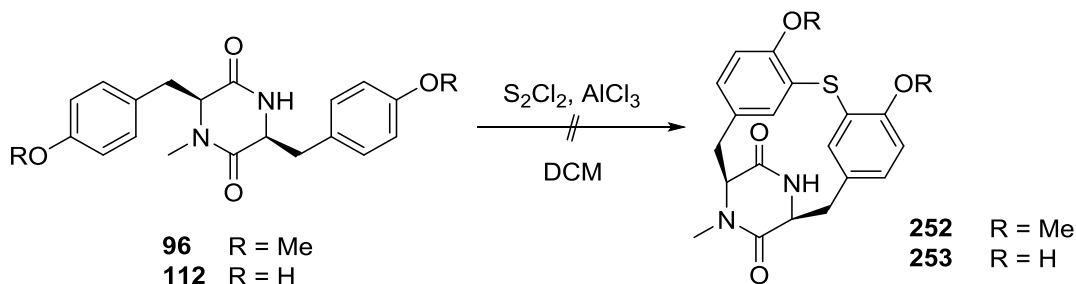
4-chloroanisole to S_2Cl_2 and $AlCl_3$ in dichloromethane, it was pleasing to see the formation of diaryl sulfide **251** in 81% yield.



Scheme 3.57

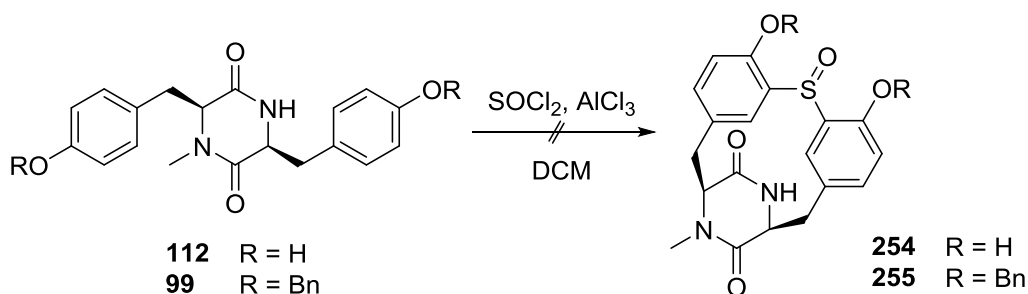
Fascinated by the palladium-catalysed detelluration of diaryl tellurides, the extrusion of the sulfur atom within **251** was also attempted with the combination of $Pd(OAc)_2$ and triethylamine. However, no reaction occurred in this case. This inertness might be due to the strong C–S bond compared with the C–Te bond. It was then hoped that the alternative Raney nickel-mediated conversion of diaryl sulfide to biaryl product would be an efficient transformation to form the desired C–C bond.

The intramolecular sulfuration was explored first with DKP substrates (Scheme 3.58). When **96** was treated with S_2Cl_2 and $AlCl_3$, mainly starting material was recovered with dimeric products being detected by mass spectrometry. Further diluting the reaction mixture did not essentially change the outcome. For the reaction with bis-phenol **112** as the substrate, no reaction was furnished.



Scheme 3.58

Effort has also been made on the synthesis of cyclic sulfoxide that was anticipated to be converted to sulfide after subsequent deoxygenation.^{119,120} However, no promising result was achieved in this approach (Scheme 3.59). While the employed conditions mainly effected the debenzylation of DKP **99**, the reaction between bis-phenol **112** and thionyl chloride in the presence of AlCl_3 gave a mixture of products, without the formation of the desired diaryl sulfoxide **254**.



Scheme 3.59

At this stage, most attempts to the synthesis of biaryl piperazines had been fruitless. Since the yields of the piperazine coupling products from the Pd-catalysed Suzuki-Miyaura coupling approach were too low, the synthesis was not carried on for further transformations. However, the less efficiency of the intramolecular piperazine coupling than the DKP coupling indicated a conformational difference between these two classes of substrates, which is analysed below.

3.4 Comparison of the Conformation of DKPs and Piperazines

Thorough experimentation revealed that the intramolecular coupling of piperazines could be accomplished, but the reactions were not as satisfactorily efficient as those with DKP substrates. Clues for the different reactivity between these two classes of structures might be found from the conformational analysis of DKP and piperazine substrates and the

corresponding coupling products which were considered to be highly strained structures. Presumably, the final coupling products should be able to reflect the conformations of the intermediates involved in the transition states of the intramolecular coupling processes.

In terms of DKP compounds, the central diketopiperazine ring is considered to be a semi-rigid structure and can exist in either a boat form or an essentially flat conformation (Figure 3.9).¹²¹ Studies have shown that the boat form is the lowest-energy structure, but the energy difference between these two forms is small (less than 5 kcal/mol). Therefore the boat and the planar conformers can easily exchange with the affect of weak external forces.¹²²

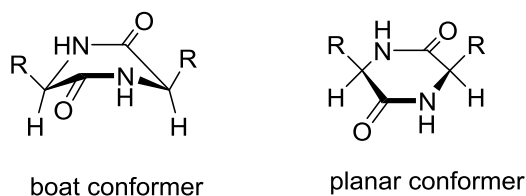


Figure 3.9: Possible conformations of 2,5-diketopiperazines.

It seems plausible that during the Pd-catalysed coupling reaction the DKP ring tends to adopt a planar conformation in which the two aromatic rings could rotate along the corresponding C–C bonds to render them in close proximity. Favourable side chain orientations would then be achieved for the new C–C bond formation. Interestingly, the X-ray crystal structure of **34** reported by Hutton and co-workers showed that the DKP ring adopts a flattened-boat conformation, very close to a planar form (Figure 3.10).²³ This feature, accompanied by other distortions balanced and minimised the steric constraint within the molecule.

Without the cyclic amide functionalities, the piperazine ring is not as flat or rigid as the DKP moiety. And the intramolecular coupling turned out to be more difficult at this stage.

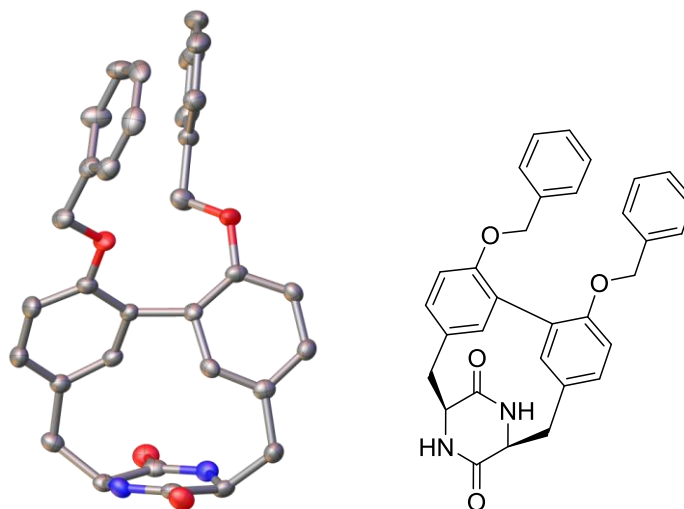


Figure 3.10: Crystal structure of DKP **34** (Reproduced using data requested from the Cambridge Crystallographic Data Centre).

Referring to the Suzuki-Miyaura coupling approach, only the reactions with piperazine substrates **171**, **213** and **215** successfully produced small amounts of coupling products, other than those with **169**, **217** and **161** (Figure 3.11), which were initially proposed to be the superior substrates for intramolecular aryl coupling according to the conformational analysis in Section 3.1.2.

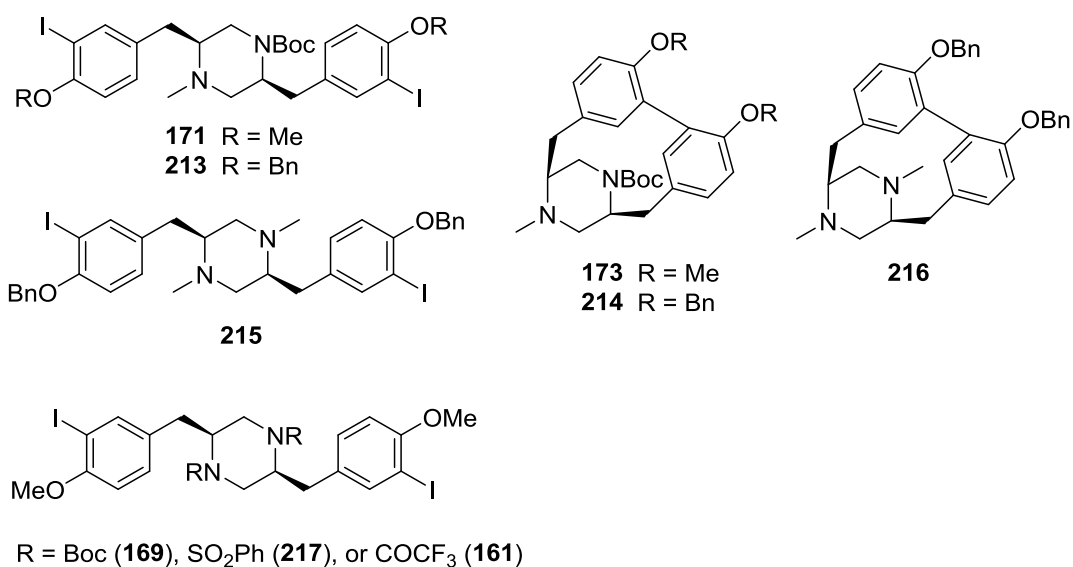


Figure 3.11

On the one hand, while all the piperazines **171**, **213** and **215** tend to adopt chair conformations at room temperature, conformational equilibrium might provide a substantial extent of favourable conformers for the intramolecular coupling process under the Pd-catalysed reaction conditions. In the cases of **169**, **217** and **161**, even though the piperazine rings were assumed to exist in a large degree of the boat conformers with the methylene groups in the *pseudo*-axial positions, the orientations of the two aromatic rings might be unsuitable for the formation of the biaryl linkage.

On the other hand, one could imagine that the piperazine coupling products **173**, **214** and **216** would represent a class of strained structures, even though no X-ray crystal structures were obtained. Referring to the relevant structure of piperazinomycin (**21**), the piperazine ring prefers to exist in a chair form, which was supported by the crystal structure of this natural product (Figure 3.12).¹⁸

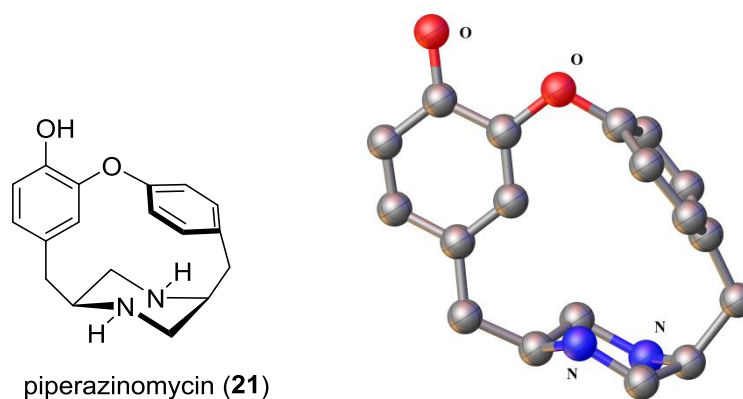
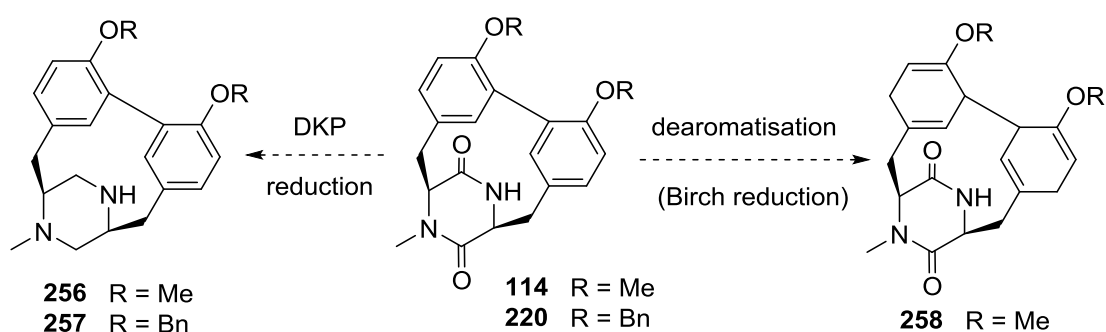


Figure 3.12: Piperazinomycin and its X-ray crystal structure (Reproduced using data requested from the Cambridge Crystallographic Data Centre).

While it is unlikely that the piperazine units within **173**, **214** and **216** would adopt ordinary chair conformations, certain favourable dispositions would be attained by these molecules which potentially possess higher strain energy than the corresponding DKP coupling products.

3.5 Attempted Transformations with Biaryl Coupling Products

As the DKP products **114** and **220** were synthesised in the Pd-catalysed coupling approach, they possessed potential synthetic utility and could serve as advanced intermediates for the synthesis of herquiline A and B. Herein, two transformations were proposed as shown in Scheme 3.60: the reduction of the DKP ring to a piperazine moiety and the reductive dearomatisation of the biphenyl unit.



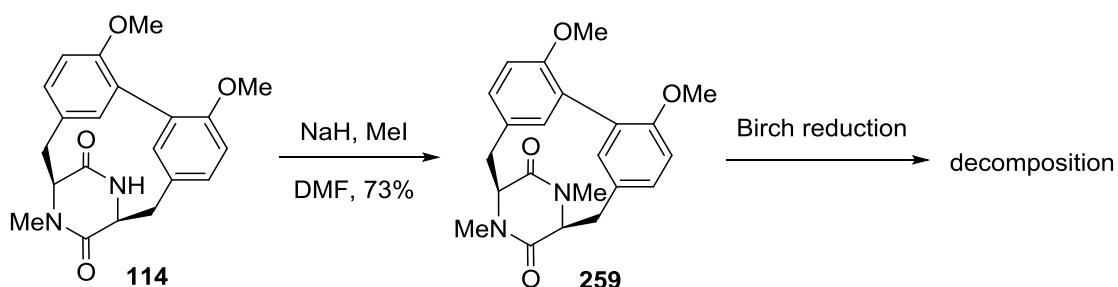
Scheme 3.60

Our efforts started from the oxidation state adjustment of the DKP ring within **220**. Treatment of this DKP substrate with LAH failed to afford the desired piperazine **257**. Instead, decomposition occurred and no reduction product was detected by mass spectrometry. Reduction of **220** with $\text{BH}_3\cdot\text{THF}$ complex in THF did not proceed at room temperature. When the reaction system was heated to reflux, slow decomposition was again observed and no isolable entity was delivered from the system. These negative results might reveal that the conversion of DKP **220** to a considerably more strained structure **257** was a difficult process.

Alternatively, the Birch reduction of **114** could be carried out before the reduction of the DKP ring. Referring to the literature, while the Birch reduction of simple linear biphenyl substrate often led to a mixture of regioisomers,^{123,124} no precedent Birch reduction of cyclic rigid biphenyl substrates has been reported. It was conceived that DKP **258** was the most

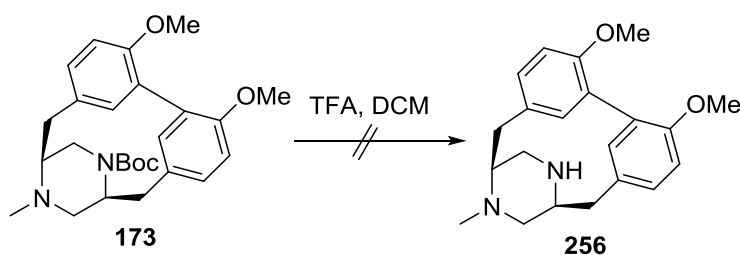
favourable and flexible product since the replacement of the Csp²–Csp² linkage in **114** with the Csp³–Csp³ one would substantially reduce the strain energy within the molecule. The attained flexibility was also presumed to be beneficial for subsequent DKP reduction process.

Initial conduction of the Birch reduction (Na/NH₃) in the presence of proton source (EtOH or *t*BuOH) did not provide the desired product **258**. Instead, an inseparable mixture of multiple reduced products was isolated from the reaction system. Based on NMR and mass spectral analysis, it was found that one aromatic ring persisted under the conditions while two double bonds from the other phenyl ether moiety were reduced. The obtained intermediates were found to be inert to a further Birch reduction. On the contrary, subsection of the symmetrical DKP **259** to a similar Birch reduction resulted in complete decomposition without producing any valuable substances (Scheme 3.61).



Scheme 3.61

Decomposition was also observed during the attempt in the cleavage of the Boc protecting group within **173** (Scheme 3.62).

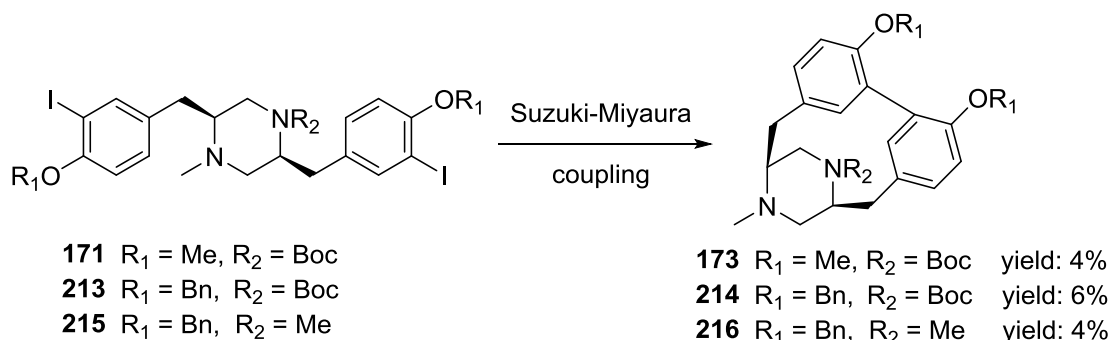


Scheme 3.62

Since both **173** and the potential deprotected piperazine product **256** were considered to be very strained molecules, it was likely that other reaction pathways dominated under acidic conditions to release the strain energy.

3.6 Summary

This Chapter described the investigation on Cu- and Pd-mediated intramolecular aryl coupling of piperazines. While the oxidative coupling of organocuprates led to oxygenated piperazine products exclusively, small amounts of the desired coupling products were successfully afforded *via* a Pd-catalysed Suzuki-Miyaura coupling protocol (Scheme 3.63).



Scheme 3.63

Further attempts in optimising the reaction conditions failed to improve the yields. And the low efficiency of the coupling reactions was attributed to the unfavourable conformations of piperazine substrates.

In contrast to piperazines, DKP derivatives were found to be superior substrates for Suzuki-Miyaura coupling reactions. The corresponding coupling products, analogues of the natural product mycocyclusin, were obtained in relatively higher yields. Further operations on these

DKP coupling products were unsuccessful towards the synthesis of the herqulines. The conformational analysis of the diketopiperazine and piperazine substrates was also presented.

The viability of C–C bond formation from organochalcogenides has also been tested. Unfortunately, our efforts were limited by the difficulty in constructing cyclic biaryl sulfides or tellurides from piperazine substrates.

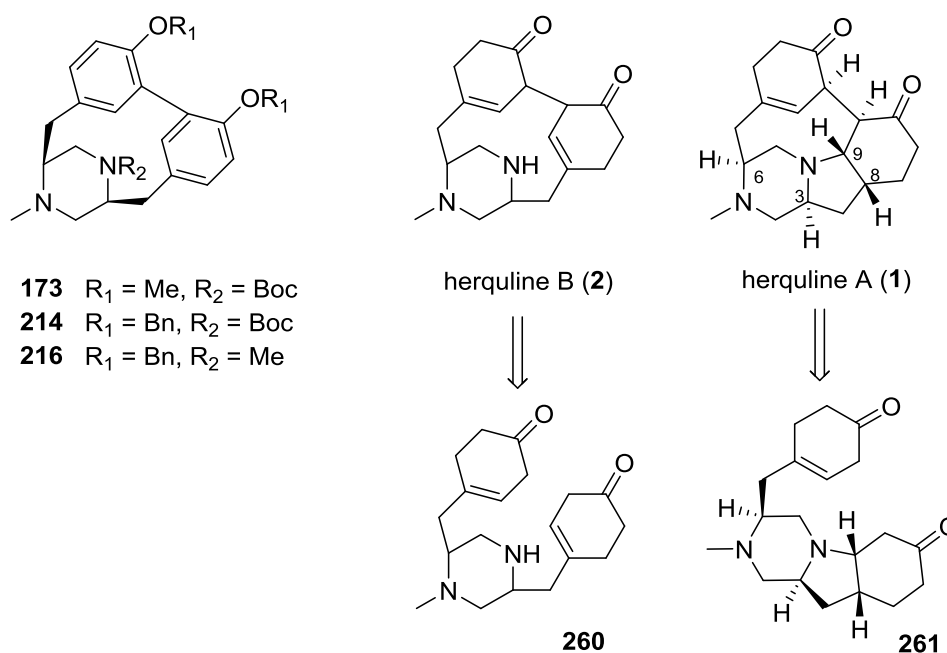
At this stage, all our aryl coupling approaches towards herquline A and B appeared to be challenging and difficult. A conceptually different strategy featuring the intramolecular enolate or enol silane coupling was employed and discussed in the next Chapter.

CHAPTER 4 OXIDATIVE ENOL SILANES OR ENOLATES

COUPLING APPROACH

4.1 Initial Considerations and Retrosynthetic Analysis of Herquiline A

Our efforts in the aryl coupling approach towards herquiline A and B indicated that piperazines were not the ideal substrates for intramolecular coupling reactions to give biaryl products which were considered to be the key intermediates during the synthesis. This low reactivity was attributed to the unfavourable conformation of piperazine substrates and the high strain energy of the corresponding biaryl coupling products.



Scheme 4.1

Close scrutiny of the structure of herquiline B as shown in Scheme 4.1, one could imagine that the existence of the $\text{Csp}^3\text{-Csp}^3$ bond within the 1,4-dicarbonyl unit renders this molecule

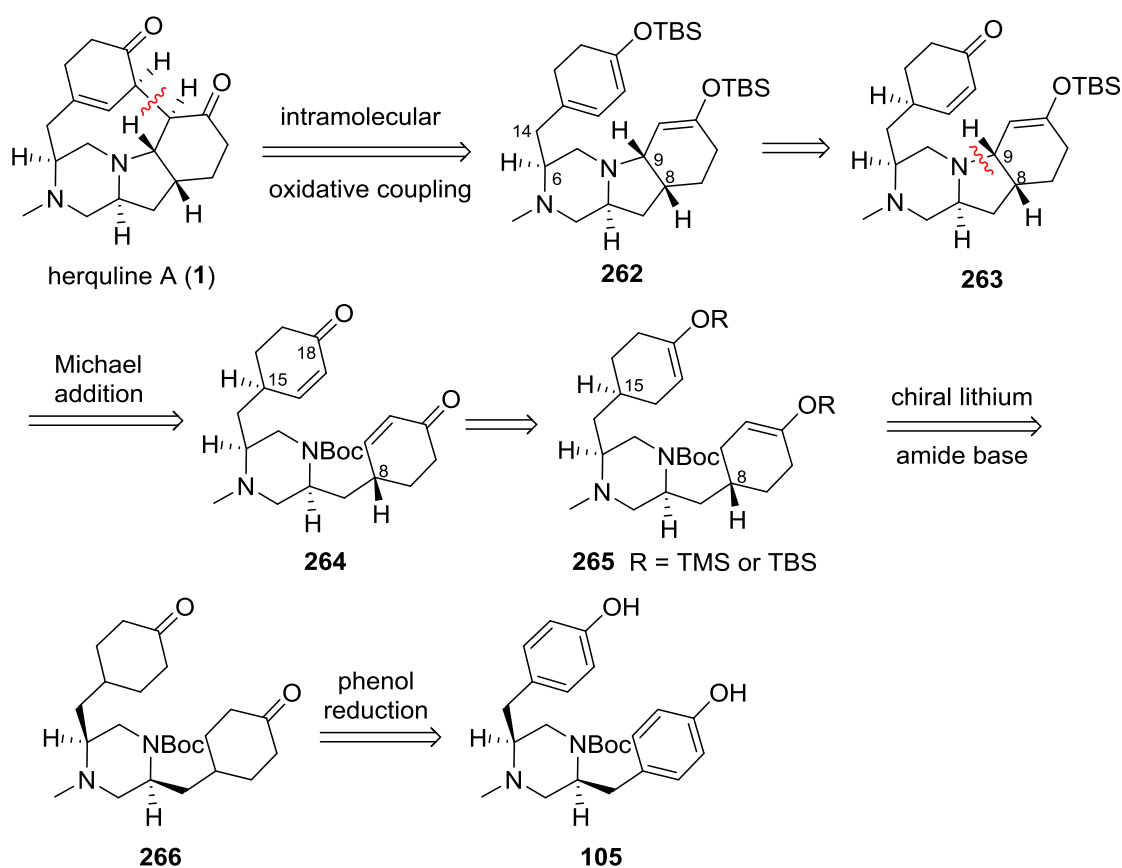
more flexible than the biaryl piperazines **173**, **214** and **216** possessing Csp²–Csp² biaryl linkages.

In order to perform the intramolecular coupling reaction at the piperazine stage, it seemed reasonable that the cyclisation of **260** would be more favourable than the previously investigated biaryl couplings, hoping that the flexibility brought from the two Csp³ centers within the 1,4-dicarbonyl moiety would compensate for the unfavourable conformation issue with the piperazine rings. Similarly, herquline A could derive from the cyclisation of **261** or its derivatives.

Based on the above analysis, a conceptually distinct approach evolved to tackle the challenging cyclisation problem, that is, formation of the 1,4-diketone functionality at the piperazine stage. For the synthesis of herquline A whose absolute structure has been elucidated, success in this new strategy would require addressing its two conspicuous structural features: the 1,4-dicarbonyl unit and the stereochemistry within the tricyclic ring system. For the former one, various methods have been developed for the construction of 1,4-diketone motifs.^{125,126} At a practical level, the oxidative coupling of silyl enol ethers or enolates provided a promising route, since no complex functionalisation of the bis-ketone precursors was required compared with other methods. For the generation of the asymmetric centers within the fused tricyclic ring, while the two stereogenic centers at C-3 and C-6 could derive from L-tyrosine starting material, those at C-8 and C-9 were conceived to be generated by using a chiral lithium amide base during the synthesis.

As outlined in Scheme 4.2, the retrosynthesis of herquline A commenced from the disconnection of the 1,4-dicarbonyl group, anticipating that herquline A (**1**) could be synthesised *via* the intramolecular oxidative coupling of bis-silyl enol ether **262** and that the

fused tricyclic system would be constructed prior to the formation of the nine-membered ring. This sequence was based on the assumption that the rotational freedom of one enol silane ring would be constrained due to the rigidity of the tricyclic ring system, which was quite different from the situation with aryl coupling substrates whose two aromatic moieties could both move freely.



Scheme 4.2

Nevertheless, it was difficult to predict at this stage whether this entropic advantage would be beneficial or not for the intramolecular coupling to occur, considering the structure of **262**. If this bis-silyl enol ether could be obtained with the specific stereochemistry at the C-8 and C-9 positions, which is in accord with that of the natural product, the shape of the molecule, especially the tricycle in which the H-8 and H-9 adopt a *cis* configuration, causes the enol

ether ring to pose away from the dienone ether coupling partner, which could be partially reflected by the X-ray crystal structure of herquline A (Figure 4.1). Even though the dienone ether ring of **262** could rotate along the C6–C14 bond to reside toward the tricycle, the challenge of generating a highly strained product was a concern.

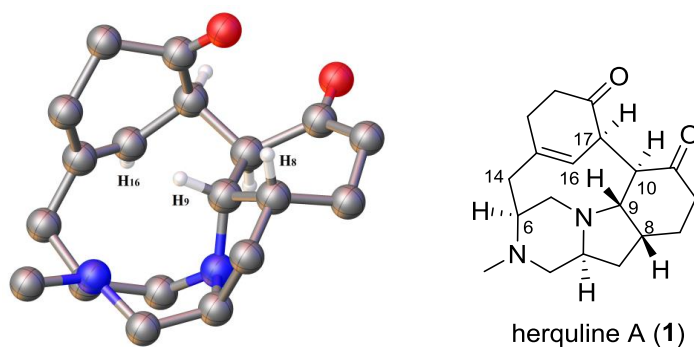


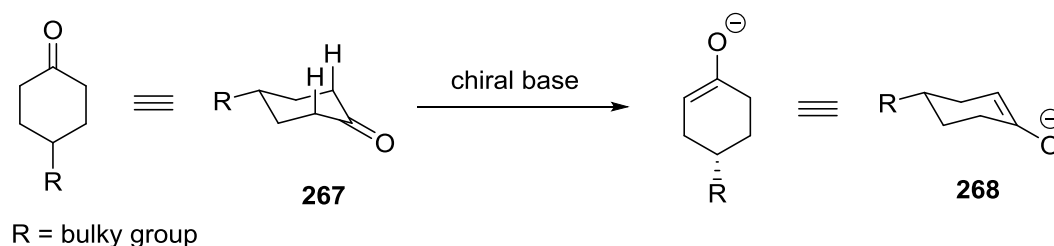
Figure 4.1: X-ray crystal structure of herquline A (Reproduced using data requested from the Cambridge Crystallographic Data Centre).

Another uncertainty with this approach is the diastereoselectivity of the intramolecular oxidative coupling of the silyl enol ethers, as a mixture of diastereoisomers may be obtained with respect to the stereochemistry within the 1,4-dicarbonyl moiety. Referring to the X-ray crystal structure of the natural product in Figure 4.1, it can be found that the alkenyl hydrogen H-16 within the cyclohexenone ring poses away from the tricyclic ring system to avoid the potential interaction with H-9, while the two hydrogens within the 1,4-diketone unit adopt a *cis* configuration. Therefore, one could imagine that the structure possessed by herquline A should be one of the most favourable products with minimal steric energy, if the intramolecular enol silane oxidative coupling could be furnished.

To carry on the retrosynthesis, the conjugated dienol ether derivative **262** was proposed to derive from **263** utilising the combination of MeMgBr/FeCl₃ (the Kharasch reagent), which has been reported to effect the generation of 'thermodynamic' silyl dienol ether from cyclic

enone with high regioselectivity.^{127,128} Intermediate **263** could arise from **264** through a three-step sequence involving the cleavage of the Boc protecting group, the intramolecular *aza*-Michael addition of the deprotected piperazine to the enone moiety and the *in situ* generation of silyl enol ether from the resultant enolate. It was anticipated that this challenging transformation could be accomplished thermally by treating bis-enone **264** with TBSOTf and 2,6-lutidine. The stereochemistry of the *aza*-Michael addition was expected to be directed by the stereogenic center at C-8 position within molecule **264** and a *cis* configuration would be adopted between H-8 and H-9.

At this stage, it seemed clear that the stereocontrolled installation of the stereogenic center at C-8 within piperazine **264** would be crucial for the whole synthesis. Based on the previous systematic work on chiral lithium amide bases in the Simpkins group,^{129,131} it was proposed that the asymmetric deprotonation of bis-ketone **266** with a proper chiral base would generate the stereogenic centers at C-8 and C-15, rendering bis-enol silane **265** as the intermediate after trapping the bis-enolate with TMSOTf or TBSOTf.

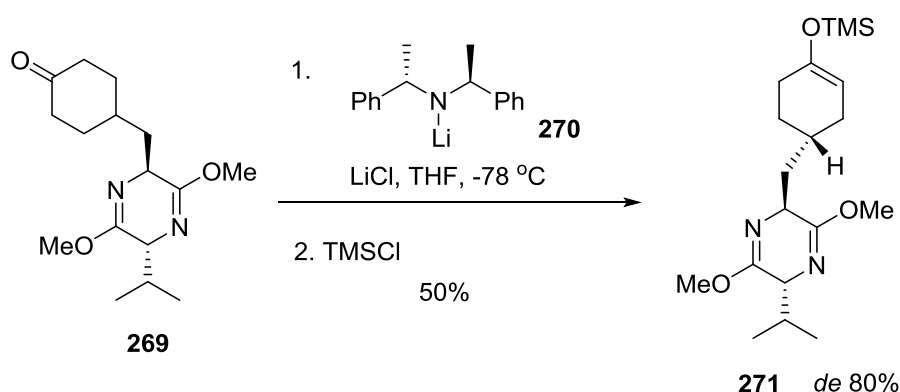


Scheme 4.3

Various chiral lithium amide bases have been developed and used successfully in enantioselective deprotonation of prochiral cyclic ketones, especially conformationally locked cyclohexanones, such as **267** in Scheme 4.3.¹²⁹⁻¹³¹ While studies on chiral bases mainly

concentrated on methodology development with structurally simple substrates, few reports have been published regarding using chiral bases in target-oriented synthesis.¹³²⁻¹³⁴

One example related to this topic is the total syntheses of chlorotetaine, bacilysin and anticapsin, a series of structurally similar antifungal natural products.^{132,133} During the synthesis, cyclohexanone **269**, which was tethered with a six-membered ring by a methylene group, was deprotonated using lithium (*S,S*)-bis(1-phenylethyl)amide **270** and was subsequently converted to silyl enol ether **271** with a *de* of 80% (Scheme 4.4). In our case, even though the configuration at C-15 position of **265** would be lost in subsequent operations, it was anticipated that both cyclohexanones within **266** would be converted into the corresponding silyl enol ethers in the chiral base step, which increased the challenge of synthesis.



Scheme 4.4: Deprotonation of cyclohexanone with chiral lithium amide base.

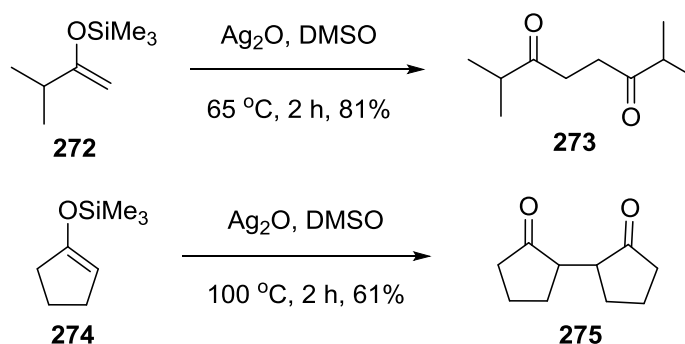
The previously synthesised bis-phenol **105** could then serve as the precursor of bis-ketone **266**. In the forward direction, a catalytic hydrogenation of bis-phenol **105** could be employed, followed by oxidation of the resultant bis-cyclohexanol to deliver the desired bis-cyclohexanone **266** (Scheme 4.2).

4.2 Introduction to the Oxidative Coupling of Enol Silanes and Enolates

4.2.1 1,4-Dicarbonyl Formation *via* Enol Silane Oxidative Coupling

Silyl enol ethers are important and versatile enol derivatives and have been employed in different types of C–C bond forming transformations, among which the oxidative coupling of two silyl enol ethers is a direct and powerful method for the construction of 1,4-dicarbonyl motifs. To date, a variety of oxidants have been developed for this coupling method, most of which are metallic species, including Ag(I), Mn(III), Ce(IV) and V(V) oxides or salts.

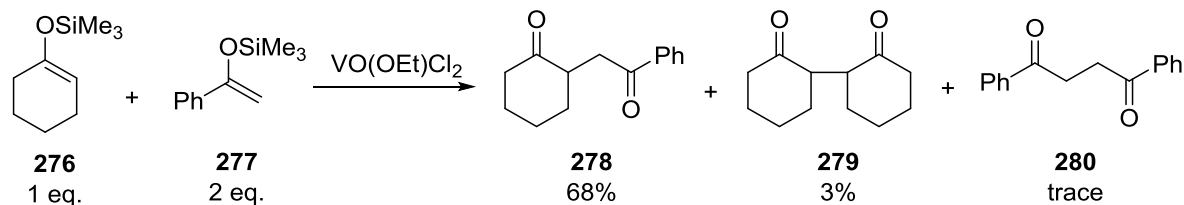
In 1975, Saegusa and co-workers reported that reactions between less substituted silyl enol ethers and Ag₂O in DMSO gave 1,4-diketones in high yields (Scheme 4.5).¹³⁵ Cyclic or more substituted substrates were found to be less reactive toward oxidation with Ag₂O. Higher temperature was usually needed in these cases and relatively lower yields were obtained, such as the case with silyl enol ether **274**.



Scheme 4.5

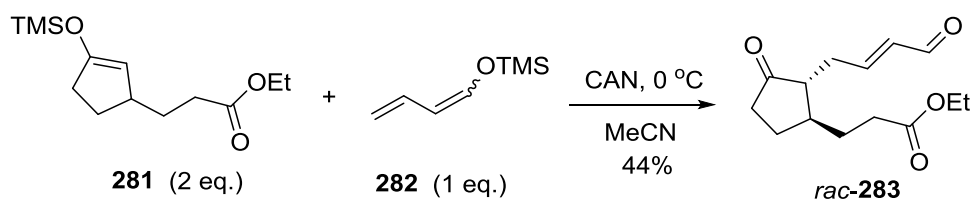
Unsymmetrical 1,4-diketones could be fashioned from the cross-coupling of two different silyl enol ethers. In this case, a superstoichiometric quantity of one coupling partner was usually used in order to obtain a higher degree of chemoselectivity. As exemplified by the coupling reaction between **276** (1.0 eq.) and **277** (2.0 eq.) in Scheme 4.6, diketone **278** was

delivered as the main product, due to the excess quantity and the low oxidisability of the styrene-type substrate **277**.¹³⁶



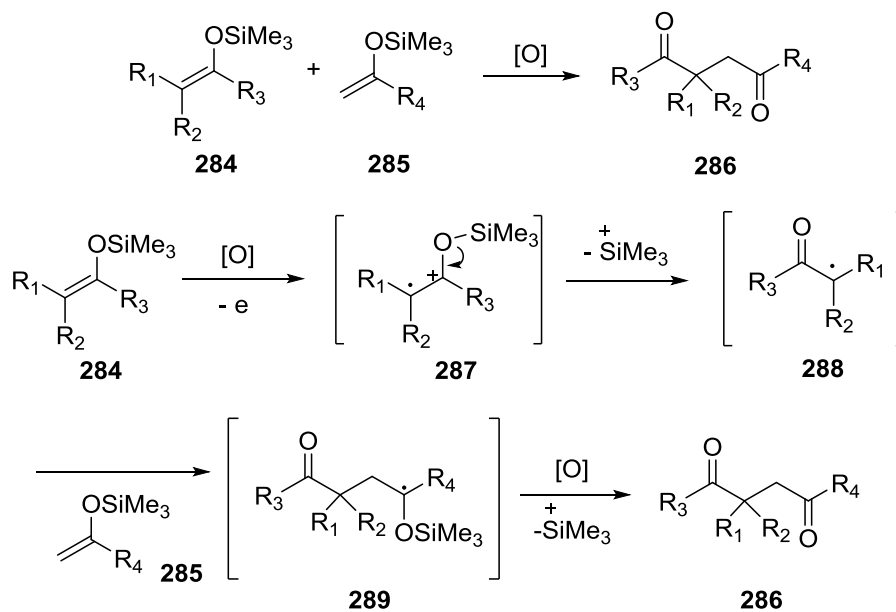
Scheme 4.6

A similar concept was also applied in the cross-coupling between silyl dienol ether and silyl enol ether in Ruzziconi and co-workers' studies (Scheme 4.7).¹³⁷ Since dienol ether was more susceptible to oxidation with respect to silyl enol ether, upon treating **282** (1.0 eq.) and **281** (2.0 eq.) with CAN, racemic diketone **283** was fashioned exclusively with high γ -selectivity.



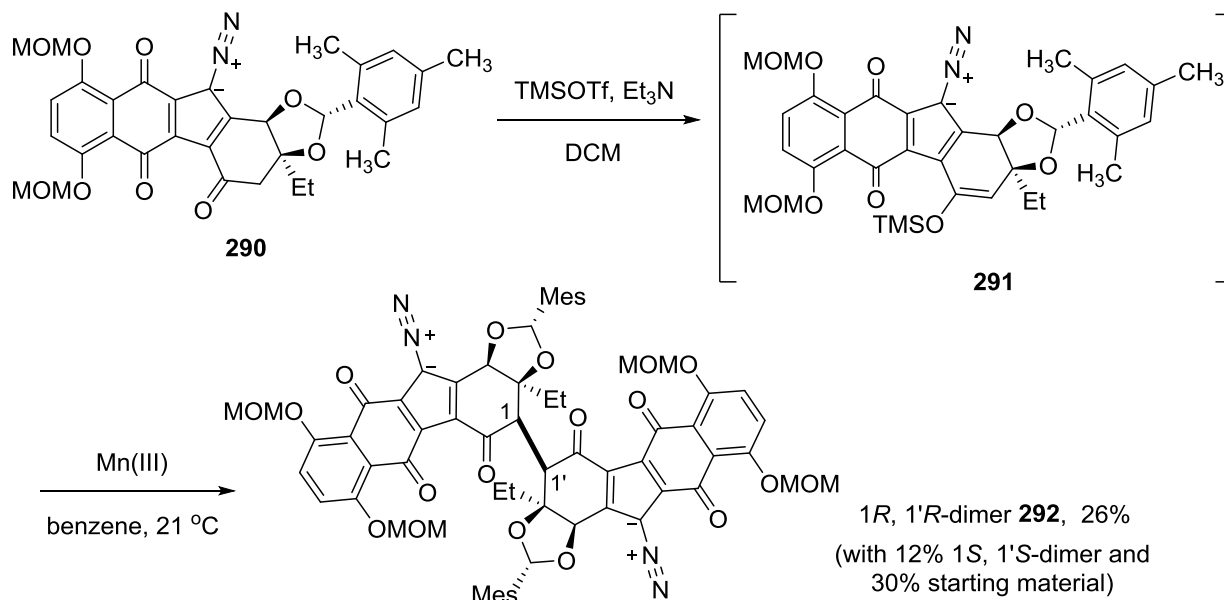
Scheme 4.7

A mechanistic hypothesis has been proposed for oxidative silyl enol ether coupling.^{136,138} As shown in Scheme 4.8, one electron oxidation of silyl enol ether **284** by the oxidant would lead to a transient radical cation **287**, which could undergo a desilylation process to generate the electrophilic radical **288**. Cross-coupling was accomplished after the intermolecular addition of radical **288** to a second silyl enol ether to form radical adduct **289**. After further oxidation of the resultant radical followed by desilylation, the final diketone **286** was afforded.



Scheme 4.8

This methodology was adopted by the Herzon research group in the synthesis of lomaiviticin aglycon (Scheme 4.9).^{139,140}



Scheme 4.9

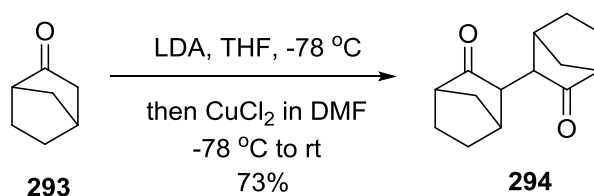
Treatment of monomeric diazo-containing TMS enol ether **291** with Mn(III) hexafluoroacetoacetate led to C–C bond formation to give the desired 1,4-diketone **292** in 26%

yield, along with starting material and the undesired bis-epimer. Although the yield of this dimerisation was modest, the enol silane oxidative coupling approach was truly impressive to construct such molecular complexity.

4.2.2 Advances in Oxidative Enolate Coupling

Oxidative enolate coupling is another method for the convergent synthesis of 1,4-dicarbonyl moieties. The enolates generated *in situ* from the corresponding carbonyl substrates are oxidised directly without any separation of the enol intermediates, which is different from the silyl enol ether coupling strategy. The earliest studies largely focused on the C–C bond formation process with the stereochemical courses being rarely addressed.

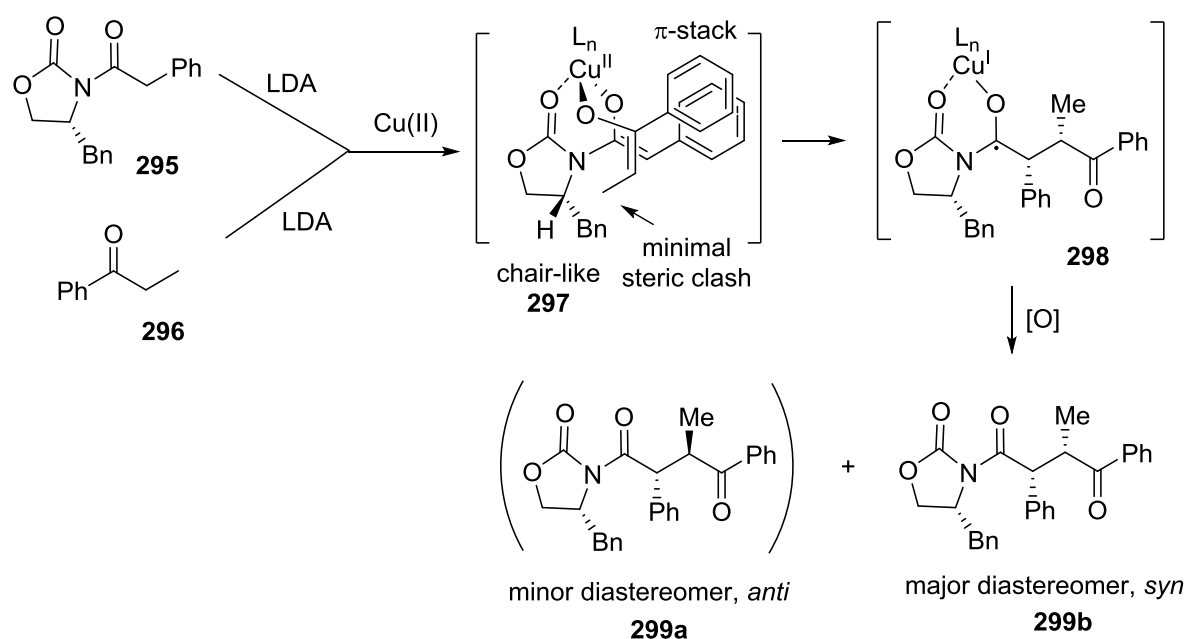
Saegusa and co-workers reported the CuCl₂-mediated oxidative coupling of ketone enolates in 1975.¹⁴¹ Representatively, the coupling of the lithium enolate generated from ketone **293** proceeded smoothly upon treatment with CuCl₂ in DMF to give dimer **294** in 73% yield (Scheme 4.10).



Scheme 4.10

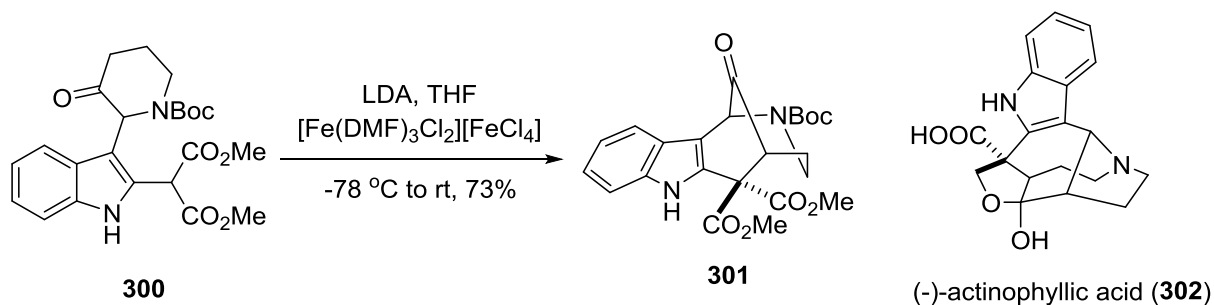
Baran and co-workers published their extensive study on the intermolecular hetero-coupling of enolates in 2008.^{142,143} A wide range of 1,4-dicarbonyl compounds were synthesised from the cross-coupling of oxazolidinone- and ketone-derived enolates in good yields. By

combining chiral oxazolidinone substrates with appropriate oxidants, synthetically useful levels of diastereocontrol could be achieved (Scheme 4.11). For example, treating the lithium enolates generated from **295** and **296** with copper(II) 2-ethylhexanoate afforded the cross-coupled product **299** as a 1.6:1 mixture of diastereomers in 55% yield. According to the proposed mechanism, the observed diastereoselectivity was attributed to the Cu(II)-chelated intermediate **297** as shown below.



Scheme 4.11

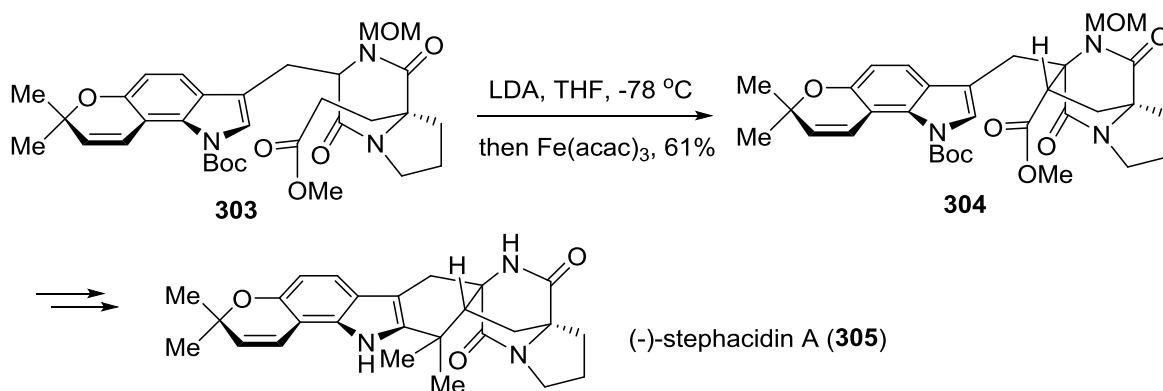
The utility of intramolecular enolate coupling in natural product syntheses is more appealing and relevant to our project. In this case, a dienolate is usually involved and one example can be found in the total synthesis of actinophyllic acid (**302**) accomplished by Overman and co-workers (Scheme 4.12).¹⁴⁴ After treating racemic keto-malonate **300** with LDA, the Fe(III)-mediated intramolecular coupling of the malonate and ketone enolates took place to afford the tetracyclic ketone *rac*-**301** in 73% yield. It was noteworthy that the cyclisation proceeded smoothly without any protection of the indole moiety in **300** and therefore three equivalents of LDA were essentially needed to assure an acceptable yield.



Scheme 4.12

The racemic ketone **301** was transformed into the indole alkaloid (\pm)-actinophyllic acid after several further operations. Following a similar sequence, the enantioselective synthesis of (-)-actinophyllic acid was also accomplished.¹⁴⁵

Another application of intramolecular oxidative enolate coupling to natural product synthesis was exemplified in the total synthesis of stephacidins reported by Baran and co-workers.^{146,147}

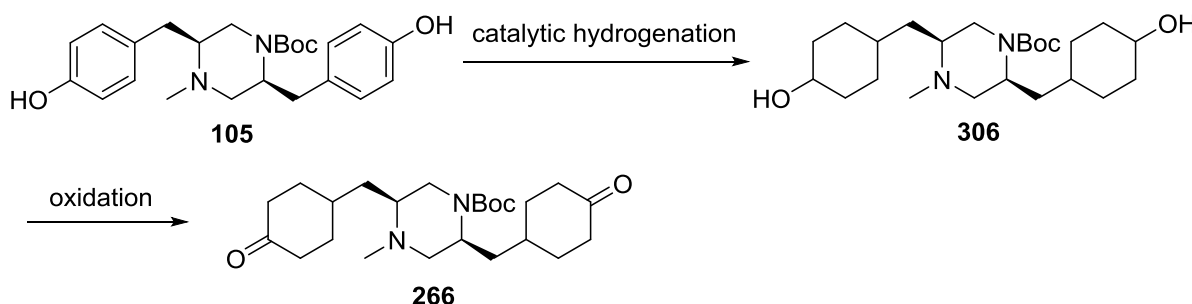


Scheme 4.13

The bridged diketopiperazine motif possessed by stephacidin A and B was constructed through the oxidative coupling of the corresponding ester and amide enolates derived from **303** (Scheme 4.13). The successful generation of the bicyclo[2.2.2]diazaoctane core within **304** demonstrated the oxidative enolate coupling as a powerful method for C–C bond formation with complex systems.

4.3 Initial Forward Synthesis

Based on the retrosynthesis of herquiline A, the conversion of bis-phenol **105** to bis-ketone **266** was initially investigated. It has been reported that the production of cyclohexanones could be realised from the direct hydrogenation of phenol substrates. However, during this type of selective reduction process, designed catalysts with special supports were usually employed, such as the Pd/mpg-C₃N₄ catalyst (Pd nanoparticles supported on a mesoporous graphitic carbon nitride).¹⁴⁸ With ordinary and commercially available catalysts, the selective catalytic hydrogenation of phenols in the literature usually led to a mixture of cyclohexanones and cyclohexanols, even under modified conditions.^{149,150} Concerned that the contamination of bis-ketone **266** with alcohols would be problematic for further operations, a step-wise protocol was adopted as shown in Scheme 4.14.

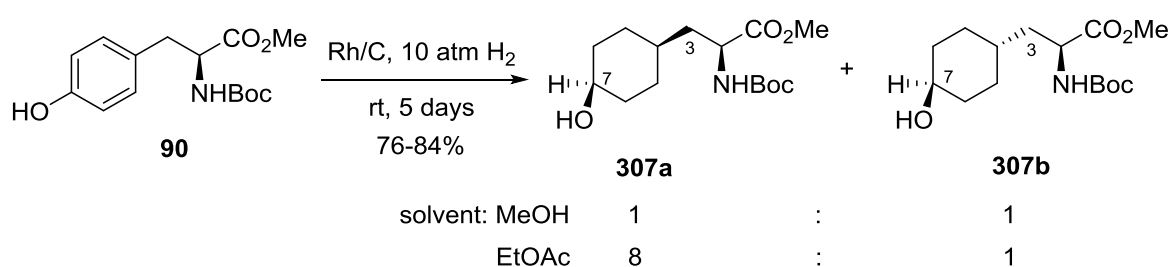


Scheme 4.14

Among the transition-metal catalysts that have been developed, rhodium and platinum derived catalysts are found to be effective for the transformation of phenols to cyclohexanols under mild conditions, compared with Ni, Ru or Pd catalysts, the reactions with which usually require higher temperature and/or pressure.¹⁵¹ In addition, Rh catalysts seem to be superior to Pt ones since the production of cyclohexane derivatives were usually observed during the hydrogenation of phenols with Pt catalysts, due to partial hydrogenolysis.^{152,153} Therefore, the hydrogenation of **105** with a rhodium catalyst was investigated in our project.

The reactions were initially carried out with 5% Rh/C (10 wt%) under 1 atm of H₂ in methanol or ethyl acetate at room temperature. Unfortunately, no hydrogenation was effected. When the pressure was increased to 5 atm, a slight degree of conversion (6%) of **105** to **306** and the half-reduced piperazine intermediates was observed after 3 days. To drive the reaction to completion, a higher pressure (12 atm) was employed consequently. However, the reaction was still sluggish and only 32% conversion of **105** was achieved after 8 days. The use of Rh/Al₂O₃ as the catalyst was not beneficial for the progress of the reaction. Further increasing the catalyst loading to 20-30 wt% and warming up the reaction system (50-60 °C) were only slightly effective in accelerating the reaction. Most of our attempted reactions appeared not to be efficient in providing the desired bis-alcohol product. Due to the pressure limit on hydrogen supply, no hydrogenation was performed at an even higher pressure.

In order to examine the effectiveness of the hydrogenation conditions we employed, model reactions were performed with mono-phenolic substrate **90** (Scheme 4.15). Surprisingly, the hydrogenation proceeded smoothly by treating the substrate with Rh/C (20 wt%) in methanol at room temperature under a H₂ pressure of 10 atm. An increase in temperature in this case was successful in shortening the reaction time.



Scheme 4.15

According to the NMR spectra, two diastereoisomers of the cyclohexanol derivative were obtained. Presumably, the C-3 amino acid side chain within **307** would reside in the equatorial

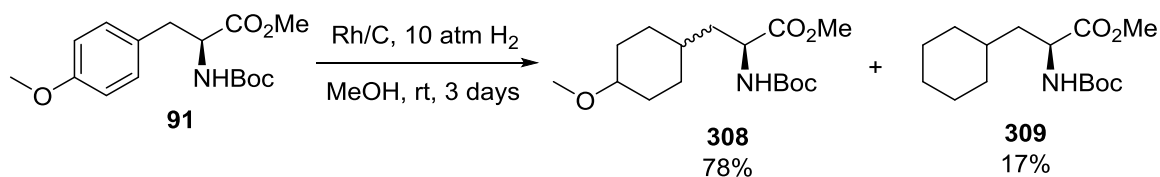
position of the chair conformer and therefore the two isomers could be differentiated by the chemical shifts of the corresponding protons geminal to the secondary hydroxy group. Since the chemical shift of the equatorial proton is usually downfield of the axial one and the signal for the axial proton tends to be invariably broader, the multiplet at 3.53 ppm was assumed to derive from the *trans*-isomer **307b** whose H-7 was proposed to be in the axial position.* The proton with a chemical shift of 3.97 ppm was then correlated to the one from the *cis*-isomer **307a**. Therefore, the ratio of the *cis*-isomer to the *trans*-isomer was determined to be around 1:1.

Interestingly, when ethyl acetate was used as the solvent, the hydrogenation favoured the *cis*-alcohol, with a ratio of 8:1 for the two isomers. A trace amount of by-product arising from the hydrogenolytic cleavage of the hydroxy group was also isolated from the reaction system this time.

While the reaction pathway for hydrogenation is still undefined and usually varies with different systems, it has been reported that solvent along with substrate structure, catalyst and other parameters could affect the stereoselectivity of the reaction.¹⁵⁴⁻¹⁵⁶

The hydrogenation of phenol ether **91** was a more favourable transformation compared to the one with phenol **90** (Scheme 4.16). When the reaction was conducted in methanol at room temperature, all starting material was completely hydrogenated within 3 days to afford the desired product **308** as the major component.

* The designation of *cis* or *trans* refers to the spatial location of the hydroxy group relative to the C-3 side chain on the cyclohexanol ring.

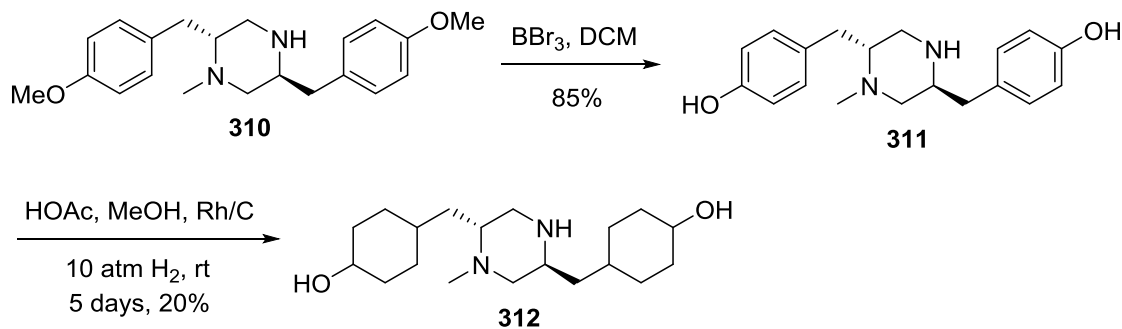


Scheme 4.16

Byproduct **309** was isolated in 17% yield in this case, indicating that the reduction of phenol ether tended to result in a larger degree of hydrogenolysis than that of phenol substrate under current conditions.

The success of these model reactions revealed that the adopted conditions were effective and suitable for the hydrogenation of phenols. Theoretically, the hydrogenation of bis-phenol **105** should be complete with sufficient reaction time, even though two phenol groups are present in the substrate. However, all our attempts indicated the low efficiency of these conditions. It is unlikely that the conformation of the substrate would have a substantially negative effect on hydrogenation process since no distinct steric hindrance exists to prevent the phenol moieties from being absorbed on the surface of the catalyst. It is possible that the catalyst was deactivated by the tertiary amino group within the substrate because amines have been reported to be potential catalyst poisons.¹⁵⁷

According to previous studies in the literature, the addition of organic acid to the hydrogenation system could prevent the inhibition or reduction of the catalyst activity by amino functionality.^{158,159} This strategy was not attempted with bis-phenol **105** due to the co-existing acid-sensitive Boc protecting group. Instead, the hydrogenation under acidic conditions was conducted with bis-phenol **311**, which derived from the demethylation of piperazine **310**, a by-product during our synthesis (Scheme 4.17).

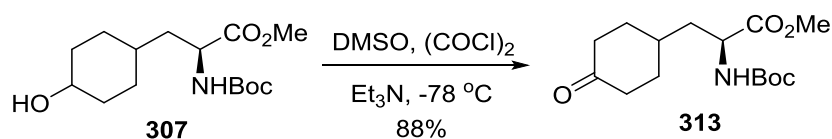


Scheme 4.17

Treatment of bis-phenol **311** with Rh/C or Rh/Al₂O₃ in 1:8 of acetic acid and MeOH (v/v) under 10 atm H₂ at room temperature led to a mixture of compounds after 5 days. The fully hydrogenated product **312** was isolated in 20% yield, along with starting material and the partially reduced intermediates. The products arising from hydrogenolysis process were also identified by mass spectrometry.

Since no improvement was made from this approach, the neutral hydrogenation conditions were employed as the standard ones for our system. And the synthesis was carried on with this low-efficiency hydrogenation step.

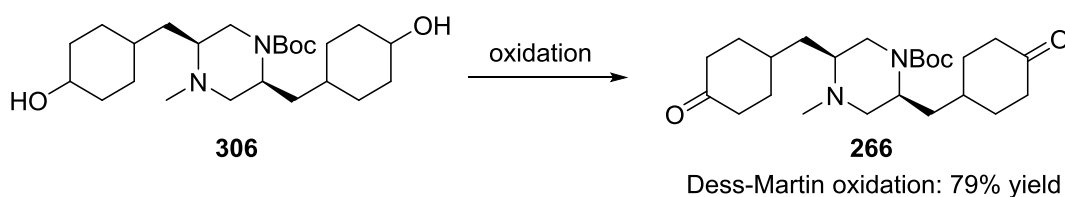
The oxidation of alcohols **307** to **313** was initially investigated as a model reaction. Under Swern oxidation conditions, ketone **313** was fashioned in high yield (Scheme 4.18).



Scheme 4.18

When the same oxidation conditions were applied to the bis-alcohol system, the desired bis-ketone **266** was delivered as the main product, accompanied by starting material and partially oxidised intermediates (Scheme 4.19). It turned out that the bis-ketone product and the

starting material **306** had similar polarity and could not be separated by column chromatography. A larger excess of oxidation reagents was employed in order to drive the reaction to completion. However, the product was still contaminated by a small amount of alcohol derivatives. The complete conversion of bis-alcohol **306** to bis-ketone product was finally realised in 79% yield with Dess-Martin periodinane in the presence of NaHCO_3 as an acid scavenger to prevent the cleavage of the Boc protecting group.



Scheme 4.19

With bis-ketone **266** in hand, the double deprotonation was studied. It was envisioned that the enolate anions could be trapped subsequently in the form of silyl enol ethers. A first attempt was performed by treating substrate **266** with LDA (2.5 eq.) followed by quenching the reaction with TMSCl (Entry 1, Table 4.1). The bis-silyl enol ether **314** was isolated in low yield, along with starting material and mono-silyl enol ether intermediates. A degree of degradation was observed for **314** during the purification process, presumably due to the presence of the labile TMS groups.

Accordingly, the bulkier TBS group was adopted to protect the bis-enolate. Either adding TBSCl to the bis-enolate solution or conducting the deprotonation in the presence of TBSCl, reactions were incomplete and a mixture of products was obtained (Entry 2, Table 4.1).

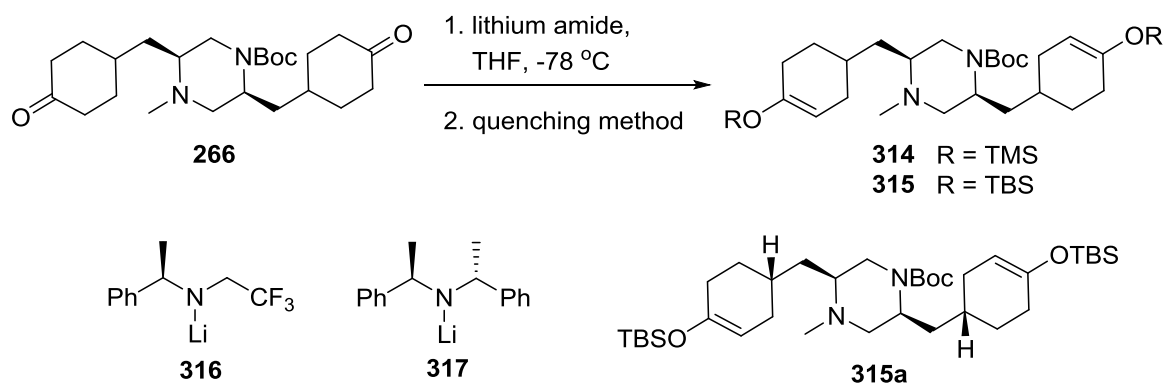


Table 4.1

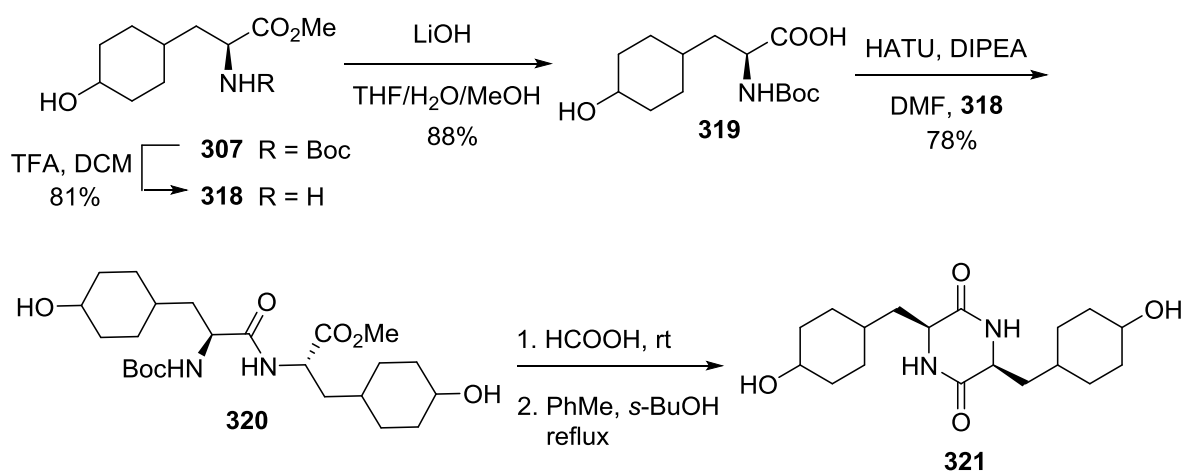
Entry	Deprotonation conditions	Quenching method	Reaction outcome
1	LDA (2.5 eq.), -78 °C, 1 h	TMSCl (5.0 eq.), -78 °C to 0 °C	314 (19%), 266 and other intermediates
2	LDA (3.0 eq.), -78 °C, 1 h	TBSCl (6.0 eq.), -78 °C to 0 °C (or rt)	315 (11%), 266 and other intermediates
3	317 (3.0 eq.), -78 °C, 1 h	TBSOTf (6.0 eq.), -78 °C to 0 °C	315 (44%) and other intermediates
4	317 (4.0 eq.), -78 °C, 1 h	TBSOTf (8.0 eq.), -78 °C to 0 °C	315 (48%)
5	316 (4.0 eq.), -78 °C, 1 h	TBSOTf (8.0 eq.), -78 °C to 0 °C	315 (41%)

Considering that TBSOTf is far more reactive than TBSCl, the bis-enolate was reacted with TBSOTf after the deprotonation of **266** with lithium amide chiral base **317** (Entry 3, Table 4.1). Improvement was made in this case since no starting material remained. Bis-silyl enol ether **315** was the main product, accompanied by mono-silyl enol ethers. Presumably, **315a** was the major diastereoisomer obtained from the asymmetric double enolisation process according to previous studies on the deprotonation of cyclohexanones with this specific chiral base.¹²⁹⁻¹³¹ Further increasing the amount of the chiral amide base was not found to be

beneficial for improving the yield of **315**, as shown in Entry 4 in Table 4.1. The use of chiral lithium amide base **316** gave a comparable result to the reaction with **317** (Entry 5, Table 4.1).

At this stage, it turned out that the hydrogenation and the enol silane synthesis were challenging operations with our system since both of the two phenol rings within **105** or cyclohexanone moieties in **266** should react during the corresponding transformations. Even though the formation of bis-silyl enol ether **315** was confirmed by ^1H NMR and mass spectra, insufficient material was brought up for the conversion of **315** to the more stable bis-enone **264** according to the retrosynthesis of herquiline A in Section 4.1 and the diastereoselectivity of the chiral base step was not determined.

To solve the material supply issue, another approach was considered. According to the model reaction in Scheme 4.15, hydrogenation of tyrosine derivative **90** could readily deliver alcohol **307**, which might serve as the starting material for bis-ketone **266**. Even though a mixture of diastereomers would be delivered in each of the following transformations due to the existence of the isomeric alcohol functionalities, it was anticipated that these stereogenic centers were not consequential for the synthesis and all isomers would be converted to the final bis-ketone product at a late stage.

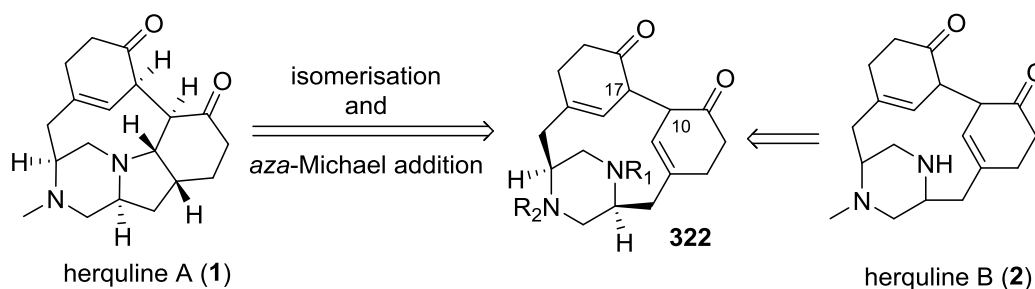


Scheme 4.20

Acid **319** was initially synthesised as a mixture of two diastereoisomers after the hydrolysis of **307** (Scheme 4.20). Deprotection of **307** with TFA in DCM delivered amine **318** in 81% yield. Following a similar procedure as we previously employed, the coupling reaction between acid **319** and amine **318** gave amide **320**, which was confirmed by NMR spectroscopy and mass spectrometry. Regrettably, the following deprotection and cyclisation steps afforded a complex mixture of products. While the formation of DKP **321** was supported by mass spectrometry, the yield was very low and the NMR spectra were complex at this stage. This route was finally abandoned and the synthetic plan was reconsidered.

4.4 Revised Retrosynthesis

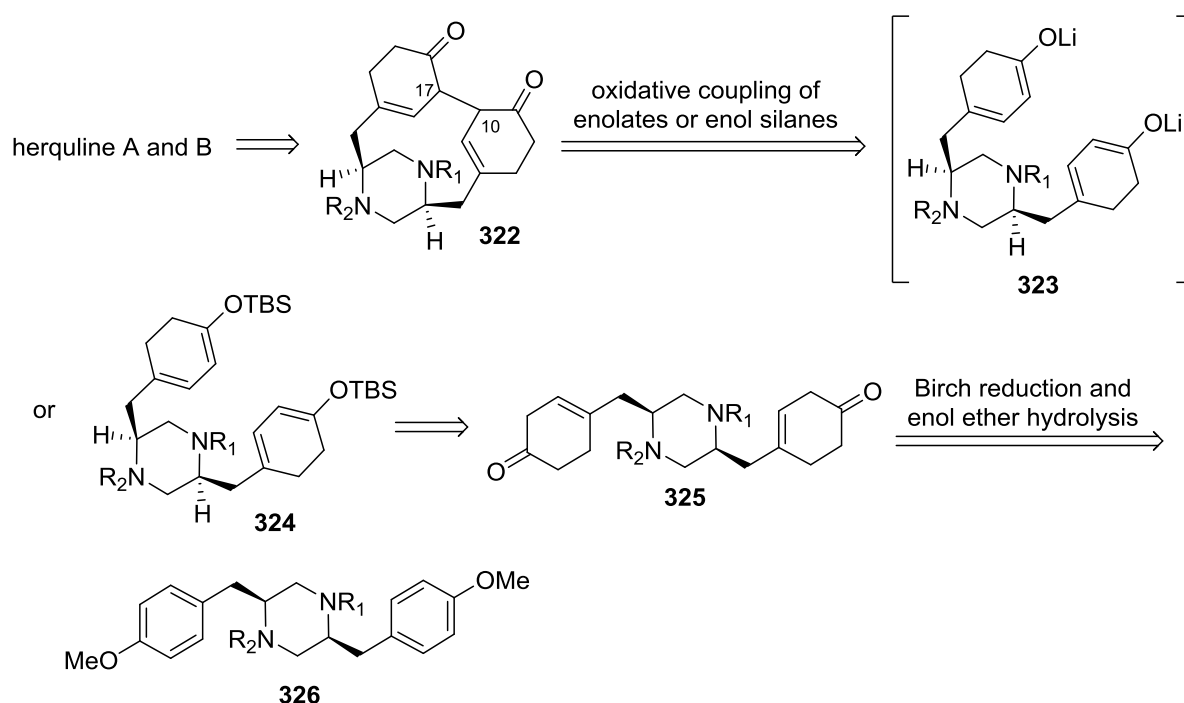
As an alternative approach, formation of the 1,4-diketone moiety could be fashioned at an early stage (Scheme 4.21). The C10–C17 linkage within **322** would be anticipated to facilitate the intramolecular *aza*-Michael addition reaction after the isomerisation of one double bond to its conjugated enone form to give herquiline A. Potentially, the synthesis of **322** would also provide valuable evidence for the absolute stereochemistry of herquiline B.



Scheme 4.21

This advanced bis-ketone structure **322** could derive from the oxidative coupling of the conjugated bis-dienolate **323** or silyl enol ether **324**, which could be traced back to bis-ketone

325 (Scheme 4.22). It was noteworthy that the intramolecular coupling at the piperazine stage in this approach was comparable to the direct oxidative phenol coupling and the transition metal-mediated aryl coupling, which appeared to be difficult transformations. However, it was envisioned that the formation of diketone **322** should be more favourable since the Csp³-Csp³ linkage within the 1,4-dicarbonyl group would increase the flexibility of the molecular structure, in contrast to the Csp²-Csp² linkages possessed by biaryl coupling products which would inevitably increase the strain of the molecules.



Scheme 4.22

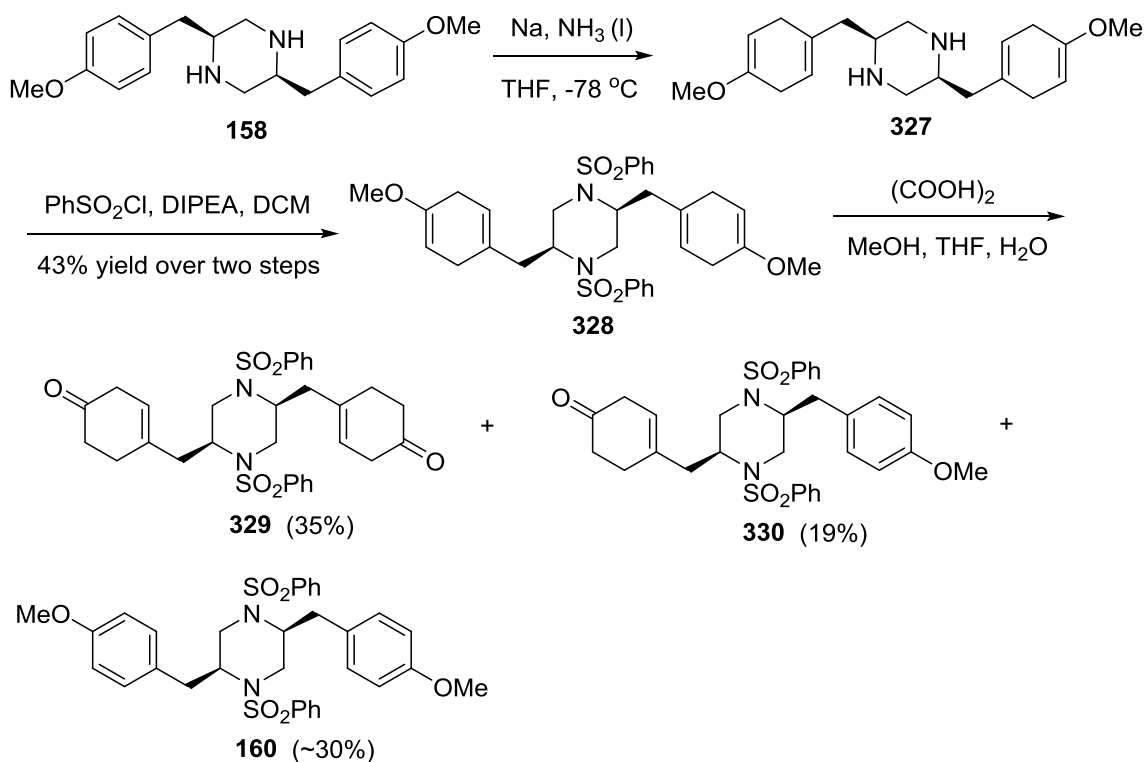
Noting that although no precedent examples of oxidative coupling between two conjugated dienolate derivatives, such as **323** and **324**, have been reported, it was anticipated that both of the two intermediates could undergo similar oxidative coupling processes to those involving simple enolate substrates as introduced in Section 4.2.1 and 4.2.2. Moreover, diketone **322** seemed to be the only possible regioisomer if the coupling reaction could proceed in an

intramolecular manner. Only the formation of the two stereogenic centers at C10 and C17 remained to be negotiated during the synthesis.

Assuming this sequence to be feasible, the formation of piperazine intermediate **323** or **324** could be realised from the selective deprotonation of bis-ketone **325** which would derive from precursor **326**. Instead of using hydrogenation methods to reduce the aromatic rings, it was anticipated that the Birch reduction of **326** followed by hydrolysis would give the bis-ketone product.

4.5 Formation of the 1,4-Dicarbonyl Functionality

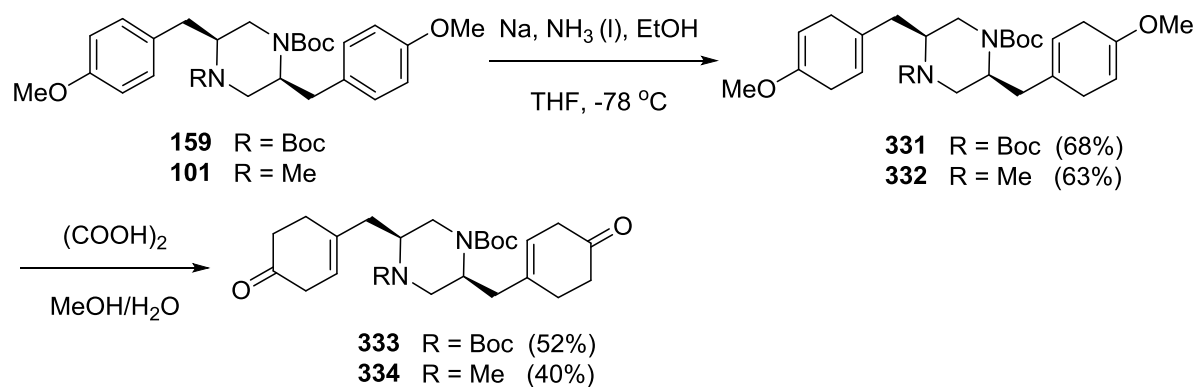
Exploration on the envisioned route towards herquiline A and B commenced from the Birch reduction of piperazine **158** (Scheme 4.23).



Scheme 4.23

Bis-diene **327** was successfully afforded after the subjection of **158** to standard Birch reduction conditions with sufficient reaction time. It was noticed that this intermediate was not stable and tended to rearomatise during the work-up process. The crude product was then treated with PhSO₂Cl and DIPEA to give the benzenesulfonyl-protected piperazine **328**, which was hydrolysed readily to bis-ketone **329** upon treatment with oxalic acid. Monoketone **330** and **160** were also isolated from the reaction mixture, possibly due to the rearomatisation of the cyclohexadiene moieties during the course of several operations.

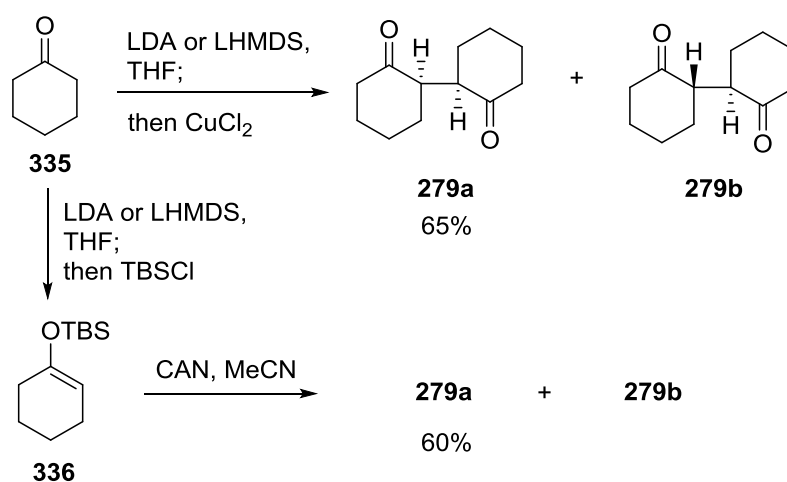
Following a similar procedure, bis-ketones **333** and **334** were also reached from **159** and **101** respectively (Scheme 4.24). Even though the overall yields for these sequences were relatively low, the success in the synthesis of the advanced piperazine intermediates **329**, **333** and **334** provided a chance for the investigation of the intriguing intramolecular oxidative enolate or enol silane coupling, a key step for the construction of the 1,4-diketone unit within the herquiline natural products.



Scheme 4.24

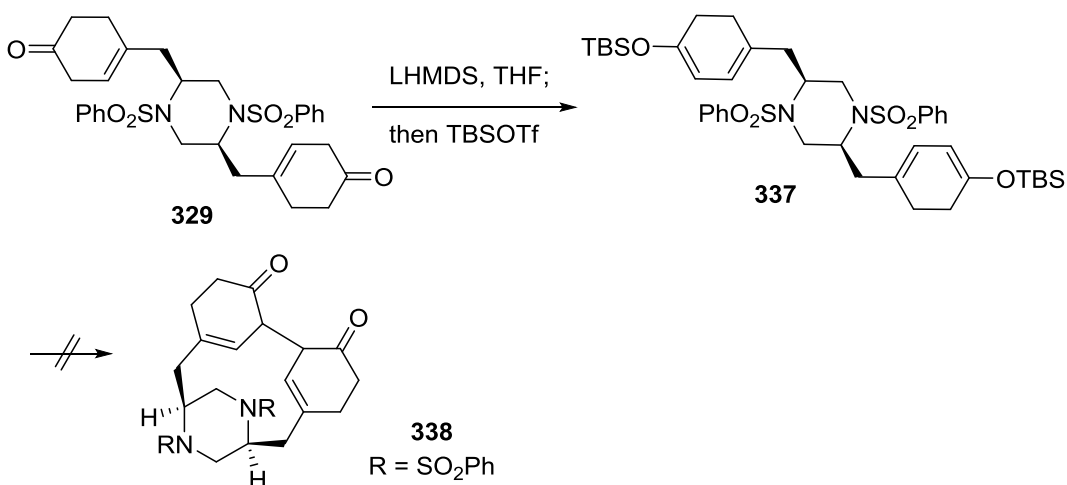
Before moving on, model reactions of oxidative enolate or enol silane coupling were performed with simple substrates (Scheme 4.25). With CuCl₂ as the oxidant, the oxidative coupling of the lithium enolate derived from cyclohexanone **335** delivered predominantly the racemic diketone **279a**, which is a known structure in the literature,^{160,161} accompanied by a

trace amount of **279b**. A comparable result was obtained from CAN-mediated oxidative coupling of silyl enol ether **336**. Since TBS enol ethers were not employed frequently as the substrates for oxidative coupling reactions in the literature, this positive outcome revealed that the enol silane with a bulkier silyl group than TMS could also serve as a coupling partner in this kind of transformation.



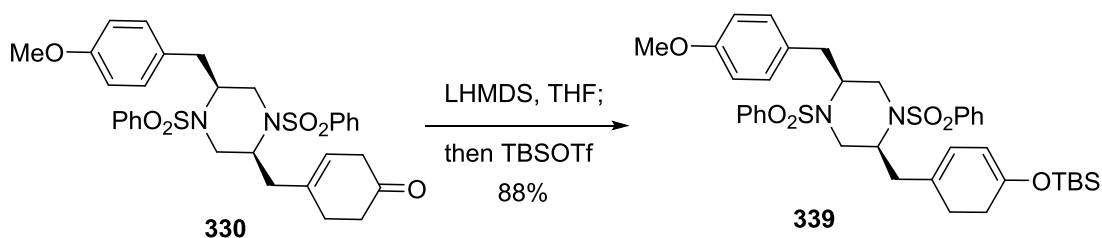
Scheme 4.25

The intramolecular oxidative coupling of silyl enol ethers was primarily investigated with the piperazine system as outlined in Scheme 4.26.



Scheme 4.26

Upon treatment of bis-dienone **329** with LHMDS, followed by trapping the bis-dienolate with TBSOTf, bis-silyl enol ether **337** was proposed to be the main product since the regioselectivity of the enolisation was confirmed with ketone **330** which was converted predominantly to the 'thermodynamic' endocyclic enol silane **339** (Scheme 4.27).



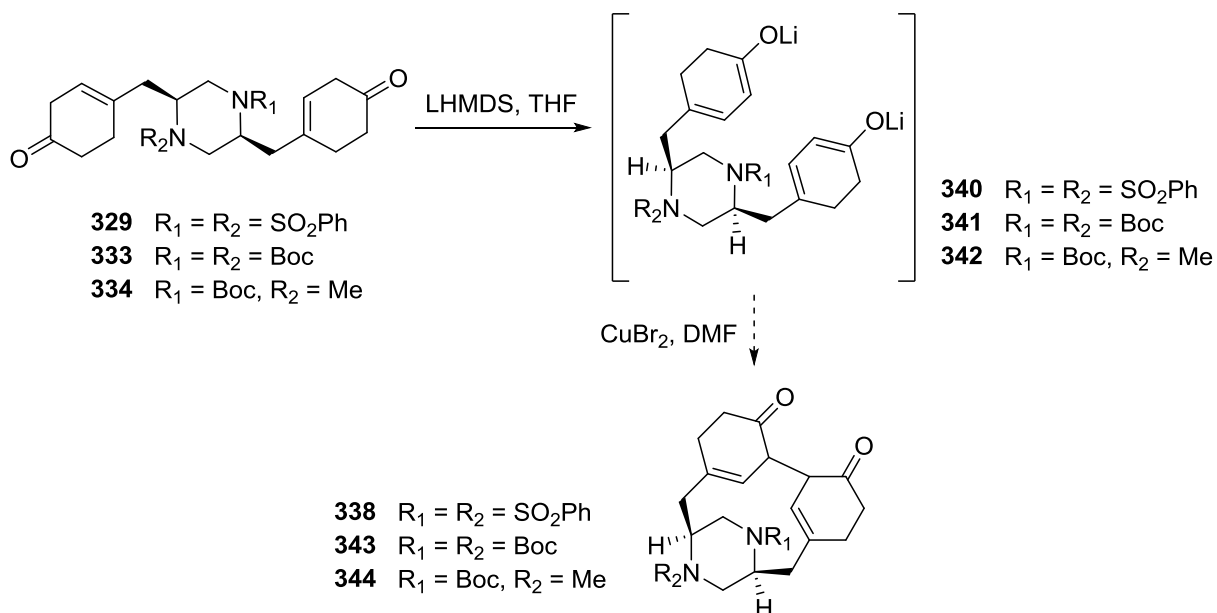
Scheme 4.27

However, the purification of **337** was found to be difficult due to partial regeneration of the corresponding ketone intermediates. Subjecting the crude sample of **337** to CAN-mediated oxidation in acetonitrile gave no cyclised product. Only isomerised bis-ketones were produced according to the ^1H NMR spectra and dimeric compounds were also detected by mass spectrometry.

The intramolecular enolate oxidative coupling approach was attempted with several different substrates, as shown in Scheme 4.28. Extensive experimentation revealed that the intramolecular oxidative coupling was not a favourable process. Specifically, when CuBr_2 was employed as the oxidant, the reaction involving **333** or unsymmetrical piperazine **334** delivered mainly isomerised bis-ketones and dimeric products, without any detection of the coupling products by mass spectrometry.

In the case of **329**, similar reaction pathways were observed. Noteworthily, a trace amount of the desired bis-ketone **338** was isolated from the reaction system this time and was further confirmed by mass spectrometry. The mass spectrum showed a $[\text{M}+\text{Na}]^+$ peak at m/z

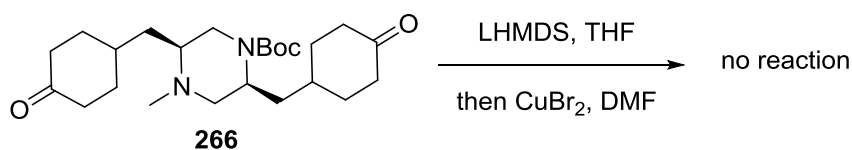
603.1597 which matches the molecular formula of product **338** ($C_{30}H_{32}N_2O_6S_2Na$ requires 603.1600). Even though this new entity was not fully characterised due to the low quantity, it was hoped that optimisation of the reaction conditions would improve the yield.



Scheme 4.28

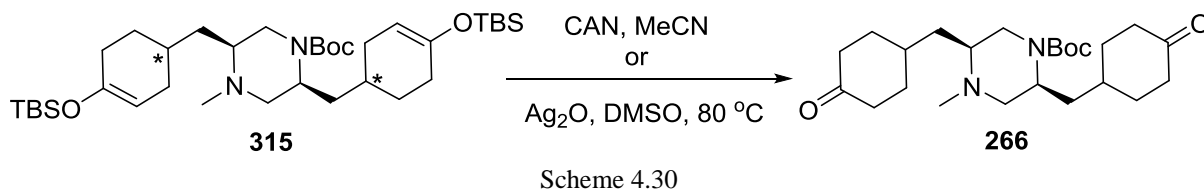
To modify the coupling conditions, other oxidants were examined, such as $Fe(acac)_3$ and $CuCl_2$. While the reaction with $CuCl_2$ provided a similar result to that with $CuBr_2$, the use of $Fe(acac)_3$ as the oxidant was found to be less efficient. Further attempts using LDA or NaHMDS as alternative bases in the enolisation step led to no improvement.

Bis-ketone **266** was also employed as the substrate for the oxidative enolate coupling protocol (Scheme 4.29). Upon treating the isomeric enolates derived from **266** with $CuBr_2$, only starting material was recovered.

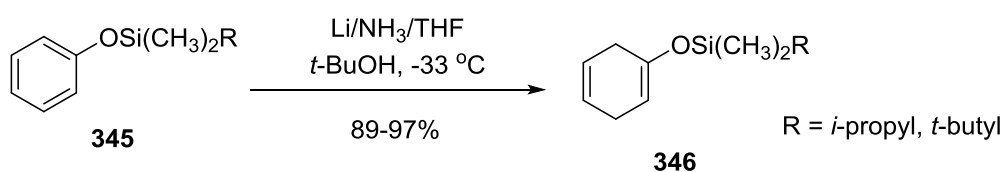


Scheme 4.29

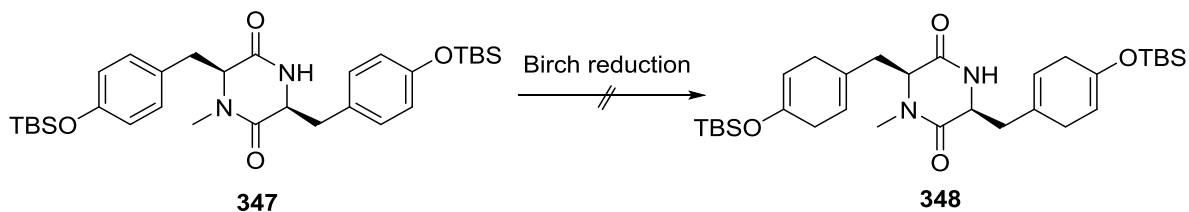
In the cases of the oxidative coupling of bis-silyl enol ethers **315**, the regeneration of **266** proceeded exclusively without giving any traces of coupling products (Scheme 4.30).



The intramolecular coupling once again turned out to be a pitfall for the total synthesis. According to our previous efforts, DKP substrates tended to give better results than the corresponding piperazines in the intramolecular aryl coupling reactions. To obtain suitable DKP substrates for oxidative enolate or enol silane coupling, the generation of bis-enolate or bis-silyl enol ether from a bis-ketone precursor would be problematic due to the epimerisation tendency of the DKP moiety under basic conditions. It has been reported that the Birch reduction of silyl aryl ethers with bulkier silyl groups could deliver 1,4-dihydroaryl silyl ethers in high yields (Scheme 4.31).¹⁶²



Potentially, a bis-silyl enol ether substrate could be fashioned from the Birch reduction of DKP **347** (Scheme 4.32). Even though the double bonds within **348** were not at the right positions for herquiline synthesis, the oxidative coupling of **348** would provide valuable information on the reactivity of diketopiperazines.



Scheme 4.32

However, when DKP **347** was subjected to Birch reduction conditions, no desired product was obtained and the reaction gave a mixture of irrelevant by-products.

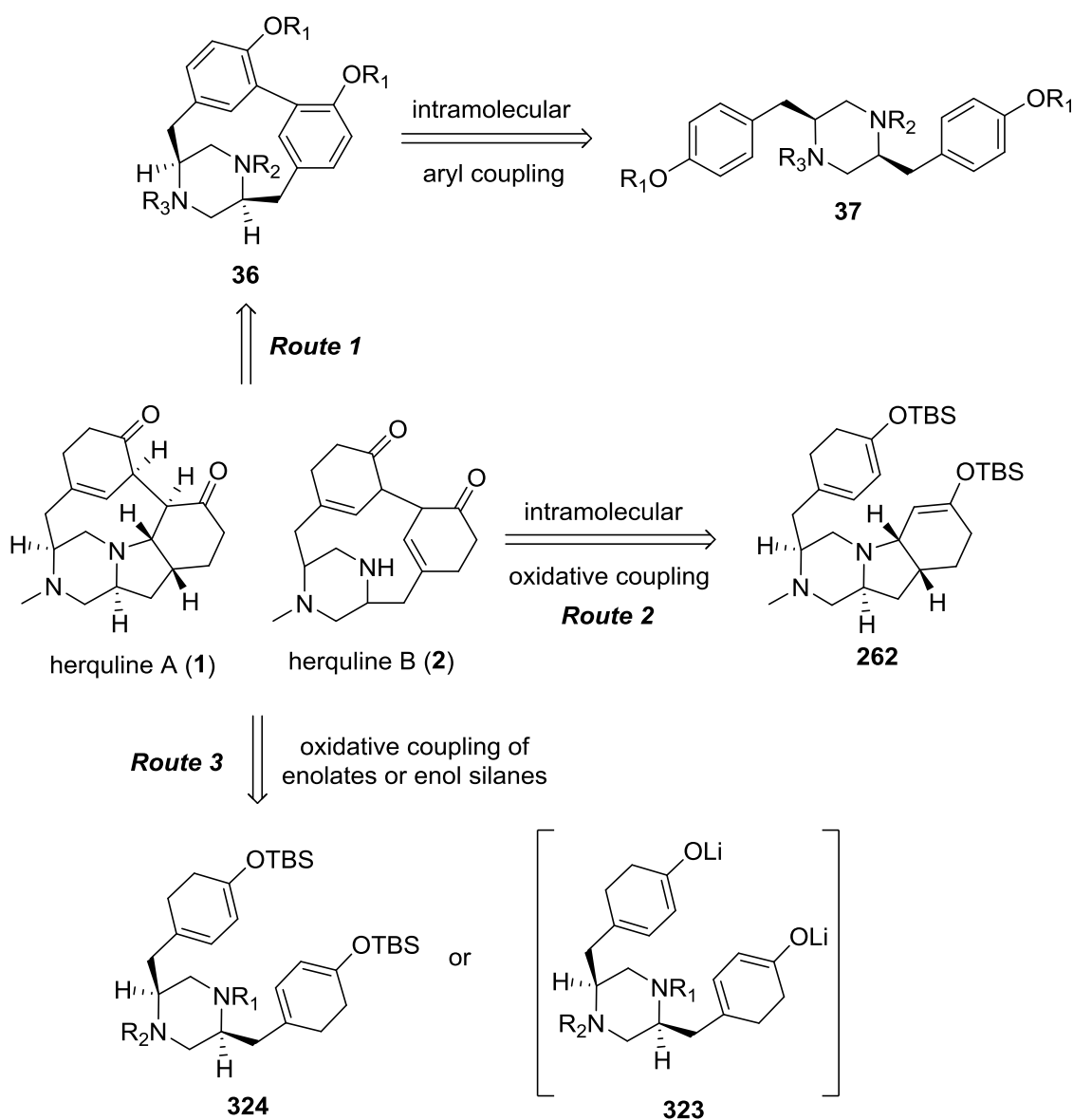
4.6 Summary

In summary, the oxidative enolate or enol silane coupling approach was explored. Based on the retrosynthesis of herquiline A, an asymmetric deprotonation of bis-ketone with a chiral base was envisioned for the generation of the stereogenic centers within the fused tricyclic ring system of herquiline A. While the bis-silyl enol ether was successfully fashioned, potentially as a mixture of diastereoisomers, the synthesis was not progressed following the proposed sequence due to the low efficiency of the hydrogenation step. No success was achieved in overcoming this material supply issue.

For the intramolecular oxidative coupling of bis-dienolates, detailed investigation led to the detection of a trace amount of the coupling product with a 1,4-dicarbonyl moiety. It was speculated that the intramolecular coupling at the piperazine stage was a challenging process.

CHAPTER 5 CONCLUSIONS

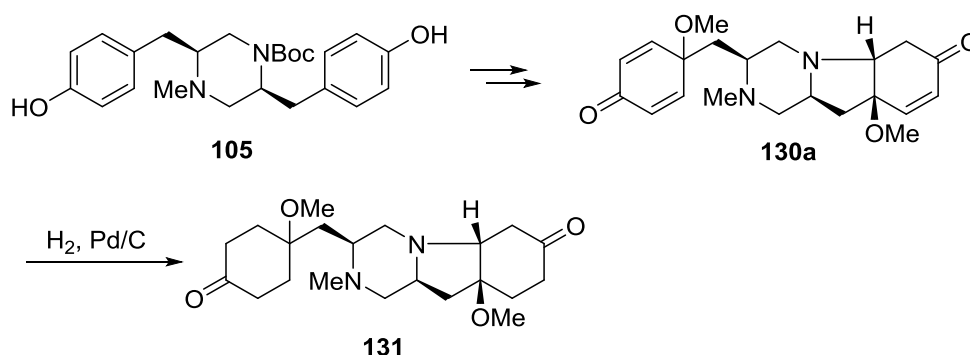
This thesis presented the synthetic efforts from several novel approaches towards herquiline A and B. From a tactical standpoint, the intramolecular coupling strategy was attempted as the mainstream of the studies in order to construct the key skeleton of the two natural products.



Scheme 5.1

Inspired by the biosynthesis of the herquiline alkaloids, a biomimetic approach was initially explored in Chapter 2 (Route 1, Scheme 5.1). Following the successful synthesis of several piperazine intermediates, the direct oxidative coupling of phenol or phenol ether substrates was examined with different oxidants to mimic Nature's way of constructing biaryl intermediate **36** for the synthesis of herquiline A and B. However, extensive experimentation failed to deliver the cyclised products.

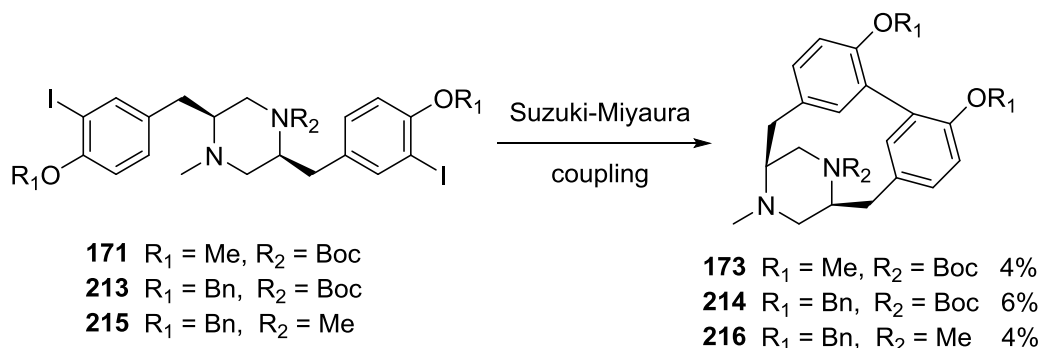
The advanced intermediate **130a** was accessed *via* an intramolecular *aza*-Michael addition reaction (Scheme 5.2). Even though no further operations were performed on **130a** or **131** towards the herquiline natural products, these molecules share close structural resemblance to the fused tricyclic ring system within herquiline A.



Scheme 5.2

The transition metal-mediated intramolecular aryl coupling strategy was emphasised in Chapter 3 (Route 1, Scheme 5.1). Based on conformational analysis, the reactivity of piperazine substrates towards intramolecular coupling was rationalised. While the oxidative coupling of organocuprates was unsuccessful in generating biaryl linkages, small amounts of the coupling products were fashioned from the Pd-catalysed domino Suzuki-Miyaura

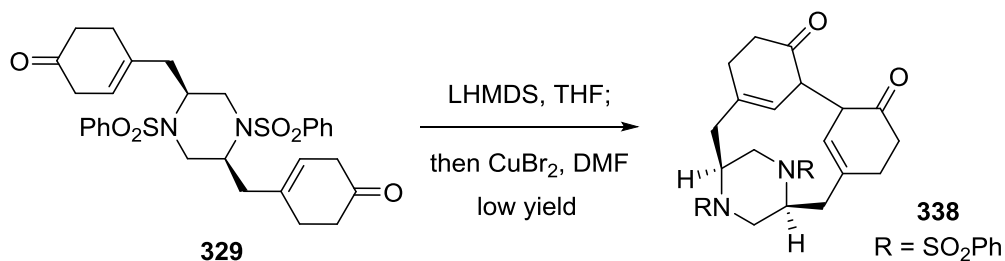
coupling approach (Scheme 5.3). Due to the low quantities of these coupling products, the synthesis was not carried on towards the herquiline natural products.



Scheme 5.3

In contrast to piperazine coupling, the intramolecular Suzuki-Miyaura coupling reactions with DKP substrates were more efficient and the corresponding coupling products, several analogues of the natural product mycocyclosin, were provided in relatively higher yields. However, further transformations on these DKP coupling products towards herquiline A and B turned out to be unsuccessful.

An alternative approach was highlighted in Chapter 4, which featured an intramolecular oxidative coupling of enolates or enol silanes as the critical steps (Route 2 and 3, Scheme 5.1). Based on the retrosynthetic analysis of herquiline A, a bis-silyl enol ether was synthesised in moderate yield. Due to the low efficiency in material supply, no further investigations were undertaken following this route. In terms of the oxidative coupling of the conjugated endocyclic dienolates or dienol silanes, trace bis-ketone product formation was successfully detected but the synthesis was limited by the low yield of the coupling reaction (Scheme 5.4).



Scheme 5.4

Overall, the intramolecular coupling of piperazines was conceived to be a highly desired process for the total synthesis of herquiline A and B in this study. However, our efforts indicated that it was challenging and difficult to perform this transformation at the piperazine oxidation state. While it seems not obvious to propose an alternative synthetic approach towards herquiline A and B, other strategy might employ different building blocks other than tyrosine derivatives as the starting materials and further deft tactics are awaited to address the specific and precise structural features possessed by herquiline A and B.

CHAPTER 6 EXPERIMENTAL

6.1 Materials and Methods

All glassware was oven-dried before use unless otherwise stated. Anhydrous THF was distilled from sodium/benzophenone immediately prior to use, or collected from a PureSolv™ solvent purification system. MeOH, MeCN, Et₂O and CH₂Cl₂ were collected from a PureSolv™ solvent purification system. All other solvents and reagents were used as received from commercial suppliers unless otherwise stated.

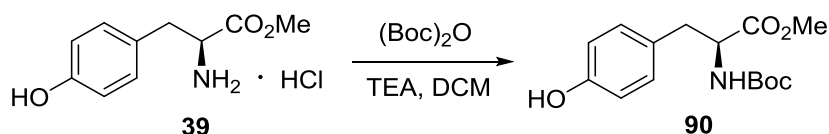
All ¹H NMR and ¹³C NMR experiments were recorded on a Bruker AC300, AVIII300, AVIII400, AV400 or DRX500 spectrometer at 298 K unless otherwise stated. ¹³C NMR spectra were recorded using the PENDANT pulse sequence and/or the UDEFT pulse sequence from the Bruker standard pulse program library. DEPT 90, DEPT 135 and two-dimensional (COSY, HSQC or HMBC) NMR spectroscopy were used to assist the assignment of signals in the ¹H and ¹³C NMR spectra where appropriate. The resonances of the residual solvent peaks of CDCl₃ ($\delta_{\text{H}} = 7.26$ ppm, $\delta_{\text{C}} = 77.16$ ppm), MeOD-*d*₄ ($\delta_{\text{H}} = 3.34$ ppm, $\delta_{\text{C}} = 49.86$ ppm) or DMSO-*d*₆ ($\delta_{\text{H}} = 2.50$ ppm, $\delta_{\text{C}} = 39.52$ ppm) were used as internal references. Chemical shifts (δ) are quoted in ppm and coupling constants (*J*) are quoted in Hz. The following abbreviations are used for multiplicity in ¹H NMR spectra: s (singlet), d (doublet), t (triplet), q (quartet), m (multiplet), br (broad) or combination of these.

Reaction progress was monitored by thin layer chromatography (TLC) performed on Merck silica gel 60 F₂₅₄ plates, which were visualised under UV light (254 nm) and with potassium permanganate or *p*-anisaldehyde dip. Flash column chromatography was carried out using

silica gel 60 (230-400 mesh, Merck and Co.) and the indicated solvent systems. Infrared spectra were recorded on a Perkin-Elmer Spectrum 100 FTIR spectrometer. Wavelengths (ν) are reported in cm^{-1} . Optical rotations were recorded as dilute solutions in the indicated solvents in a 25 mm glass cell using an Optical Activity PolAAr 2001 automatic polarimeter. The concentrations are reported in grams per 100 mL. EI mass spectra were recorded on a VG ZabSpec magnetic sector mass spectrometer and ESI mass spectra were recorded on a Micromass LCT time-of-flight mass spectrometer by the analytical services at the University of Birmingham. Melting points were measured with a Gallenkamp melting point apparatus and are uncorrected. The experiments under microwave irradiation were conducted with a CEM Discover S-Class microwave reaction station. The high pressure hydrogenation reactions were carried out with a Parr series 5500 high pressure compact reactor (100 mL).

6.2 Preparative Procedures for Chapter 2

Preparation of *N*-Boc-L-tyrosine methyl ester **90**

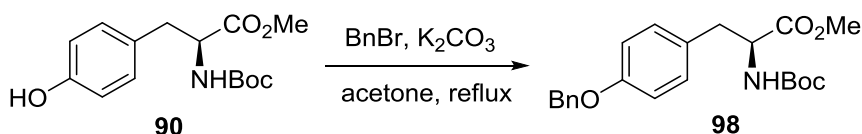


To a suspension of L-tyrosine methyl ester hydrochloride (3.48 g, 15.1 mmol) in DCM (30 mL) was added Et₃N (4.60 mL, 33.0 mmol) at 0 °C and the reaction mixture was stirred for 30 min. A solution of (Boc)₂O (3.57 g, 15.9 mmol) in DCM (10 mL) was added to the mixture and the reaction system was warmed to rt and stirred for 12 h. Upon completion, the reaction mixture was washed with saturated NaHCO₃ solution (30 mL) and then brine (20 mL). The organic layer was separated, dried over MgSO₄ and concentrated under reduced pressure. The residue was purified by flash column chromatography using 30% EtOAc in petroleum ether as

the eluent to provide compound **90** (3.84 g, 87% yield) as an oil, which solidified as a white solid in the fridge. M.p. 100-101 °C (lit.¹⁶³ m.p. 101-103 °C); $R_f = 0.40$ (EtOAc/petroleum ether 1:1); $[\alpha]_D^{18} = +46.8$ ($c = 1.0$, CHCl_3) (lit.¹⁶⁴ $[\alpha]_D^{20} = +41.2$, $c = 1.0$, CHCl_3); FTIR (film) ν_{max} 3359, 2977, 2932, 1687, 1516, 1223, 1163; ^1H NMR (CDCl_3 , 300 MHz) δ 6.89 (d, $J = 8.4$ Hz, ArH, 2H), 6.66 (d, $J = 8.4$ Hz, ArH, 2H), 6.28 (br s, OH, 1H), 4.97 (d, $J = 8.3$ Hz, NH, 1H), 4.51-4.43 (m, CHNH, 1H), 3.64 (s, COOCH_3 , 3H), 2.96 (dd, $J = 14.0, 6.0$ Hz, ArCH_aH_b , 1H), 2.89 (dd, $J = 14.0, 6.2$ Hz, ArCH_aH_b , 1H), 1.35 (s, $\text{COOC}(\text{CH}_3)_3$, 9H); ^{13}C NMR (CDCl_3 , 100 MHz) δ 171.7 (CO_2Me), 154.4 (COO^tBu), 154.3 (Ar), 129.3 (Ar), 126.4 (Ar), 114.5 (Ar), 79.2 ($\text{COOC}(\text{CH}_3)_3$), 53.6 (CHNH), 51.3 (CO_2CH_3), 36.6 (ArCH_2), 27.3 ($\text{COOC}(\text{CH}_3)_3$).

The NMR data are in accord with published values.¹⁶³

Preparation of *N*-Boc-*O*-benzyl-*L*-tyrosine methyl ester **98**

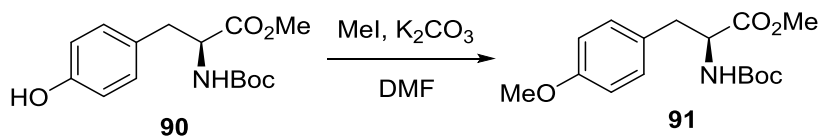


To a mixture of compound **90** (3.00 g, 10.2 mmol) and K_2CO_3 (1.82 g, 13.2 mmol) in acetone (25 mL) was added BnBr (1.45 mL, 12.2 mmol). The mixture was heated under reflux for 10 h and then cooled to rt. The solid was filtered off and washed with acetone (3×6 mL). The organic solvent was concentrated under reduced pressure and the crude product was purified by column chromatography using 30% ethyl acetate in petroleum ether as the eluent to afford compound **98** (3.68 g, 93% yield) as a white solid. M.p. 83-84 °C (lit.¹⁶⁵ m.p. 83-86 °C); $R_f = 0.35$ (EtOAc/petroleum ether 2:1); $[\alpha]_D^{19} = +53.7$ ($c = 1.5$, CHCl_3); FTIR (film) ν_{max} 3374, 2957, 2928, 2871, 1745, 1713, 1511, 1242, 1225, 696; ^1H NMR (CDCl_3 , 300 MHz) δ 7.50-7.31 (m, ArH, 5H), 7.06 (d, $J = 8.6$ Hz, ArH, 2H), 6.93 (d, $J = 8.6$ Hz, ArH, 2H), 5.06 (s, PhCH_2 , 2H), 5.00 (d, $J = 8.0$ Hz, NH, 1H), 4.60-4.54 (m, CHNH, 1H), 3.73 (s, COOCH_3 , 3H),

3.08 (dd, $J = 13.9, 5.8$ Hz, ArCH_aH_b , 1H), 3.02 (dd, $J = 13.9, 6.1$ Hz, ArCH_aH_b , 1H), 1.45 (s, $\text{COOC}(\text{CH}_3)_3$, 9H); ^{13}C NMR (CDCl_3 , 100 MHz) δ 172.4 (CO_2Me), 157.9 (Ar), 155.1 (COO^tBu), 137.0 (Ar), 130.3 (Ar), 128.6 (Ar), 128.3 (Ar), 128.0 (Ar), 127.5 (Ar), 114.9 (Ar), 79.9 ($\text{COOC}(\text{CH}_3)_3$), 70.0 (PhCH_2), 54.5 (CHNH), 52.2 (COOCH_3), 37.5 (ArCH_2), 28.3 ($\text{COOC}(\text{CH}_3)_3$).

The observed data are in accord with published values.¹⁶⁵

Preparation of *N*-Boc-*O*-methyl-*L*-tyrosine methyl ester **91**

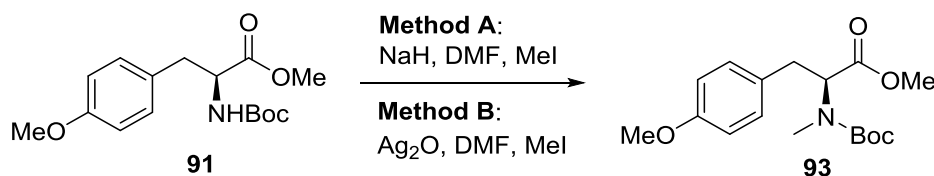


A mixture of Boc-protected tyrosine derivative **90** (3.84 g, 13.0 mmol), K_2CO_3 (1.97 g, 14.3 mmol) and MeI (1.20 mL, 19.3 mmol) in DMF (25 mL) was stirred for 12 h at rt. Water (40 mL) was added to the reaction suspension and the mixture was extracted with DCM (3×30 mL). The organic layers were combined and washed with brine (3×30 mL). After being dried over MgSO_4 and filtration, the organic solvent was concentrated under reduced pressure to give a colourless oil. The crude product was purified by column chromatography eluting with 30% ethyl acetate in petroleum ether to afford **91** (3.66 g, 91% yield) as a white solid. M.p. 55-56 °C (lit.¹⁶⁶ m.p. 52-53 °C); $R_f = 0.55$ (EtOAc/petroleum ether 1:1); $[\alpha]_{\text{D}}^{20} = +55.5$ ($c = 1.8$, CHCl_3) (lit.¹⁶⁶ $[\alpha]_{\text{D}}^{20} = +50.0$, $c = 1.8$, CHCl_3); FTIR (film) ν_{max} 3374, 2977, 1745, 1715, 1513, 1248, 1167; ^1H NMR (CDCl_3 , 300 MHz) δ 7.05 (d, $J = 8.4$ Hz, ArH, 2H), 6.84 (d, $J = 8.4$ Hz, ArH, 2H), 5.00 (d, $J = 7.7$ Hz, NH, 1H), 4.55 (dd, $J = 13.8, 6.0$ Hz, CHNH, 1H), 3.79 (s, ArOCH_3 , 3H), 3.72 (s, COOCH_3 , 3H), 3.22-2.82 (m, ArCH_2 , 2H), 1.43 (s, $\text{COOC}(\text{CH}_3)_3$, 9H); ^{13}C NMR (CDCl_3 , 100 MHz) δ 171.4 (COOMe), 157.7 (Ar), 154.1 (COO^tBu), 129.3

(Ar), 127.0 (Ar), 113.0 (Ar), 78.8 (COOC(CH₃)₃), 54.2 (ArOCH₃), 53.6 (CHNH), 51.1 (CO₂CH₃), 36.5 (CH₂Ar), 27.3 (COOC(CH₃)₃).

The observed data are in accord with published values.¹⁶⁶

Preparation of *N*-Boc-*N*, *O*-dimethyl-*L*-tyrosine methyl ester **93**



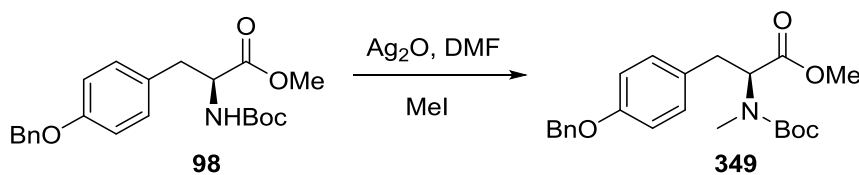
Method A: To a solution of compound **91** (2.50 g, 8.08 mmol) in anhydrous DMF (25 mL) at 0 °C was added MeI (0.75 mL, 12.10 mmol), followed by a suspension of NaH (60% dispersion in mineral oil, 0.34 g, 8.48 mmol) in DMF (3 mL). The mixture was stirred at 0 °C for 1 h and then at rt overnight. Water (20 mL) was slowly added and the resulting mixture was extracted with DCM (3×30 mL). The organic layers were combined and washed twice with brine (2×15 mL). After being dried over MgSO₄ and filtration, the organic solvent was concentrated under reduced pressure. The crude product was used in the next step without further purification.

Method B: A mixture of tyrosine derivative **91** (2.50 g, 8.08 mmol), Ag₂O (2.80 g, 12.10 mmol) and MeI (0.75 mL, 12.10 mmol) in anhydrous DMF (20 mL) was stirred at rt for 36 h. The reaction system was diluted with ethyl acetate (25 mL) and the resulting mixture was filtered through a layer of Celite pad. The solid was washed twice with ethyl acetate (2×15 mL) and the filtrate was transferred to a separating funnel. The organic phase was washed with brine (3×20 mL), dried over MgSO₄, filtered and concentrated *in vacuo*. The crude product was purified by column chromatography eluting with 30% ethyl acetate in petroleum ether to afford the desired product **93** as a colourless oil (2.30 g, 88% yield). R_f = 0.56

(EtOAc/petroleum ether 1:1); $[\alpha]_D^{18} = -56.9$ ($c = 1.0$, CHCl_3); FTIR (film) ν_{max} 2976, 1743, 1694, 1514, 1248, 1176; ^1H NMR (CDCl_3 , 300 MHz) (major rotamer) δ 7.12 (d, $J = 8.4$ Hz, ArH, 2H), 6.84 (d, $J = 8.4$ Hz, ArH, 2H), 4.48 (dd, $J = 10.7$, 4.6 Hz, CHNMe, 1H), 3.79 (s, ArOCH₃, 3H), 3.76 (s, COOCH₃, 3H), 3.22 (dd, $J = 14.4$, 4.6 Hz, ArCH_aH_b, 1H), 2.97 (dd, $J = 14.4$, 10.7 Hz, ArCH_aH_b, 1H), 2.73 (s, NCH₃, 3H), 1.36 (s, COOC(CH₃)₃, 9H); ^{13}C NMR (CDCl_3 , 100 MHz) (major rotamer) δ 175.5 (CO₂Me), 158.4 (Ar), 155.0 (COO'Bu), 129.9 (Ar), 129.6 (Ar), 113.5 (Ar), 80.1 (COOC(CH₃)₃), 61.8 (CHNMe), 52.0 (COOCH₃), 34.6 (ArCH₂CH), 32.6 (NCH₃), 28.3 (COOC(CH₃)₃).

The observed data are in accord with published values.¹⁶⁸

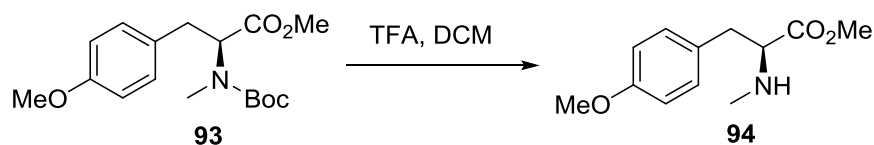
Preparation of *N*-Boc-*N*-methyl-*O*-benzyl-*L*-tyrosine methyl ester **349**



N-Boc-*N*-methyl-*O*-benzyl-*L*-tyrosine methyl ester **349** was prepared from **98** (1.36 g, 3.53 mmol) following a similar procedure to that for the synthesis of **93** (Method B) and was obtained as a white solid (1.27 g, 3.18 mmol, 90% yield). M.p. 131-132 °C (lit.¹⁶⁹ m.p. 130-134 °C); $R_f = 0.65$ (EtOAc/petroleum ether 1:1); $[\alpha]_D^{20} = -68$ ($c = 1.2$, CHCl_3); FTIR (film) ν_{max} 3035, 2976, 1742, 1693, 1512, 1223, 1174, 1142; ^1H NMR (CDCl_3 , 300 MHz) (major rotamer) δ 7.46-7.33 (m, ArH, 5H), 7.13 (d, $J = 8.4$ Hz, ArH, 2H), 6.93 (d, $J = 8.4$ Hz, ArH, 2H), 5.05 (s, PhCH₂, 2H), 4.50 (dd, $J = 10.8$, 5.0 Hz, CHNMe, 1H), 3.76 (s, COOCH₃, 3H), 3.26 (dd, $J = 14.0$, 5.0 Hz, ArCH_aH_b, 1H), 2.98 (dd, $J = 14.0$, 10.8 Hz, ArCH_aH_b, 1H), 2.75 (s, NCH₃, 3H), 1.37 (s, COOC(CH₃)₃, 9H); ^{13}C NMR (CDCl_3 , 100 MHz) (major rotamer) δ 171.6 (CO₂Me), 157.6 (Ar), 155.8 (COO'Bu), 137.1 (Ar), 129.7 (Ar), 128.6 (Ar), 127.9 (Ar),

127.4 (Ar), 115.0 (Ar), 114.8 (Ar), 80.2 (COOC(CH₃)₃), 70.1 (PhCH₂), 61.8 (CHNMe), 52.1 (COOCH₃), 34.7 (ArCH₂CH), 32.6 (NCH₃), 28.2 (COOC(CH₃)₃); HRMS (ESI) calculated for C₂₃H₃₀NO₅ [M+H]⁺ 400.2124, found 400.2120.

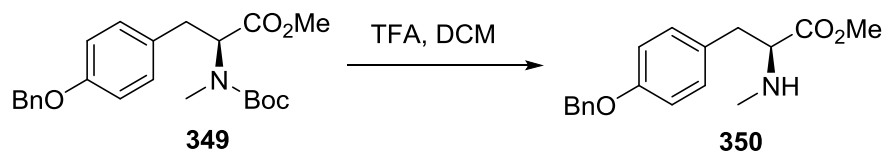
Preparation of *N*, *O*-dimethyl-L-tyrosine methyl ester **94**



To a solution of *N*-Boc tyrosine derivative **93** (2.40 g, 7.40 mmol) in DCM (20 mL) was added TFA (3.0 mL, 39.2 mmol). After stirring for 5 h, saturated NaHCO₃ solution (25 mL) was slowly added to the reaction solution. The mixture was extracted with DCM (3×30 mL). After being dried over MgSO₄ and filtration, the organic solvent was concentrated under reduced pressure. The crude product was purified by column chromatography using 50% ethyl acetate in petroleum ether as the eluent to give tyrosine derivative **94** (1.56 g, 94% yield) as a colourless oil. *R*_f = 0.20 (EtOAc); [α]_D¹⁹ = +25.5 (*c* = 0.7, CHCl₃) (lit.¹⁷⁰ [α]_D²³ = +24, *c* = 0.65, CHCl₃); FTIR (film) *v*_{max} 3339, 2950, 2837, 1732, 1512, 1245, 1174, 1033; ¹H NMR (CDCl₃, 300 MHz) δ 7.09 (d, *J* = 8.4 Hz, Ar*H*, 2H), 6.84 (d, *J* = 8.4 Hz, Ar*H*, 2H), 3.79 (s, ArOCH₃, 3H), 3.68 (s, COOCH₃, 3H), 3.43 (t, CHNH, *J* = 6.6 Hz, 1H), 2.91 (d, *J* = 6.6 Hz, ArCH₂, 2H), 2.37 (s, NCH₃, 3H); ¹³C NMR (CDCl₃, 100 MHz) δ 174.7 (COOCH₃), 158.5 (Ar), 130.1 (Ar), 129.1 (Ar), 113.9 (Ar), 64.8 (CHNH), 55.2 (ArOCH₃), 51.6 (COOCH₃), 38.5 (ArCH₂), 34.7 (NCH₃).

The observed data are in accord with published values.¹⁷⁰

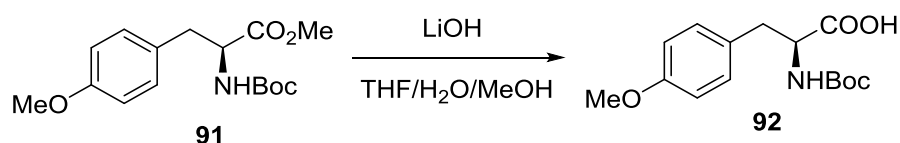
Preparation of *N*-methyl-*O*-benzyl-*L*-tyrosine methyl ester **350**



N-methyl-*O*-Benzyl-*L*-tyrosine methyl ester **350** was prepared from **349** (1.24 g, 3.10 mmol) following a similar procedure to that for the synthesis of **94**. Compound **350** was obtained as a colourless oil (0.83 g, 2.76 mmol, 89% yield). $R_f = 0.25$ (EtOAc); $[\alpha]_D^{20} = +27.5$ ($c = 1.0$, CHCl₃) (lit.¹⁷⁰ $[\alpha]_D^{23} = +20$, $c = 1.0$, CHCl₃); FTIR (film) ν_{\max} 3338, 3032, 2949, 2799, 1732, 1511, 1238, 1016, 736; ¹H NMR (CDCl₃, 300 MHz) δ 7.49-7.32 (m, ArH, 5H), 7.11 (d, $J = 8.6$ Hz, ArH, 2H), 6.92 (d, $J = 8.6$ Hz, ArH, 2H), 5.06 (s, PhCH₂, 2H), 3.69 (s, COOCH₃, 3H), 3.44 (t, $J = 6.8$ Hz, CHNMe, 1H), 2.92 (d, $J = 6.8$ Hz, ArCH₂, 2H), 2.38 (s, NCH₃, 3H); ¹³C NMR (CDCl₃, 100 MHz) δ 174.6 (COOMe), 157.7 (Ar), 137.1 (Ar), 130.1 (Ar), 129.3 (Ar), 128.6 (Ar), 127.9 (Ar), 127.5 (Ar), 114.9 (Ar), 70.0 (PhCH₂), 64.7 (CHNMe), 51.7 (COOCH₃), 38.5 (ArCH₂), 34.7 (NCH₃).

The observed data are in accord with published values.¹⁷⁰

Preparation of *N*-Boc-*O*-methyl tyrosine **92**

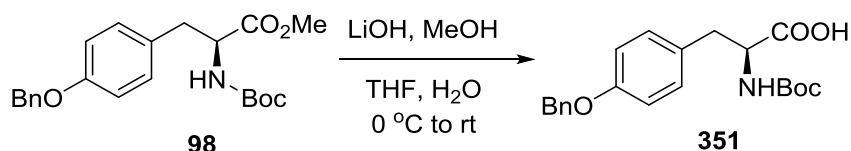


To a solution of compound **91** (2.97 g, 9.60 mmol) in THF (8 mL), MeOH (8 mL) and H₂O (6 mL) was added lithium hydroxide monohydrate (0.61 g, 14.4 mmol) at 0 °C. The mixture was stirred at 0 °C for 1 h and then at rt for 6 h. To the hydrolysis system was added water (15 mL) and the pH of the reaction system was adjusted to 4~5 with 5% HCl (aq). The mixture was extracted with DCM (3×20 mL). The organic layers were combined and dried over MgSO₄.

After filtration and concentration, the crude product was purified by column chromatography using 50% ethyl acetate in petroleum ether as the eluent to give acid **92** (2.76 g, 97% yield) as a colourless oil which solidified in the fridge. M.p. 95-96 °C (lit.¹⁷¹ m.p. 92-94 °C); $R_f = 0.35$ (EtOAc/petroleum ether 1:2); $[\alpha]_D^{20} = +39.5$ ($c = 1.0$, EtOH) (lit.¹⁷¹ $[\alpha]_D^{25} = +42.2$, $c = 1.0$, EtOH); FTIR (film) ν_{\max} 3322, 2978, 2933, 1714, 1513, 1248, 1164; $^1\text{H NMR}$ (CDCl_3 , 300 MHz) (major rotamer) δ 7.12 (d, $J = 8.6$ Hz, ArH, 2H), 6.86 (d, $J = 8.6$ Hz, ArH, 2H), 4.96 (d, $J = 7.8$ Hz, NH, 1H), 4.59 (dd, $J = 12.6, 7.8$ Hz, CHNH, 1H), 3.81 (s, OCH₃, 3H), 3.18-3.02 (m, ArCH₂, 2H), 1.44 (s, COOC(CH₃)₃, 9H); $^{13}\text{C NMR}$ (CDCl_3 , 100 MHz) (major rotamer) δ 176.5 (COOH), 158.7 (Ar), 155.4 (COO'Bu), 130.4 (Ar), 127.7 (Ar), 114.1 (Ar), 80.3 (COOC(CH₃)₃), 55.2 (OCH₃), 54.4 (CHNH), 36.9 (ArCH₂), 28.3 (COOC(CH₃)₃).

The observed data are in accord with published values.¹⁷¹

Preparation of *N*-Boc-*O*-benzyl tyrosine **351**

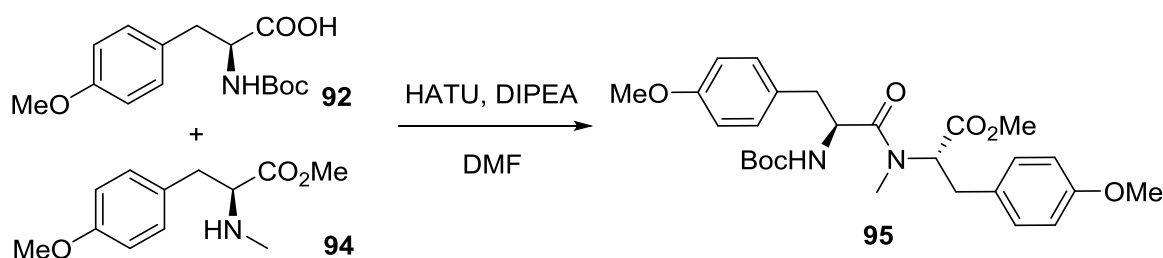


N-Boc-*O*-benzyl-L-tyrosine **351** was prepared from **98** (1.80 g, 4.67 mmol) following a similar procedure to that for the synthesis of **92**. Compound **351** was obtained as a white solid (1.54 g, 4.15 mmol, 89% yield). M.p. 106-108 °C (lit.¹⁷² m.p. 109-111 °C); $R_f = 0.40$ (EtOAc/petroleum ether 1:2); $[\alpha]_D^{20} = +17.4$ ($c = 2.0$, CHCl_3); FTIR (film) ν_{\max} 3429, 3320, 2979, 2557, 1711, 1511, 1240, 1161, 734; $^1\text{H NMR}$ (CDCl_3 , 300 MHz) (major rotamer) δ 10.63 (br s, COOH, 1H), 7.48-7.26 (m, ArH, 5H), 7.13 (d, $J = 8.4$ Hz, ArH, 2H), 6.95 (d, $J = 8.4$ Hz, ArH, 2H), 5.06 (s, PhCH₂, 2H), 5.07-4.97 (m, NH, 1H), 4.62 (dd, $J = 13.1, 5.8$ Hz, CHNH, 1H), 3.17 (dd, $J = 14.0, 5.1$ Hz, ArCH_aH_bCH, 1H), 3.07 (dd, $J = 14.0, 6.1$ Hz,

ArCH_aH_bCH, 1H), 1.46 (s, COOC(CH₃)₃, 9H); ¹³C NMR (CDCl₃, 100 MHz) (major rotamer) δ 176.7 (COOH), 158.0 (Ar), 155.4 (COO^tBu), 137.0 (Ar), 130.5 (Ar), 128.6 (Ar), 128.1 (Ar), 128.0 (Ar), 127.5 (Ar), 115.0 (Ar), 80.3 (COOC(CH₃)₃), 70.0 (PhCH₂), 54.4 (CHNH), 37.0 (ArCH₂CH), 28.3 (COOC(CH₃)₃).

The observed data are in accord with published values.¹⁷²

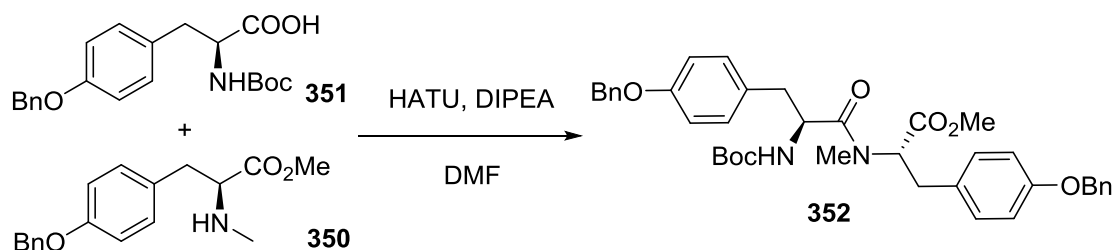
Preparation of dipeptide **95**



To a solution of acid **92** (0.37 g, 1.25 mmol) in DMF (8 mL) was added HATU (0.52 g, 1.38 mmol) and the mixture was stirred for 30 min at 0 °C. A solution of amine **94** (0.28 g, 1.25 mmol) in DMF (5 mL) was added to the reaction solution, followed by DIPEA (0.22 mL, 1.25 mmol). The resulting mixture was warmed to rt and stirred overnight. To the system was added water (20 mL) and the mixture was extracted with DCM (3×20 mL). The organic layers were combined and washed with brine (20 mL). After being dried over MgSO₄ and filtration, the organic solvent was concentrated under reduced pressure. The crude product was purified by column chromatography eluting with 25% ethyl acetate in petroleum ether to give dipeptide **95** (0.45 g, 71% yield) as a white solid. M.p. 114-116 °C; R_f = 0.40 (EtOAc/petroleum ether 1:2); [α]_D²⁰ = -45.2 (c = 1.0, CHCl₃); FTIR (film) ν_{max} 3307, 2988, 2956, 2837, 1735, 1682, 1513, 1243, 1160, 1030; ¹H NMR (CDCl₃, 300 MHz) (major rotamer) δ 7.12 (d, *J* = 8.4 Hz, ArH, 2H), 7.04 (d, *J* = 8.5 Hz, ArH, 2H), 6.81 (d, *J* = 8.5 Hz, ArH, 2H), 6.79 (d, *J* = 8.4 Hz, ArH, 2H), 5.20 (dd, *J* = 9.7, 6.0 Hz, CHNCH₃, 1H), 5.11 (d, *J* = 8.9 Hz,

NH, 1H), 4.71 (dd, $J = 14.0, 9.2$ Hz, *CHNH*, 1H), 3.78 (s, *ArOCH*₃, 3H), 3.77 (s, *ArOCH*₃, 3H), 3.71 (s, *COOCH*₃, 3H), 3.28 (dd, $J = 14.4, 6.0$ Hz, *CH*_a*H*_b*CHNMe*, 1H), 2.92 (dd, $J = 14.4, 9.7$ Hz, *CH*_a*H*_b*CHNH*, 1H), 2.83 (dd, $J = 9.2, 4.0$ Hz, *CH*_a*H*_b*CHNMe*, 1H), 2.77 (s, *NCH*₃, 3H), 2.46 (dd, $J = 14.0, 4.0$ Hz, *CH*_a*H*_b*CHNH*, 1H), 1.40 (s, *COOC(CH*₃*)*₃, 9H); ¹³C NMR (CDCl₃, 100 MHz) δ 172.2 (*CONMe*), 170.9 (*COOMe*), 158.5 (*Ar*), 155.0 (*COO*^t*Bu*), 130.6 (*Ar*), 129.9 (*Ar*), 128.7 (*Ar*), 128.4 (*Ar*), 113.9 (*Ar*), 113.8 (*Ar*), 79.6 (*COOC(CH*₃*)*₃), 58.8 (*CHNMe*), 55.2 (*ArOCH*₃), 55.1 (*ArOCH*₃), 52.2 (*COOCH*₃), 51.6 (*CHNH*), 38.3 (*CH*₂*CHNH*), 33.8 (*CH*₂*CHNMe*), 32.6 (*NCH*₃), 28.3 (*COOC(CH*₃*)*₃); HRMS (ESI) calculated for C₂₇H₃₆N₂O₇Na [M+Na]⁺ 523.2420, found 523.2426.

Preparation of dipeptide **352**

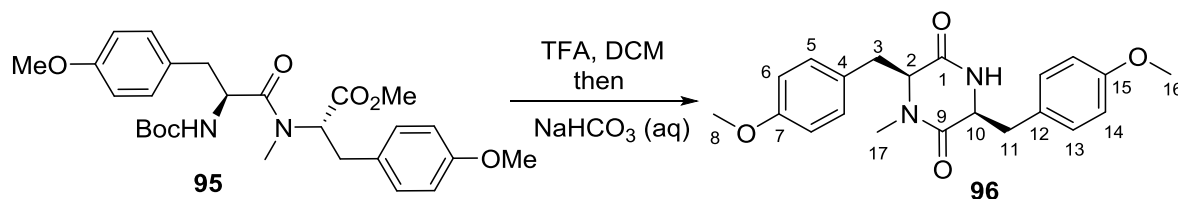


Dipeptide **352** was prepared from acid **351** (0.65 g, 1.75 mmol) and amine **350** (0.52 g, 1.75 mmol) following a similar procedure to that for the synthesis of **95** and was obtained as a colourless oil (0.89 g, 1.36 mmol, 78% yield). $R_f = 0.46$ (EtOAc:hexane = 1:1); $[\alpha]_D^{20} = -38.2$ ($c = 2.2$, CHCl₃); FTIR (film) ν_{\max} 3425, 3317, 3033, 2979, 2932, 2879, 1740, 1706, 1645, 1611, 1510, 1238, 1167, 1015, 732, 696; ¹H NMR (CDCl₃, 400 MHz) (major rotamer) δ 7.46-7.31 (m, *ArH*, 10H), 7.18-7.06 (m, *ArH*, 3H), 6.95-6.84 (m, *ArH*, 5H), 5.32 (d, $J = 8.8$ Hz, *NH*, 1H), 5.24-5.15 (m, *CHNMe*, 1H), 5.04 (s, *PhCH*₂, 2H), 5.03 (s, *PhCH*₂, 2H), 4.79-4.73 (m, *CHNH*, 1H), 3.75 (s, *OCH*₃, 3H), 3.30 (dd, $J = 14.4, 5.4$ Hz, *CH*_a*H*_b*CHNMe*, 1H), 2.95 (dd, $J = 14.4, 4.1$ Hz, *CH*_a*H*_b*CHNMe*, 1H), 2.70 (dd, $J = 13.8, 6.7$ Hz, *CH*_a*H*_b*CHNH*, 1H),

2.58 (dd, $J = 13.8, 6.4$ Hz, $\text{CH}_a\text{H}_b\text{CHNH}$, 1H), 1.43 (s, $\text{COOC}(\text{CH}_3)_3$, 9H); ^{13}C NMR (CDCl_3 , 100 MHz) δ 172.7 (CONMe), 170.9 (COOMe), 157.8 (Ar), 157.7 (Ar), 155.1 (COO^tBu), 137.1 (Ar), 136.9 (Ar), 130.0 (Ar), 129.9 (Ar), 129.1 (Ar), 128.7 (Ar), 128.6 (Ar), 127.9 (Ar), 127.4 (Ar), 115.0 (Ar), 114.9 (Ar), 114.8 (Ar), 114.7 (Ar), 79.5 ($\text{COOC}(\text{CH}_3)_3$), 70.0 (d, PhCH_2), 58.9 (CHNMe), 52.3 (OCH₃), 51.7 (CHNH), 38.3 (CH_2CHNH), 33.8 (CH_2CHNMe), 32.8 (NCH₃), 28.3 ($\text{COOC}(\text{CH}_3)_3$); HRMS (ESI) calculated for $\text{C}_{39}\text{H}_{44}\text{N}_2\text{O}_7\text{Na}$ $[\text{M}+\text{Na}]^+$ 675.3046, found 675.3048;

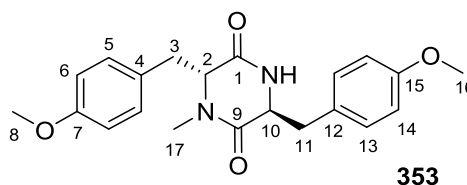
Although compound **352** was mentioned in the literature and confirmed by mass spectrometry,¹⁷³ no further characterisation has been reported.

Preparation of *cis*-diketopiperazine **96**

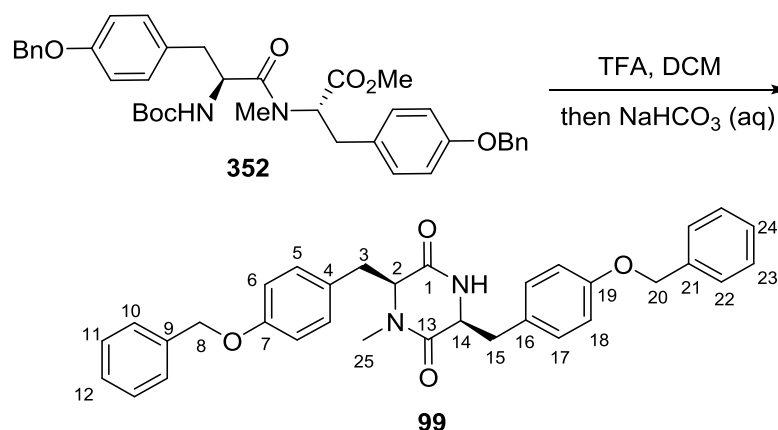


To a solution of dipeptide **95** (0.54 g, 1.08 mmol) in dry DCM (10 mL) was added TFA (1.0 mL, 13.1 mmol) and the mixture was stirred overnight. Another portion of DCM (10 mL) was added to the system, followed by slow addition of saturated NaHCO₃ solution (20 mL). After thoroughly stirring, the organic layer was separated and the aqueous layer was extracted twice with DCM (2×20 mL). The organic layers were combined, dried over MgSO₄ and concentrated under reduced pressure. The crude product was purified by column chromatography using ethyl acetate as the eluent to afford DKP **96** (0.26 g, 62% yield) as a colourless oil. $R_f = 0.20$ (EtOAc/MeOH 6:1); $[\alpha]_D^{22} = -47.5$ ($c = 6.5$, CHCl_3); FTIR (film) ν_{max} 3228, 2934, 1681, 1652, 1513, 1248; ^1H NMR (CDCl_3 , 400 MHz) δ 7.11 (d, $J = 8.7$ Hz, H-5, 2H), 6.94 (d, $J = 8.7$ Hz, H-6, 2H), 6.87 (d, $J = 8.8$ Hz, H-14, 2H), 6.82 (d, $J = 8.8$ Hz, H-13,

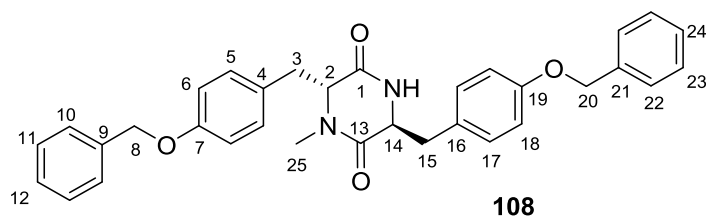
2H), 5.68 (s, *NH*, 1H), 4.17 (t, $J = 3.8$ Hz, H-2, 1H), 3.85 (dt, $J = 11.5, 2.8$ Hz, H-10, 1H), 3.78 (s, H-8 or H-16, 3H), 3.76 (s, H-16 or H-8, 3H), 3.22 (dd, $J = 14.2, 3.8$ Hz, H-3a, 1H), 3.11 (dd, $J = 14.2, 3.8$ Hz, H-3b, 1H), 3.11 (s, H-17, 3H), 2.91 (dd, $J = 13.6, 2.8$ Hz, H-11a, 1H), 0.93 (dd, $J = 13.6, 11.5$ Hz, H-11b, 1H); ^{13}C NMR (CDCl_3 , 100 MHz) δ 165.8 (C-1 or C-9), 165.5 (C-9 or C-1), 159.3 (C-7), 158.8 (C-15), 131.4 (C-5), 130.1 (C-13), 128.0 (C-4 or C-12), 126.8 (C-12 or C-4), 114.4 (C-6 and C-14), 63.2 (C-2), 56.9 (C-10), 55.4 (C-8 or C-16), 55.3 (C-16 or C-8), 39.8 (C-11), 35.8 (C-3), 33.1 (C-17); HRMS (ESI) calculated for $\text{C}_{21}\text{H}_{24}\text{N}_2\text{O}_4\text{Na}$ $[\text{M}+\text{Na}]^+$ 391.1634, found 391.1649.



The *trans*-DKP **353** was obtained as a by-product when the methylation of tyrosine derivative **91** was conducted with Method A (NaH/MeI). M.p. 156-158 °C; $R_f = 0.20$ (EtOAc); $[\alpha]_D^{22} = +4.4$ ($c = 6.5$, CHCl_3); FTIR (film) ν_{max} 3244, 2934, 1642, 1511, 1246; ^1H NMR (CDCl_3 , 400 MHz) δ 7.01 (d, $J = 8.6$ Hz, H-5 or H-13, 2H), 6.92 (d, $J = 8.6$ Hz, H-13 or H-5, 2H), 6.83 (d, $J = 8.6$ Hz, H-6 or H-14, 2H), 6.83 (d, $J = 8.6$ Hz, H-14 or H-6, 2H), 5.44 (br s, *NH*, 1H), 4.11 (t, $J = 3.9$ Hz, H-2, 1H), 3.83 (s, H-8 or H-16, 3H), 3.81 (s, H-16 or H-8, 3H), 3.26 (dd, $J = 14.0, 3.3$ Hz, H-11a, 1H), 3.20 (dd, $J = 14.1, 3.5$ Hz, H-3a, 1H), 3.08 (dd, $J = 14.0, 4.4$ Hz, H-3b, 1H), 3.07 (s, H-17, 3H), 2.61 (dd, $J = 10.5, 3.3$ Hz, H-10, 1H), 2.49 (dd, $J = 14.0, 10.5$ Hz, H-11b, 1H); ^{13}C NMR (CDCl_3 , 100 MHz) δ 167.6 (C-9), 166.3 (C-1), 159.4 (C-7 or C-15), 158.9 (C-15 or C-7), 131.0 (C-5), 130.0 (C-13), 127.5 (C-4 or C-12), 126.3 (C-12 or C-4), 114.5 (C-6 or C-14), 114.2 (C-14 or C-6), 64.1 (C-2), 55.3 (C-8 and C-16), 54.0 (C-10), 37.4 (C-11), 35.9 (C-3), 32.9 (C-17); HRMS (ESI) calculated for $\text{C}_{21}\text{H}_{24}\text{N}_2\text{O}_4\text{Na}$ $[\text{M}+\text{Na}]^+$ 391.1634, found 391.1644.

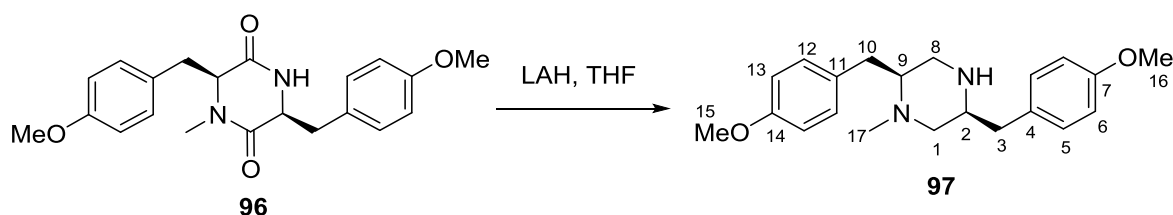
Preparation of *cis*-diketopiperazine **99**

DKP derivative **99** was prepared from dipeptide **352** (0.72 g, 1.10 mmol) following a similar procedure to that for the synthesis of **96**. Compound **99** was obtained as a colourless oil (0.42 g, 0.80 mmol, 73% yield). $R_f = 0.25$ (EtOAc/MeOH 6:1); $[\alpha]_D^{24} = -63$ ($c = 5.0$, CHCl₃); FTIR (film) ν_{\max} 3213, 2975, 2939, 1679, 1651, 1510, 1234, 1018, 730; ¹H NMR (CDCl₃, 300 MHz) δ 7.47-7.21 (m, H-10 and H-11 and H-12 and H-23 and H-24, 10H), 7.11 (d, $J = 8.6$ Hz, H-5, 2H), 7.01 (d, $J = 8.6$ Hz, H-6, 2H), 6.90 (d, $J = 8.6$ Hz, H-18, 2H), 6.85 (d, $J = 8.6$ Hz, H-17, 2H), 5.56 (d, $J = 1.2$ Hz, NH, 1H), 5.06 (s, H-8 or H-20, 2H), 5.05 (s, H-20 or H-8, 2H), 4.19 (t, $J = 3.8$ Hz, H-2, 1H), 3.83 (m, H-14, 1H), 3.26 (dd, $J = 14.2, 3.8$ Hz, H-3a, 1H), 3.13 (s, H-25, 3H), 3.12 (dd, $J = 14.2, 3.8$ Hz, H-3b, 1H), 2.86 (dd, $J = 13.6, 2.8$ Hz, H-15a, 1H), 0.82 (dd, $J = 13.6, 11.7$ Hz, H-15b, 1H); ¹³C NMR (CDCl₃, 100 MHz) δ 165.7 (C-1 or C-13), 165.4 (C-13 or C-1), 158.4 (C-7 or C-19), 158.0 (C-19 or C-7), 136.9 (C-9 or C-21), 136.7 (C-21 or C-9), 131.5 (C-5), 130.2 (C-17), 128.6 (C-11 or C-23), 128.5 (C-23 or C-11), 128.3 (C-12 or C-24), 128.0 (C-24 or C-12), 127.9 (C-16), 127.4 (C-10 or C-22), 127.2 (C-22 or C-10), 127.0 (C-4), 115.5 (C-6), 115.4 (C-18), 70.1 (C-8 or C-20), 70.0 (C-20 or C-8), 63.2 (C-2), 56.9 (C-14), 39.8 (C-15), 35.7 (C-3), 33.1 (C-25); HRMS (ESI) calculated for C₃₃H₃₂N₂O₄Na [M+Na]⁺ 543.2260, found 543.2278.



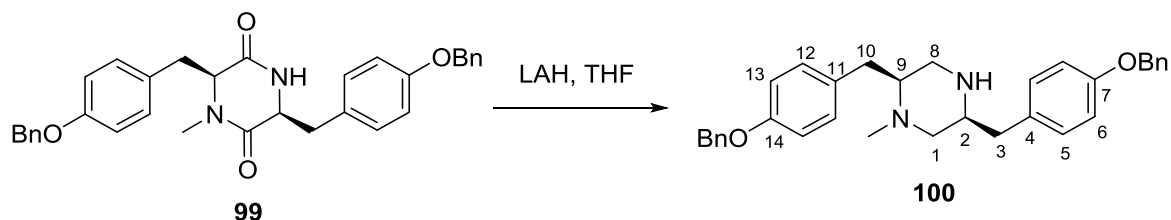
The *trans*-DKP **108** was obtained as a by-product when the methylation of **98** was conducted with Method A (NaH/MeI). M.p. 165-166 °C; $R_f = 0.30$ (EtOAc); $[\alpha]_D^{22} = +3.0$ ($c = 6.5$, CHCl₃); FTIR (film) ν_{\max} 3225, 2930, 1682, 1656, 1510, 1240, 1025; ¹H NMR (CDCl₃, 400 MHz) δ 7.54-7.32 (m, H-10 and H-11 and H-12 and H-22 and H-23 and H-24, 10H), 7.02 (d, $J = 8.6$ Hz, H-5 or H-17, 2H), 6.91 (d, $J = 8.6$ Hz, H-17 or H-5, 2H), 6.90 (d, $J = 8.6$ Hz, H-6 and H-18, 4H), 5.51 (s, NH, 1H), 5.07 (d, $J = 4.3$ Hz, H-8 or H-20, 2H), 5.05 (s, H-20 or H-8, 2H), 4.10 (t, $J = 3.9$ Hz, H-2, 1H), 3.25 (dd, $J = 14.2, 3.3$ Hz, H-15a, 1H), 3.20 (dd, $J = 14.0, 3.2$ Hz, H-3a, 1H), 3.09 (dd, $J = 14.0, 4.4$ Hz, H-3b, 1H), 3.07 (s, H-25, 3H), 2.65 (dd, $J = 10.4, 3.3$ Hz, H-14, 1H), 2.52 (dd, $J = 14.2, 10.4$ Hz, H-15b, 1H); ¹³C NMR (CDCl₃, 100 MHz) δ 167.6 (C-13), 166.3 (C-1), 158.6 (C-7 or C-19), 158.1 (C-19 or C-7), 136.9 (C-9 or C-21), 136.7 (C-21 or C-9), 131.0 (C-5), 130.1 (C-17), 128.7 (C-11 or C-23), 128.6 (C-23 or C-11), 128.1 (C-12 or C-24), 128.0 (C-24 or C-12), 127.8 (C-16), 127.5 (C-10 or C-22), 127.4 (C-22 or C-10), 126.7 (C-4), 115.5 (C-6 or C-18), 115.1 (C-18 or C-6), 70.1 (C-8 and C-20), 64.1 (C-2), 54.0 (C-14), 37.5 (C-15), 35.9 (C-3), 32.9 (C-25); HRMS (ESI) calculated for C₃₃H₃₂N₂O₄Na [M+Na]⁺ 543.2260, found 543.2249.

Reduction of DKP **96** to piperazine **97**



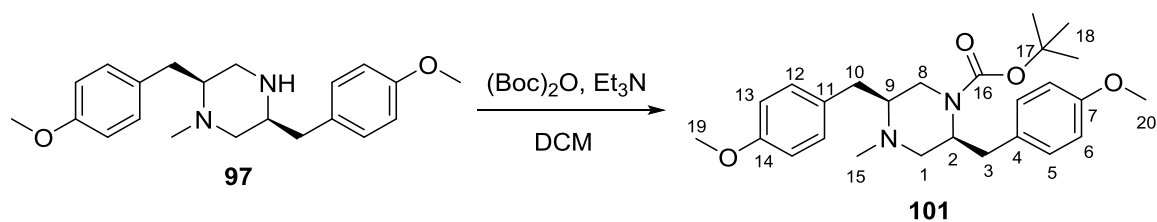
At 0 °C, to a solution of DKP **96** (0.22 g, 0.60 mmol) in anhydrous THF (10 mL) was added lithium aluminium hydride solution (1.0 M in THF, 1.80 mL, 1.80 mmol) dropwise. The system was maintained at the same temperature for 3 h and then warmed to rt. After being stirred for 4 days at rt, the mixture was cooled to 0 °C and ethyl acetate (10 mL) was added to quench the reaction, followed by addition of saturated NaOH aqueous solution (2 mL) and THF (15 mL). After being stirred for 15 min, the mixture was filtered and the solid was washed thoroughly with DCM (4×10 mL). The filtrate was dried over MgSO₄ and concentrated under reduced pressure. The crude product was purified by column chromatography using ethyl acetate/MeOH (10:1) as the eluent to afford piperazine **97** (0.13 g, 65% yield) as a white film. $R_f = 0.30$ (EtOAc/MeOH 3:1); $[\alpha]_D^{24} = +26.5$ ($c = 0.65$, CHCl₃); FTIR (film) ν_{\max} 3031, 2929, 2835, 2796, 1509, 1241, 1026, 804, 733; ¹H NMR (CDCl₃, 400 MHz) δ 7.16 (d, $J = 8.4$ Hz, H-5 or H-12, 2H), 7.12 (d, $J = 8.4$ Hz, H-12 or H-5, 2H), 6.87 (d, $J = 8.8$ Hz, H-6 or H-13, 2H), 6.84 (d, $J = 8.4$ Hz, H-13 or H-6, 2H), 3.81 (s, H-15 or H-16, 3H), 3.80 (s, H-16 or H-15, 3H), 3.01 (ddd, $J = 14.9, 7.5, 3.6$ Hz, H-2, 1H), 2.86-2.84 (m, H-10, 2H), 2.80-2.77 (dd, $J = 11.9, 3.6$ Hz, H-8a, 1H), 2.71-2.64 (m, H-3 and H-8b and H-9, 4H), 2.51-2.46 (dd, $J = 11.9, 3.6$ Hz, H-1a, 1H), 2.46 (s, H-17, 3H), 2.44-2.41 (dd, $J = 11.9, 3.6$ Hz, H-1b, 1H); ¹³C NMR (CDCl₃, 100 MHz) δ 157.1 (C-7 or C-14), 156.8 (C-14 or C-7), 131.6 (C-4 or C-11), 130.0 (C-11 or C-4), 129.2 (C-5 or C-12), 129.1 (C-12 or C-5), 112.9 (C-6 or C-13), 112.8 (C-13 or C-6), 61.1 (C-9), 55.3 (C-2), 54.7 (C-1), 54.2 (C-15 and C-16), 45.7 (C-8), 42.1 (C-17), 38.2 (C-3), 27.3 (C-10); HRMS (ESI) calculated for C₂₁H₂₉N₂O₂ [M+H]⁺ 341.2229, found 341.2240.

Reduction of DKP to piperazine 100



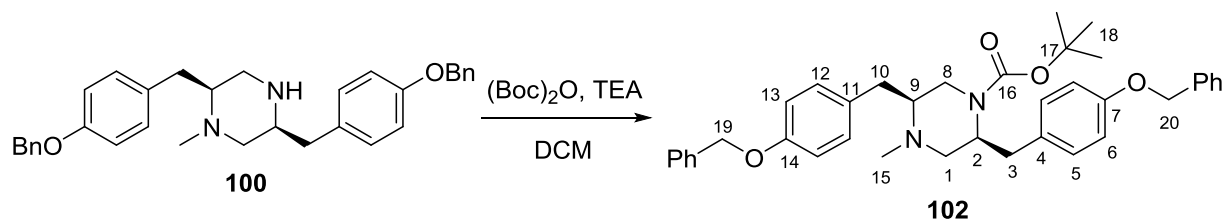
Piperazine derivative **100** was prepared from the reduction of **99** (0.36 g, 0.69 mmol) following a similar procedure to that for the synthesis of **97**. Compound **100** was obtained as a white solid (0.23 g, 0.47 mmol, 68% yield). M.p. 129-131 °C; $R_f = 0.35$ (EtOAc/MeOH 3:1); $[\alpha]_D^{24} = +16.5$ ($c = 0.80$, CHCl_3); FTIR (film) ν_{max} 3031, 2924, 2796, 1509, 1237, 1017, 801; $^1\text{H NMR}$ (CDCl_3 , 300 MHz) δ 7.40-7.20 (m, PhH, 10H), 7.06 (d, $J = 8.6$ Hz, H-5 or H-12, 2H), 7.03 (d, $J = 8.6$ Hz, H-12 or H-5, 2H), 6.84 (d, $J = 8.8$ Hz, H-6 or H-13, 2H), 6.81 (d, $J = 8.8$ Hz, H-13 or H-6, 2H), 4.96 (s, PhCH_2 , 2H), 4.94 (s, PhCH_2 , 2H), 3.02-2.90 (m, H-2, 1H), 2.80-2.57 (m, H-10 and H-8 and H-3 and H-9, 7H), 2.42-2.36 (m, H-1, 2H), 2.38 (s, NCH_3 , 3H); $^{13}\text{C NMR}$ (CDCl_3 , 100 MHz) δ 157.4 (C-7 or C-14), 157.1 (C-14 or C-7), 137.2 (Ph), 132.6 (C-4 or C-11), 131.0 (C-11 or C-4), 130.3 (C-5 or C-12), 130.2 (C-12 or C-5), 128.6 (Ph), 127.9 (Ph), 127.5 (Ph), 114.9 (C-6 or C-13), 114.8 (C-13 or C-6), 70.1 (PhCH_2), 61.9 (C-9), 56.1 (C-2), 55.4 (C-1), 46.4 (C-8), 43.0 (NCH_3), 39.0 (C-3), 28.5 (C-10); HRMS (ESI) calculated for $\text{C}_{33}\text{H}_{37}\text{N}_2\text{O}_2$ $[\text{M}+\text{H}]^+$ 493.2855, found 493.2863.

Preparation of piperazine 101



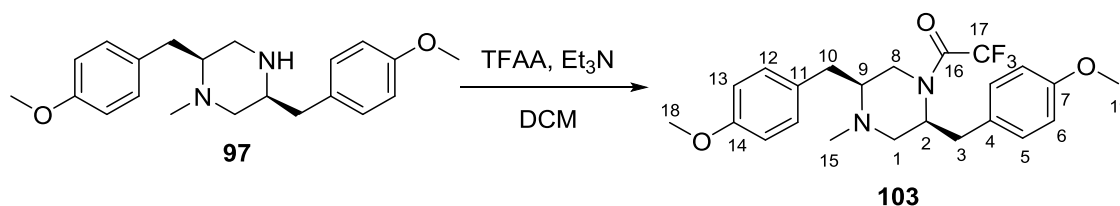
To a solution of piperazine derivative **97** (0.51 g, 1.51 mmol) in DCM (8 mL) was added a solution of (Boc)₂O (0.40 g, 1.81 mmol) in DCM (2 mL), followed by Et₃N (0.25 mL, 1.81 mmol). The mixture was stirred at rt for 10 h. Upon completion, DCM (10 mL) was added and the reaction mixture was washed with saturated NaHCO₃ (aq) (10 mL). The organic layer was dried over MgSO₄, filtered and concentrated under reduced pressure. The crude product was purified by column chromatography eluting with ethyl acetate/petroleum ether (1:6) to afford product **101** (0.51 g, 77% yield) as a white solid. M.p. 118-119 °C; R_f = 0.60 (EtOAc/petroleum ether 1:1); [α]_D²⁰ = -99 (*c* = 0.4, CHCl₃); FTIR (film) ν_{max} 2966, 2927, 2862, 2792, 1688, 1612, 1511, 1243, 1165, 1035, 820; ¹H NMR (CDCl₃, 400 MHz) δ 7.15 (d, *J* = 8.5 Hz, H-5 and H-12, 4H), 6.85 (d, *J* = 8.5 Hz, H-6 and H-13, 4H), 4.15-4.04 (br m, H-2, 1H), 3.86-3.74 (br m, H-8a, 1H), 3.80 (s, H-19 or H-20, 3H), 3.79 (s, H-20 or H-19, 3H), 3.13 (dd, *J* = 13.8, 4.0 Hz, H-10a, 1H), 3.06-2.95 (br m, H-3a, 1H), 2.89-2.67 (m, H-3b and H-8b and H-1a, 3H), 2.55-2.47 (m, H-10b, 1H), 2.38 (s, H-15, 3H), 2.26-2.10 (m, H-1b and H-9, 2H), 1.32 (s, H-18, 9H); ¹³C NMR (CDCl₃, 100 MHz) δ 158.2 (C-7 or C-14), 158.1 (C-14 or C-7), 154.4 (C-16), 131.4 (C-4 and C-11), 130.3 (C-5 or C-12), 130.2 (C-12 or C-5), 113.9 (C-6 or C-13), 113.8 (C-13 or C-6), 79.4 (C-17), 64.2 (C-9), 57.8 (C-1), 55.3 (C-19 and C-20), 53.7 (C-2), 43.2 (C-15), 43.1 (C-8), 36.9 (C-10), 35.2 (C-3), 28.2 (C-18); HRMS (ESI) calculated for C₂₆H₃₇N₂O₄ [M+H]⁺ 441.2753, found 441.2760.

Preparation of piperazine derivative **102**



The *N*-Boc-protected compound **102** was prepared from piperazine **100** (0.35 g, 0.71 mmol) following a similar procedure to that for the synthesis of **101** and was obtained as a white solid (0.37 g, 0.63 mmol, 88% yield). M.p. 105-106 °C; $R_f = 0.40$ (EtOAc/petroleum ether 1:3); $[\alpha]_D^{20} = -34$ ($c = 0.6$, CHCl_3); FTIR (film) ν_{max} 3032, 2975, 2928, 2860, 2792, 1687, 1509, 1239, 1166; $^1\text{H NMR}$ (CDCl_3 , 300 MHz) δ 7.51-7.31 (m, ArH, 10H), 7.16 (d, $J = 8.6$ Hz, H-5 and H-12, 4H), 6.93 (d, $J = 8.6$ Hz, H-6 and H-13, 4H), 5.07 (s, H-19 and H-20, 4H), 4.17-4.04 (br m, H-2, 1H), 3.85-3.81 (br m, H-8a, 1H), 3.14 (dd, $J = 13.8, 3.9$ Hz, H-10a, 1H), 3.08-2.94 (br m, H-3a, 1H), 2.92-2.65 (m, H-3b and H-8b and H-1a, 3H), 2.57-2.44 (br m, H-10b, 1H), 2.38 (s, H-15, 3H), 2.21-2.13 (br m, H-1b and H-9, 2H), 1.33 (s, H-18, 9H); $^{13}\text{C NMR}$ (CDCl_3 , 100 MHz) δ 157.4 (C-7 or C-14), 157.3 (C-14 or C-7), 154.4 (C-16), 137.2 (Ph), 131.8 (C-4 and C-11), 130.4 (C-5 or C-12), 130.3 (C-12 or C-5), 128.6 (Ph), 127.9 (Ph), 127.5 (Ph), 114.9 (C-6 and C-13), 79.4 (C-17), 70.1 (C-19 and C-20), 64.1 (C-9), 58.0 (C-1), 53.7 (C-2), 43.3 (C-15), 43.2 (C-8), 37.0 (C-10), 35.2 (C-3), 28.3 (C-18); HRMS (ESI) calculated for $\text{C}_{38}\text{H}_{45}\text{N}_2\text{O}_4$ $[\text{M}+\text{H}]^+$ 593.3379, found 593.3384.

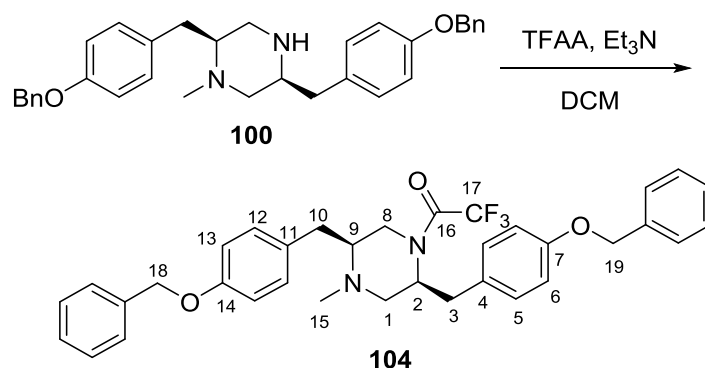
Preparation of piperazine derivative **103**



To a solution of piperazine **97** (51 mg, 0.15 mmol) in DCM (5 mL) at 0 °C was added Et_3N (25 μL , 0.18 mmol), followed by a solution of trifluoroacetic anhydride (25 μL , 0.18 mmol) in DCM (2 mL). The resulting mixture was stirred at room temperature overnight. Upon completion, the reaction system was washed with saturated NaHCO_3 solution (10 mL). The aqueous phase was extracted with DCM (2 \times 10 mL). The combined organic fractions were

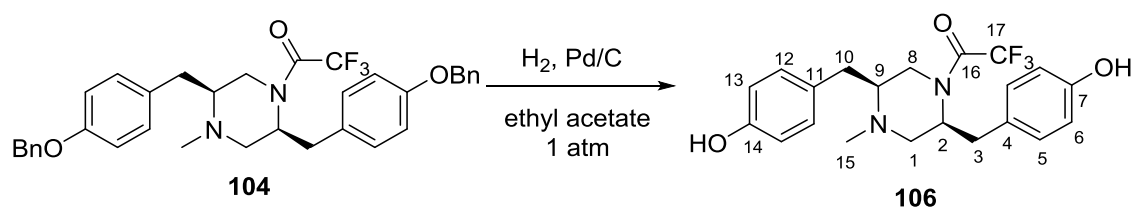
dried over MgSO_4 , filtered and concentrated under reduced pressure. The crude product was purified by column chromatography eluting with 30% EtOAc in petroleum ether to afford desired product **103** (55 mg, 84% yield) as a white solid. M.p. 143-144 °C; $R_f = 0.55$ (EtOAc/petroleum ether 1:1); $[\alpha]_D^{20} = -83$ ($c = 0.6$, CHCl_3); FTIR (film) ν_{max} 2959, 2801, 1689, 1513, 1464, 1249, 1142, 1038, 822; $^1\text{H NMR}$ (CDCl_3 , 300 MHz) δ 7.17 (d, $J = 8.6$ Hz, H-5 or H-12, 2H), 7.13 (d, $J = 8.7$ Hz, H-12 or H-5, 2H), 6.89 (d, $J = 8.6$ Hz, H-6 or H-13, 2H), 6.85 (d, $J = 8.7$ Hz, H-13 or H-6, 2H), 4.66-4.58 (br m, H-2, 1H), 4.14 (dd, $J = 13.4, 2.4$ Hz, H-8a, 1H), 3.83 (s, H-18 or H-19, 3H), 3.82 (s, H-19 or H-18, 3H), 3.49 (d, $J = 13.4$ Hz, H-10a, 1H), 3.23-3.00 (m, H-3a and H-10b, 2H), 2.89-2.64 (m, H-1a and H-3b and H-8b, 3H), 2.40 (s, H-15, 3H), 2.23-2.18 (m, H-1b and H-9, 2H); $^{13}\text{C NMR}$ (CDCl_3 , 100 MHz) δ 158.5 (C-7 or C-14), 158.4 (C-14 or C-7), 155.6 (q, $^2J_{\text{FC}} = 36$ Hz, C-16), 130.3 (C-5 or C-12), 130.0 (C-12 or C-5), 129.7 (C-4 and C-11), 117.6 (q, $^1J_{\text{FC}} = 286$ Hz, C-17), 114.1 (C-6 or C-13), 114.0 (C-13 or C-6), 64.4 (C-9), 56.7 (C-1), 55.3 (C-18 and C-19), 52.2 (C-2), 45.3 (C-10), 42.8 (C-8 and C-15), 34.5 (C-3); HRMS (ESI) calculated for $\text{C}_{23}\text{H}_{28}\text{F}_3\text{N}_2\text{O}_3$ $[\text{M}+\text{H}]^+$ 437.2052, found 437.2051.

Preparation of piperazine derivative **104**



N-trifluoroacetyl-protected piperazine derivative **104** was prepared from piperazine **100** (0.35 g, 0.71 mmol) following a similar procedure to that for the synthesis of **103** and was obtained as a white solid (0.31 g, 0.53 mmol, 75% yield). M.p. 146-147 °C; $R_f = 0.50$ (EtOAc:hexane = 1:1); $[\alpha]_D^{20} = -3.2$ ($c = 2.5$, CHCl_3); FTIR (film) ν_{max} 3666, 2972, 2923, 1680, 1512, 1454, 1247, 1180, 1137, 1041, 813, 729; $^1\text{H NMR}$ (CDCl_3 , 400 MHz) δ 7.52-7.33 (m, PhH, 10H), 7.19 (d, $J = 8.6$ Hz, H-5 or H-12, 2H), 7.15 (d, $J = 8.6$ Hz, H-12 or H-5, 2H), 6.98 (d, $J = 8.6$ Hz, H-6 or H-13, 2H), 6.97 (d, $J = 8.6$ Hz, H-13 or H-6, 2H), 5.11 (s, H-18 or H-19, 2H), 5.07 (s, H-19 or H-18, 2H), 4.69-4.61 (br m, H-2, 1H), 4.18 (dd, $J = 13.4, 2.6$ Hz, H-8a, 1H), 3.51 (d, $J = 13.6$ Hz, H-10a, 1H), 3.21-3.09 (m, H-3a and H-10b, 3H), 2.93-2.68 (m, H-1a and H-3b and H-8b, 3H), 2.42 (s, H-15, 3H), 2.26-2.20 (m, H-1b and H-9, 2H); $^{13}\text{C NMR}$ (CDCl_3 , 100 MHz) δ 157.8 (C-7 or C-14), 157.7 (C-14 or C-7), 155.2 (q, $^2J_{\text{FC}} = 35$ Hz, C-16), 137.1 (Ph), 137.0 (Ph), 130.4 (C-5 or C-12), 130.1 (C-12 or C-5), 128.6 (Ph), 128.0 (C-4 and C-11), 127.9 (Ph), 127.5 (Ph), 117.7 (q, $^1J_{\text{FC}} = 286$ Hz, C-17), 115.2 (C-6 or C-13), 115.0 (C-13 or C-6), 70.1 (C-18 and C-19), 64.4 (C-9), 56.7 (C-1), 52.2 (C-2), 45.3 (C-10), 42.8 (C-8 and C-15), 34.6 (C-3); HRMS (ESI) calculated for $\text{C}_{35}\text{H}_{36}\text{F}_3\text{N}_2\text{O}_3$ $[\text{M}+\text{H}]^+$ 589.2678, found 589.2681.

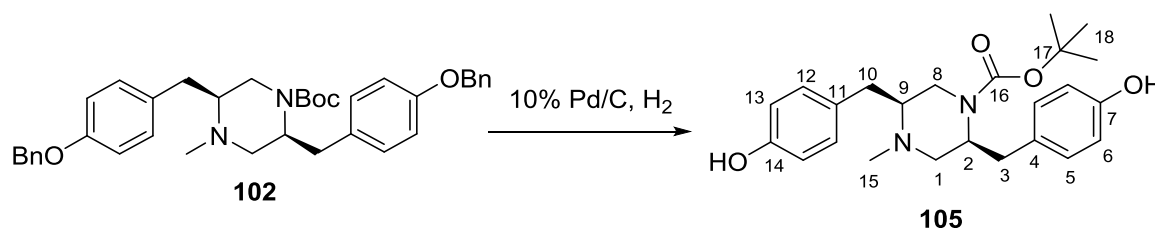
Preparation of bis-phenol **106**



A mixture of piperazine **104** (0.32 g, 0.54 mmol) and 10% Pd/C catalyst (0.09 g) in ethyl acetate (5.0 mL) was stirred under H_2 atmosphere (1 atm) for 48 h. Upon completion, the reaction was filtered through a layer of Celite pad and the catalyst was washed with MeOH (2×10 mL). The filtrate was concentrated and the crude product was purified by column

chromatography eluting with 40% EtOAc in petroleum ether to afford the desired product **106** (0.20 g, 89% yield) as a colourless oil. $R_f = 0.37$ (EA:Hexane = 1:1); $[\alpha]_D^{19} = +58$ ($c = 0.2$, MeOH); FTIR (film) ν_{\max} 3389, 2971, 2926, 1675, 1516, 1447, 1211, 1149, 1047, 824; ^1H NMR (MeOD- d_4 , 300 MHz) δ 7.07 (d, $J = 8.5$ Hz, H-5 or H-12, 2H), 7.04 (d, $J = 8.5$ Hz, H-12 or H-5, 2H), 6.77 (d, $J = 8.5$ Hz, H-6 or H-13, 2H), 6.70 (d, $J = 8.5$ Hz, H-13 or H-6, 2H), 4.62-4.55 (m, H-2, 1H), 4.09 (dd, $J = 13.4, 2.4$ Hz, H-8a, 1H), 3.47 (d, $J = 14.2$ Hz, H-10a, 1H), 3.26-3.09 (m, H-3a and H-10b, 2H), 3.04-2.80 (m, H-1a and H-3b and H-8b, 3H), 2.33 (s, H-15, 3H), 2.26 (dd, $J = 12.1, 4.1$ Hz, H-1b, 1H), 2.21-2.12 (m, H-9, 1H); ^{13}C NMR (MeOD- d_4 , 100 MHz) δ 157.4 (C-7 or C-14), 157.2 (C-14 or C-7), 155.2 (q, $^2J_{\text{FC}} = 36$ Hz, C-16), 131.4 (C-5 or C-12), 131.3 (C-12 or C-5), 129.6 (C-4 and C-11), 117.6 (q, $^1J_{\text{FC}} = 286$ Hz, C-17), 116.5 (C-6 or C-13), 116.4 (C-13 or C-6), 66.2 (C-9), 58.1 (C-1), 53.8 (C-2), 46.2 (C-10), 43.1 (C-8 and C-15), 35.4 (C-3); HRMS (ESI) calculated for $\text{C}_{21}\text{H}_{23}\text{F}_3\text{N}_2\text{NaO}_3$ $[\text{M}+\text{Na}]^+$ 431.1558, found 431.1574.

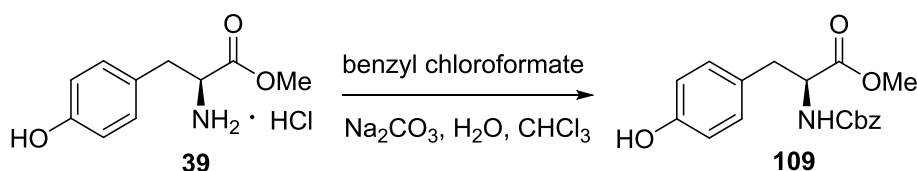
Preparation of bis-phenol **105**



Following a similar procedure to that for the synthesis of **106**, compound **105** was obtained from piperazine **102** (0.26 g, 0.44 mmol) as a white solid (0.16 g, 0.38 mmol, 87% yield). M.p. 94-95 °C; $R_f = 0.40$ (MeOH:EtOAc = 1:10); $[\alpha]_D^{20} = +76$ ($c = 0.1$, MeOH); FTIR (film) ν_{\max} 3320, 2977, 2927, 2857, 2800, 1658, 1515, 1427, 1241, 1162, 734; ^1H NMR (CDCl_3 , 300 MHz) δ 7.02 (m, H-5 and H-12, 4H), 6.71 (m, H-6 and H-13, 4H), 4.26-4.10 (m, H-2, 1H),

3.88 (d, $J = 11.2$ Hz, H-8a, 1H), 3.12 (m, H-10a, 1H), 3.00-2.70 (m, H-1a and H-8b and H-3, 4H), 2.48 (dd, $J = 13.1, 10.0$ Hz, H-10b, 1H), 2.39 (s, H-15, 3H), 2.33-2.13 (m, H-1b and H-9, 2H), 1.27 (s, H-18, 9H); ^{13}C NMR (CDCl_3 , 100 MHz) δ 154.9 (C-16), 154.7 (C-14 and C-7), 130.4 (C-5 or C-12), 130.3 (C-12 or C-5), 128.8 (C-4 and C-11), 115.6 (C-6 or C-13), 115.4 (C-13 or C-6), 80.3 (C-17), 64.4 (C-9), 58.3 (C-1), 53.6 (C-2), 43.3 (C-15), 42.9 (C-8), 36.5 (C-10), 35.2 (C-3), 28.2 (C-18); HRMS (ESI) calculated for $\text{C}_{22}\text{H}_{34}\text{N}_2\text{O}_4\text{Na}$ $[\text{M}+\text{Na}]^+$ 413.2416, found 413.2420.

Synthesis of *N*-Cbz-L-tyrosine methyl ester **109**

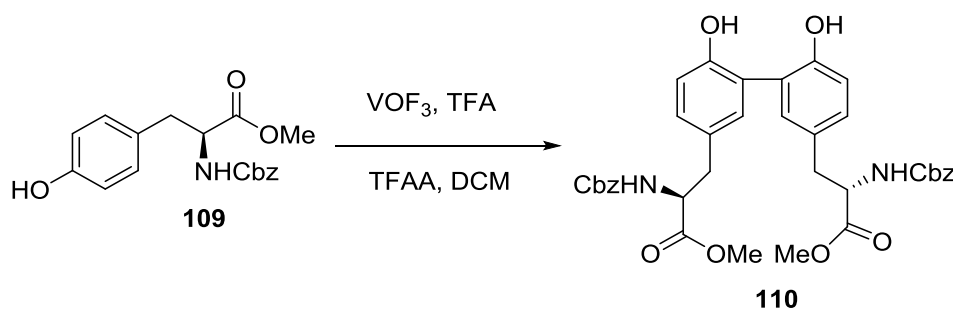


At 0 °C, a solution of Na_2CO_3 (0.21 g, 1.99 mmol) in water (2 mL) was added to a suspension of L-tyrosine methyl ester hydrochloride (0.46 g, 1.99 mmol) in chloroform (10 mL). After stirring for 15 min at 0 °C, another solution of Na_2CO_3 (0.21 g, 1.99 mmol) in water (2 mL) was added, followed by benzyl chloroformate (0.30 mL, 1.99 mmol). The mixture was warmed up to room temperature and stirred vigorously for 5 h. Upon completion, saturated NaHCO_3 solution (10 mL) was added and the organic layer was separated after vigorously stirring the resulting mixture for 5 min. The aqueous layer was extracted with DCM (3×10 mL). The combined organic fractions were washed with brine (15 mL), dried over MgSO_4 and concentrated under reduced pressure. The crude product was purified by column chromatography eluting with 50% EtOAc in petroleum ether to afford the desired product **109** (0.51 g, 79% yield) as a colourless oil. $R_f = 0.45$ (EtOAc/petroleum ether 1:1); $[\alpha]_{\text{D}}^{20} = +36.6$ ($c = 0.5$, CHCl_3); FTIR (film) ν_{max} 3336, 2954, 1694, 1515, 1215; ^1H NMR (300 MHz, CDCl_3)

δ 7.34-7.18 (m, ArH, 5H), 6.84 (d, $J = 8.3$ Hz, ArH, 2H), 6.62 (d, $J = 8.3$ Hz, ArH, 2H), 5.22 (m, NH, 1H), 5.04 (s, PhCH₂, 2H), 4.59-4.51 (m, CHNH, 1H), 3.65 (s, COOCH₃, 3H), 3.08 (dd, $J = 14.0, 5.6$ Hz, CH_aH_bCHNH, 1H), 3.00 (dd, $J = 14.0, 6.2$ Hz, CH_aH_bCHNH, 1H); ¹³C NMR (CDCl₃, 100 MHz) δ 172.5 (COOCH₃), 156.1 (Ar), 155.4 (CO₂CH₂Ph), 136.0 (Ar), 130.4 (Ar), 128.6 (Ar), 128.3 (Ar), 128.1 (Ar), 127.0 (Ar), 115.6 (Ar), 67.2 (PhCH₂), 55.1 (CHNH), 52.5 (OCH₃), 37.4 (CH₂CHNH).

The observed data are in accord with published values.^{174,175}

Intermolecular phenol oxidative coupling (Synthesis of dityrosine **110**)

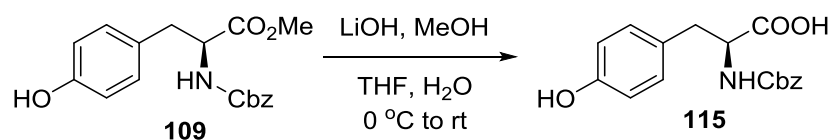


At -10 °C, to a solution of tyrosine derivative **109** (0.15 g, 0.47 mmol) in anhydrous DCM (8 mL), trifluoroacetic acid (1.90 mL, 24.8 mmol) and trifluoroacetic anhydride (95 μ L, 0.67 mmol) was slowly added a solution of VOF₃ (0.15 g, 1.17 mmol) in ethyl acetate (0.75 mL), trifluoroacetic acid (0.71 mL, 9.27 mmol) and trifluoroacetic anhydride (35 μ L, 0.25 mmol). The mixture was stirred at -10 °C for 3 h and then quenched by adding saturated NaHCO₃ solution (15 mL). The organic layer was separated and the aqueous layer was extracted with DCM (2 \times 10 mL). The combined organic fractions were washed with brine (10 mL), dried over MgSO₄, filtered and concentrated under reduced pressure. The crude product was purified by column chromatography eluting with 15% EtOAc in petroleum ether to afford dityrosine derivative **110** (0.07 g, 45% yield) as a colourless oil. R_f = 0.35 (EtOAc/petroleum

ether 1:1); $[\alpha]_D^{20} = +24.5$ ($c = 0.5$, CHCl_3) (lit.⁷⁷ $[\alpha]_D^{28} = +18.6$, $c = 0.3$, CHCl_3); FTIR (film) ν_{max} 3334, 2954, 1699, 1513, 1498, 1216; ^1H NMR (CDCl_3 , 400 MHz) δ 7.36-7.25 (m, ArH, 10H), 7.06 (s, ArH, 2H), 7.01 (d, $J = 8.2$ Hz, ArH, 2H), 6.91 (d, $J = 8.2$ Hz, ArH, 2H), 5.38 (d, $J = 8.5$ Hz, NH, 2H), 5.05 (d, $J = 12.0$ Hz, PhCH_aH_b , 2H), 5.01 (d, $J = 12.0$ Hz, PhCH_aH_b , 2H), 4.68 (dd, $J = 13.0, 7.5$ Hz, CHNH, 1H), 3.75 (s, OCH₃, 6H), 3.16 (dd, $J = 13.8, 4.8$ Hz, ArCH_aH_b, 2H), 2.89 (dd, $J = 13.8, 7.6$ Hz, ArCH_aH_b, 2H); ^{13}C NMR (CDCl_3 , 100 MHz) δ 172.1 (COOCH₃), 155.8 (CO₂CH₂Ph), 152.8 (Ar), 136.0 (Ar), 131.7 (Ar), 130.9 (Ar), 128.5 (Ar), 128.2 (Ar), 128.1 (Ar), 123.5 (Ar), 117.0 (Ar), 67.1 (PhCH₂), 55.1 (CHNH), 52.5 (OCH₃), 38.1 (ArCH₂); HRMS (ESI) calculated for $\text{C}_{36}\text{H}_{36}\text{N}_2\text{O}_{10}\text{Na}$ $[\text{M}+\text{Na}]^+$ 679.2268, found 679.2264.

The observed data are in accord with published values.⁷⁷

Synthesis of *N*-Cbz-L-tyrosine **115**

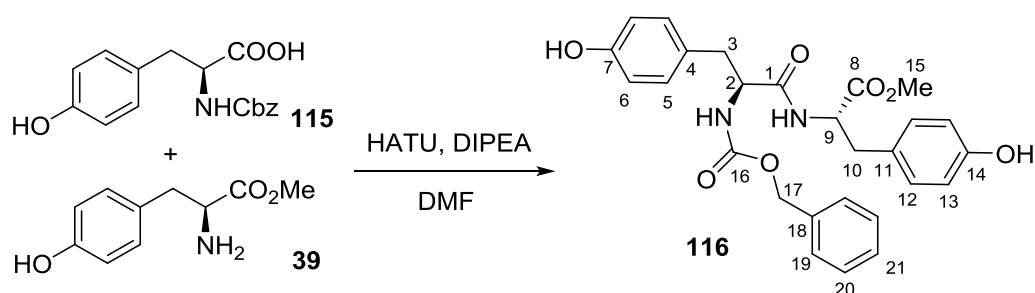


N-Cbz-L-tyrosine **115** was prepared from **109** (0.31 g, 0.94 mmol) following a similar procedure to that for the synthesis of **92**. This product was obtained as a colourless oil which solidified in the fridge (0.27 g, 0.86 mmol, 92% yield). M.p. 95-96 °C; $R_f = 0.25$ (EtOAc/petroleum ether 1:1); $[\alpha]_D^{20} = +34.0$ ($c = 1.0$, CHCl_3); FTIR (film) ν_{max} 3320, 3032, 2963, 1694, 1515, 1222, 1055; ^1H NMR (CDCl_3 , 400 MHz) (major rotamer) δ 8.93 (br s, COOH, 1H), 7.48-7.25 (m, ArH, 5H), 6.96 (d, $J = 8.4$ Hz, ArH, 2H), 6.70 (d, $J = 8.4$ Hz, ArH, 2H), 5.51 (d, $J = 8.2$ Hz, NH, 1H), 5.11 (s, PhCH₂, 2H), 4.66 (dd, $J = 13.8, 5.8$ Hz, CHNH, 1H), 3.10 (dd, $J = 14.0, 5.2$ Hz, ArCH_aH_bCH, 1H), 3.02 (dd, $J = 14.0, 6.0$ Hz, ArCH_aH_bCH, 1H); ^{13}C NMR (CDCl_3 , 100 MHz) (major rotamer) δ 175.3 (COOH), 156.2 (Ar), 155.2

(CO₂CH₂Ph), 136.0 (Ar), 130.5 (Ar), 128.6 (Ar), 128.3 (Ar), 128.1 (Ar), 127.0 (Ar), 115.7 (Ar), 68.0 (PhCH₂), 54.8 (CHNH), 37.0 (CH₂CHNH).

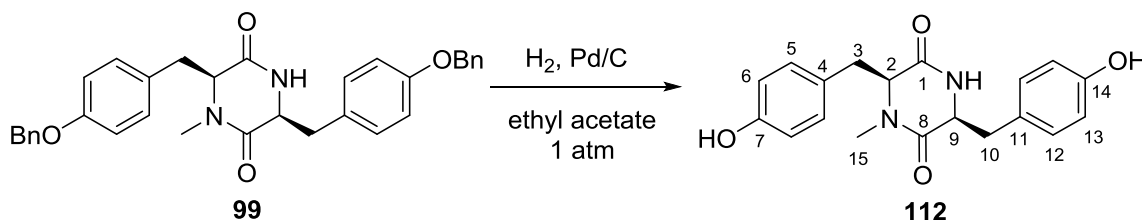
The observed data are in accord with published values.¹⁷²

Synthesis of dipeptide **116**



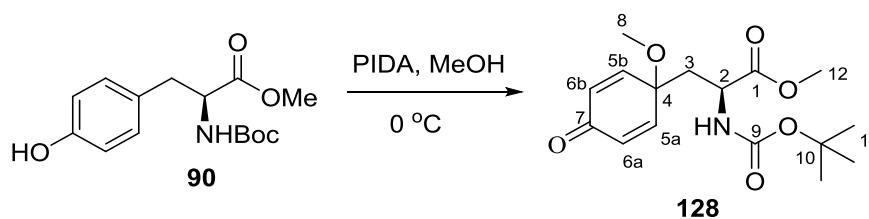
Dipeptide **116** was prepared from acid **115** (0.25 g, 0.79 mmol) and amine **39** (0.15 g, 0.79 mmol) following a similar procedure to that for the synthesis of **95**. This product was obtained as a white solid (0.28 g, 0.57 mmol, 72% yield). M.p. 159-161 °C; $R_f = 0.30$ (EtOAc); $[\alpha]_D^{20} = +34.0$ ($c = 1.0$, CHCl₃); FTIR (film) ν_{\max} 3373, 2943, 1654, 838; ¹H NMR (MeOD-*d*₄, 400 MHz) δ 7.37-7.22 (m, H-19 and H-20 and H-21, 5H), 7.03 (d, $J = 8.4$ Hz, H-5 or H-12, 2H), 7.00 (d, $J = 8.4$ Hz, H-12 or H-5, 2H), 6.71 (d, $J = 8.4$ Hz, H-6 or H-13, 2H), 6.69 (d, $J = 8.4$ Hz, H-13 or H-6, 2H), 5.08 (d, $J = 12.6$ Hz, H-17a, 1H), 5.00 (d, $J = 12.6$ Hz, H-17b, 1H), 4.60 (dd, $J = 7.9, 6.0$ Hz, H-9, 1H), 4.33 (dd, $J = 9.2, 5.9$ Hz, H-2, 1H), 3.66 (s, H-15, 3H), 3.03 (dd, $J = 13.9, 6.0$ Hz, H-10a, 1H), 2.97 (dd, $J = 14.0, 5.9$ Hz, H-3a, 1H), 2.91 (dd, $J = 13.9, 7.9$ Hz, H-10b, 1H), 2.71 (dd, $J = 14.0, 9.2$ Hz, H-3b, 1H); ¹³C NMR (MeOD-*d*₄, 100 MHz) δ 174.0 (C-1), 173.2 (C-8), 158.2 (C-16), 157.4 (C-7 or C-14), 157.2 (C-14 or C-7), 138.2 (C-18), 131.4 (C-5 and C-12), 129.5 (C-20), 129.1 (C-4 or C-11), 128.9 (C-21), 128.6 (C-19), 128.5 (C-11 or C-4), 116.3 (C-6 or C-13), 116.2 (C-13 or C-6), 67.6 (C-17), 57.9 (C-2), 55.4 (C-9), 52.7 (C-15), 38.3 (C-3), 37.8 (C-10); HRMS (ESI) calculated for C₂₇H₂₈N₂O₇Na [M+Na]⁺ 515.1794, found 515.1797.

Preparation of bis-phenol **112**



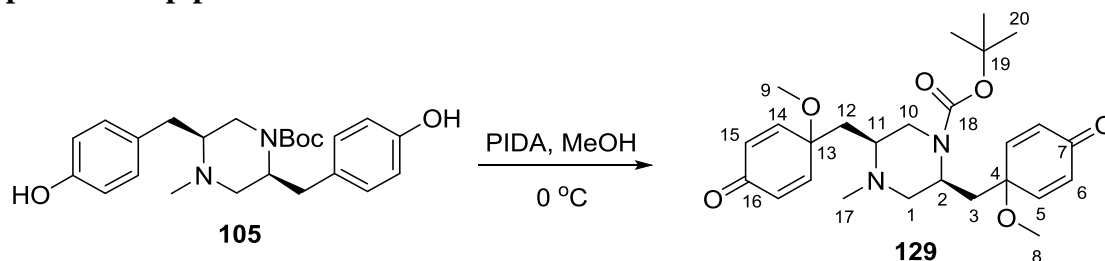
Bis-phenol **112** was prepared from **99** (0.31 g, 0.60 mmol) following a similar procedure to that for the synthesis of **106** and was obtained as a colourless crystalline solid (0.19 g, 0.55 mmol, 93% yield). M.p. 196-199 °C; $R_f = 0.20$ (EtOAc/MeOH 5:1); $[\alpha]_D^{20} = -176$ ($c = 0.8$, MeOH); FTIR (film) ν_{\max} 3248, 2926, 2854, 1682, 1512, 1453, 1247; ^1H NMR (MeOD- d_4 , 300 MHz) δ 6.99 (d, $J = 8.5$ Hz, H-5 or H-12, 2H), 6.88 (d, $J = 8.5$ Hz, H-12 or H-5, 2H), 6.81 (d, $J = 8.6$ Hz, H-6 or H-13, 2H), 6.74 (d, $J = 8.6$ Hz, H-13 or H-6, 2H), 4.18 (t, $J = 4.2$ Hz, H-2, 1H), 3.94 (dd, $J = 9.4, 3.6$ Hz, H-9, 1H), 3.02 (dd, $J = 14.4, 4.2$ Hz, H-3a, 1H), 2.98 (s, H-15, 3H), 2.73 (dd, $J = 14.4, 4.2$ Hz, H-3b, 1H), 2.65 (dd, $J = 13.7, 3.6$ Hz, H-10a, 1H), 1.43 (dd, $J = 13.7, 9.4$ Hz, H-10b, 1H); ^{13}C NMR (MeOD- d_4 , 100 MHz) δ 167.3 (C-1 or C-8), 166.7 (C-8 or C-1), 156.7 (C-7 or C-14), 156.2 (C-14 or C-7), 130.9 (C-5 or C-12), 130.3 (C-12 or C-5), 126.9 (C-4 or C-11), 126.3 (C-11 or C-4), 115.3 (C-6 or C-13), 115.1 (C-13 or C-6), 63.3 (C-2), 56.7 (C-9), 39.6 (C-10), 36.0 (C-3), 32.4 (C-15); HRMS (ESI) calculated for $\text{C}_{19}\text{H}_{20}\text{N}_2\text{O}_4\text{Na}$ $[\text{M}+\text{Na}]^+$ 363.1321, found 363.1324.

Preparation of dienone **128**



To a solution of tyrosine derivative **90** (0.21 g, 0.71 mmol) in MeOH (20 mL) at $-40\text{ }^{\circ}\text{C}$ was added $\text{PhI}(\text{OAc})_2$ (0.23 g, 0.71 mmol) and the reaction mixture was stirred at the same temperature for 6 h. Upon completion, the mixture was partitioned between brine (20 mL) and DCM (30 mL). The organic phase was separated and the aqueous phase was extracted with DCM (2×15 mL). The combined organic fractions were washed with brine (20 mL), dried over MgSO_4 , filtered and concentrated under reduced pressure. The crude product was purified by flash column chromatography eluting with 50% EtOAc in petroleum ether to afford product **128** as a colourless oil (0.14 g, 61% yield). $R_f = 0.30$ (EtOAc/petroleum ether 1:1); FTIR (film) ν_{max} 3671, 3352, 2976, 1699, 1394, 1174, 1080; $[\alpha]_{\text{D}}^{20} = +6$ ($c = 0.45$, CHCl_3); $^1\text{H NMR}$ (CDCl_3 , 400 MHz) δ 6.83 (dd, $J = 12.0, 1.6$ Hz, H-5a and H-5b, 2H), 6.40-6.35 (m, H-6a and H-6b, 2H), 5.21 (d, $J = 7.4$ Hz, NH, 1H), 4.52-4.41 (m, H-2, 1H), 3.74 (s, H-12, 3H), 3.20 (s, H-8, 3H), 2.29 (dd, $J = 14.3, 3.7$ Hz, H-3a, 1H), 2.04 (dd, $J = 14.3, 8.3$ Hz, H-3b, 1H), 1.45 (s, H-11, 9H); $^{13}\text{C NMR}$ (CDCl_3 , 100 MHz) δ 184.7 (C-7), 172.6 (C-1), 154.9 (C-9), 149.3 (C-5a), 149.2 (C-5b), 131.6 (C-6a), 131.4 (C-6b), 80.3 (C-10), 74.1 (C-4), 53.1 (C-12), 52.5 (C-8), 50.3 (C-2), 42.6 (C-3), 28.3 (C-11); HRMS (ESI) calculated for $\text{C}_{16}\text{H}_{23}\text{NO}_6\text{Na}$ $[\text{M}+\text{Na}]^+$ 348.1423, found 348.1430.

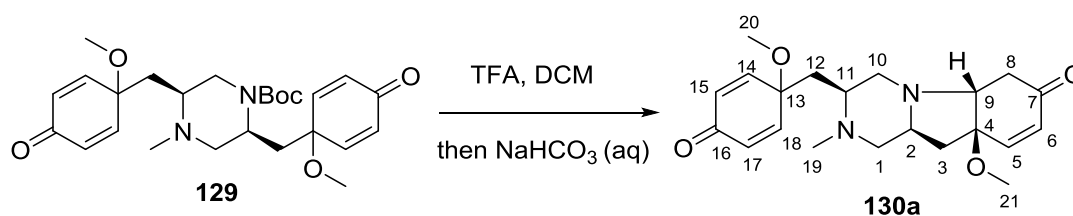
Preparation of piperazine **129**



To a solution of bis-phenol **105** (0.51 g, 1.24 mmol) in MeOH (20 mL) at $0\text{ }^{\circ}\text{C}$ was added $\text{PhI}(\text{OAc})_2$ (1.18 g, 3.72 mmol) and the reaction solution was stirred at the same temperature

for 12 h. Upon completion, the mixture was partitioned between brine (20 mL) and DCM (30 mL). The organic phase was separated and the aqueous phase was extracted with DCM (2×15 mL). The combined organic fractions were washed with brine (20 mL), dried over MgSO₄, filtered and concentrated under reduced pressure. The crude product was purified by flash column chromatography eluting with EtOAc to afford the product **129** as a colourless oil (0.30 g, 52% yield). $R_f = 0.46$ (MeOH:EtOAc = 1:4); $[\alpha]_D^{20} = +184$ ($c = 0.2$, CHCl₃); FTIR (film) ν_{\max} 2975, 2935, 1692, 1671, 1168, 1057; ¹H NMR (CDCl₃, 300 MHz) δ 6.94-6.69 (m, H-6 and H-15, 4H), 6.54-6.24 (m, H-5 and H-14, 4H), 4.03-3.85 (br m, H-2, 1H), 3.21 (s, H-8 or H-9, 3H), 3.20 (s, H-9 or H-8, 3H), 3.08-2.57 (m, H-11 and H-12, 3H), 2.37-1.99 (m, H-1 and H-3 and H-10, 6H), 2.15 (s, H-17, 3H), 1.46 (s, H-20, 9H); ¹³C NMR (CDCl₃, 100 MHz) δ 185.1 (C-7 and C-16), 152.2 (C-18), 150.8 (C-5 or C-14), 149.9 (C-14 or C-5), 131.7 (C-6 or C-15), 131.1 (C-15 or C-6), 79.8 (C-19), 74.5 (C-4 or C-13), 74.3 (C-13 or C-4), 60.9 (C-2 or C-11), 60.6 (C-11 or C-2), 58.4 (C-1), 53.0 (C-8 and C-9), 43.3 (C-17), 40.9 (C-10), 40.2 (C-3 and C-12), 28.4 (C-20); HRMS (ESI) calculated for C₂₆H₃₇N₂O₆ [M+H]⁺ 473.2652, found 473.2643.

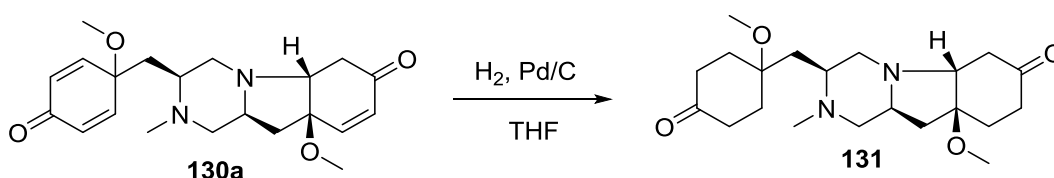
Preparation of piperazine **130a**



To a solution of piperazine derivative **129** (47 mg, 0.10 mmol) in DCM (8 mL) was added TFA (1.0 mL) and the resultant mixture was stirred at rt for 6 h. The reaction solution was then diluted with DCM (20 mL) and saturated NaHCO₃ solution (25 mL) was added dropwise to neutralise excess TFA. After stirring the mixture vigorously, the organic layer was

separated and the aqueous phase was extracted with DCM (3×15 mL). The combined organic fractions were washed with brine (20 mL), dried over MgSO₄, filtered and concentrated under reduced pressure. The crude product was purified by flash column chromatography eluting with 15% MeOH in EtOAc to afford the cyclised product **130a** as a colourless oil (23 mg, 62% yield). $R_f = 0.35$ (MeOH:EtOAc = 1:2); $[\alpha]_D^{24} = +45$ ($c = 0.7$, MeOH); FTIR (film) ν_{\max} 2927, 2854, 2823, 1688, 1670, 1090; ¹H NMR (CDCl₃, 300 MHz) δ 6.80 (dd, $J = 10.1, 3.1$ Hz, H-14 or H-18, 1H), 6.67 (dd, $J = 9.9, 2.9$ Hz, H-18 or H-14, 1H), 6.61 (dd, $J = 10.3, 1.9$ Hz, H-5, 1H), 6.44-6.34 (m, H-15 and H-17, 2H), 6.03 (d, $J = 10.3$ Hz, H-6, 1H), 3.34 (s, H-21, 3H), 3.18 (s, H-20, 3H), 2.87-2.84 (m, H-9, 1H), 2.82 (dd, $J = 10.7, 2.1$ Hz, H-10a, 1H), 2.68 (dd, $J = 9.2, 5.5$ Hz, H-11, 1H), 2.64-2.58 (m, H-8 and H-1a, 3H), 2.58-2.53 (m, H-2, 1H), 2.28 (s, H-19, 3H), 2.22 (d, $J = 10.7$ Hz, H-10b, 1H), 2.12-2.01 (m, H-1b and H-3a and H-12a, 3H), 1.72 (d, $J = 14.0$ Hz, H-12b, 1H), 1.47 (dd, $J = 13.3, 10.3$ Hz, H-3b, 1H); ¹³C NMR (CDCl₃, 100 MHz) δ 197.2 (C-7), 185.4 (C-16), 151.1 (C-14 and C-18), 148.8 (C-5), 131.4 (C-15 and C-17), 128.2 (C-6), 79.5 (C-4), 75.3 (C-13), 65.3 (C-9), 59.6 (C-2), 54.1 (C-11), 53.3 (C-1), 53.1 (C-10), 52.9 (C-20), 52.5 (C-21), 42.1 (C-19), 42.1 (C-3), 37.8 (C-8), 33.3 (C-12); HRMS (ESI) calculated for C₂₁H₂₉N₂O₄ [M+H]⁺ 373.2127, found 373.2130.

Hydrogenation of **130a** to piperazine **131**

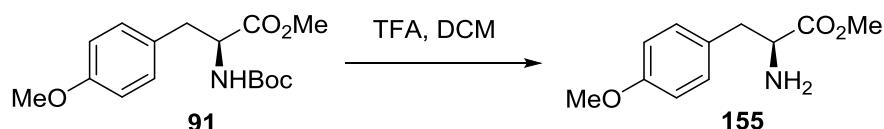


A mixture of piperazine derivative **130a** (53 mg, 0.14 mmol) and 10% Pd/C (10 mg) in THF (10 mL) was stirred under an atmosphere of H₂ for 10 h. Upon completion, the reaction was filtered through a layer of Celite pad. The catalyst was washed with THF (3×10 mL). The

filtrate was concentrated under reduced pressure and the crude product was purified by flash column chromatography eluting with 20% MeOH in EtOAc to afford the reduced product **131** as a colourless oil (32 mg, 68% yield). $R_f = 0.30$ (MeOH:EtOAc = 1:2); $[\alpha]_D^{20} = -108$ ($c = 0.2$, CHCl_3); FTIR (film) ν_{max} 2944, 2828, 1714, 1456, 1224, 1067; $^1\text{H NMR}$ (CDCl_3 , 300 MHz) δ 3.29 (s, OCH_3 , 3H), 3.28 (s, OCH_3 , 3H), 2.93 (d, $J = 6.3$ Hz, 1H), 2.75-2.65 (m, 3H), 2.63-2.50 (m, 4H), 2.46 (dd, $J = 15.4, 3.1$ Hz, 1H), 2.38 (s, NCH_3 , 3H), 2.32-2.01 (m, 10H), 1.87-1.59 (m, 2H), 1.46-1.31 (m, 2H); $^{13}\text{C NMR}$ (CDCl_3 , 100 MHz) δ 211.7 (C=O), 211.0 (C=O), 82.2 (COCH_3), 73.9 (COCH_3), 67.5 (CH), 59.0 (CH), 54.0 (CH), 53.4 (CH_2), 53.0 (CH_2), 50.3 (OCH_3), 49.4 (OCH_3), 42.3 (NCH_3), 40.0 (CH_2), 36.8 (CH_2), 36.7 (CH_2), 36.3 (CH_2), 34.0 (CH_2), 33.9 (CH_2), 33.5 (CH_2), 30.2 (CH_2); HRMS (ESI) calculated for $\text{C}_{21}\text{H}_{35}\text{N}_2\text{O}_4$ $[\text{M}+\text{H}]^+$ 379.2597, found 379.2606.

6.3 Preparative Procedures for Chapter 3

Preparation of *O*-methyl-L-tyrosine methyl ester **155**

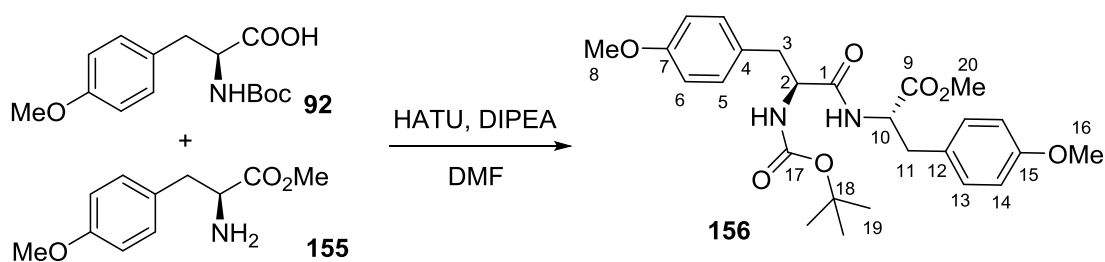


O-methyl-L-tyrosine methyl ester **155** was prepared from **91** (1.18 g, 4.00 mmol) following a similar procedure to that for the synthesis of **94**. Compound **155** was obtained as a colourless oil (0.74 g, 3.80 mmol, 95% yield). $R_f = 0.15$ (EA); $[\alpha]_D^{20} = +23.2$ ($c = 1.0$, MeOH); FTIR (film) ν_{max} 3379, 2999, 2952, 2837, 1733, 1511, 1244, 1175, 1032, 818; $^1\text{H NMR}$ (CDCl_3 , 400 MHz) δ 7.11 (d, $J = 8.7$ Hz, ArH, 2H), 6.85 (d, $J = 8.7$ Hz, ArH, 2H), 3.79 (s, ArOCH_3 , 3H), 3.72 (s, COOCH_3 , 3H), 3.70 (dd, $J = 7.7, 5.2$ Hz, CHNH_2 , 1H), 3.03 (dd, $J = 13.6, 5.2$ Hz, ArCH_aH_b , 1H), 2.82 (dd, $J = 13.6, 7.7$ Hz, ArCH_aH_b , 1H), 1.52 (br s, NH_2 , 2H); $^{13}\text{C NMR}$

(CDCl₃, 100 MHz) δ 175.6 (COOMe), 158.5(Ar), 130.2 (Ar), 129.1 (Ar), 113.9 (Ar), 55.9 (CHNH), 55.2 (ArOCH₃), 51.9 (COOCH₃), 40.2 (ArCH₂).

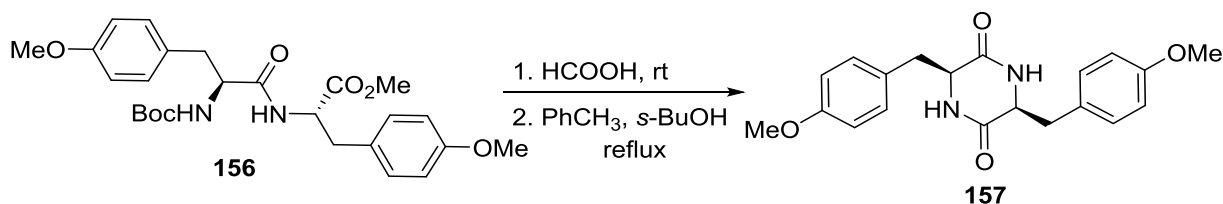
The observed data are in accord with published values.¹⁷⁶

Preparation of dipeptide **156**



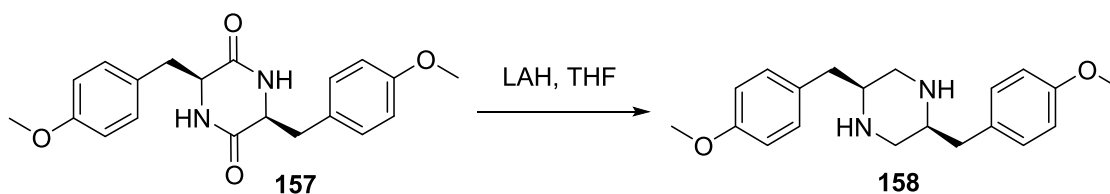
Dipeptide **156** was prepared from acid **92** (0.93 g, 3.15 mmol) and amine **155** (0.61 g, 3.15 mmol) following a similar procedure to that for the synthesis of **95** and was obtained as a white solid (1.25 g, 2.58 mmol, 82% yield). M.p. 108-109 °C; R_f = 0.63 (EA:hexane = 1:1); $[\alpha]_D^{20}$ = +34.4 (c = 2.0, CHCl₃); FTIR (film) ν_{\max} 3664, 3321, 2973, 1737, 1690, 1646, 1511, 1244, 1169, 1033; ¹H NMR (CDCl₃, 400 MHz) δ 7.12 (d, J = 8.6 Hz, H-5 or H-13, 2H), 6.91 (d, J = 8.6 Hz, H-13 or H-5, 2H), 6.84 (d, J = 8.6 Hz, H-6 or H-14, 2H), 6.78 (d, J = 8.6 Hz, H-14 or H-6, 2H), 6.26 (br s, CHCONH, 1H), 4.98 (br s, NHBoc, 1H), 4.75 (dd, J = 12.6, 5.9 Hz, H-10, 1H), 4.30 (dd, J = 12.6, 6.8 Hz, H-2, 1H), 3.79 (s, H-8 and H-16, 6H), 3.69 (s, H-20, 3H), 3.07-2.92 (m, H-3 and H-11, 4H), 1.43 (s, H-19, 9H); ¹³C NMR (CDCl₃, 100 MHz) δ 171.4 (C-9), 170.8 (C-1), 158.7 (C-7 and C-15), 155.3 (C-17), 130.4 (C-5 or C-13), 130.2 (C-13 or C-5), 128.4 (C-4 or C-12), 127.5 (C-12 or C-4), 114.1 (C-6 or C-14), 113.9 (C-14 or C-6), 80.2 (C-18), 55.8 (C-2), 55.2 (C-8 and C-16), 53.4 (C-10), 52.2 (C-20), 37.4 (C-3 or C-11), 37.1 (C-11 or C-3), 28.3 (C-19); HRMS (ESI) calculated for C₂₆H₃₄N₂O₇Na [M+Na]⁺ 509.2264, found 509.2266.

Preparation of DKP **157**



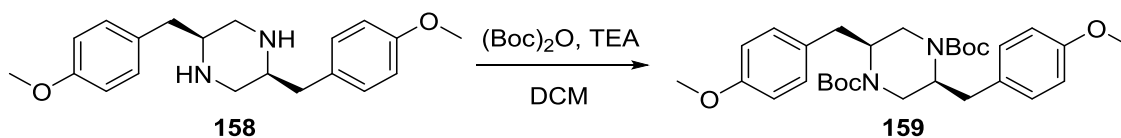
A solution of dipeptide derivative **156** (2.40 g, 5.67 mmol) in formic acid (15 mL) was stirred at rt for 8 h. The solvent was concentrated under reduced pressure and trace formic acid was removed from the dipeptide intermediate by azeotropic distillation with toluene (2×10 mL). To the residue was added 3:1 *s*-butanol:toluene (60 mL) and the resultant mixture was heated at reflux for 6 h. The reaction was cooled to rt and filtered. The solid was washed with EtOAc (2×5 mL), dried first by suction and subsequently under high vacuum with an oil pump to give DKP **157** as a white solid (1.21 g, 69% yield). M.p. 241-243 °C; $R_f = 0.20$ (EtOAc/MeOH 5:1); $[\alpha]_D^{20} = -109.9$ ($c = 1.0$, DMSO); FTIR (film) ν_{\max} 3664, 2988, 2974, 2904, 1676, 1658, 1246, 1066, 1041; ¹H NMR (DMSO-*d*₆, 400 MHz) δ 7.86 (s, NH, 2H), 6.95 (d, $J = 8.6$ Hz, ArH, 4H), 6.85 (d, $J = 8.6$ Hz, ArH, 4H), 3.92 (dd, $J = 6.1, 4.7$ Hz, CHNH, 2H), 3.70 (s, OCH₃, 6H), 2.55 (dd, $J = 13.7, 4.7$ Hz, CH_aH_b, 2H), 2.22 (dd, $J = 13.7, 6.1$ Hz, CH_aH_b, 2H); ¹³C NMR (DMSO-*d*₆, 100 MHz) δ 166.8 (C=O), 158.5 (Ar), 131.3 (Ar), 128.8 (Ar), 114.1 (Ar), 56.0 (CHNH), 55.5 (OCH₃), 38.9 (ArCH₂); HRMS (ESI) calculated for C₂₀H₂₂N₂O₄Na [M+Na]⁺ 377.1477, found 377.1481.

Reduction of DKP **157** to piperazine **158**



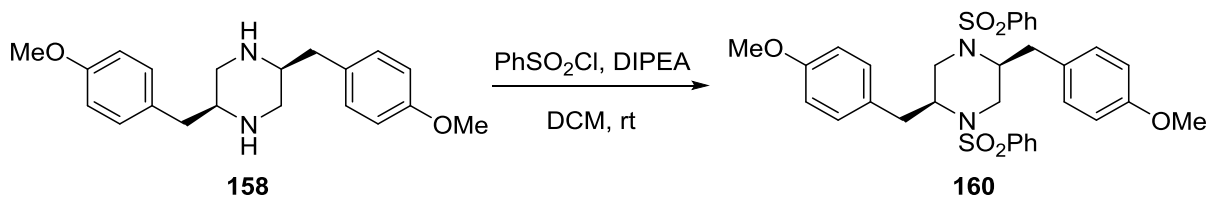
Piperazine derivative **158** was prepared from DKP **157** (0.97 g, 2.74 mmol) following a similar procedure to that for the synthesis of **97** and was obtained as a white solid (0.55 g, 1.70 mmol, 62% yield). M.p. 169-172 °C; $R_f = 0.35$ (MeOH:EtOAc = 1:2); $[\alpha]_D^{20} = +4$ ($c = 0.6$, CHCl₃); FTIR (film) ν_{\max} 3343, 2955, 2932, 2835, 1512, 1247, 1033; ¹H NMR (CDCl₃, 300 MHz) δ 7.16 (d, $J = 8.6$ Hz, ArH, 4H), 6.87 (d, $J = 8.6$ Hz, ArH, 4H), 3.81 (s, OCH₃, 6H), 2.98 (dt, $J = 13.0, 4.8$ Hz, CHNH, 2H), 2.89-2.83 (m, CH₂, 6H), 2.75 (dd, $J = 13.0, 5.5$ Hz, CH₂, 2H), 1.95 (br s, NH, 2H); ¹³C NMR (CDCl₃, 100 MHz) δ 158.1(Ar), 131.3 (Ar), 130.1 (Ar), 114.0 (Ar), 55.7 (CHNH), 55.3 (OCH₃), 47.9 (CH₂NH), 37.6 (ArCH₂); HRMS (ESI) calculated for C₂₀H₂₇N₂O₂ [M+H]⁺ 327.2073, found 327.2063.

Preparation of piperazine **159**



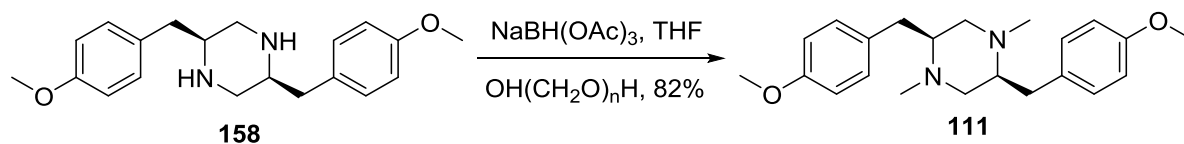
Piperazine **159** was prepared from **158** (1.50 g, 4.60 mmol) following a similar procedure to that for the synthesis of **101** and was obtained as a colourless oil (2.30 g, 4.37 mmol, 95% yield). $R_f = 0.60$ (EtOAc/petroleum ether 1:3); $[\alpha]_D^{20} = +6.7$ ($c = 1.2$, CHCl₃); FTIR (film) ν_{\max} 2973, 2933, 1686, 1511, 1404, 1245, 1152, 1110, 1035; ¹H NMR (CDCl₃, 300 MHz) δ 7.03 (d, $J = 8.6$ Hz, ArH, 4H), 6.81 (d, $J = 8.6$ Hz, ArH, 4H), 4.05 (br s, CH, 2H), 3.83 (br s, NCH_aH_b, 2H), 3.81 (s, OCH₃, 6H), 2.81 (dd, $J = 13.3, 3.8$ Hz, ArCH_aH_b, 2H), 2.73-2.30 (m, ArCH_aH_b and NCH_aH_b, 4H), 1.46 (s, COOC(CH₃)₃, 18H); ¹³C NMR (CDCl₃, 100 MHz) δ 158.3 (Ar), 155.1 (COO^tBu), 130.3 (Ar), 129.2 (Ar), 113.9 (Ar), 80.0 (COOC(CH₃)₃), 55.3 (OCH₃), 54.5 (CH), 41.1 (NCH₂), 37.1 (CH₂Ar), 28.3 (COOC(CH₃)₃); HRMS (ESI) calculated for C₃₀H₄₂N₂O₆Na [M+Na]⁺ 549.2941, found 549.2939.

Preparation of piperazine 160

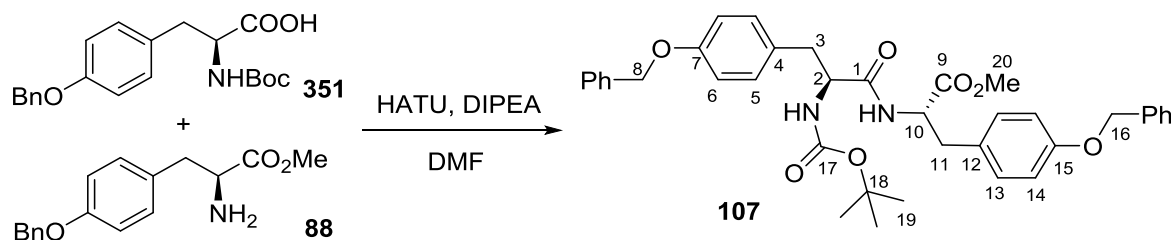


To a solution of piperazine derivative **158** (0.13 g, 0.39 mmol) in DCM (15 mL) at 0 °C was added PhSO₂Cl (0.11 mL, 0.82 mmol), followed by DIPEA (0.15 mL, 0.82 mmol). The reaction solution was stirred at 0 °C for 1 h and then at rt for 5 h. The mixture was partitioned between brine (20 mL) and DCM (15 mL). The aqueous phase was extracted with DCM (2×15 mL). The combined organic fractions were washed with brine (20 mL), dried over MgSO₄, filtered and concentrated under reduced pressure. The crude product was purified by flash column chromatography eluting with 25% EtOAc in petroleum ether to afford the protected product **160** as a white solid (0.21 g, 87% yield). M.p. 149-151 °C; R_f = 0.60 (EA:hexane = 1:4); [α]_D²⁰ = +10.8 (*c* = 1.0, CHCl₃); FTIR (film) ν_{max} 2999, 2956, 2934, 1512, 1347, 1248, 1164; ¹H NMR (CDCl₃, 400 MHz) δ 7.72 (dd, *J* = 8.3, 1.1 Hz, Ar*H*, 4H), 7.64-7.58 (m, Ar*H*, 2H), 7.55-7.48 (m, Ar*H*, 4H), 7.06 (d, *J* = 8.6 Hz, Ar*H*, 4H), 6.85 (d, *J* = 8.6 Hz, Ar*H*, 4H), 3.84 (s, OCH₃, 6H), 3.77 (td, *J* = 9.7, 6.0 Hz, NCH, 2H), 3.14 (dd, *J* = 13.4, 6.0 Hz, NCH_aH_b, 2H), 3.13 (dd, *J* = 13.4, 4.2 Hz, ArCH_aH_b, 2H), 3.00 (dd, *J* = 13.4, 4.2 Hz, NCH_aH_b, 2H), 2.95 (dd, *J* = 13.4, 9.7 Hz, ArCH_aH_b, 2H); ¹³C NMR (CDCl₃, 100 MHz) δ 158.5 (Ar), 138.5 (Ar), 133.0 (Ar), 130.5 (Ar), 129.3 (Ar), 128.8 (Ar), 127.3 (Ar), 114.1 (Ar), 56.8 (CH), 55.3 (OCH₃), 43.5 (NCH₂), 38.5 (ArCH₂); HRMS (ESI) calculated for C₃₂H₃₄N₂O₆NaS₂ [M+Na]⁺ 629.1756, found 629.1769.

Preparation of piperazine 111

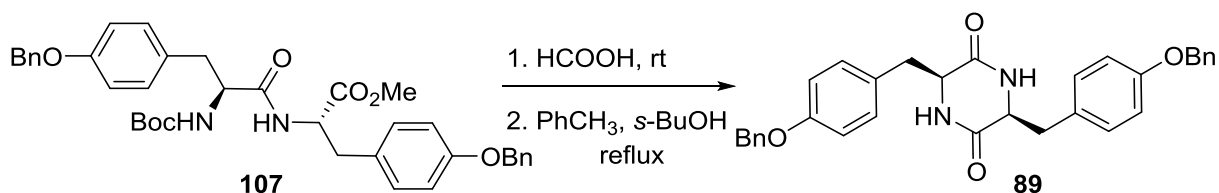


To a solution of piperazine derivative **158** (0.28 g, 0.84 mmol) in THF (10 mL) was added paraformaldehyde (0.10 g, 3.33 mmol) and the resulting mixture was stirred at room temperature for 1 h. Sodium triacetoxyborohydride (0.75 g, 3.33 mmol) was added and the reaction mixture was stirred for 12 h before the addition of another portion of paraformaldehyde (0.10 g, 3.33 mmol) followed by sodium triacetoxyborohydride (0.75 g, 3.33 mmol). After stirring for additional 12 h, water (15 mL) was added to the reaction system and the mixture was extracted with DCM (3×15 mL). The combined organic fraction was washed with saturated NaHCO₃ solution (15 mL), brine (15 mL), dried over MgSO₄, filtered and concentrated under reduced pressure. The crude product was purified by flash column chromatography eluting with 40% EtOAc in petroleum ether to yield the final product as a white solid (0.24 g, 82% yield). M.p. 117-118 °C; R_f = 0.45 (MeOH:EtOAc = 1:2); [α]_D²⁰ = +89 (*c* = 2.0, CHCl₃); FTIR (film) ν_{max} 2957, 2936, 2424, 1668, 1611, 1512, 1246, 1030, 820, 731; ¹H NMR (CDCl₃, 300 MHz) δ 7.13 (d, *J* = 8.6, Ar*H*, 4H), 6.85 (d, *J* = 8.6, Ar*H*, 4H), 3.81 (s, OCH₃, 6H), 2.93 (dd, *J* = 13.0, 3.0 Hz, ArCH_aH_b, 2H), 2.71 (dd, *J* = 13.0, 9.6 Hz, ArCH_aH_b, 2H), 2.53 (m, NCH and NCH_aH_b, 4H), 2.37 (s, NCH₃, 6H), 2.24 (dd, *J* = 10.7, 2.3 Hz, NCH_aH_b, 2H); ¹³C NMR (CDCl₃, 100 MHz) δ 157.8 (Ar), 132.1 (Ar), 130.2 (Ar), 113.8 (Ar), 62.9 (NCH), 55.4 (NCH₂), 55.2 (OCH₃), 42.8 (NCH₃), 32.0 (ArCH₂); HRMS (ESI) calculated for C₂₂H₃₁N₂O₂ [M+H]⁺ 355.2386, found 355.2392.

Preparation of dipeptide **107**

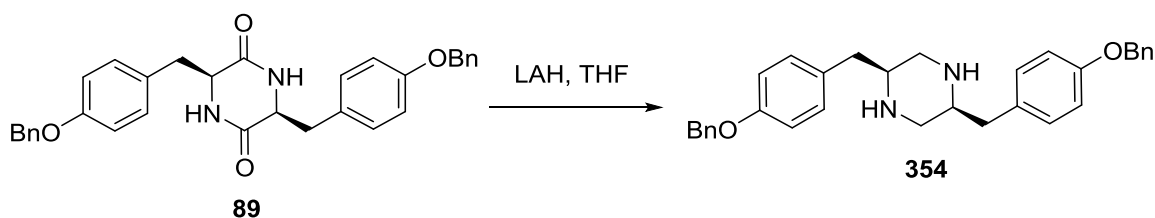
Dipeptide **107** was prepared from acid **351** (1.70 g, 4.57 mmol) and amine **88** (1.30 g, 4.57 mmol) following a similar procedure to that for the synthesis of **95** and was obtained as a white solid (2.18 g, 3.43 mmol, 75% yield). M.p. 128-131 °C (lit.¹⁷⁷ m.p. 163-165 °C); $R_f = 0.65$ (EA:hexane = 1:1); $[\alpha]_D^{20} = +29.2$ ($c = 1.5$, CHCl_3); FTIR (film) ν_{max} 3314, 2977, 2930, 1740, 1706, 1645, 1511, 1240, 1174, 1018; $^1\text{H NMR}$ (CDCl_3 , 300 MHz) δ 7.51-7.31 (m, PhH, 10H), 7.13 (d, $J = 8.6$ Hz, H-5 or H-13, 2H), 6.92 (d, $J = 8.6$ Hz, H-6 or H-14, 2H), 6.91 (d, $J = 8.6$ Hz, H-13 or H-5, 2H), 6.89 (d, $J = 8.6$ Hz, H-14 or H-6, 2H), 6.29 (d, $J = 6.8$ Hz, CHCONH, 1H), 5.04 (s, C-8 or C-16, 2H), 5.03 (s, C-16 or C-8, 2H), 4.97 (d, $J = 5.7$ Hz, NHBoc, 1H), 4.76 (dd, $J = 12.6, 5.7$ Hz, H-10, 1H), 4.31 (dd, $J = 12.6, 6.8$ Hz, H-2, 1H), 3.69 (s, H-20, 3H), 3.02-3.00 (m, H-3 and H-11, 4H), 1.43 (s, H-19, 9H); $^{13}\text{C NMR}$ (CDCl_3 , 100 MHz) δ 171.5 (C-9), 170.8 (C-1), 157.9 (C-7 and C-15), 155.3 (C-17), 137.0 (Ph), 130.5 (C-5 or C-13), 130.3 (C-13 or C-5), 128.7 (C-4 or C-12), 128.6 (Ph), 128.0 (Ph), 127.9 (C-12 or C-4), 127.5 (Ph), 127.4 (Ph), 115.0 (C-6 or C-14), 114.9 (C-14 or C-6), 80.2 (C-18), 70.0 (C-8 and C-16), 55.7 (C-2), 53.4 (C-10), 52.3 (C-20), 37.4 (C-3 or C-11), 37.1 (C-11 or C-3), 28.3 (C-19); HRMS (ESI) calculated for $\text{C}_{38}\text{H}_{42}\text{N}_2\text{O}_7\text{Na}$ $[\text{M}+\text{Na}]^+$ 661.2890, found 661.2909.

The NMR data are in accord with published values.¹⁷⁷

Preparation of DKP **89**

DKP **89** was prepared from dipeptide **107** (0.55 g, 0.86 mmol) following a similar procedure to that for the synthesis of **157** and was obtained as a white solid (0.27 g, 0.54 mmol, 63% yield). M.p. 234-237 °C; $R_f = 0.25$ (EtOAc/MeOH 5:1); $[\alpha]_D^{20} = -103.7$ ($c = 1.0$, DMSO); FTIR (film) ν_{\max} 3671, 2987, 2974, 2901, 1396, 1066, 1057; ¹H NMR (DMSO-*d*₆, 400 MHz) δ 7.87 (s, NH, 2H), 7.40-7.26 (m, ArH, 10H), 6.96 (d, $J = 9.0$ Hz, ArH, 4H), 6.93 (d, $J = 9.0$ Hz, ArH, 2H), 5.06 (s, PhCH₂, 4H), 3.91 (dd, $J = 6.2, 4.8$ Hz, CHNH, 2H), 2.55 (d, $J = 13.7, 4.8$ Hz, ArCH_aH_b, 2H), 2.21 (dd, $J = 13.7, 6.2$ Hz, ArCH_aH_b, 2H); ¹³C NMR (DMSO-*d*₆, 100 MHz) δ 166.7 (C=O), 157.6 (Ar), 137.6 (Ar), 131.3 (Ar), 129.2 (Ar), 128.8 (Ar), 128.2 (Ar), 127.9 (Ar), 115.0 (Ar), 69.6 (PhCH₂), 56.0 (CHNH), 39.0 (CH₂CHNH); HRMS (ESI) calculated for C₃₂H₃₀N₂O₄Na [M+Na]⁺ 529.2103, found 529.2098.

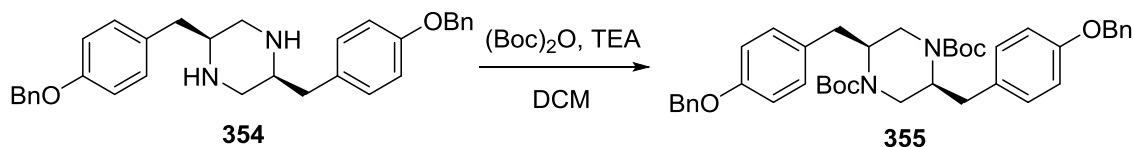
The observed data are in accord with published values.¹⁷⁸

Reduction of DKP to piperazine **354**

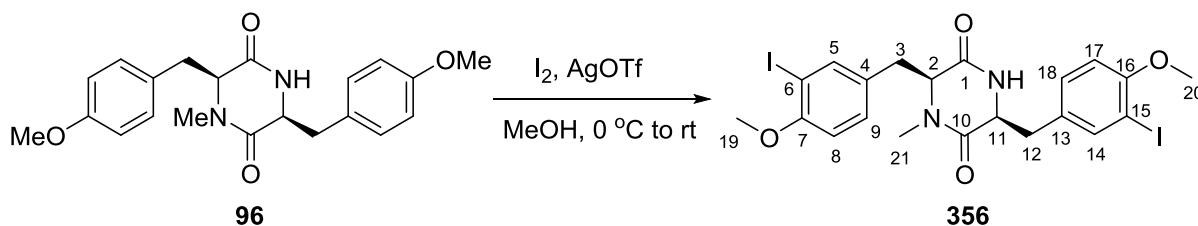
Piperazine **354** was prepared from DKP **89** (0.46 g, 0.91 mmol) following a similar procedure to that for the synthesis of **158** and was obtained as a white solid (0.29 g, 0.60 mmol, 66% yield). M.p. 111-113 °C; $R_f = 0.40$ (MeOH:EtOAc = 1:2); $[\alpha]_D^{20} = +12.5$ ($c = 0.5$, CHCl₃);

FTIR (film) ν_{\max} 3341, 2926, 2855, 1511, 1242; ^1H NMR (CDCl_3 , 400 MHz) δ 7.35-7.15 (m, ArH, 10H), 7.01 (d, $J = 8.5$ Hz, ArH, 4H), 6.77 (d, $J = 8.5$ Hz, ArH, 4H), 4.88 (s, PhCH_2 , 4H), 3.15-2.98 (m, CHNH, 2H), 2.78 (m, CH_2 , 6H), 2.60-2.33 (m, CH_2 , 2H); ^{13}C NMR (CDCl_3 , 100 MHz) δ 157.7 (Ar), 137.0 (Ar), 130.3 (Ar), 130.2 (Ar), 129.7 (Ar), 128.6 (Ar), 128.0 (Ar), 127.5 (Ar), 115.1 (Ar), 70.0 (PhCH_2), 54.7 (CHNH), 45.4 (CH_2NH), 36.3 (ArCH_2); HRMS (ESI) calculated for $\text{C}_{32}\text{H}_{35}\text{N}_2\text{O}_2$ $[\text{M}+\text{H}]^+$ 479.2699, found 479.2697.

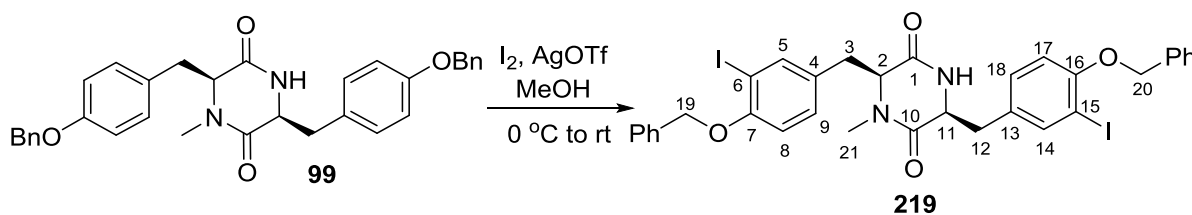
Preparation of piperazine 355



Piperazine **355** was prepared from **354** (0.38 g, 0.79 mmol) following a similar procedure to that for the synthesis of **101** and was obtained as a colourless oil (0.44 g, 0.65 mmol, 82% yield). $R_f = 0.60$ (EtOAc/petroleum ether 1:3); $[\alpha]_{\text{D}}^{20} = +16$ ($c = 1.0$, CHCl_3); FTIR (film) ν_{\max} 2973, 2930, 1686, 1511, 1246, 1174; ^1H NMR ($\text{DMSO}-d_6$, 400 MHz) δ 7.45 (d, $J = 7.2$ Hz, ArH, 4H), 7.39 (t, $J = 7.2$ Hz, ArH, 4H), 7.35-7.29 (m, ArH, 2H), 7.07 (d, $J = 8.5$ Hz, ArH, 4H), 6.95 (d, $J = 8.5$ Hz, ArH, 4H), 5.08 (s, PhCH_2 , 4H), 3.91-3.85 (m, NCH, 2H), 3.67-3.61 (m, NCH_aH_b , 2H), 2.80 (dd, $J = 14.3, 11.3$ Hz, NCH_aH_b , 2H), 2.75 (dd, $J = 13.0, 5.1$ Hz, ArCH_aH_b , 2H), 2.61 (dd, $J = 13.0, 8.4$ Hz, ArCH_aH_b , 2H), 1.31 (s, $\text{COOC}(\text{CH}_3)_3$, 18H); ^{13}C NMR ($\text{DMSO}-d_6$, 100 MHz) δ 157.4 (Ar), 154.7 (COO^tBu), 137.7 (Ar), 130.5 (Ar), 130.2 (Ar), 128.9 (Ar), 128.2 (Ar), 128.0 (Ar), 115.1 (Ar), 79.4 ($\text{COOC}(\text{CH}_3)_3$), 69.6 (PhCH_2), 55.2 (NCH), 40.8 (NCH_2), 36.9 (ArCH_2), 28.3 ($\text{COOC}(\text{CH}_3)_3$); HRMS (ESI) calculated for $\text{C}_{42}\text{H}_{50}\text{N}_2\text{O}_6\text{Na}$ $[\text{M}+\text{Na}]^+$ 701.3567, found 701.3562.

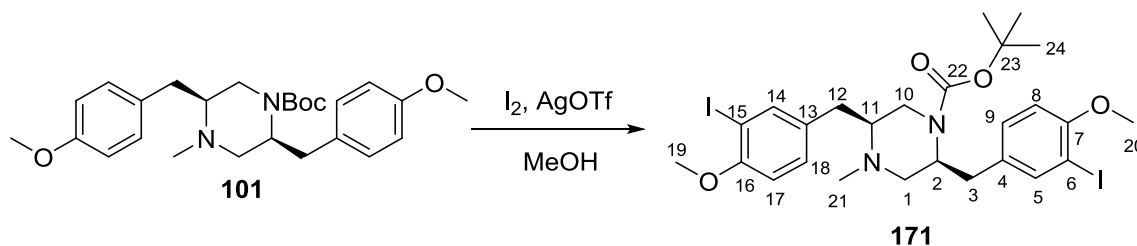
Iodination of DKP **96**

To a solution of DKP **96** (0.18 g, 0.50 mmol) in MeOH (30 mL) was added AgOTf (0.27 g, 1.05 mmol). The mixture was cooled to 0 °C and a solution of I₂ (0.27 g, 1.05 mmol) in MeOH (10 mL) was slowly added over a period of 15 min. The reaction mixture was stirred at 0 °C for 1 h and then at rt for 8 h. Sodium thiosulfate was added to the reaction system to consume excess iodine. The mixture was filtered through a layer of Celite pad and the solid was washed with DCM (3×10 mL). The filtrate was concentrated under reduced pressure and the crude product was purified by column chromatography with 5% methanol in ethyl acetate as the eluent to give DKP **356** as an off-white solid (0.21 g, 69% yield). M.p. 183-184 °C; R_f = 0.20 (EtOAc/MeOH 6:1); [α]_D²⁰ = -118 (*c* = 1.0, CHCl₃); FTIR (film) ν_{max} 3213, 2939, 1680, 1646, 1490, 1253, 1048; ¹H NMR (CDCl₃, 400 MHz) δ 7.63 (d, *J* = 2.1 Hz, H-5, 1H), 7.41 (d, *J* = 2.1 Hz, H-14, 1H), 7.08 (dd, *J* = 8.4, 2.1 Hz, H-9, 1H), 6.90 (dd, *J* = 8.4, 2.1 Hz, H-18, 1H), 6.85 (d, *J* = 8.4 Hz, H-8, 1H), 6.76 (d, *J* = 8.4 Hz, H-17, 1H), 5.83 (d, *J* = 1.9 Hz, NH, 1H), 4.16 (t, *J* = 4.0 Hz, H-2, 1H), 3.91 (dd, *J* = 5.8, 3.2 Hz, H-11, 1H), 3.85 (s, H-19 and H-20, 6H), 3.17 (dd, *J* = 14.2, 3.6 Hz, H-3a, 1H), 3.11 (s, H-21, 3H), 3.05 (dd, *J* = 14.2, 4.4 Hz, H-3b, 1H), 2.91 (dd, *J* = 13.6, 2.7 Hz, H-12a, 1H), 0.92 (dd, *J* = 13.6, 11.3 Hz, H-12b, 1H); ¹³C NMR (CDCl₃, 100 MHz) δ 165.5 (C-10), 165.1 (C-1), 157.9 (C-7), 157.4 (C-16), 141.0 (C-5), 139.8 (C-14), 131.4 (C-9), 130.7 (C-18), 130.0 (C-13), 129.0 (C-4), 111.2 (C-8), 111.1 (C-17), 86.6 (C-6 and C-15), 63.0 (C-2), 56.7 (C-11), 56.6 (C-19 or C-20), 56.5 (C-20 or C-19), 39.7 (C-12), 35.3 (C-3), 33.2 (C-21); HRMS (ESI) calculated for C₂₁H₂₂N₂O₄NaI₂ [M+Na]⁺ 642.9567, found 642.9570.

Preparation of DKP **219**

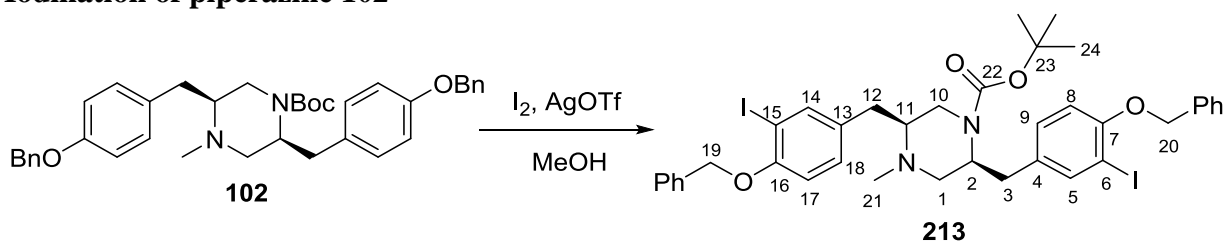
DKP **219** was prepared from **99** (0.31 g, 0.60 mmol) following a similar procedure to that for the synthesis of **356** and was obtained as a white solid (0.29 g, 0.38 mmol, 63% yield). M.p. 95-96 °C; $R_f = 0.25$ (EtOAc/MeOH 6:1); $[\alpha]_D^{24} = -48$ ($c = 0.9$, MeOH); FTIR (film) ν_{\max} 3209, 2972, 2902, 1680, 1653, 1487, 1251, 1046, 734; $^1\text{H NMR}$ (CDCl_3 , 300 MHz) δ 7.65 (d, $J = 2.1$ Hz, H-5, 1H), 7.50-7.46 (m, H-14 and PhH, 2H), 7.42-7.30 (m, PhH, 6H), 7.23-7.19 (m, PhH, 3H), 6.99 (dd, $J = 8.4, 2.1$ Hz, H-9, 1H), 6.85-6.77 (m, H-8 and H-17 and H-18, 3H), 5.57 (d, $J = 1.2$ Hz, NH, 1H), 5.16 (s, H-19 or H-20, 2H), 5.13 (s, H-20 or H-19, 2H), 4.15 (t, $J = 3.8$ Hz, H-2, 1H), 3.85-3.78 (m, H-11, 1H), 3.18 (dd, $J = 14.2, 3.8$ Hz, H-3a, 1H), 3.09 (s, H-21, 3H), 3.03 (dd, $J = 14.2, 3.8$ Hz, H-3b, 1H), 2.76 (dd, $J = 13.6, 2.8$ Hz, H-12a, 1H), 0.72 (dd, $J = 13.6, 11.5$ Hz, H-12b, 1H); $^{13}\text{C NMR}$ (CDCl_3 , 100 MHz) δ 165.3 (C-1 or C-10), 165.0 (C-10 or C-1), 156.8 (C-7), 156.5 (C-16), 141.1 (C-5), 139.9 (C-14), 136.3 (Ph), 136.0 (Ph), 131.2 (C-9), 130.5 (C-18), 130.3 (C-13), 129.2 (C-4), 128.6 (Ph), 128.5 (Ph), 128.0 (Ph), 127.9 (Ph), 127.0 (Ph), 126.8 (Ph), 113.0 (C-8 or C-17), 112.9 (C-17 or C-8), 87.5 (C-6 or C-15), 87.4 (C-15 or C-6), 71.0 (C-19 or C-20), 70.8 (C-20 or C-19), 62.9 (C-2), 56.8 (C-11), 39.7 (C-12), 35.2 (C-3), 33.1 (C-21); HRMS (ESI) calculated for $\text{C}_{33}\text{H}_{31}\text{N}_2\text{O}_4\text{I}_2$ $[\text{M}+\text{H}]^+$ 773.0373, found 773.0375.

Iodination of piperazine **101**



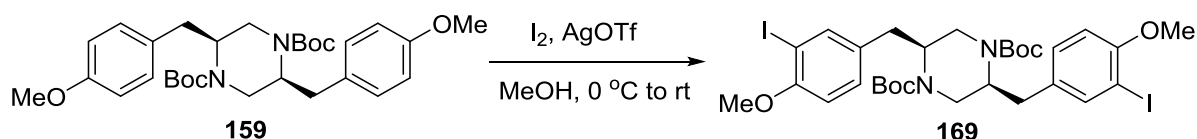
Iodination of piperazine **101** (1.30 g, 2.95 mmol) was performed following a similar procedure to that for the synthesis of **356** to afford product **171** as a colourless oil (1.16 g, 1.68 mmol, 57% yield). $R_f = 0.60$ (EtOAc/petroleum ether 1:1); $[\alpha]_D^{20} = -7.5$ ($c = 1.8$, MeOH); FTIR (film) ν_{\max} 2969, 2927, 2792, 1689, 1611, 1520, 1246, 1055, 823; $^1\text{H NMR}$ (CDCl_3 , 400 MHz) δ 7.66 (d, $J = 2.0$ Hz, H-5 and H-14, 2H), 7.16 (dd, $J = 8.4, 2.0$ Hz, H-9 and H-18, 2H), 6.75 (d, $J = 8.4$ Hz, H-8 and H-17, 2H), 4.12-4.03 (br m, H-2, 1H), 3.87 (s, H-19 or H-20, 3H), 3.85 (s, H-20 or H-19, 3H), 3.80-3.74 (br m, H-10a, 1H), 3.05 (dd, $J = 14.0, 3.9$ Hz, H-12a, 1H), 3.00-2.61 (m, H-3 and H-1a and H-10b, 4H), 2.47 (dd, $J = 13.8, 9.0$ Hz, H-12b, 1H), 2.35 (s, H-21, 3H), 2.26-2.07 (m, H-1b and H-11, 2H), 1.33 (s, H-24, 9H); $^{13}\text{C NMR}$ (CDCl_3 , 100 MHz) δ 156.7 (C-7 or C-16), 156.6 (C-16 or C-7), 154.3 (C-22), 140.1 (C-5 or C-14), 140.0 (C-14 or C-5), 133.6 (C-4 or C-13), 132.4 (C-13 or C-4), 130.4 (C-9 and C-18), 110.8 (C-8 and C-17), 86.0 (C-6 and C-15), 79.7 (C-23), 63.8 (C-11), 57.8 (C-1), 56.4 (C-19 and C-20), 53.5 (C-2), 43.2 (C-21), 42.9 (C-10), 36.2 (C-12), 34.7 (C-3), 28.3 (C-24); HRMS (ESI) calculated for $\text{C}_{26}\text{H}_{35}\text{I}_2\text{N}_2\text{O}_4$ $[\text{M}+\text{H}]^+$ 693.0686, found 693.0688.

Iodination of piperazine **102**



Iodination of piperazine **102** (0.42 g, 0.71 mmol) was performed following a similar procedure to that for the synthesis of **356** to afford product **213** as a colourless oil (0.32 g, 0.38 mmol, 53% yield). $R_f = 0.30$ (EtOAc/petroleum ether 1:3); $[\alpha]_D^{20} = -14$ ($c = 0.7$, CHCl_3); FTIR (film) ν_{max} 2975, 2927, 2793, 1689, 1488, 1249, 1046; $^1\text{H NMR}$ (CDCl_3 , 300 MHz) δ 7.69 (d, $J = 2.0$ Hz, H-5 and H-14, 2H), 7.57-7.29 (m, PhH, 10H), 7.14 (dd, $J = 8.6, 2.0$ Hz, H-9 or H-18, 1H), 7.13 (dd, $J = 8.4, 2.0$ Hz, H-18 and H-9, 1H), 6.80 (d, $J = 8.6$ Hz, H-8 or H-17 1H), 6.78 (d, $J = 8.4$ Hz, H-17 or H-8, 1H), 5.14 (s, H-19 and H-20, 4H), 4.16-4.02 (br m, H-2, 1H), 3.88-3.70 (br m, H-10a, 1H), 3.06 (dd, $J = 14.0, 3.2$ Hz, H-12a, 1H), 2.89-2.64 (m, H-3 and H-1a and H-10b, 4H), 2.51-2.42 (br m, H-12b, 1H), 2.36 (s, H-21, 3H), 2.25-2.07 (br m, H-1b and H-11, 2H), 1.33 (s, H-24, 9H); $^{13}\text{C NMR}$ (CDCl_3 , 100 MHz) δ 155.9 (C-7 or C-16), 155.8 (C-16 or C-7), 154.3 (COO'Bu), 140.2 (C-5 or C-14), 140.0 (C-14 or C-5), 136.6 (Ph), 134.0 (C-4 or C-13), 132.8 (C-13 or C-4), 130.3 (C-9 and C-18), 128.6 (Ph), 127.9 (Ph), 127.5 (Ph), 127.0 (Ph), 112.6 (C-8 and C-17), 86.9 (C-6 and C-15), 79.7 (C-23), 71.0 (C-19 and C-20), 63.7 (C-11), 57.9 (C-1), 53.7 (C-2), 43.2 (C-21), 43.0 (C-10), 36.3 (C-12), 34.8 (C-3), 28.3 (C-24); HRMS (ESI) calculated for $\text{C}_{38}\text{H}_{42}\text{N}_2\text{O}_4\text{I}_2\text{Na}$ $[\text{M}+\text{Na}]^+$ 867.1132, found 867.1152.

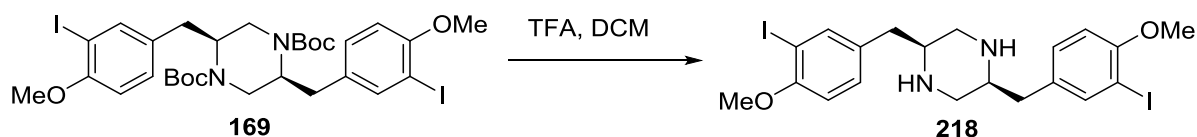
Iodination of piperazine **159**



Iodination of piperazine **159** (0.41 g, 0.78 mmol) was performed following a similar procedure to that for the synthesis of **356** to afford product **169** as a colourless oil (0.43 g, 0.55 mmol, 71% yield). $R_f = 0.58$ (EtOAc/petroleum ether 1:3); $[\alpha]_D^{20} = +4.6$ ($c = 1.2$, CHCl_3); FTIR (film) ν_{max} 2973, 2934, 1684, 1391, 1251, 1153; $^1\text{H NMR}$ (CDCl_3 , 400 MHz) δ 7.57 (d,

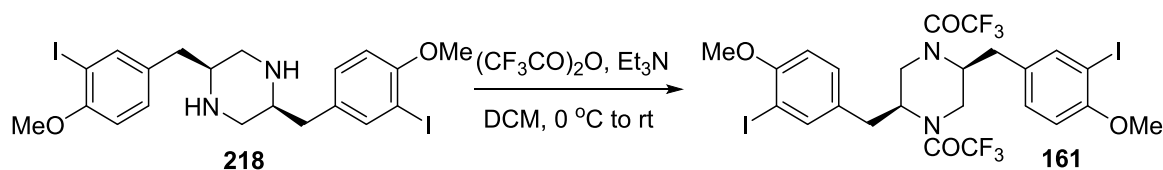
$J = 2.0$ Hz, ArH , 2H), 7.08 (dd, $J = 8.4, 2.0$ Hz, ArH , 2H), 6.74 (d, $J = 8.4$ Hz, ArH , 2H), 4.10-4.00 (br m, NCH , 2H), 3.87 (s, OCH_3 , 6H), 3.87-3.85 (m, NCH_aH_b , 2H), 2.81 (dd, $J = 13.3, 4.1$ Hz, $ArCH_aH_b$, 2H), 2.68-2.62 (m, NCH_aH_b , 2H), 2.57 (dd, $J = 13.3, 8.4$ Hz, $ArCH_aH_b$, 2H), 1.45 (s, $COOC(CH_3)_3$, 9H); ^{13}C NMR ($CDCl_3$, 100 MHz) δ 156.9 (Ar), 155.0 (COO^tBu), 140.0 (Ar), 131.5 (Ar), 130.2 (Ar), 110.9 (Ar), 86.0 (Ar), 80.3 ($COOC(CH_3)_3$), 56.4 (OCH_3), 54.6 (NCH), 41.2 (NCH_2), 36.7 ($ArCH_2$), 28.4 ($COOC(CH_3)_3$); HRMS (ESI) calculated for $C_{30}H_{40}I_2N_2O_6Na$ $[M+Na]^+$ 801.0873, found 801.0867.

Preparation of piperazine 218



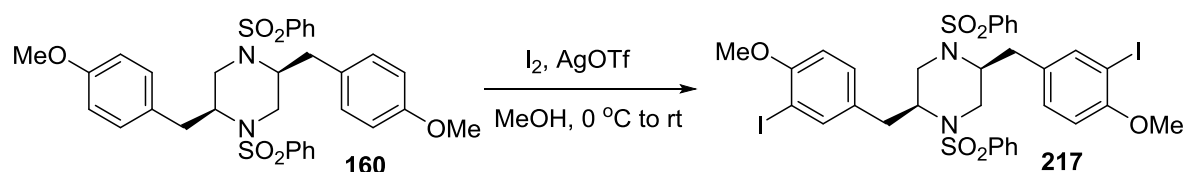
Piperazine derivative **218** was prepared from **169** (0.39 g, 0.50 mmol) following a similar procedure to that for the synthesis of **94** and was afforded as a yellow oil (0.26 g, 0.46 mmol, 92% yield). $R_f = 0.35$ (MeOH:EtOAc = 1:2); $[\alpha]_D^{22} = +14.5$ ($c = 0.8$, $CHCl_3$); FTIR (film) ν_{max} 2945, 2935, 2834, 1672, 1600, 1491, 1255, 1048; 1H NMR ($CDCl_3$, 400 MHz) δ 7.57 (d, $J = 2.0$ Hz, ArH , 2H), 7.08 (dd, $J = 8.3, 2.0$ Hz, ArH , 2H), 6.69 (d, $J = 8.3$ Hz, ArH , 2H), 3.78 (s, OCH_3 , 6H), 2.93-2.87 (m, $CHNH$, 2H), 2.79-2.65 (m, CH_2 , 8H), 2.30 (br s, NH , 2H); ^{13}C NMR ($CDCl_3$, 100 MHz) δ 156.7 (Ar), 139.9 (Ar), 133.2 (Ar), 130.2 (Ar), 111.0 (Ar), 86.2 (Ar), 56.4 (OCH_3), 55.5 ($CHNH$), 47.4 (NCH_2), 36.9 ($ArCH_2$); HRMS (ESI) calculated for $C_{20}H_{25}I_2N_2O_2$ $[M+H]^+$ 579.0005, found 579.0004.

Preparation of piperazine 161



N-trifluoroacetyl-protected piperazine derivative **161** was prepared from **218** (0.18 g, 0.31 mmol) following a similar procedure to that for the synthesis of **103** and was obtained as a colourless oil (0.20 g, 0.26 mmol, 85% yield). $R_f = 0.50$ (EtOAc/petroleum ether 1:3); $[\alpha]_{\text{D}}^{20} = +47$ ($c = 1.8$, CHCl_3); FTIR (film) ν_{max} 2970, 2949, 1691, 1492, 1203, 1139; ^1H NMR (CDCl_3 , 400 MHz) δ 7.42 (d, $J = 1.6$ Hz, ArH, 2H), 6.94 (dd, $J = 8.4, 1.6$ Hz, ArH, 2H), 6.69 (d, $J = 8.4$ Hz, ArH, 2H), 4.34 (dd, $J = 10.8, 5.0$ Hz, NCH, 2H), 3.83 (s, OCH_3 , 6H), 3.66 (dd, $J = 15.6, 5.0$ Hz, NCH_aH_b , 2H), 2.85 (dd, $J = 15.6, 10.8$ Hz, NCH_aH_b , 2H), 2.73-2.68 (m, ArCH₂, 4H); ^{13}C NMR (CDCl_3 , 100 MHz,) δ 157.5 (Ar), 156.5 (q, $^2J_{\text{FC}} = 36$ Hz, C=O), 140.0 (Ar), 130.1 (Ar), 128.7 (Ar), 115.8 (q, $^1J_{\text{FC}} = 286$ Hz, CF_3), 111.0 (Ar), 86.2 (Ar), 56.5 (OCH_3), 55.4 (NCH), 42.4 (NCH_2), 33.9 (ArCH₂); HRMS (ESI) calculated for $\text{C}_{24}\text{H}_{22}\text{I}_2\text{N}_2\text{O}_4\text{F}_6\text{Na}$ $[\text{M}+\text{Na}]^+$ 792.9471, found 792.9465.

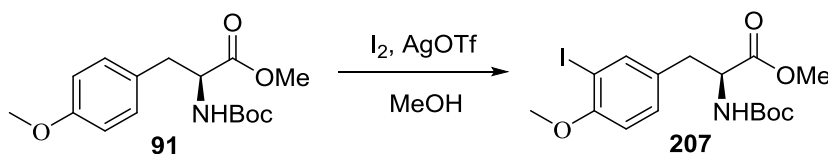
Iodination of piperazine 160



Iodination of piperazine **160** (0.14 g, 0.23 mmol) was performed following a similar procedure to that for the synthesis of **356** to afford product **217** as a white solid (0.14 g, 0.16 mmol, 70% yield). M.p. 161-163 $^\circ\text{C}$; $R_f = 0.60$ (EA:hexane = 1:4); $[\alpha]_{\text{D}}^{20} = +14$ ($c = 0.8$, CHCl_3); FTIR (film) ν_{max} 2927, 2854, 1490, 1345, 1254, 1159, 1048, 629; ^1H NMR (CDCl_3 ,

400 MHz) δ 7.71 (dd, $J = 7.2, 1.4$ Hz, ArH, 4H), 7.63 (dt, $J = 2.1, 1.4$ Hz, ArH, 2H), 7.58-7.50 (m, ArH, 6H), 7.14 (dd, $J = 8.4, 2.1$ Hz, ArH, 2H), 6.77 (d, $J = 8.4$ Hz, ArH, 2H), 3.90 (s, OCH₃, 6H), 3.73 (dd, $J = 9.9, 4.8$ Hz, CH, 2H), 3.15-3.08 (m, ArCH_aH_b and NCH_aH_b, 4H), 3.03 (dd, $J = 13.6, 4.8$ Hz, NCH_aH_b, 2H), 2.88 (dd, $J = 13.6, 9.9$ Hz, ArCH_aH_b, 2H); ¹³C NMR (CDCl₃, 100 MHz) δ 157.1 (Ar), 139.9 (Ar), 138.4 (Ar), 133.2 (Ar), 130.9 (Ar), 130.8 (Ar), 129.5 (Ar), 127.2 (Ar), 111.0 (Ar), 86.2 (Ar), 56.5 (CH), 56.4 (OCH₃), 43.6 (NCH₂), 38.0 (ArCH₂); HRMS (ESI) calculated for C₃₂H₃₂N₂O₆NaS₂¹²⁷I₂ [M+Na]⁺ 880.9689, found 880.9695.

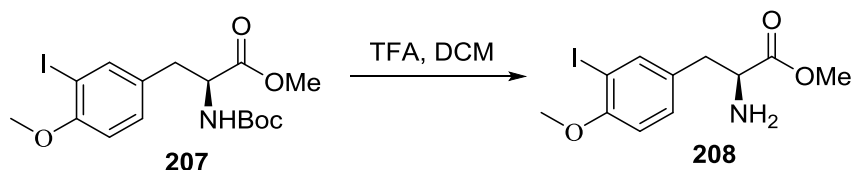
Preparation of tyrosine derivative **207**



The iodination of **91** (1.80 g, 5.82 mmol) was conducted following a similar procedure to that for the synthesis of **356** and **207** was obtained as a colourless oil (2.07 g, 4.77 mmol, 82% yield). $R_f = 0.53$ (EtOAc/petroleum ether 1:1); $[\alpha]_D^{20} = +35.9$ ($c = 1.2$, CHCl₃); FTIR (film) ν_{\max} 3374, 2976, 1743, 1712, 1491, 1253, 1164, 1050, 1018; ¹H NMR (CDCl₃, 300 MHz) δ 7.48 (d, $J = 1.5$ Hz, ArH, 1H), 7.02 (dd, $J = 8.4, 1.5$ Hz, ArH, 1H), 6.67 (d, $J = 8.4$ Hz, ArH, 1H), 5.07 (d, $J = 7.7$ Hz, NH, 1H), 4.53 (dd, $J = 13.8, 6.0$ Hz, CHNH, 1H), 3.78 (s, ArOCH₃, 3H), 3.67 (s, COOCH₃, 3H), 3.18 (dd, $J = 14.0, 5.5$ Hz, ArCH_aH_b, 1H), 2.98 (dd, $J = 14.0, 6.0$ Hz, ArCH_aH_b, 1H), 1.37 (s, COOC(CH₃)₃, 9H); ¹³C NMR (CDCl₃, 100 MHz) δ 172.1 (COOMe), 157.2 (Ar), 155.0 (COO^tBu), 140.2 (Ar), 130.3 (Ar), 130.2 (Ar), 110.8 (Ar), 85.9 (Ar), 80.0 (COOC(CH₃)₃), 56.4 (ArOCH₃), 54.5 (CHNH), 52.3 (COOCH₃), 36.9 (ArCH₂), 28.3 (COOC(CH₃)₃).

The observed data are in accord with published values.¹⁷⁹

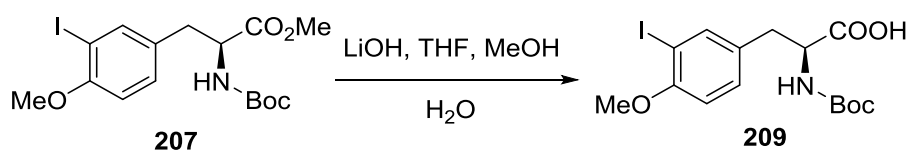
Preparation of amine 208



Amine **208** was prepared from **207** (0.80 g, 1.84 mmol) following a similar procedure to that for the synthesis of **94** and was obtained as a colourless oil (0.56 g, 1.67 mmol, 91% yield). $R_f = 0.20$ (EtOAc); $[\alpha]_D^{20} = +32$ ($c = 0.5$, MeOH); FTIR (film) ν_{\max} 3377, 2948, 2838, 1733, 1490, 1252, 1197, 1176, 1048, 811; $^1\text{H NMR}$ (CDCl_3 , 300 MHz) δ 7.63 (d, $J = 2.1$ Hz, ArH, 1H), 7.16 (dd, $J = 8.4, 2.1$ Hz, ArH, 1H), 6.77 (d, $J = 8.4$ Hz, ArH, 1H), 3.88 (s, ArOCH_3 , 3H), 3.74 (s, COOCH_3 , 3H), 3.68 (dd, $J = 7.8, 5.2$ Hz, CHNH, 1H), 3.01 (dd, $J = 13.7, 5.2$ Hz, ArCH_aH_b , 1H), 2.80 (dd, $J = 13.7, 7.8$ Hz, ArCH_aH_b , 1H), 1.75 (br s, NH_2 , 2H); $^{13}\text{C NMR}$ (CDCl_3 , 100 MHz) δ 175.1 (COOMe), 157.1 (Ar), 140.1 (Ar), 131.3 (Ar), 130.4 (Ar), 110.9 (Ar), 86.1 (Ar), 56.4 (ArOCH_3), 55.8 (CHNH), 52.1 (COOCH_3), 39.4 (ArCH_2).

The observed data are in accord with published values.¹⁸⁰

Preparation of acid 209

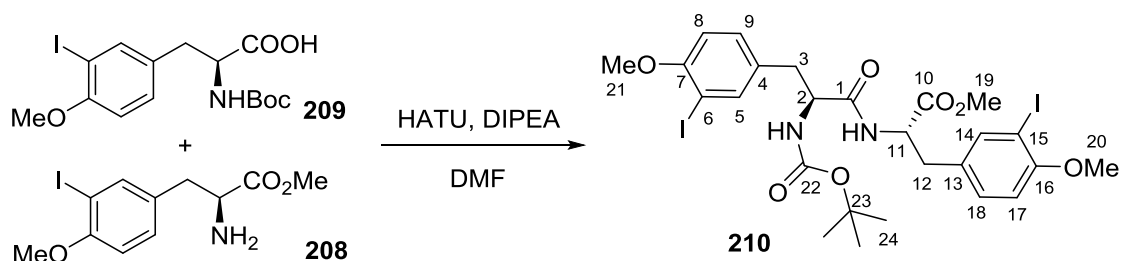


Acid **209** was prepared from **207** (0.98 g, 2.25 mmol) following a similar procedure to that for the synthesis of **92** and was obtained as a colourless oil (0.83 g, 1.98 mmol, 88% yield). $R_f = 0.35$ (EtOAc/petroleum ether 1:2); $[\alpha]_D^{20} = +34.4$ ($c = 1.0$, CHCl_3); FTIR (film) ν_{\max} 3326, 2978, 1712, 1492, 1254, 1166, 1050; $^1\text{H NMR}$ (CDCl_3 , 300 MHz) (major rotamer) δ 9.99 (s, COOH , 1H), 7.59 (d, $J = 2.0$ Hz, ArH, 1H), 7.14 (dd, $J = 8.4, 2.0$ Hz, ArH, 1H), 6.75 (d, $J = 8.4$ Hz, ArH, 1H), 5.09 (d, $J = 7.9$ Hz, NH, 1H), 4.55 (dd, $J = 13.4, 5.9$ Hz, CHNH, 1H), 3.85

(s, OCH₃, 3H), 3.17-3.11 (m, ArCH₂, 2H), 1.44 (s, COOC(CH₃)₃, 9H); ¹³C NMR (CDCl₃, 100 MHz) (major rotamer) δ 175.5 (COOH), 157.2 (Ar), 155.3 (COO^tBu), 140.3 (Ar), 130.4 (Ar), 130.1 (Ar), 110.9 (Ar), 85.9 (Ar), 80.4 (COOC(CH₃)₃), 56.4 (OCH₃), 54.3 (CHNH), 36.5 (ArCH₂CH), 28.3 (COOC(CH₃)₃).

The observed data are in accord with published values.¹⁸¹

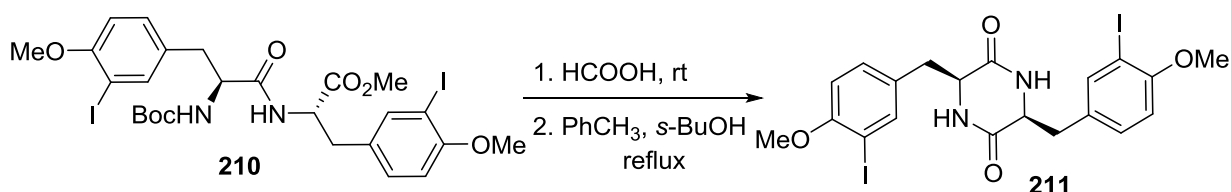
Preparation of dipeptide **210**



Dipeptide **210** was prepared from acid **209** (0.80 g, 1.90 mmol) and amine **208** (0.63 g, 1.90 mmol) following a similar procedure to that for the synthesis of **95** and was obtained as a colourless oil (1.11 g, 1.50 mmol, 79% yield). $R_f = 0.60$ (EtOAc:hexane = 1:1); $[\alpha]_D^{20} = +37.6$ ($c = 1.8$, CHCl₃); FTIR (film) ν_{\max} 3309, 2974, 2938, 1742, 1657, 1491, 1253, 1168, 1049; ¹H NMR (CDCl₃, 400 MHz) δ 7.63 (d, $J = 2.0$ Hz, H-5 or H-14, 1H), 7.42 (d, $J = 2.0$ Hz, H-14 or H-5, 1H), 7.17 (dd, $J = 8.4, 2.0$ Hz, H-9 or H-18, 1H), 6.95 (dd, $J = 8.4, 2.0$ Hz, H-18 or H-9, 1H), 6.75 (d, $J = 8.4$ Hz, H-8 or H-17, 1H), 6.71 (d, $J = 8.4$ Hz, H-17 or H-8, 1H), 6.38 (d, $J = 7.4$ Hz, CHCONH, 1H), 5.09 (d, $J = 7.1$ Hz, NHBoc, 1H), 4.74 (dd, $J = 12.7, 7.4$ Hz, H-11, 1H), 4.30 (dd, $J = 13.2, 7.1$ Hz, H-2, 1H), 3.86 (s, H-20 and H-21, 6H), 3.72 (s, H-19, 3H), 3.03-2.95 (m, H-3 and H-12, 4H), 1.43 (s, H-24, 9H); ¹³C NMR (CDCl₃, 100 MHz) δ 171.2 (C-10), 170.7 (C-1), 157.2 (C-7 and C-16), 155.3 (C-22), 140.1 (C-5 and C-14), 130.7 (C-4 or C-13), 130.4 (C-9 or C-18), 130.3 (C-18 or C-9), 129.8 (C-13 or C-4), 110.0 (C-8 or C-17), 110.8 (C-17 or C-8), 86.1 (C-6 or C-15), 85.8 (C-15 or C-6), 80.3 (C-23), 56.4 (C-20 or C-21),

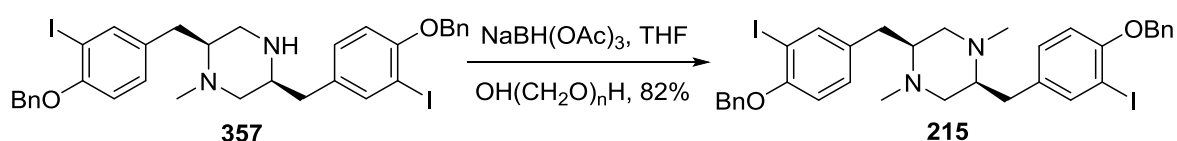
56.3 (C-21 or C-20), 55.7 (C-2), 53.3 (C-11), 52.5 (C-19), 36.9 (C-3 or C-12), 36.5 (C-12 or C-3), 28.3 (C-24); HRMS (ESI) calculated for $C_{26}H_{32}N_2O_7I_2Na$ $[M+Na]^+$ 761.0197, found 761.0194.

Preparation of DKP **211**



DKP **211** was prepared from dipeptide **210** (1.51 g, 2.13 mmol) following a similar procedure to that for the synthesis of **157** and was obtained as a white solid (0.89 g, 1.47 mmol, 69% yield). M.p. 189-190 °C; $R_f = 0.20$ (EtOAc/MeOH 5:1); $[\alpha]_D^{20} = -130.2$ ($c = 0.55$, CHCl₃); FTIR (film) ν_{max} 3192, 2971, 1666, 1492, 1254, 1050, 760; ¹H NMR (DMSO-*d*₆, 300 MHz) δ 8.07 (s, NH, 2H), 7.44 (d, $J = 1.6$ Hz, ArH, 2H), 7.00 (dd, $J = 8.4, 1.6$ Hz, ArH, 2H), 6.87 (d, $J = 8.4$ Hz, ArH, 2H), 3.97 (dd, $J = 5.4, 4.7$ Hz, CHNH, 2H), 3.79 (s, OCH₃, 6H), 2.55 (dd, $J = 13.7, 4.7$ Hz, ArCH_aH_b, 2H), 2.33 (dd, $J = 13.7, 5.4$ Hz, ArCH_aH_b, 2H); ¹³C NMR (DMSO-*d*₆, 100 MHz) δ 166.2 (C=O), 156.4 (Ar), 140.0 (Ar), 131.0 (Ar), 130.6 (Ar), 111.0 (Ar), 85.8 (Ar), 56.2 (CHNH), 55.2 (OCH₃), 37.5 (ArCH₂); HRMS (ESI) calculated for $C_{20}H_{21}N_2O_4I_2$ $[M+H]^+$ 606.9591, found 606.9598.

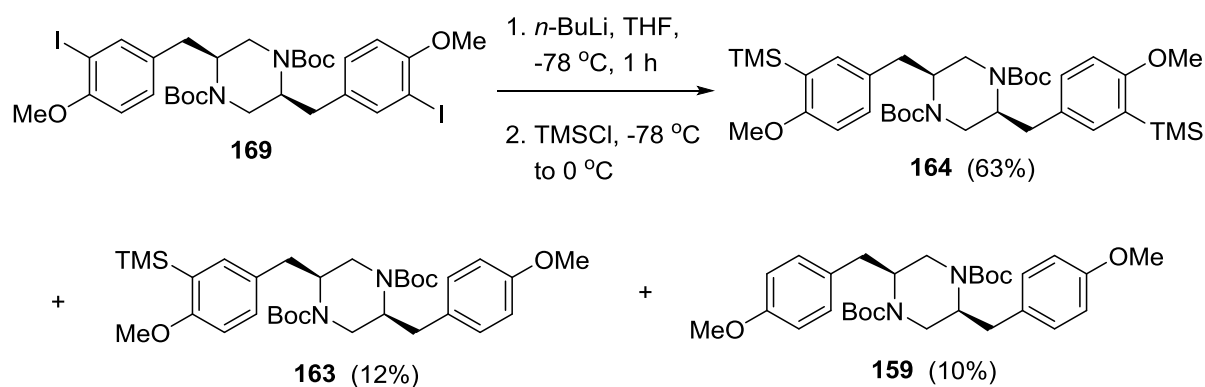
Preparation of piperazine **215**



Piperazine **215** was prepared from **357** (0.70 g, 0.96 mmol) following a similar procedure to

that for the synthesis of **111** and was obtained as a colourless oil (0.44 g, 0.58 mmol, 60% yield). $R_f = 0.50$ (MeOH:EtOAc = 1:2); $[\alpha]_D^{20} = +81$ ($c = 1.2$, CHCl_3); FTIR (film) ν_{max} 2925, 2852, 2792, 1509, 1487, 1453, 1241, 734; $^1\text{H NMR}$ (CDCl_3 , 400 MHz) δ 7.70 (d, $J = 2.0$ Hz, *ArH*, 2H), 7.53 (d, $J = 7.3$ Hz, *ArH*, 4H), 7.42 (t, $J = 7.3$ Hz, *ArH*, 4H), 7.36 (d, $J = 7.3$ Hz, *ArH*, 2H), 7.13 (dd, $J = 8.4, 2.0$ Hz, *ArH*, 2H), 6.81 (d, $J = 8.4$ Hz, *ArH*, 2H), 5.15 (s, PhCH_2 , 4H), 2.87 (dd, $J = 13.2, 3.3$ Hz, ArCH_aH_b , 2H), 2.69 (dd, $J = 13.2, 10.0$ Hz, ArCH_aH_b , 2H), 2.58-2.52 (br m, *NCH*, 2H), 2.46 (dd, $J = 11.5, 6.2$ Hz, NCH_aH_b , 2H), 2.37 (s, NCH_3 , 6H), 2.25 (dd, $J = 11.5, 3.1$ Hz, NCH_aH_b , 2H); $^{13}\text{C NMR}$ (CDCl_3 , 100 MHz) δ 155.6 (*Ar*), 140.1 (*Ar*), 136.9 (*Ar*), 134.8 (*Ar*), 130.3 (*Ar*), 128.6 (*Ar*), 127.9 (*Ar*), 127.0 (*Ar*), 112.6 (*Ar*), 86.8 (*Ar*), 70.5 (PhCH_2), 62.5 (*NCH*), 55.3 (ArCH_2), 42.7 (NCH_3), 31.6 (NCH_2); HRMS (ESI) calculated for $\text{C}_{34}\text{H}_{37}\text{N}_2\text{O}_2\text{I}_2$ $[\text{M}+\text{H}]^+$ 759.0944, found 759.0952.

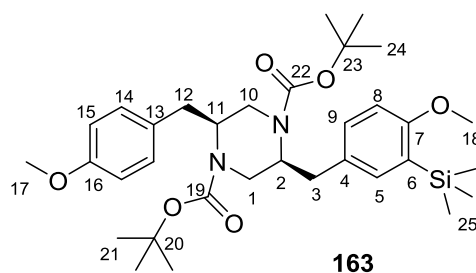
Preparation of piperazine **164** (Li-I exchange approach)



n-Butyllithium (0.23 mL, 0.36 mmol, 1.6 M solution in hexanes) was added dropwise to a solution of piperazine derivative **169** (95 mg, 0.12 mmol) in anhydrous THF (6 mL) at -78 °C. The mixture was stirred at -78 °C for 1 h before the addition of freshly distilled chlorotrimethylsilane (77 μL , 0.60 mmol). The resultant mixture was stirred at -78 °C for 30 min and then at 0 °C for 2 h. Saturated NaHCO_3 aqueous solution (15 mL) was added to

quench the reaction and the mixture was extracted with DCM (3×15 mL). The combined organic fractions were washed with brine (15 mL), dried over MgSO₄ and concentrated under reduced pressure. The residue was purified by flash column chromatography eluting with 15% EtOAc in petroleum ether to afford **164** (63% yield) and **163** (12% yield) as colourless oils, along with deiodinated material **159** (10% yield).

Data for 164: $R_f = 0.62$ (EtOAc/petroleum ether 1:3); $[\alpha]_D^{20} = +20$ ($c = 0.2$, CHCl₃); FTIR (film) ν_{\max} 2961, 2936, 1693, 1402, 1239, 1157, 838; ¹H NMR (CDCl₃, 300 MHz) δ 7.11 (d, $J = 2.2$ Hz, ArH, 2H), 7.08 (dd, $J = 8.2, 2.2$ Hz, ArH, 2H), 6.73 (d, $J = 8.2$ Hz, ArH, 2H), 4.12-4.01 (br m, CH, 2H), 3.97-3.85 (br m, NCH_aH_b, 2H), 3.79 (s, OCH₃, 6H), 2.86 (dd, $J = 13.2, 4.0$ Hz, ArCH_aH_b, 2H), 2.67-2.51 (m, ArCH_aH_b and NCH_aH_b, 4H), 1.45 (s, COOC(CH₃)₃, 18H), 0.26 (s, Si(CH₃)₃, 18H); ¹³C NMR (CDCl₃, 100 MHz) δ 164.1 (Ar), 156.0 (COO^tBu), 136.6 (Ar), 132.3 (Ar), 129.6 (Ar), 129.0 (Ar), 110.6 (Ar), 80.8 (COOC(CH₃)₃), 56.1 (OCH₃), 55.6 (CH), 42.1 (NCH₂), 38.4 (CH₂Ar), 29.4 (COOC(CH₃)₃), 0.0 (Si(CH₃)₃); HRMS (ESI) calculated for C₃₆H₅₈N₂O₆²⁸Si₂Na [M+Na]⁺ 693.3731, found 693.3738.

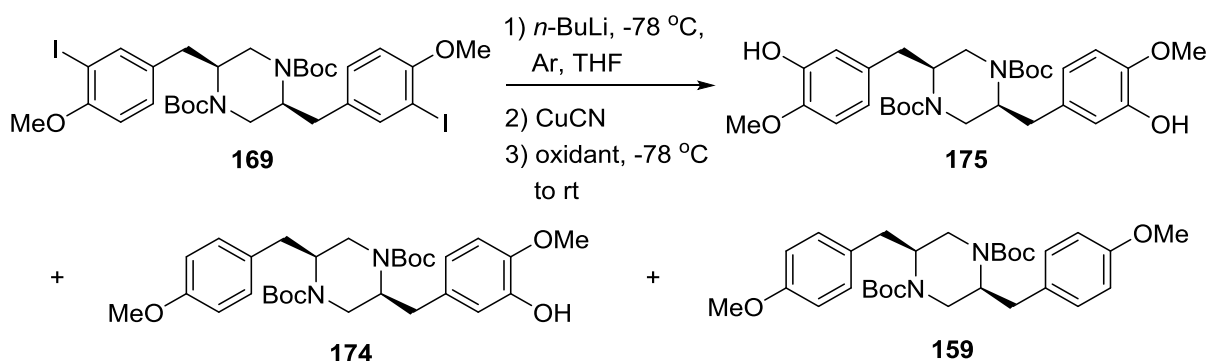


Data for 163: $R_f = 0.61$ (EtOAc/petroleum ether 1:3); $[\alpha]_D^{20} = +25.6$ ($c = 0.5$, CHCl₃); FTIR (film) ν_{\max} 2970, 2936, 1693, 1404, 1244, 1163, 840; ¹H NMR (CDCl₃, 300 MHz) δ 7.09 (d, $J = 2.1$ Hz, H-5, 1H), 7.08 (dd, $J = 8.2, 2.1$ Hz, H-9, 1H), 7.03 (d, $J = 8.6$ Hz, H-14, 2H), 6.81 (d, $J = 8.6$ Hz, H-15, 2H), 6.72 (d, $J = 8.2$ Hz, H-8, 1H), 4.14-4.00 (br m, H-2 and H-11, 2H), 3.92-3.80 (m, H-1a and H-10a, 2H), 3.81 (s, H-18, 3H), 3.80 (s, H-17, 3H), 2.87-2.78 (m, H-

3a and H-12a, 2H), 2.65-2.54 (m, H-1b and H-3b and H-10b and H-12b, 4H), 1.46 (s, H-21 or H-24, 9H), 1.45 (s, H-24 or H-21, 9H), 0.27 (s, H-25, 9H); ^{13}C NMR (CDCl_3 , 100 MHz) δ 164.1 (C-7), 159.2 (C-16), 156.0 (C-19 and C-22), 136.7 (C-5), 132.4 (C-9), 131.2 (C-14), 130.1 (C-13), 129.5 (C-4), 129.0 (C-6), 114.9 (C-15), 110.5 (C-8), 80.9 (C-19 and C-22), 56.2 (C-17 or C-18), 56.1 (C-18 or C-17), 55.4 (C-2 and C-11), 42.1 (C-1 and C-10), 38.1 (C-3 and C-12), 29.4 (C-19 and C-22), 0.0 (C-25); HRMS (ESI) calculated for $\text{C}_{33}\text{H}_{50}\text{N}_2\text{O}_6^{28}\text{SiNa}$ $[\text{M}+\text{Na}]^+$ 621.3336, found 621.3337.

General procedure for oxidative cuprate coupling

Attempted intramolecular oxidative cuprate coupling with piperazine 169:

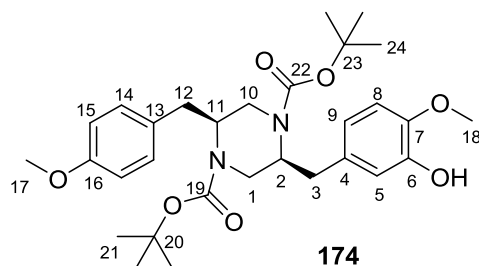


Oxidation using nitrobenzene: To a solution of piperazine derivative **169** (0.36 g, 0.46 mmol) in anhydrous THF (10 mL) was added *n*-butyllithium (0.63 mL, 1.01 mmol, 1.6 M in hexanes) dropwise at -78 °C under N_2 . The reaction mixture was stirred at the same temperature for 30 min before being transferred to a pre-cooled flask at -78 °C containing a suspension of CuCN (42 mg, 0.46 mmol) in THF (15 mL). The resultant mixture was stirred at -78 °C for 30 min and then at -40 °C for 1 h. Upon warming up, the reaction mixture became homogeneous and the colour of the system changed from light yellow to light green. The reaction solution was then cooled to -78 °C and nitrobenzene (0.19 mL, 1.86 mmol) was added in one portion. The

resultant mixture was allowed to warm up to rt within 2 h and stirred for 3 h. Upon fully consumption of the starting material, the mixture was partitioned between water (20 mL) and DCM (20 mL). The aqueous phase was extracted with DCM (3×15 mL). The organic fractions were combined, washed with brine (15 mL), dried over MgSO₄, filtered and concentrated under reduced pressure. The residue was purified by flash column chromatography (gradient eluent: 20% to 35% EtOAc in petroleum ether) to afford **175** (0.12 g, 0.23 mmol, 50% yield) and **174** (0.05 g, 0.09 mmol, 20% yield) as colourless oils, along with deiodinated material **159** (41 mg, 0.078 mmol, 17% yield).

Oxidation using O₂: *n*-Butyllithium (0.31 mL, 0.50 mmol, 1.6 M solution in hexanes) was added dropwise to a solution of piperazine derivative (0.18 g, 0.23 mmol) in anhydrous THF (8 mL) at -78 °C under N₂. The reaction mixture was stirred at the same temperature for 30 min before being transferred to a pre-cooled flask at -78 °C containing a suspension of CuCN (21 mg, 0.23 mmol) in THF (8 mL). The resultant mixture was stirred at -78 °C for 30 min and then at -40 °C for 1 h. The reaction solution was then cooled to -78 °C and dry molecular oxygen was bubbled through the reaction mixture for 1 h. The mixture was then allowed to warm to rt and stirred for 3 h under an atmosphere of O₂. The system was cooled to 0 °C and water (5 mL) was added. The mixture was partitioned between water (15 mL) and DCM (20 mL). The aqueous phase was extracted with DCM (3×10 mL). The combined organic fractions were washed with brine (15 mL), dried over MgSO₄, filtered and concentrated under reduced pressure. The residue was purified by flash column chromatography (gradient eluent: 20% to 35% EtOAc in petroleum ether) to afford **175** (68 mg, 0.12 mmol, 53% yield) and **174** (32 mg, 0.060 mmol, 26% yield) as colourless oils, along with deiodinated material **159** (17 mg, 0.032 mmol, 14% yield).

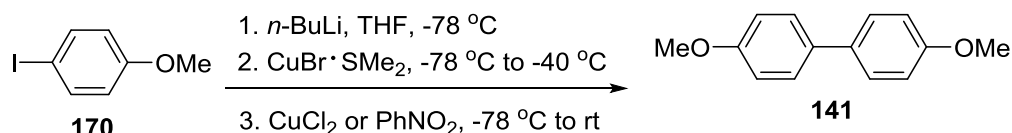
Data for 175: $R_f = 0.30$ (EtOAc/petroleum ether 1:2); $[\alpha]_D^{20} = +66.4$ ($c = 0.5$, CHCl_3); FTIR (film) ν_{max} 3670, 2973, 2931, 1685, 1405, 1244, 1153, 1023; ^1H NMR (CDCl_3 , 300 MHz) δ 6.76 (d, $J = 8.2$ Hz, ArH, 2H), 6.70 (d, $J = 1.8$ Hz, ArH, 2H), 6.60 (dd, $J = 8.2, 1.8$ Hz, ArH, 2H), 5.63 (br s, OH, 2H), 4.11-3.98 (br m, CH, 2H), 3.93-3.83 (br m, NCH_aH_b , 2H), 3.88 (s, OCH_3 , 6H), 2.82 (dd, $J = 13.2, 3.9$ Hz, ArCH_aH_b , 2H), 2.62-2.56 (m, ArCH_aH_b and NCH_aH_b , 4H), 1.46 (s, $\text{COOC}(\text{CH}_3)_3$, 18H); ^{13}C NMR (CDCl_3 , 100 MHz) δ 155.1 (COO^tBu), 145.5 (Ar), 145.3 (Ar), 130.4 (Ar), 120.7 (Ar), 115.6 (Ar), 110.8 (Ar), 80.0 ($\text{COOC}(\text{CH}_3)_3$), 56.0 (OCH_3), 54.5 (CH), 41.2 (NCH_2), 37.5 (CH_2Ar), 28.4 ($\text{COOC}(\text{CH}_3)_3$); HRMS (ESI) calculated for $\text{C}_{30}\text{H}_{42}\text{N}_2\text{O}_8\text{Na}$ $[\text{M}+\text{Na}]^+$ 581.2839, found 581.2834.



Data for 174: $R_f = 0.35$ (EtOAc/petroleum ether 1:2); $[\alpha]_D^{20} = +118$ ($c = 0.2$, CHCl_3); FTIR (film) ν_{max} 3369, 2973, 2930, 1683, 1511, 1406, 1245, 1153, 1121, 734; ^1H NMR (CDCl_3 , 300 MHz) δ 7.04 (d, $J = 8.6$ Hz, H-14, 2H), 6.82 (d, $J = 8.6$ Hz, H-15, 2H), 6.75 (d, $J = 8.2$ Hz, H-8, 1H), 6.70 (d, $J = 1.9$ Hz, H-5, 1H), 6.59 (dd, $J = 8.2, 1.9$ Hz, H-9, 1H), 5.60 (br s, OH, 1H), 4.07-4.03 (br m, H-2 and H-11, 2H), 3.88 (s, H-18, 3H), 3.88-3.80 (br m, H-1a and H-10a, 2H), 3.81 (s, H-17, 3H), 2.86-2.78 (m, H-3a and H-12a, 2H), 2.66-2.55 (m, H-1b and H-3b and H-10b and H-12b, 4H), 1.46 (s, H-21 or H-24, 9H), 1.45 (s, H-24 or H-21, 9H); ^{13}C NMR (CDCl_3 , 100 MHz) δ 158.3 (C-16), 155.1 (C-19 and C-22), 145.5 (C-7), 145.3 (C-6), 130.4 (C-4), 130.3 (C-14), 129.2 (C-13), 120.7 (C-9), 115.5 (C-5), 113.9 (C-15), 110.7 (C-8), 80.0 (C-19 and C-22), 56.0 (C-18), 55.3 (C-17), 54.5 (C-2 and C-11), 41.2 (C-1 and C-10), 37.5

(C-3), 37.1 (C-12), 28.4 (C-21 and C-24); HRMS (ESI) calculated for $C_{30}H_{42}N_2O_7Na$ $[M+Na]^+$ 565.2890, found 565.2892.

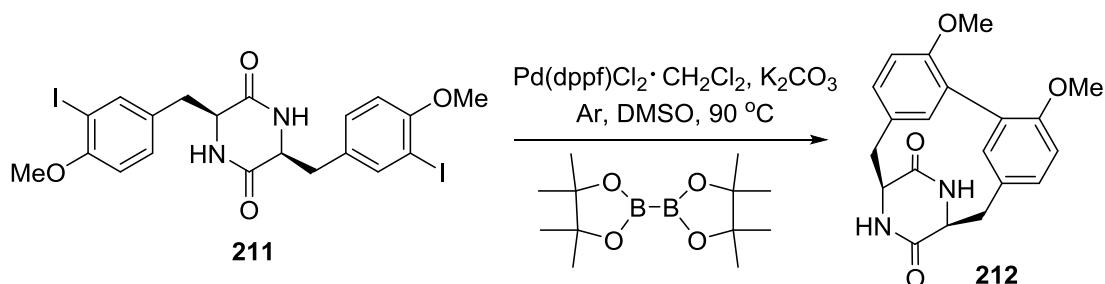
Model reactions with 4-iodoanisole:



The reaction with **170** (0.16 g, 0.68 mmol) was conducted following a similar procedure to that for the synthesis of **175** and biphenyl **141** was obtained as a colourless crystalline solid in 79% yield (57 mg, 0.27 mmol, CuCl_2 as the oxidant) or 86% yield (63 mg, 0.29 mmol, PhNO_2 as the oxidant). M.p. 177-178 °C; $R_f = 0.55$ (hexane:EtOAc = 15:1); FTIR (film) ν_{max} 2958, 2840, 1608, 1502, 1276, 1251, 1041, 824, 737; $^1\text{H NMR}$ (CDCl_3 , 300 MHz) δ 7.50 (d, $J = 8.8$ Hz, 4H), 6.98 (d, $J = 8.8$ Hz, 4H), 3.87 (s, 6H); $^{13}\text{C NMR}$ (CDCl_3 , 100 MHz) δ 158.7, 133.5, 127.7, 114.2, 55.4.

The observed data are in accord with published values.¹⁸²

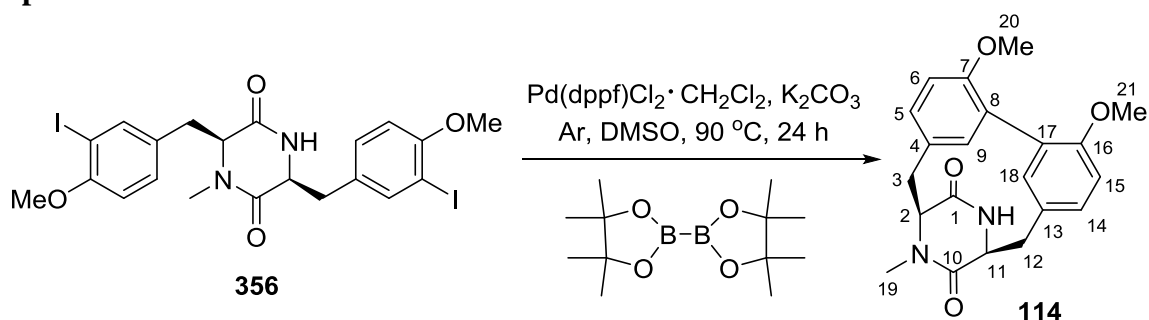
General procedure for intramolecular Suzuki-Miyaura coupling



To a mixture of DKP **211** derivative (62 mg, 0.10 mmol), $\text{Pd(dppf)Cl}_2\cdot\text{CH}_2\text{Cl}_2$ (16 mg, 0.02 mmol), bis(pinacolato)diboron (28 mg, 0.11 mmol) and K_2CO_3 (80 mg, 0.60 mmol) was added degassed anhydrous DMSO (30 mL). The reaction mixture was stirred at 90 °C under

argon for 20 h. The mixture was then cooled to rt and partitioned between 5% HCl (30 mL) and 3:1 CHCl₃/isopropanol (40 mL). The aqueous phase was extracted with 3:1 CHCl₃/isopropanol (2×40 mL). The combined organic fractions were washed with brine (30 mL), dried over MgSO₄, filtered and concentrated under reduced pressure. The crude product was purified by flash column chromatography eluting with 5% MeOH in DCM to afford the coupling DKP product **212** as a white solid (15 mg, 39% yield). M.p. (dec.) 252-256 °C; $[\alpha]_D^{20} = +32$ ($c = 0.2$, CHCl₃); FTIR (film) ν_{\max} 3181, 3041, 2958, 1664, 1512, 1266; ¹H NMR (DMSO-*d*₆, 400 MHz) δ 8.00 (s, NH, 2H), 7.02 (dd, $J = 8.2, 1.7$ Hz, ArH, 2H), 6.84 (d, $J = 8.2$ Hz, ArH, 2H), 6.49 (d, $J = 1.7$ Hz, ArH, 2H), 4.34 (d, $J = 5.2$ Hz, CHNH, 2H), 3.80 (s, OCH₃, 6H), 3.55 (d, $J = 15.3$ Hz, ArCH_aH_b, 2H), 2.66 (dd, $J = 15.3, 5.7$ Hz, ArCH_aH_b, 2H); ¹³C NMR (DMSO-*d*₆, 100 MHz) δ 168.2 (C=O), 154.9 (Ar), 141.4 (Ar), 130.5 (Ar), 129.2 (Ar), 126.9 (Ar), 111.3 (Ar), 56.2 (ArOCH₃), 55.5 (CHNH), 33.4 (ArCH₂); HRMS (ESI) calculated for C₂₀H₂₁N₂O₄ [M+H]⁺ 353.1501, found 353.1499.

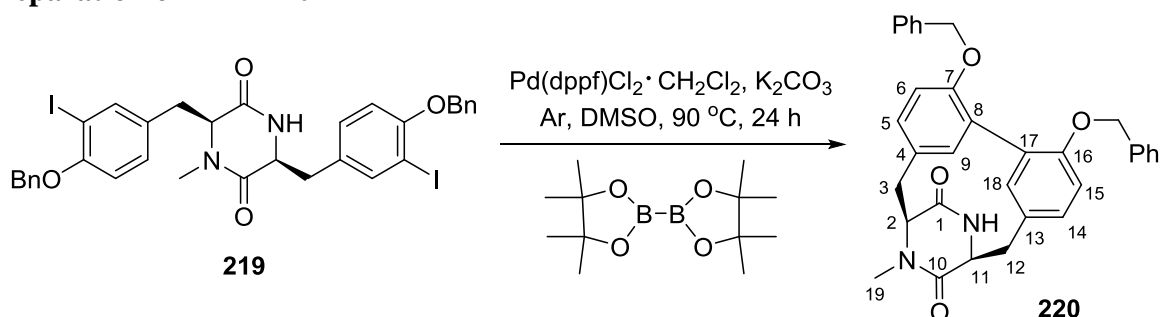
Preparation of DKP **114**



DKP **114** was prepared from **356** (109 mg, 0.17 mmol) following a similar procedure to that for the synthesis of **212** and was obtained as a white solid (29 mg, 0.08 mmol, 48% yield). M.p. 118-119 °C; $R_f = 0.25$ (MeOH/EtOAc = 1:6); $[\alpha]_D^{20} = +74$ ($c = 0.7$, MeOH); FTIR (film) ν_{\max} 3242, 2959, 2929, 1674, 1651, 1510, 1263, 1247; ¹H NMR (CDCl₃, 300 MHz) δ 7.06 (dd, $J = 8.0, 2.2$ Hz, H-5 or H-14, 1H), 6.99 (dd, $J = 8.2, 1.8$ Hz, H-14 or H-5, 1H), 6.78 (d, $J = 8.0$

Hz, H-6 or H-15, 1H), 6.76 (d, $J = 8.2$ Hz, H-15 or H-6, 1H), 6.53 (d, $J = 2.2$ Hz, H-9 or H-18, 1H), 6.45 (d, $J = 1.8$ Hz, H-18 or H-9, 1H), 5.71 (s, NH, 1H), 4.50 (dd, $J = 9.4, 5.8$ Hz, H-11, 1H), 4.35 (dd, $J = 9.4, 6.3$ Hz, H-2, 1H), 4.07 (dd, $J = 15.9, 9.4$ Hz, H-12a, 1H), 4.02 (dd, $J = 15.9, 9.4$ Hz, H-3a, 1H), 3.93 (s, H-20 or H-21, 3H), 3.91 (s, H-21 or H-20, 3H), 2.98 (dd, $J = 15.9, 6.3$ Hz, H-3b, 1H), 2.80 (s, H-19, 3H), 2.65 (dd, $J = 15.9, 5.8$ Hz, H-12b, 1H); ^{13}C NMR (CDCl₃, 100 MHz) δ 167.9 (C-10), 166.9 (C-1), 155.7 (C-7 or C-16), 155.5 (C-16 or C-7), 141.9 (C-9 or C-18), 141.6 (C-18 or C-9), 129.9 (C-5 or C-14), 129.6 (C-14 or C-5), 129.5 (C-4 or C-13), 129.1 (C-13 or C-4), 125.4 (C-8 or C-17), 125.2 (C-17 or C-8), 112.2 (C-6 or C-15), 111.8 (C-15 or C-6), 62.2 (C-2), 56.3 (C-11), 56.1 (C-20 or C-21), 56.0 (C-21 or C-20), 34.7 (C-12), 34.1 (C-3), 31.7 (C-19); HRMS (ESI) calculated for C₂₁H₂₂N₂O₄Na [M+Na]⁺ 389.1477, found 389.1471.

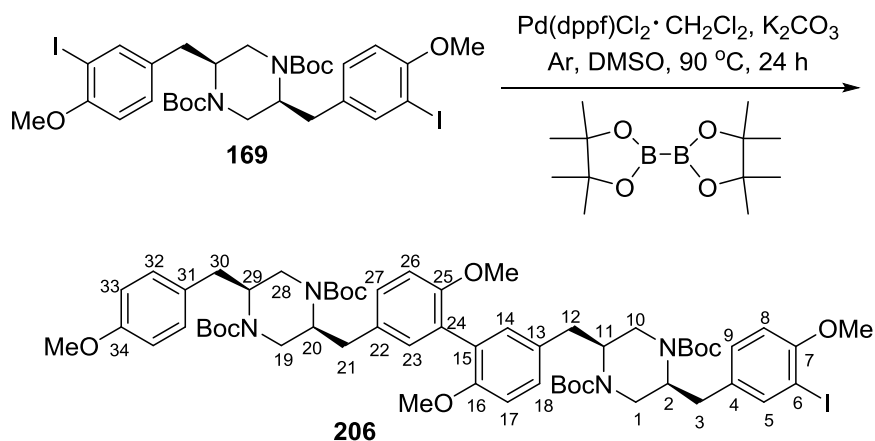
Preparation of DKP **220**



DKP **220** was prepared from **219** (0.21 g, 0.27 mmol) following a similar procedure to that for the synthesis of **212** and was obtained as a white solid (73 mg, 0.14 mmol, 52% yield). M.p. 169-172 °C; $R_f = 0.22$ (EtOAc/MeOH 6:1); $[\alpha]_D^{25} = +116$ ($c = 0.4$, CHCl₃); FTIR (film) ν_{max} 3221, 2974, 2901, 1677, 1664, 1507, 1251, 1052, 736; ^1H NMR (CDCl₃, 300 MHz) δ 7.40-7.32 (m, PhH, 4H), 7.31-7.24 (m, PhH, 6H), 7.03 (dd, $J = 8.3, 2.3$ Hz, H-5 or H-14, 1H), 6.96 (dd, $J = 8.2, 2.1$ Hz, H-14 or H-5, 1H), 6.81 (d, $J = 8.3$ Hz, H-6 or H-15, 1H), 6.75 (d, $J = 8.3$ Hz, H-15 or H-6, 1H), 6.57 (d, $J = 2.3$ Hz, H-9 or H-18, 1H), 6.51 (d, $J = 2.1$ Hz, H-18

or H-9, 1H), 5.98 (s, NH, 1H), 5.26 (d, $J = 11.8$ Hz, PhCH_aH_b, 1H), 5.19 (d, $J = 11.8$ Hz, PhCH_aH_b, 1H), 5.13 (s, PhCH₂, 2H), 4.50 (d, $J = 6.4$ Hz, H-11, 1H), 4.35 (d, $J = 6.4$ Hz, H-2, 1H), 4.07 (d, $J = 5.9$ Hz, H-12a, 1H), 4.02 (d, $J = 5.9$ Hz, H-3a, 1H), 2.98 (dd, $J = 15.9, 6.4$ Hz, H-3b, 1H), 2.80 (s, H-19, 3H), 2.67 (dd, $J = 15.9, 6.4$ Hz, H-12b, 1H); ¹³C NMR (CDCl₃, 100 MHz) δ 167.8 (C-10), 166.8 (C-1), 154.9 (C-7 or C-16), 154.8 (C-16 or C-7), 141.9 (C-9 or C-18), 141.6 (C-18 or C-9), 137.4 (Ph), 137.3 (Ph), 130.4 (C-4 or C-13), 129.9 (C-13 or C-4), 129.7 (C-5 or C-14), 129.4 (C-14 or C-5), 128.4 (Ph), 127.6 (Ph), 127.5 (Ph), 127.4 (Ph), 125.7 (C-8 or C-17), 125.6 (C-17 or C-8), 114.2 (C-6 or C-15), 113.6 (C-15 or C-6), 70.8 (PhCH₂), 70.7 (PhCH₂), 62.2 (C-2), 56.3 (C-11), 34.8 (C-12), 34.1 (C-3), 31.7 (C-19); HRMS (ESI) calculated for C₃₃H₃₀N₂O₄Na [M+Na]⁺ 541.2103, found 541.2115.

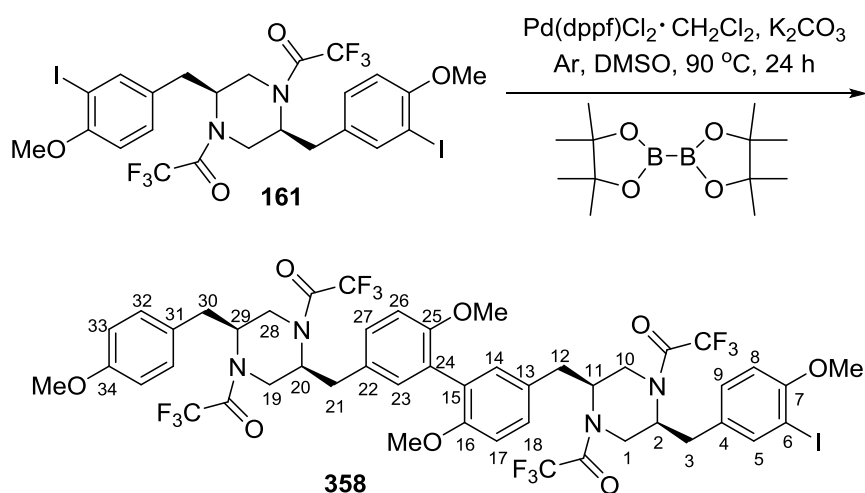
Intramolecular Suzuki-Miyaura coupling of **169**



The coupling reaction of piperazine **169** (0.13 g, 0.17 mmol) was performed following a similar procedure to that for the synthesis of **212** and dimeric compound **206** was isolated as a white solid (18 mg, 0.015 mmol, 18% yield). M.p. 160-161 °C; $R_f = 0.40$ (EtOAc/petroleum ether 1:2); $[\alpha]_D^{20} = +30$ ($c = 0.2$, CHCl₃); FTIR (film) ν_{max} 2974, 2930, 1688, 1246, 1153, 1115; ¹H NMR (CDCl₃, 300 MHz) δ 7.57 (d, $J = 2.0$ Hz, H-5, 1H), 7.14-7.01 (m, H-9 and H-

14 and H-18 and H-23 and H-27 and H-32, 7H), 6.89 (d, $J = 8.4$ Hz, H-17 or H-26, 1H), 6.88 (d, $J = 8.4$ Hz, H-26 or H-17, 1H), 6.81 (d, $J = 8.6$ Hz, H-33, 2H), 6.72 (d, $J = 8.4$ Hz, H-8, 1H), 4.18-4.00 (br m, H-2 and H-11 and H-20 and H-29, 4H), 3.99-3.72 (m, H-1a and H-10a and H-19a and H-28a, 4H), 3.85 (s, OCH_3 , 3H), 3.79 (s, OCH_3 , 3H), 3.76 (s, OCH_3 , 6H), 2.94-2.76 (m, H-3a and H-12a and H-21a and H-30a, 4H), 2.72-2.48 (m, H-1b and H-3b and H-10b and H-12b and H-19b and H-21b and H-28b and H-30b, 8H), 1.46 (s, $\text{COOC}(\text{CH}_3)_3$, 9H), 1.45 (s, $\text{COOC}(\text{CH}_3)_3$, 18H), 1.44 (s, $\text{COOC}(\text{CH}_3)_3$, 9H); ^{13}C NMR (CDCl_3 , 100 MHz) δ 158.3 (C-34), 156.9 (C-7), 155.8 (C-16 and C-25), 155.1 (COO^tBu), 155.0 (COO^tBu), 140.0 (C-5), 132.5 (C-32), 131.7 (C-13 and C-22), 130.2 (C-9 and C-14 and C-23), 129.3 (C-4 or C-31), 129.1 (C-18 and C-27), 128.7 (C-31 or C-4), 127.4 (C-15 and C-24), 113.9 (C-33), 111.3 (C-17 and C-26), 110.9 (C-8), 86.0 (C-6), 80.0 ($\text{COOC}(\text{CH}_3)_3$), 79.9 ($\text{COOC}(\text{CH}_3)_3$), 56.4 (OCH_3), 55.8 (OCH_3), 55.3 (OCH_3), 54.7 and 54.6 (C-2 and C-11 and C-20 and C-29), 41.1 (C-1 and C-10 and C-19 and C-28), 37.3 (C-3 and C-12 and C-21 and C-30), 28.4 ($\text{COOC}(\text{CH}_3)_3$); HRMS (ESI) calculated for $\text{C}_{60}\text{H}_{82}\text{N}_4\text{O}_{12}\text{I}$ $[\text{M}+\text{H}]^+$ 1177.4974, found 1177.4980.

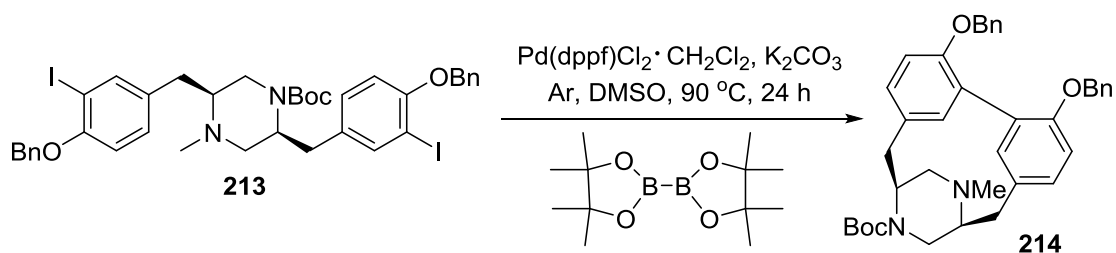
Intramolecular Suzuki-Miyaura coupling of 161



The coupling reaction of piperazine **161** (96 mg, 0.12 mmol) was performed following a similar procedure to that for the synthesis of **212** and dimeric compound **358** was isolated as a colourless viscous oil (8 mg, 0.007 mmol, 12% yield). $R_f = 0.45$ (EtOAc/petroleum ether 1:2); $[\alpha]_D^{20} = +43$ ($c = 0.3$, CHCl_3); FTIR (film) ν_{max} 2924, 2854, 1690, 1444, 1240, 1204, 1138; ^1H NMR (CDCl_3 , 300 MHz) δ 7.44 (d, $J = 1.0$ Hz, H-5, 1H), 7.04-6.79 (m, H-9 and H-14 and H-17 and H-18 and H-23 and H-26 and H-27 and H-32, 9H), 6.72 (d, $J = 8.4$ Hz, H-33, 2H), 6.64 (d, $J = 8.4$ Hz, H-8, 1H), 4.45-4.28 (m, H-2 and H-11 and H-20 and H-29, 4H), 3.78 (s, OCH_3 , 3H), 3.71 (s, OCH_3 , 3H), 3.70 (s, OCH_3 , 3H), 3.70 (s, OCH_3 , 3H), 3.80-3.59 (m, H-1a and H-10a and H-19a and H-28a, 4H), 3.07-2.54 (m, H-1b and H-3 and H-10b and H-12 and H-19b and H-21 and H-28b and H-30, 12H); HRMS (ESI) calculated for $\text{C}_{48}\text{H}_{46}\text{N}_4\text{O}_8\text{IF}_{12}$ $[\text{M}+\text{H}]^+$ 1161.2169, found 1161.2220.

Due to the small quantity of material, ^{13}C NMR spectrum was not obtained. The ^1H NMR signals of **358** were assigned by referring to the cases of dimeric product **206** and piperazine **161**.

Preparation of piperazine **214**

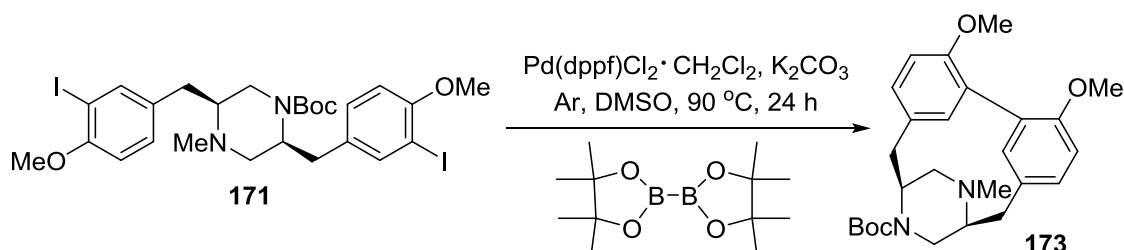


Piperazine **214** was prepared from **213** (0.12 g, 0.14 mmol) following a similar procedure to that for the synthesis of **212** and was obtained as a colourless oil (5 mg, 0.008 mmol, 6% yield). $R_f = 0.65$ (EA/hexane = 1:5); $[\alpha]_D^{20} = -83.2$ ($c = 0.5$, MeOH); FTIR (film) ν_{max} 2961, 2929, 1692, 1252, 1152; ^1H NMR ($\text{DMSO}-d_6$, 300 MHz) δ 7.40-7.28 (m, ArH, 6H), 7.26-7.17

(m, ArH, 6H), 6.86-6.78 (m, ArH, 2H), 6.74 (dd, $J = 8.2, 2.4$ Hz, ArH, 2H), 5.25 (br s, PhCH₂, 4H), 4.18-4.03 (m, NCH, 1H), 3.50-3.37 (m, CH₂, 1H), 3.30-3.09 (m, CH₂, 2H), 2.58-2.39 (m, CH₂, 2H), 2.34-2.08 (m, NCH and CH₂, 4H), 1.94 (s, NCH₃, 3H), 1.37 (s, COOC(CH₃)₃, 9H); ¹³C NMR (DMSO-*d*₆, 100 MHz) δ 154.3 (Ar), 154.0 (Ar), 153.0 (Ar), 142.9 (Ar), 137.5 (Ar), 137.4 (Ar), 129.7 (Ar), 129.3 (Ar), 129.0 (Ar), 128.5 (Ar), 128.2 (Ar), 127.5 (Ar), 127.4 (Ar), 113.6 (Ar), 79.0 (COOC(CH₃)₃), 70.3 (PhCH₂), 70.0 (PhCH₂), 61.9 (CH), 50.6 (CH and NCH₂), 45.1 (NCH₂), 42.5 (NCH₃), 36.0 (ArCH₂), 33.3 (ArCH₂), 28.0 (COOC(CH₃)₃); HRMS (ESI) calculated for C₃₈H₄₃N₂O₄ [M+H]⁺ 591.3223, found 591.3231.

Due to the small quantity of material, suitable 2D NMR spectra were not obtained.

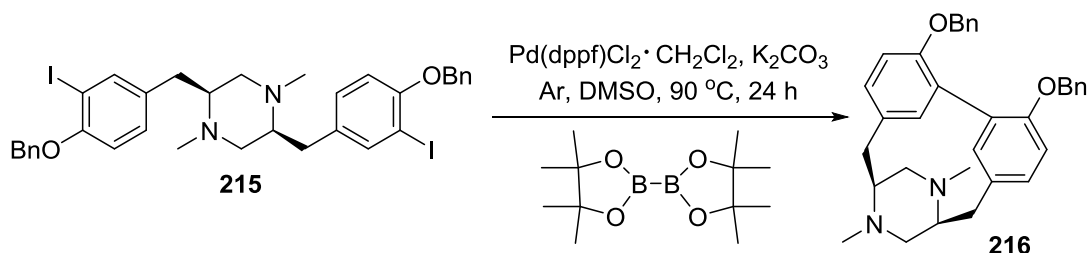
Preparation of piperazine 173



Piperazine **173** was prepared from precursor **171** (0.13 g, 0.19 mmol) following a similar procedure to that for the synthesis of **212** and was obtained as a colourless oil (3 mg, 0.008 mmol, 4% yield). $R_f = 0.60$ (EA/hexane = 1:4); FTIR (film) ν_{\max} 3230, 2957, 2927, 2850, 1673, 1651, 1509, 1263; ¹H NMR (CDCl₃, 300 MHz) δ 7.39 (br s, 2H), 6.97-6.88 (m, 2H), 6.77 (dd, $J = 7.6, 6.3$ Hz, 2H), 4.27-4.14 (m, 1H), 3.99 (s, 2×OCH₃, 6H), 3.59-3.43 (m, 1H), 3.39-3.17 (m, 2H), 2.70-2.49 (m, 2H), 2.46-2.16 (m, 4H), 2.03 (s, NCH₃, 3H), 1.45 (s, COOC(CH₃)₃, 9H); HRMS (ESI) calculated for C₂₆H₃₅N₂O₄ [M+H]⁺ 439.2597, found 439.2593.

Due to the small quantity of material, ¹³C NMR spectrum was not obtained.

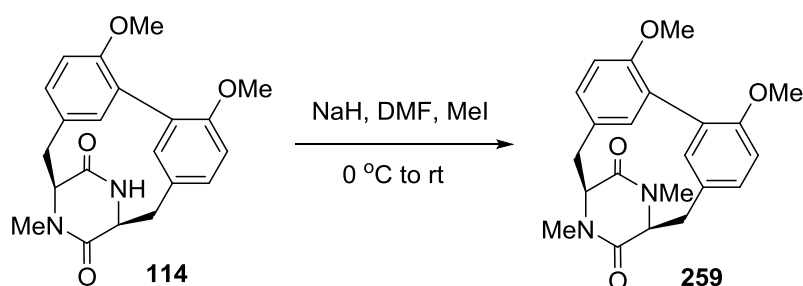
Preparation of piperazine **216**



Piperazine **216** was prepared from precursor **215** (101 mg, 0.13 mmol) following a similar procedure to that for the synthesis of **212** and was obtained as a white solid (3 mg, 0.005 mmol, 4% yield). M.p. 149-150 °C; $R_f = 0.30$ (EA:Hexane = 2:3); FTIR (film) ν_{max} 2963, 2922, 1685, 1673, 1507, 1455, 1380, 1263, 1057; $^1\text{H NMR}$ (CDCl_3 , 400 MHz) δ 8.20 (d, $J = 2.2$ Hz, 2H), 7.42 (dd, $J = 7.3, 2.0$ Hz, 4H), 7.27-7.20 (m, 6H), 6.95 (dd, $J = 8.1, 2.2$ Hz, 2H), 6.73 (d, $J = 8.1$ Hz, 2H), 5.21 (s, PhCH_2 , 4H), 3.11-2.90 (m, 4H), 2.83-2.73 (m, 2H), 2.73-2.66 (m, 2H), 2.65-2.55 (m, 2H), 1.80 (s, NCH_3 , 6H); HRMS (ESI) calculated for $\text{C}_{34}\text{H}_{37}\text{N}_2\text{O}_2$ $[\text{M}+\text{H}]^+$ 505.2855, found 505.2844.

Due to the small quantity of material, $^{13}\text{C NMR}$ spectrum was not obtained.

Preparation of piperazine **259**

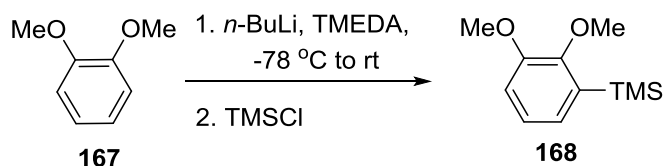


The methylation of **114** (0.19 g, 0.52 mmol) was performed following a similar procedure to that for the synthesis of **93** (Method A) and DKP **259** was obtained as a white solid (0.14 g, 0.38 mmol, 73% yield). M.p. 180-182 °C; $R_f = 0.30$ (MeOH:EtOAc = 1:6); $[\alpha]_{\text{D}}^{20} = +101$ ($c = 0.5$, CHCl_3); FTIR (film) ν_{max} 2956, 2929, 2851, 1655, 1648, 1508, 1255; $^1\text{H NMR}$ (CDCl_3 ,

400 MHz) δ 7.05 (dd, $J = 8.3, 2.0$ Hz, ArH, 2H), 6.77 (d, $J = 8.3$ Hz, ArH, 2H), 6.46 (d, $J = 2.0$ Hz, ArH, 2H), 4.34 (d, $J = 6.4$ Hz, CH, 2H), 4.10 (d, $J = 16.0$ Hz, CH_aH_b, 2H), 3.92 (s, OCH₃, 6H), 2.94 (dd, $J = 16.0, 6.4$ Hz, CH_aH_b, 2H), 2.80 (s, NCH₃, 6H); ¹³C NMR (CDCl₃, 100 MHz) δ 166.6 (C=O), 155.5 (Ar), 141.9 (Ar), 129.4 (Ar), 129.1 (Ar), 125.3 (Ar), 111.9 (Ar), 62.1 (CH), 56.0 (OCH₃), 33.8 (CH₂), 31.5 (NCH₃); HRMS (ESI) calculated for C₂₂H₂₄N₂O₄Na [M+Na]⁺ 403.1634, found 403.1635.

General procedure for directed *ortho* lithiation

Model reaction with 1,2-dimethoxybenzene:

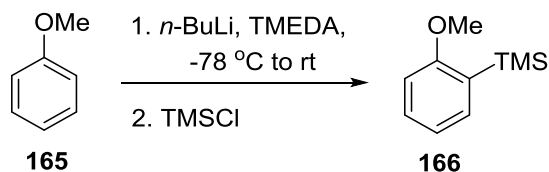


n-Butyllithium (1.42 mL, 2.28 mmol, 1.6 M solution in hexanes) was added dropwise to a solution of 1,2-dimethoxybenzene (0.21 g, 1.52 mmol) and freshly distilled TMEDA (0.45 mL, 4.56 mmol) in anhydrous THF (10 mL) at -78 °C. The mixture was warmed up to rt and stirred for 3 h. The system was then cooled to -78 °C and freshly distilled chlorotrimethylsilane (0.58 mL, 4.56 mmol) was added to the reaction mixture. The resultant mixture was stirred at -78 °C for 30 min and then at rt for 5 h. Saturated NaHCO₃ aqueous solution (15 mL) was added slowly to quench the reaction and the mixture was extracted with Et₂O (3×15 mL). The combined organic fractions were washed with brine (15 mL), dried over MgSO₄ and concentrated under reduced pressure. The residue was purified by flash column chromatography eluting with 10% EtOAc in petroleum ether to afford **168** (0.27 g, 85% yield) as a colourless oil. $R_f = 0.60$ (EA:hexane = 1:10); FTIR (film) ν_{max} 2954, 2901, 2835, 1457, 1415, 1260, 828, 755; ¹H NMR (CDCl₃, 300 MHz) δ 7.14-7.07 (m, 1H), 7.02 (dd, $J = 7.3, 1.7$

Hz, 1H), 6.99 (dd, $J = 7.5, 1.7$ Hz, 1H), 3.91 (s, 3H), 3.90 (s, 3H), 0.34 (s, 9H); ^{13}C NMR (CDCl₃, 100 MHz) δ 154.2, 152.4, 133.8, 126.7, 124.4, 114.4, 61.0, 56.0, 0.0.

The observed data are in accord with published values.⁹⁵

Model reactions with anisole:

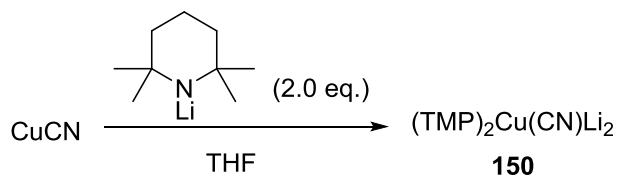


Anisole derivative **166** was prepared from anisole **165** (62 mg, 0.57 mmol) following a similar procedure to that for the synthesis of **168** and was obtained as a colourless oil (75 mg, 0.42 mmol, 73% yield). $R_f = 0.55$ (EA:hexane = 1:30); FTIR (film) ν_{max} 2955, 2930, 2838, 1732, 1513, 1248; ^1H NMR (CDCl₃, 300 MHz) δ 7.45-7.32 (m, 2H), 6.98 (td, $J = 7.3, 0.8$ Hz, 1H), 6.86 (d, $J = 8.2$ Hz, 1H), 3.83 (s, 3H), 0.29 (s, 9H); ^{13}C NMR (CDCl₃, 100 MHz) δ 165.3, 135.9, 131.7, 128.9, 121.3, 110.5, 56.0, 0.0.

The observed data are in accord with published values.¹⁸³

General procedure for direct *ortho* cupration

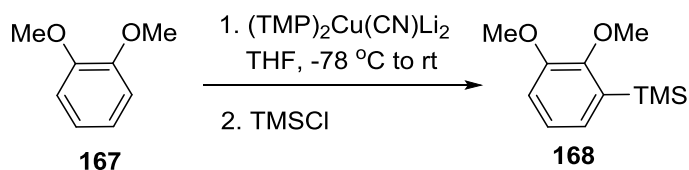
Preparation of the solution of amidocuprate (TMP)₂Cu(CN)Li₂ in THF:



At -78 °C, to a solution of TMP (1.15 mL, 6.78 mmol) in THF (5 mL) was added *n*-butyllithium (4.85 mL, 6.78 mmol, 1.4 M solution in hexanes) dropwise over a period of 15 min. The mixture was then warmed to 0 °C and stirred for 30 min. The LTMP solution was

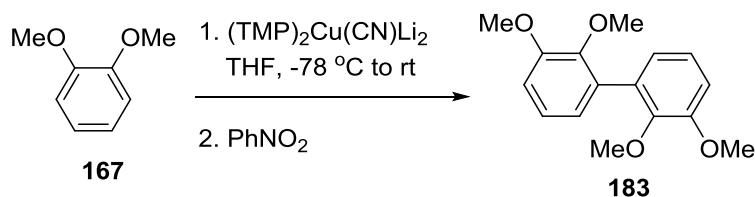
slowly transferred to a pre-cooled flask containing a suspension of CuCN (0.31 g, 3.39 mmol) in THF (3 mL). The resultant mixture was allowed to warm to 0 °C within 20 min and stirred for further 30 min at 0 °C to give a solution of (TMP)₂Cu(CN)Li₂ in THF (0.26 mol/L).

Direct ortho cupration of 1,2-dimethoxybenzene (Preparation of silane 168):



At -78 °C, to a stirred solution of 1,2-dimethoxybenzene (69 mg, 0.50 mmol) in anhydrous THF (3 mL) was added dropwise a solution of (TMP)₂Cu(CN)Li₂ (5.75 mL, 1.50 mmol, 0.26 mol/L) in THF. The reaction solution was warmed to rt and stirred for 3 h at the same temperature. The system was then cooled to -78 °C and freshly distilled TMSCl (0.25 mL, 2.0 mmol) was added. After the reaction mixture being warmed up and stirred for 10 h at rt, saturated NaHCO₃ aqueous solution (15 mL) was added slowly to quench the reaction and the mixture was extracted with Et₂O (3×15 mL). The combined organic fractions were washed with brine (15 mL), dried over MgSO₄ and concentrated under reduced pressure. The residue was purified by flash column chromatography eluting with 10% EtOAc in petroleum ether to afford **168** (69 mg, 66% yield).

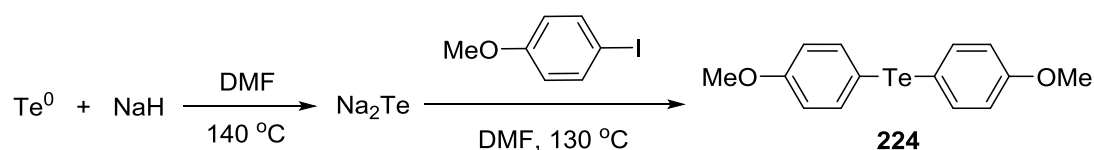
Direct ortho cupration of 1,2-dimethoxybenzene (Preparation of biphenyl 183):



At -78 °C, to a stirred solution of 1,2-dimethoxybenzene (69 mg, 0.50 mmol) in anhydrous THF (3 mL) was added dropwise a solution of (TMP)₂Cu(CN)Li₂ (5.75 mL, 1.50 mmol, 0.26 mol/L) in THF. The reaction solution was warmed to rt and stirred for 3 h at the same temperature. The system was then cooled to -78 °C and PhNO₂ (0.31 mL, 3.0 mmol) was added. After the reaction mixture being stirred for 8 h at rt, saturated NaHCO₃ aqueous solution (15 mL) was added slowly to quench the reaction and the mixture was extracted with Et₂O (3×15 mL). The combined organic fractions were washed with brine (15 mL), dried over MgSO₄ and concentrated under reduced pressure. The residue was purified by flash column chromatography eluting with 20% EtOAc in petroleum ether to afford **183** (50 mg, 73% yield) as a white crystalline solid. M.p. 105-106 °C; R_f = 0.50 (EA:hexane = 1:10); FTIR (film) ν_{max} 2996, 2938, 2835, 1465, 1261, 1031; ¹H NMR (CDCl₃, 300 MHz) δ 7.10 (dd, *J* = 8.2, 7.6 Hz, 2H), 6.96 (dd, *J* = 8.2, 1.6 Hz, 2H), 6.89 (dd, *J* = 7.6, 1.6 Hz, 2H), 3.93 (s, 6H), 3.68 (s, 6H); ¹³C NMR (CDCl₃, 100 MHz) δ 152.8, 146.8, 132.9, 123.3, 111.7, 60.6, 55.8; HRMS (ESI) calculated for C₁₆H₁₉O₄ [M+H]⁺ 275.1283, found 275.1280.

The observed data are in accord with published values.¹⁸⁴

Preparation of telluride **224**

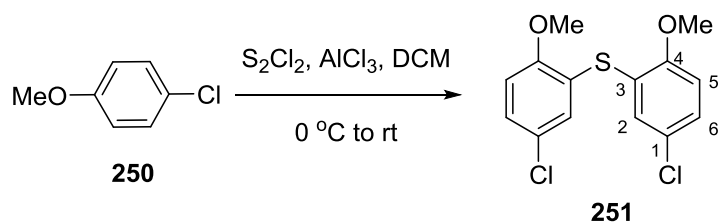


A mixture of Te powder (0.10 g, 0.80 mmol) and NaH (71 mg, 1.76 mmol, 60% dispersion in mineral oil) in anhydrous DMF (6 mL) was stirred at 140 °C for 1.5 h under Ar to give a purple suspension. The system was cooled to rt and a solution of 4-iodoanisole (0.37 g, 1.60 mmol) in DMF (2 mL) was added. The resulting mixture was then heated to 130 °C and

stirred for 15 h before being cooled to rt. Saturated NH_4Cl (aq) (10 mL) was added to the reaction mixture and the system was extracted with Et_2O (3×15 mL). The combined organic phases were washed with brine (10 mL), dried over MgSO_4 and concentrated under reduced pressure. The residue was purified by flash column chromatography eluting with 2% EtOAc in petroleum ether to afford **224** (97 mg, 65% yield) as a yellow solid. M.p. 50-52 °C (lit.¹¹⁵ m.p. 51-52 °C); $R_f = 0.45$ (EA:hexane = 1:15); FTIR (film) ν_{max} 3408, 1587, 1493, 1253, 1178; ^1H NMR (CDCl_3 , 300 MHz) δ 7.65 (d, $J = 8.8$ Hz, 1H), 6.78 (d, $J = 8.8$ Hz, 1H), 3.80 (s, 2H); ^{13}C NMR (CDCl_3 , 100 MHz) δ 159.7, 139.7, 115.4, 104.3, 55.2.

The observed data are in accord with published values.¹¹⁵

Preparation of sulfide **251**

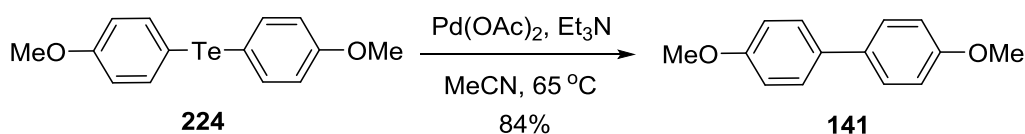


To a solution of 4-chloroanisole (0.13 mL, 1.04 mmol) in DCM (5 mL) at $0\text{ }^\circ\text{C}$ was added AlCl_3 (70 mg, 0.52 mmol), followed by S_2Cl_2 (42 μL , 0.52 mmol). The reaction mixture was stirred at $0\text{ }^\circ\text{C}$ for 1 h and then warmed up to rt for 2 h. Upon completion, water (15 mL) was added to the system and the mixture was extracted with DCM (3×15 mL). The combined organic phases were washed with brine (10 mL), dried over MgSO_4 and concentrated under reduced pressure. The crude product was purified by flash column chromatography eluting with 5% EtOAc in petroleum ether to afford **251** (0.13 g, 81% yield) as a yellow crystalline solid. M.p. 107-108 °C; $R_f = 0.45$ (EA:hexane = 1:4); FTIR (film) ν_{max} 3008, 2965, 2937, 2838, 1474, 1462, 1241; ^1H NMR (CDCl_3 , 300 MHz) δ 7.25 (dd, $J = 8.7, 2.6$ Hz, H-6, 2H), 7.04 (d, $J = 2.6$ Hz, H-2, 2H), 6.87 (d, $J = 8.7$ Hz, H-5, 2H), 3.88 (s, OCH_3 , 6H); ^{13}C NMR

(CDCl₃, 100 MHz) δ 156.4 (C-4), 131.2 (C-2), 128.5 (C-6), 126.0 (C-1), 123.7 (C-3), 111.9 (C-5), 56.2 (OCH₃); HRMS (ESI) calculated for C₁₄H₁₂O₂SCl₂ [M+H]⁺ 313.9935, found 313.9922.

Although **251** was mentioned in the literature,¹⁸⁵ no characterization has been reported.

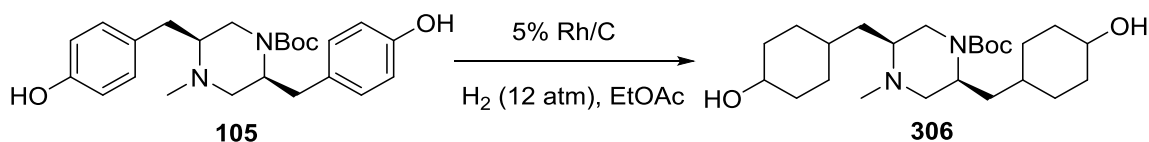
Preparation of biphenyl **141** from telluride **224**



Under Ar, Et₃N (57 μ L, 0.42 mmol) was added to a mixture of telluride **224** (70 mg, 0.21 mmol) and Pd(OAc)₂ (46 mg, 0.21 mmol) in MeCN (10 mL). The resultant mixture was stirred at 65 °C for 6 h. Upon completion, the reaction system was cooled to rt and filtered through a layer of Celite pad. The solid was washed with Et₂O (2 \times 5 mL). The filtrate was concentrated under reduced pressure and the residue was purified by flash column chromatography eluting with petroleum ether to afford **141** (37 mg, 68% yield) as a white solid.

6.4 Preparative Procedures for Chapter 4

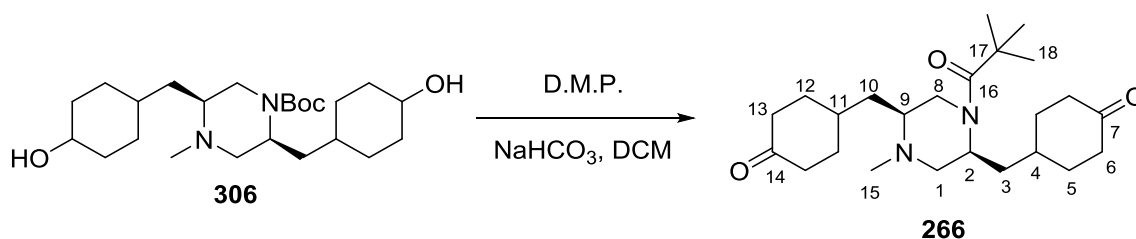
Catalytic hydrogenation of bis-phenol **105** to bis-alcohol **306**



A mixture of compound **105** (0.21 g, 0.51 mmol) and 5% Rh/C (0.10 g) in ethyl acetate (15 mL) was stirred at rt under 12 atm H₂ for 5 days. The catalyst was filtered off through a layer

of Celite pad and the filtrate was concentrated under reduced pressure. The crude product was purified by column chromatography using MeOH/EtOAc (1:6) as the eluent to afford the desired compound **306** (colourless oil, 70 mg, 32% yield) as a mixture of diastereoisomers. $R_f = 0.45$ (MeOH:EA = 1:2); FTIR (film) ν_{\max} 3662, 2988, 2905, 1691, 1407, 1243, 1168, 1056, 879, 730; $^1\text{H NMR}$ (300 MHz, CDCl_3) δ 4.15-3.79 (m, CHNBoc and $\text{CH}_a\text{H}_b\text{NBoc}$, 2H), 3.66-3.35 (m, CHOH , 2H), 2.73-2.48 (m, $\text{CH}_a\text{H}_b\text{NBoc}$ and $\text{CH}_a\text{H}_b\text{NMe}$, 2H), 2.42-2.22 (m, $\text{CH}_a\text{H}_b\text{NMe}$ and CHNMe , 2H), 2.20 (s, NCH_3 , 3H), 2.01-1.61 (m, CH_2 , 9H), 1.62-1.47 (m, CH_2 , 3H), 1.44 (s, $\text{COOC}(\text{CH}_3)_3$, 9H), 1.33-0.80 (m, CH and CH_2 , 10H); $^{13}\text{C NMR}$ (CDCl_3 , 100 MHz) δ 154.5 (COO^tBu), 79.7 ($\text{COOC}(\text{CH}_3)_3$), 70.8 (CHOH), 66.9 (CHOH), 61.3 (NCH), 59.8 (NCH_2), 49.1 (NCH), 48.9 (CH_2), 43.1 (NCH_3), 42.9 (CH_2), 38.1 (CH_2), 35.5 (CH_2), 35.4 (CH_2), 35.3 (CH_2), 33.7 (CH_2), 32.3 (CH), 32.1 (CH), 28.5 ($\text{COOC}(\text{CH}_3)_3$); HRMS (ESI) calculated for $\text{C}_{24}\text{H}_{44}\text{N}_2\text{NaO}_4$ $[\text{M}+\text{Na}]^+$ 447.3199, found 447.3204.

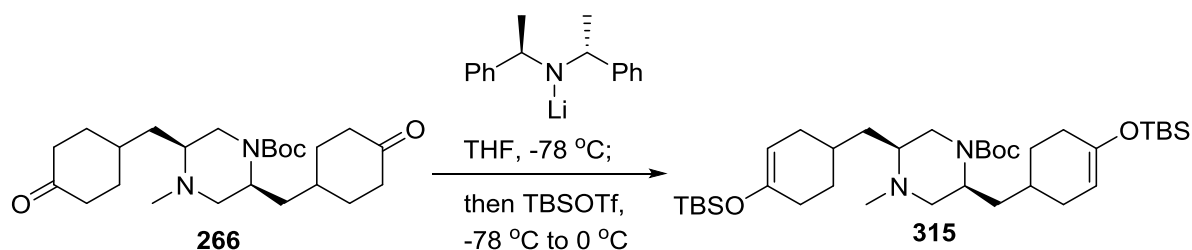
Oxidation of piperazine **306** to bis-ketone **266**



To a solution of diol **306** (45 mg, 0.11 mmol) in DCM (10 mL) was slowly added Dess-Martin periodinane (110 mg, 0.27 mmol) at 0 °C, followed by NaHCO_3 (45 mg, 0.27 mmol). The mixture was allowed to warm to rt and stirred for 6 h. To the reaction system was added DCM (10 mL) and the mixture was filtered through a layer of Celite pad. The Celite pad was washed with DCM (2×10 mL). The filtrate was concentrated and the crude product was purified by column chromatography eluting with ethyl acetate/methanol (15:1) to afford

diketone **266** (35 mg, 79% yield) as a colourless oil. $R_f = 0.45$ (MeOH:EA = 1:2); $[\alpha]_D^{20} = -28$ ($c = 0.2$, CHCl_3); FTIR (film) ν_{max} 2972, 2927, 2868, 1690, 1417, 1248, 1162, 764; $^1\text{H NMR}$ (CDCl_3 , 300 MHz) δ 4.14-3.97 (m, H-2 and H-8a, 2H), 2.68-2.53 (m, H-1 and H-8b, 3H), 2.40-2.20 (m, H-6 and H-9 and H-13, 9H), 2.19 (s, H-15, 3H), 2.01-1.69 (m, H-5 and H-12 8H), 1.67-1.51 (m, H-3 and H-4 and H-10 and H-11, 6H), 1.43 (s, H-18, 9H); $^{13}\text{C NMR}$ (CDCl_3 , 100 MHz) δ 211.7 (C-7 or C-14), 211.2 (C-14 or C-7), 154.5 (C-16), 80.0 (C-17), 61.2 (C-9), 59.8 (C-1), 49.2 (C-2), 43.1 (C-15), 42.9 (C-8), 40.8 (C-6 or C-13), 40.5 (C-13 or C-6), 35.6 (C-3 or C-10), 34.2 (C-10 or C-3), 33.1 (C-5 or C-12), 32.7 (C-4 and C-11), 32.4 (C-12 or C-5), 28.5 (C-18); HRMS (ESI) calculated for $\text{C}_{24}\text{H}_{40}\text{N}_2\text{NaO}_4$ $[\text{M}+\text{Na}]^+$ 443.2886, found 443.2888.

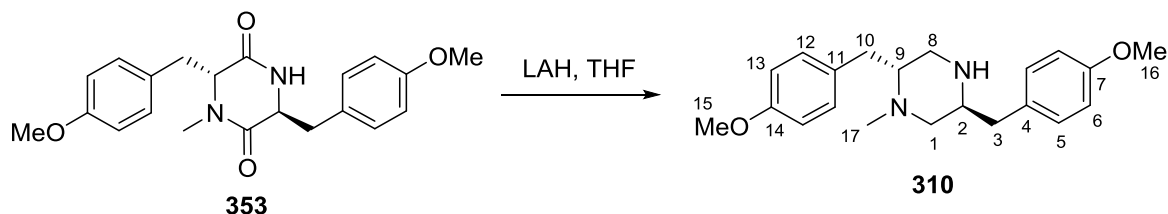
General procedure for the preparation of bis-silyl enol ether **315**



To a suspension of (*-*)-bis[(*R*)-1-phenylethyl]amine hydrochloride (0.19 g, 0.73 mmol) in anhydrous THF (4.0 mL) at $-78\text{ }^\circ\text{C}$ was added *n*-butyllithium (1.18 mL, 1.54 mmol, 1.3 M solution in hexanes) over a period of 10 min. The mixture was stirred at $-78\text{ }^\circ\text{C}$ for 20 min and then $0\text{ }^\circ\text{C}$ for 30 min before being cooled to $-78\text{ }^\circ\text{C}$. To the lithium amide base solution was added slowly a solution of bis-ketone **266** (77 mg, 0.18 mmol) in THF (3 mL). The resulting mixture was stirred for 1 h at $-78\text{ }^\circ\text{C}$ and TBSOTf (0.34 mL, 1.46 mmol) was added to the reaction system. After being stirred for 30 min at $-78\text{ }^\circ\text{C}$, the mixture was warmed to $0\text{ }^\circ\text{C}$ and stirred for another 3 h. Saturated NaHCO_3 aqueous solution (10 mL) was added to the

reaction solution slowly and the mixture was extracted with DCM (3×15 mL). The combined organic fractions were washed with brine (15 mL), dried over MgSO₄ and concentrated under reduced pressure. The residue was purified by flash column chromatography eluting with 25% EtOAc in petroleum ether to afford **315** (colourless oil, 55 mg, 45% yield) as a mixture of diastereoisomers. $R_f = 0.60$ (EA:hexane = 1:3); ¹H NMR (CDCl₃, 300 MHz) δ 4.83 (br s, C=CH, 2H), 4.33-3.83 (m, CHNBoc and CH_aH_bNBoc, 2H), 2.73-2.57 (m, 2H), 2.35-2.18 (m, 2H), 2.23 (s, NCH₃, 3H), 2.16-1.96 (m, 4H), 1.92-1.80 (m, 2H), 1.78-1.57 (m, 8H), 1.47 (br s, COOC(CH₃)₃, 9H), 1.34-1.12 (m, 4H), 0.94 (2s, (CH₃)₂SiC(CH₃)₃, 18H), 0.14 (2s, (CH₃)₂SiC(CH₃)₃, 12H); HRMS (ESI) calculated for C₃₆H₆₉N₂O₄Si₂ [M+H]⁺ 649.4796, found 649.4798.

Reduction of DKP **353** to piperazine **310**



Piperazine derivative **310** was prepared from the reduction of **353** (0.57 g, 1.55 mmol) following a similar procedure to that for the synthesis of **97** and was obtained as a white solid (0.35 g, 1.02 mmol, 66% yield). M.p. 164-166 °C; $R_f = 0.35$ (EtOAc/MeOH 3:1); $[\alpha]_D^{20} = -25.6$ ($c = 0.25$, CHCl₃); ¹H NMR (CDCl₃, 400 MHz) δ 7.09 (d, $J = 8.6$ Hz, H-5 or H-12, 2H), 7.05 (d, $J = 8.6$ Hz, H-12 or H-5, 2H), 6.83 (d, $J = 8.6$ Hz, H-6 or H-13, 2H), 6.79 (d, $J = 8.6$ Hz, H-13 or H-6, 2H), 3.78 (s, H-15 or H-16, 3H), 3.77 (s, H-16 or H-15, 3H), 3.11 (dd, $J = 13.5, 4.1$ Hz, H-3a, 1H), 3.01-2.91 (m, H-9, 1H), 2.85 (dd, $J = 11.2, 2.5$ Hz, H-8a, 1H), 2.72 (dd, $J = 11.8, 2.8$ Hz, H-1a, 1H), 2.64 (dd, $J = 13.6, 5.1$ Hz, H-10a, 1H), 2.47 (dd, $J = 13.6,$

8.7 Hz, H-10b, 1H), 2.41 (s, H-17, 3H), 2.36 (dd, $J = 11.8, 1.7$ Hz, H-1b, 1H), 2.31 (dd, $J = 13.5, 9.5$ Hz, H-3b, 1H), 2.23-2.13 (m, H-2, 1H), 2.00 (t, $J = 10.8$ Hz, H-8b, 1H), 1.81 (s, NH, 1H); ^{13}C NMR (CDCl_3 , 100 MHz) δ 157.2 (C-7 or C-14), 157.0 (C-14 or C-7), 129.8 (C-4 or C-11), 129.2 (C-11 or C-4), 129.1 (C-5 and C-12), 112.9 (C-6 or C-13), 112.7 (C-13 or C-6), 63.7 (C-2), 61.8 (C-8), 55.6 (C-9), 54.2 (C-15 and C-16), 50.0 (C-1), 42.2 (C-17), 38.9 (C-10), 36.0 (C-3); HRMS (ESI) calculated for $\text{C}_{21}\text{H}_{29}\text{N}_2\text{O}_2$ $[\text{M}+\text{H}]^+$ 341.2229, found 341.2237.

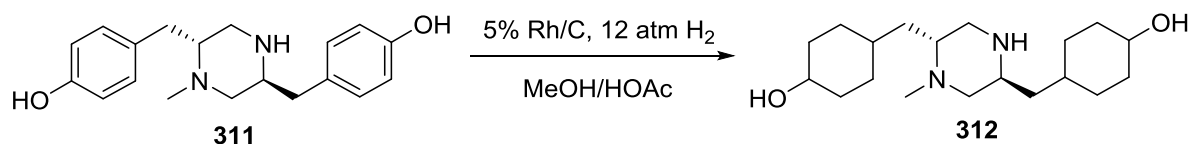
Demethylation of **310** to bis-phenol **311**



To a solution of **310** (0.13 g, 0.38 mmol) in DCM (5 mL) was slowly added BBr_3 (1.0 M in DCM, 3.82 mL, 3.82 mmol) over 10 min at 0 °C. The system was allowed to warm to rt and the mixture was stirred for 20 h. Upon completion, MeOH (10 mL) was slowly added to quench the reaction, followed by water (10 mL). The product started to precipitate from the solution. The solid was collected by filtration, washed with water (3×3 mL) and thoroughly dried under high vacuum to afford piperazine **311** (0.10 g, 85%) as an off-white solid. M.p (dec) 250-260 °C; $R_f = 0.30$ (EtOAc/MeOH 2:1); $[\alpha]_D^{20} = -33$ ($c = 0.20$, MeOH); FTIR (film) ν_{max} 3525, 3230, 2807, 2586, 1612, 1514, 1468, 1247, 819; ^1H NMR (acetic acid- d_4 , 300 MHz) δ 7.09 (d, $J = 8.4$ Hz, H-5 or H-12, 2H), 7.07 (d, $J = 8.4$ Hz, H-12 or H-5, 2H), 6.83 (d, $J = 8.4$ Hz, H-6 or H-13, 2H), 6.80 (d, $J = 8.4$ Hz, H-13 or H-6, 2H), 4.18-4.00 (br m, H-2 and H-9, 2H), 3.83-3.66 (m, H-8, 2H), 3.60-3.50 (m, H-1a, 1H), 3.44 (dd, $J = 13.6, 4.1$ Hz, H-3a, 1H), 3.34 (dd, $J = 13.9, 2.5$ Hz, H-1b, 1H), 3.08 (s, H-15, 3H), 2.98 (d, $J = 6.9$ Hz, H-10, 2H), 2.83 (dd, $J = 13.6, 10.6$ Hz, H-3b, 1H); ^{13}C NMR (acetic acid- d_4 , 100 MHz) δ 156.1 (C-7 or

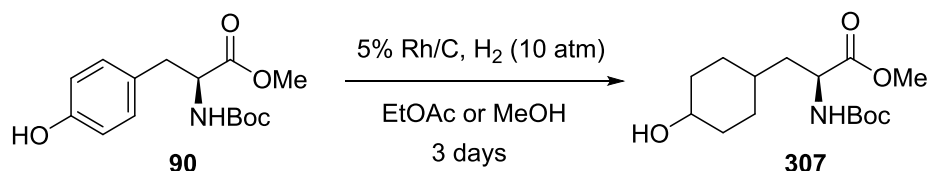
C-14), 155.9 (C-14 or C-7), 130.5 (C-5 or C-12), 130.1 (C-12 or C-5), 125.3 (C-4 or C-11), 124.5 (C-11 or C-4), 115.8 (C-6 or C-13), 115.7 (C-13 or C-6), 60.9 (C-2), 54.9 (C-8), 53.9 (C-9), 44.3 (C-1), 39.9 (C-15), 35.0 (C-10), 32.7 (C-3); HRMS (ESI) calculated for $C_{19}H_{25}N_2O_2$ $[M+H]^+$ 313.1916, found 313.1918.

Catalytic hydrogenation of **311**



The hydrogenation of piperazine **311** (0.22 g, 0.71 mmol) was performed in HOAc/MeOH (1:4, v/v) following a similar procedure to that for the synthesis of **306**. After 5 days, TLC indicated a low conversion of bis-phenol. From the mixture recovered most of the starting material and 46 mg (0.14 mmol, 20% yield) of the desired bis-alcohol **312** as a mixture of diastereoisomers as a colourless oil. $R_f = 0.35$ (EtOAc/MeOH 2:1); 1H NMR ($CDCl_3$, 300 MHz) δ 3.21-2.97 (br m, $CHOH$, 2H), 2.49-1.90 (m, NCH and NCH_2 , 6H), 2.07 (s, NCH_3 , 3H), 1.80-1.00 (m, CH and CH_2 , 22H); HRMS (ESI) calculated for $C_{19}H_{36}N_2NaO_2$ $[M+Na]^+$ 347.2674, found 347.2676.

Catalytic hydrogenation of tyrosine derivative **90** to alcohol **307**

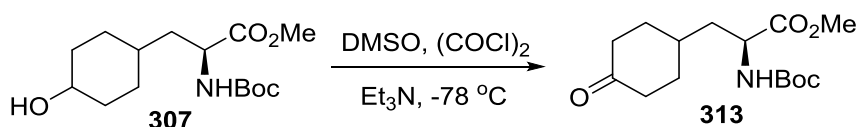


The hydrogenation reaction of **90** was performed following a similar procedure to that for the synthesis of **306** and alcohol **307** was obtained as a mixture of diastereoisomers as a

colourless oil (gram scale, 76-84% yield). $R_f = 0.30$ (EtOAc/petroleum ether 1:1); $^1\text{H NMR}$ (CDCl_3 , 300 MHz) δ 4.98 (d, $J = 8.6$ Hz, NH, 1H), 4.37-4.30 (m, CHNH, 1H), 3.97-3.95 (m, CHOH, 1H), 3.72 (s, OCH_3 , 3H), 1.79-1.37 (m, CH and CH_2 , 11H), 1.43 (s, $\text{COOC}(\text{CH}_3)_3$, 9H); ESI-MS calculated for $\text{C}_{15}\text{H}_{27}\text{NO}_5\text{Na}$ $[\text{M}+\text{Na}]^+$ 324.1, found 324.1.

The observed data are in accord with published values.¹⁸⁶

Swern oxidation of alcohol **307** to ketone **313**

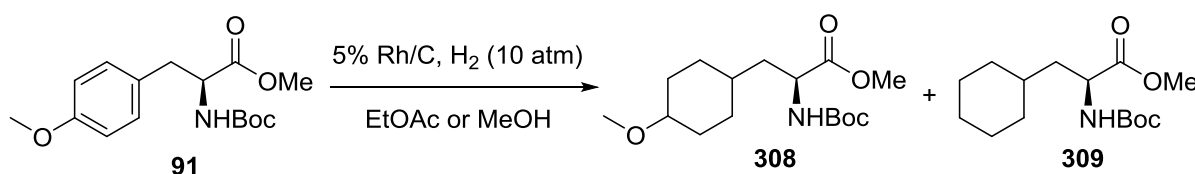


To a stirred solution of oxalyl chloride (0.14 mL, 1.59 mmol) in DCM (10 mL) was added anhydrous DMSO (0.23 mL, 3.18 mmol) dropwise at -78 °C over a period of 15 min. After stirring the reaction mixture for an additional 15 min, a solution of alcohol **307** (0.32 g, 1.06 mmol) in DCM (3 mL) was added and the resultant mixture was stirred at -78 °C for 40 min. Et_3N (0.45 mL, 3.12 mmol) was added and the reaction system was allowed to warm to rt over a period of 30 min. After being stirred for 40 min at rt, the reaction mixture was quenched with saturated NaHCO_3 (aq) (15 mL) and the mixture was extracted with DCM (3×15 mL). The combined organic phases were washed with brine (10 mL), dried over MgSO_4 and concentrated under reduced pressure. The crude product was purified by flash column chromatography eluting with 30% EtOAc in petroleum ether to afford ketone **313** (0.28 g, 88% yield) as a colourless oil. $R_f = 0.35$ (EtOAc/petroleum ether 1:1); $[\alpha]_D^{20} = +4$ ($c = 1.5$, CHCl_3); FTIR (film) ν_{max} 3356, 2957, 2933, 1705, 1515, 1163; $^1\text{H NMR}$ (CDCl_3 , 300 MHz) δ 5.09 (d, $J = 8.6$ Hz, NH, 1H), 4.36 (td, $J = 9.0, 5.0$ Hz, CHNH, 1H), 3.72 (s, OCH_3 , 3H), 2.43-2.26 (m, $\text{CO}(\text{CH}_2)_2$, 4H), 2.24-2.10 (m, 1H), 2.06-1.94 (m, 1H), 1.91-1.66 (m, 2H), 1.64-1.55 (m, 1H), 1.48-1.33 (m, 2H), 1.42 (s, $\text{COOC}(\text{CH}_3)_3$, 9H); $^{13}\text{C NMR}$ (CDCl_3 , 100

MHz) δ 211.5 (CO(CH₂)₂), 173.4 (COOMe), 155.5 (COO'Bu), 80.0 (COOC(CH₃)₃), 52.3 (COOCH₃), 51.6 (CHNH), 40.6 (CO(CH₂)₂), 38.8 (CH₂), 32.9 (CH₂), 32.6 (CH), 28.3 (COOC(CH₃)₃); HRMS (ESI) calculated for C₁₅H₂₅NO₅Na [M+Na]⁺ 322.1630, found 322.1629.

The observed data are in accord with published values.¹⁸⁶

Catalytic hydrogenation of tyrosine derivative **91**



The hydrogenation of **91** (1.68 g, 5.44 mmol) was performed following a similar procedure to that for the synthesis of **306** and the desired product **308** was obtained as mixture of diastereoisomers (colourless oil, 1.34 g, 4.24 mmol, 78% yield), accompanied by **309** (0.26 g, 0.92 mmol, 17%).

Data for 308: R_f = 0.45 (EtOAc/petroleum ether 1:1); ¹H NMR (CDCl₃, 300 MHz) δ 4.96 (d, J = 8.4 Hz, NH, 1H), 4.34-4.26 (m, CHNH, 1H), 3.69 (s, COOCH₃, 3H), 3.37 (br s, CHOCH₃, 1H), 3.26 (s, CHOCH₃, 3H), 1.91-1.75 (m, 2H), 1.68-1.62 (m, 1H), 1.56-1.27 (m, 8H), 1.41 (s, COOC(CH₃)₃, 9H); ESI-MS calculated for C₁₆H₃₀NO₅ [M+H]⁺ 316.2, found 316.2.

Data for 309: R_f = 0.65 (EtOAc/petroleum ether 1:1); ¹H NMR (CDCl₃, 300 MHz) δ 4.89 (d, J = 8.4 Hz, NH, 1H), 4.35 (td, J = 8.9, 5.2 Hz, CHNH, 1H), 3.74 (s, OCH₃, 3H), 1.83 (d, J = 12.6 Hz, CH₂CHNH, 1H), 1.74-1.60 (m, 6H), 1.46 (s, COOC(CH₃)₃, 9H), 1.27-1.16 (m, 4H), 0.98-0.88 (m, 2H); ESI-MS calculated for C₁₅H₂₈NO₄ [M+H]⁺ 286.2, found 286.2.

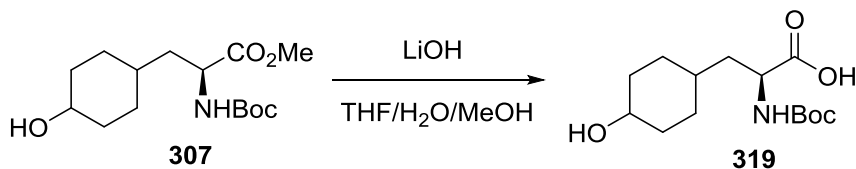
The observed data are in accord with published values.¹⁸⁷

Preparation of amine 318



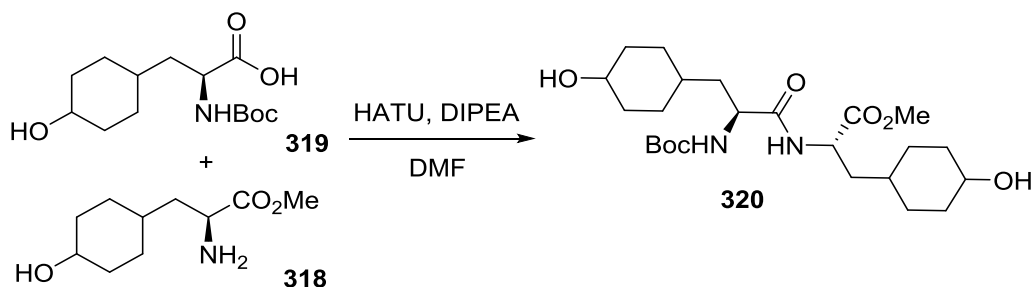
Amine **318** was prepared from **307** (0.41 g, 1.36 mmol) following a similar procedure to that for the synthesis of **94** and was obtained as a mixture of diastereoisomers (colourless oil, 0.22 g, 1.10 mmol, 81% yield). $R_f = 0.65$ (EtOAc/MeOH 8:1); $^1\text{H NMR}$ (CDCl_3 , 400 MHz) δ 6.94 (d, $J = 7.6$ Hz, NH_2 , 2H), 4.79-4.62 (m, CHNH_2 , 1H), 4.04-3.95 (m, CHOH , 1H), 3.80 (s, OCH_3 , 3H), 2.48 (br s, OH , 1H), 1.99 (dd, $J = 11.0, 2.2$ Hz, $\text{CH}_a\text{H}_b\text{CHNH}_2$, 1H), 1.93-0.94 (m, 10H); ESI-MS calculated for $\text{C}_{10}\text{H}_{19}\text{NO}_3\text{Na}$ $[\text{M}+\text{Na}]^+$ 224.1, found 224.1.

Preparation of acid 319



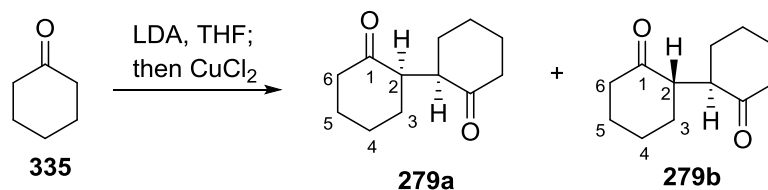
Acid **319** was prepared from **307** (0.56 g, 1.86 mmol) following a similar procedure to that for the synthesis of **92** and was obtained as a mixture of diastereoisomers (colourless oil, 0.47 g, 1.64 mmol, 88% yield). $R_f = 0.50$ (EtOAc/MeOH 10:1); $^1\text{H NMR}$ (CDCl_3 , 400 MHz) δ 6.63 (br s, COOH , 1H), 5.09 (d, $J = 8.3$ Hz, NH , 1H), 4.38-4.29 (m, CHNH , 1H), 4.00 (s, OH , 1H), 1.99 (d, $J = 10.6$ Hz, $\text{CH}_a\text{H}_b\text{CHNH}$, 1H), 1.92-0.91 (m, 10H), 1.45 (s, $\text{COOC}(\text{CH}_3)_3$, 9H); ESI-MS calculated for $\text{C}_{14}\text{H}_{25}\text{NO}_5\text{Na}$ $[\text{M}+\text{Na}]^+$ 310.1, found 310.1.

Preparation of dipeptide **320**



Dipeptide **320** was synthesised from acid **319** (0.24 g, 0.84 mmol) and amine **318** (0.17 g, 0.84 mmol) following a similar procedure to that for the synthesis of **95** and was obtained as a mixture of diastereoisomers (colourless oil, 0.31 g, 0.65 mmol, 78% yield). $R_f = 0.30$ (EtOAc); $^1\text{H NMR}$ (CDCl_3 , 300 MHz) δ 7.02 (d, $J = 7.8$ Hz, NH, 1H), 4.96 (d, $J = 8.5$ Hz, NH, 1H), 4.77-4.61 (m, CHNH, 1H), 4.42-4.27 (m, CHNH, 1H), 3.99-3.97 (m, CHOH, 2H), 3.74 (s, COOCH_3 , 3H), 2.03-0.92 (m, 22H), 1.44 (s, $\text{COOC}(\text{CH}_3)_3$, 9H); ESI-MS calculated for $\text{C}_{24}\text{H}_{42}\text{N}_2\text{O}_7\text{Na}$ $[\text{M}+\text{Na}]^+$ 493.3, found 493.3.

General procedure for oxidative coupling of enolate (Model reaction with cyclohexanone)



To a solution of diisopropylamine (0.20 mL, 1.43 mmol) at -78 °C was added *n*-butyllithium (1.02 mL, 1.43 mmol, 1.4 M solution in toluene) over a period of 10 min and the mixture was stirred at the same temperature for 30 min. The reaction solution was warmed to 0 °C and stirred for further 30 min before being cooled to -78 °C. To the reaction system was added a solution of cyclohexanone (0.12 mL, 1.19 mmol) in THF (2 mL) and the resulting mixture was stirred for 30 min at -78 °C and then 30 min at 0 °C. The enolate solution was then

transferred to a pre-cooled flask containing CuCl_2 (0.17 g, 1.26 mmol) at $-78\text{ }^\circ\text{C}$ and the reaction system was stirred for 30 min before being warmed up to rt. After 4 h, H_2O (10 mL) was added to quench the reaction and the mixture was extracted with Et_2O (3×15 mL). The combined organic fractions were washed with brine (15 mL), dried over MgSO_4 and concentrated under reduced pressure. The residue was purified by flash column chromatography eluting with 2% EtOAc in petroleum ether to afford **279a** (71 mg, 65% yield) and **279b** (5 mg, 5%) as colourless oils.

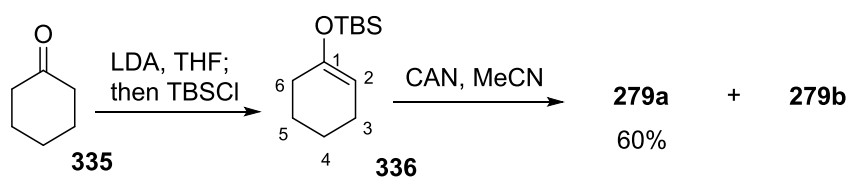
Data for 279a: M.p. $70\text{--}71\text{ }^\circ\text{C}$; $R_f = 0.30$ (EA:hexane = 1:8); FTIR (film) ν_{max} 2957, 2869, 1707, 1468, 1366, 1228; $^1\text{H NMR}$ (CDCl_3 , 300 MHz) δ 2.92 (m, H-2, 2H), 2.46–2.38 (m, H-6, 4H), 2.17–2.01 (m, H-5, 4H), 1.97–1.85 (m, H-3a, 2H), 1.78–1.58 (m, H-4, 4H), 1.43–1.22 (m, H-3b, 2H); $^{13}\text{C NMR}$ (CDCl_3 , 100 MHz) δ 211.8 (C-1), 49.0 (C-2), 42.3 (C-6), 30.1 (C-3), 28.1 (C-5), 25.4 (C-4); HRMS (EI) calculated for $\text{C}_{12}\text{H}_{18}\text{O}_2$ $[\text{M}]^+$ 194.1307, found 194.1305.

The observed data are in accord with published values.^{160,161}

Data for 279b: $R_f = 0.31$ (EA:hexane = 1:8); FTIR (film) ν_{max} 2946, 2868, 1707, 1461, 1357, 1218; $^1\text{H NMR}$ (CDCl_3 , 300 MHz) δ 2.69–2.60 (m, H-2, 2H), 2.44–2.27 (m, H-6, 4H), 2.08–1.85 (m, H-3a and H-5, 6H), 1.77–1.62 (m, H-3b and H-4, 6H); $^{13}\text{C NMR}$ (CDCl_3 , 100 MHz) δ 210.7 (C-1), 50.3 (C-2), 41.8 (C-6), 29.1 (C-3), 26.5 (C-5), 25.0 (C-4); HRMS (EI) calculated for $\text{C}_{12}\text{H}_{18}\text{O}_2$ $[\text{M}]^+$ 194.1307, found 194.1310.

The observed data are in accord with published values.¹⁶¹

Model reaction of oxidative coupling of silyl enol ether 336



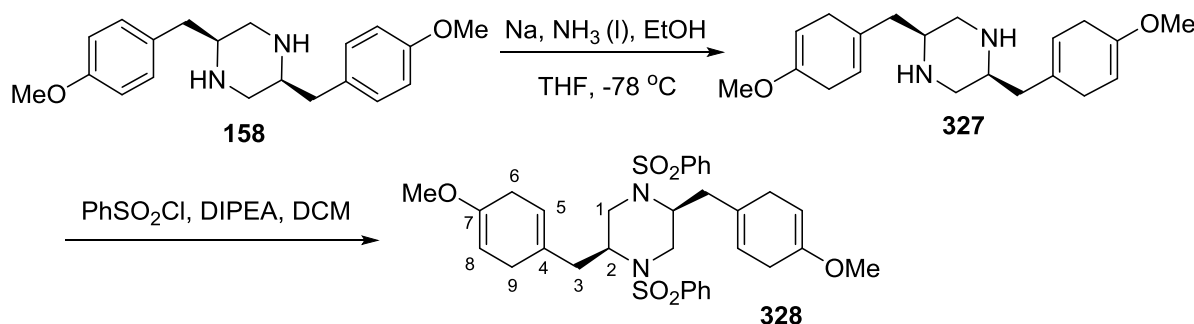
Preparation of 336: At -78 °C, to a solution of LDA in THF prepared from diisopropylamine (0.41 mL, 2.93 mmol) and *n*-butyllithium (1.94 mL, 2.70 mmol, 1.4 M solution in toluene) was added a solution of cyclohexanone (0.23 mL, 2.27 mmol) in THF (2 mL) and the mixture was stirred for 30 min before being warmed up to 0 °C. The reaction mixture was stirred for another 30 min at 0 °C and TBSCl (0.78 mL, 4.55 mol, 50 wt.% in toluene) was added over a period of 5 min. The resulting solution was stirred for 10 min at 0 °C and 2 h at rt before the addition of triethylamine (1.0 mL) followed by saturated NaHCO₃ (aq) (15 mL). The mixture was extracted with Et₂O (3×15 mL) and the combined organic fractions were washed with brine (15 mL), dried over MgSO₄ and concentrated under reduced pressure. The residue was purified by flash column chromatography eluting with petroleum ether to afford **336** (0.39 g, 83% yield) as a colourless oil. *R*_f = 0.65 (Hexane:EtOAc = 20:1); FTIR (film) ν_{\max} 2929, 2858, 1670, 1194, 1182, 891, 837, 776; ¹H NMR (CDCl₃, 400 MHz) δ 4.74 (ddd, *J* = 3.8, 2.6, 1.3 Hz, H-2, 1H), 1.92-1.84 (m, H-3 and H-6, 4H), 1.57-1.49 (m, H-5, 2H), 1.41-1.35 (m, H-4, 2H), 0.79 (s, SiC(CH₃)₃, 9H), 0.00 (s, SiCH₃, 6H); ¹³C NMR (CDCl₃, 100 MHz) δ 150.5 (C-1), 104.4 (C-2), 29.9 (C-6 and SiC(CH₃)₃), 25.7 (SiC(CH₃)₃), 23.8 (C-3), 23.2 (C-5), 22.4 (C-4), -4.4 (SiCH₃).

The observed data are in accord with published values.¹⁸⁸

Oxidative coupling of 336: A solution of silyl enol ether (96 mg, 0.45 mmol) in MeCN (2.0 mL) was slowly added to a mixture of CAN (0.27 g, 0.54 mmol) and NaHCO₃ (76 mg, 0.90 mmol) in MeCN (4.0 mL). The resulting mixture was stirred for 1 h at rt. Upon complete consumption of the starting material, H₂O (15 mL) was added and the mixture was extracted with Et₂O (3×15 mL). The combined organic fractions were washed with brine (15 mL), dried over MgSO₄ and concentrated under reduced pressure. The residue was purified by flash

column chromatography eluting with 2% EtOAc in petroleum ether to afford **279a** (53 mg, 60% yield) and a trace amount of **279b**.

Preparation of piperazine **328**

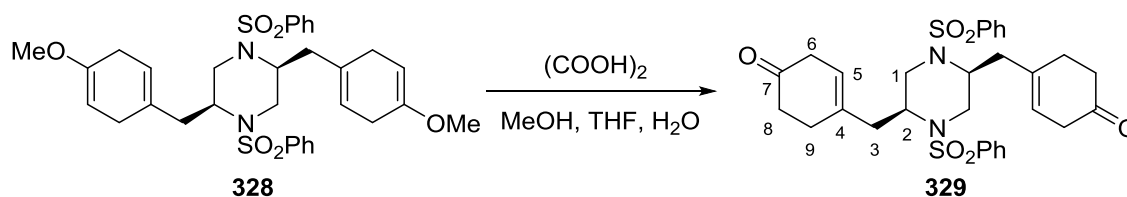


Birch reduction of piperazine 158: Liquid ammonia (30 mL) was collected by condensing ammonia into a three-neck flask at -78 °C. Sodium (0.10 g, 4.34 mmol) was added and the mixture was stirred for 20 min to give a deep-blue solution. A solution of piperazine **158** (0.25 g, 0.77 mmol) and EtOH (0.5 mL) in THF (8 mL) was added to the liquid ammonia solution over a period of 1 h. More sodium was added when necessary to maintain a blue colour of the system. The reaction mixture was stirred at -78 °C for 5 h before being quenched with EtOH (5 mL). The ammonia was allowed to evaporate overnight and the residue was partitioned between water (20 mL) and DCM (20 mL). The organic phase was separated and the aqueous phase was extracted with DCM (3×15 mL). The combined organic fractions were washed with brine (20 mL), dried over MgSO₄, filtered and concentrated under reduced pressure. The crude product **327** was used directly in the next step to avoid rearomatisation during the purification process.

Preparation of piperazine 328: The crude piperazine substrate **327** from the Birch reduction was dissolved in DCM (10 mL). To the solution was added PhSO₂Cl (0.25 mL, 1.96 mmol) at

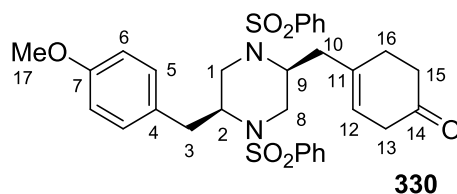
0 °C, followed by DIPEA (0.34 mL, 1.96 mmol). The reaction solution was allowed to warm to rt and stirred for 6 h. Upon completion, the mixture was diluted with DCM (20 mL) and the mixture was washed with NaHCO₃(aq) (15 mL) and brine (15 mL) successively. The organic phase was separated, dried over MgSO₄, filtered and concentrated under reduced pressure. The crude product was purified by flash column chromatography eluting with 20% EtOAc in hexane to afford bis-enol ether **328** as a colourless oil (0.19 g, 43% yield). $R_f = 0.60$ (EA:hexane = 1:4); $[\alpha]_D^{20} = +24$ ($c = 0.5$, CHCl₃); FTIR (film) ν_{\max} 2932, 1513, 1343, 1164, 730; ¹H NMR (CDCl₃, 300 MHz) δ 7.80-7.73 (m, ArH, 4H), 7.65-7.48 (m, ArH, 6H), 5.34 (br s, H-5, 2H), 4.63 (s, H-8, 2H), 3.74 (dt, $J = 10.0, 5.7$ Hz, H-2, 2H), 3.58 (s, OCH₃, 6H), 3.27-3.22 (m, H-1, 4H), 2.82-2.62 (m, H-6 and H-9, 8H), 2.52 (dd, $J = 13.6, 3.3$ Hz, H-3a, 2H), 2.35 (dd, $J = 13.6, 10.2$ Hz, H-3b, 2H); ¹³C NMR (CDCl₃, 300 MHz) δ 152.7 (C-7), 132.9 (C-4), 130.8 (Ar), 129.3 (Ar), 127.2 (Ar), 125.0 (Ar), 122.7 (C-5), 90.2 (C-8), 54.6 (OCH₃), 54.0 (C-2), 44.8 (C-1), 39.9 (C-3), 29.2 (C-6 and C-9); HRMS (ESI) calculated for C₃₂H₃₈N₂O₆NaS₂ [M+Na]⁺ 633.2069, found 633.2063.

Preparation of bis-ketone **329**



To a solution of piperazine **328** (66 mg, 0.11 mmol) in MeOH (10 mL) and THF (5 mL) was added a solution of oxalic acid (24 mg, 0.26 mmol) in water (1.0 mL). The resulting system was stirred at rt for 10 h. Upon completion, the mixture was partitioned between water (15 mL) and DCM (20 mL). The organic phase was separated and the aqueous phase was extracted with DCM (3×10 mL). The combined organic fractions were washed with brine (20

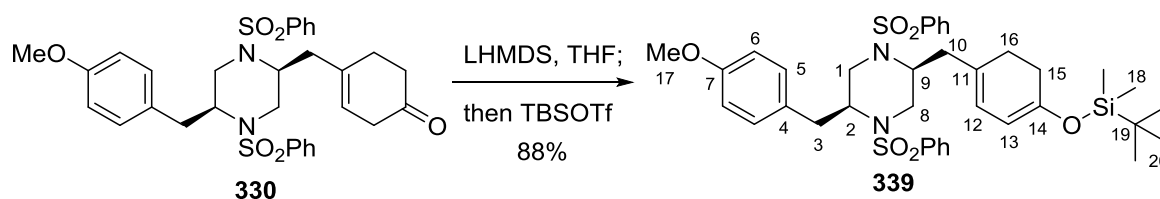
mL), dried over MgSO₄, filtered and concentrated under reduced pressure. The crude product was purified by flash column chromatography eluting with 40% EtOAc in hexane to afford bis-ketone **329** as a white foam (0.16 g, 35% yield). M.p. 75-77 °C; R_f = 0.25 (EA:hexane = 1:1); [α]_D²⁰ = +50.0 (*c* = 0.4, CHCl₃); FTIR (film) ν_{max} 2925, 2867, 1714, 1342, 1163, 735; ¹H NMR (CDCl₃, 300 MHz) δ 7.77-7.69 (m, ArH, 4H), 7.64-7.46 (m, ArH, 6H), 5.43 (br s, H-5, 2H), 3.68 (td, *J* = 9.9, 4.6 Hz, H-2, 2H), 3.26 (dd, *J* = 13.6, 9.9 Hz, H-1a, 2H), 3.15 (dd, *J* = 13.6, 4.6 Hz, H-1b, 2H), 2.81 (br s, H-6, 4H), 2.66-2.57 (dd, *J* = 13.6, 1.6 Hz, H-3a, 2H), 2.54-2.28 (m, H-3b and H-8 and H-9, 10H); ¹³C NMR (CDCl₃, 100 MHz) δ 209.6 (C-7), 138.6 (Ar), 134.0 (C-4), 133.2 (Ar), 129.4 (Ar), 127.2 (Ar), 122.8 (C-5), 53.4 (C-2), 44.6 (C-1), 40.4 (C-3), 39.6 (C-6), 38.5 (C-8), 28.3 (C-9); HRMS (ESI) calculated for C₃₀H₃₄N₂O₆NaS₂ [M+Na]⁺ 605.1756, found 605.1755.



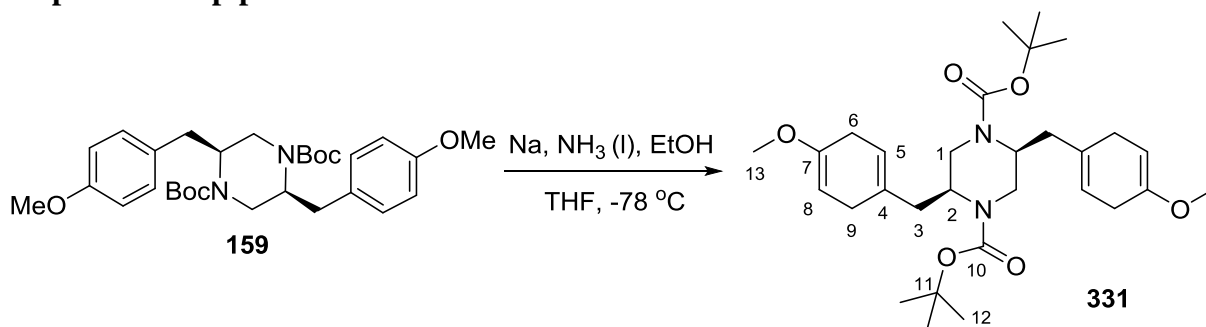
Piperazine **330** was also isolated from the reaction mixture as an off-white film (0.09 g, 19% yield), possibly arising from the rearomatisation of bis-dienes. R_f = 0.25 (EA:hexane = 1:1); [α]_D²⁰ = +31 (*c* = 0.6, CHCl₃); FTIR (film) ν_{max} 2932, 1715, 1513, 1346, 1249, 1166; ¹H NMR (CDCl₃, 400 MHz) δ 7.80-7.74 (m, PhH, 2H), 7.71-7.66 (m, PhH, 2H), 7.65-7.58 (m, PhH, 2H), 7.56-7.48 (m, PhH, 4H), 7.03 (d, *J* = 8.6 Hz, H-5, 2H), 6.84 (d, *J* = 8.6 Hz, H-6, 2H), 5.45 (br s, H-12, 1H), 3.82 (s, H-17, 1H), 3.77 (dd, *J* = 9.9, 5.0 Hz, H-9, 1H), 3.70 (dd, *J* = 10.1, 5.5 Hz, H-2, 1H), 3.28-3.02 (m, H-1 and H-3a and H-8, 5H), 2.89 (dd, *J* = 13.8, 10.3 Hz, H-3b, 1H), 2.85 (br s, H-13, 2H), 2.65 (dd, *J* = 13.5, 1.7 Hz, H-10a, 1H), 2.55-2.38 (m, H-10b and H-15 and H-16, 5H); ¹³C NMR (CDCl₃, 100 MHz) δ 209.8 (C-14), 158.6 (C-7), 138.7 (Ph), 138.6 (Ph), 134.1 (C-11), 133.2 (Ph), 133.0 (Ph), 130.4 (C-5), 129.4 (Ph), 128.6 (C-4),

127.3 (Ph), 127.2 (Ph), 122.7 (C-12), 114.1 (C-6), 56.7 (C-2), 55.3 (C-17), 53.5 (C-9), 44.5 (C-8), 43.8 (C-1), 40.6 (C-10), 39.6 (C-13), 38.5 (C-15), 38.1 (C-3), 28.4 (C-16); HRMS (ESI) calculated for $C_{31}H_{34}N_2O_6NaS_2$ $[M+Na]^+$ 617.1756, found 617.1766.

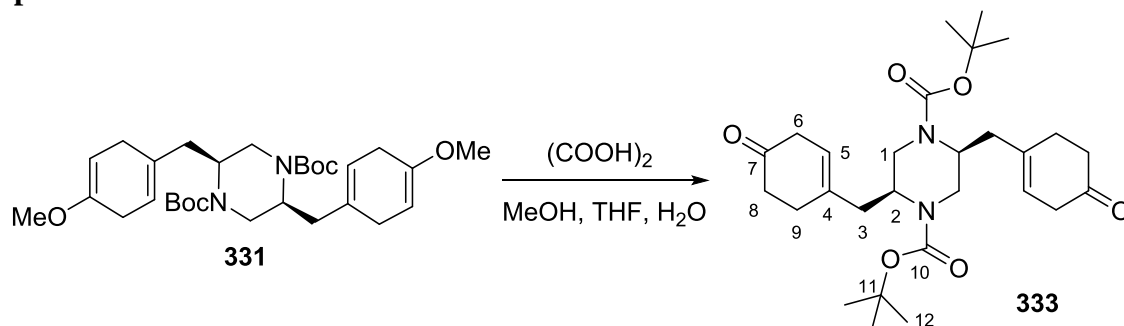
Preparation of dienol silane **339**



Silyl enol ether **339** was synthesised from **330** (83 mg, 0.14 mmol) following a similar procedure to that for the synthesis of **336** and was obtained as a colourless oil (87 mg, 0.12 mmol, 88% yield). $R_f = 0.65$ (EA:hexane = 1:4); $[\alpha]_D^{20} = +43$ ($c = 0.5$, MeOH); FTIR (film) ν_{max} 2957, 2929, 2857, 1513, 1349, 1249, 1166; 1H NMR (MeOD- d_4 , 300 MHz) δ 8.11-7.71 (m, PhH, 2H), 7.81-7.48 (m, PhH, 8H), 7.07 (d, $J = 8.7$ Hz, H-5, 2H), 6.87 (d, $J = 8.7$ Hz, H-6, 2H), 5.52 (d, $J = 5.9$ Hz, H-13, 1H), 5.06 (d, $J = 5.9$ Hz, H-12, 1H), 3.81 (s, H-17, 3H), 3.76-3.62 (m, H-2 and H-9, 2H), 3.29-3.01 (m, H-1 and H-3a and H-8, 5H), 2.84 (dd, $J = 13.4, 9.8$ Hz, H-3b, 1H), 2.54 (dd, $J = 13.4, 3.7$ Hz, H-10a, 1H), 2.34 (dd, $J = 13.4, 9.8$ Hz, H-10b, 1H), 2.26-2.14 (m, H-15 and H-16, 4H); ^{13}C NMR (MeOD- d_4 , 100 MHz) δ 158.7 (C-7), 152.6 (C-14), 139.1 (Ph), 132.8 (Ph), 130.2 (C-5 or Ph), 130.1 (Ph or C-5), 129.2 (Ph), 128.7 (C-4), 127.0 (Ph), 126.9 (Ph), 125.6 (C-11 or Ph), 122.6 (Ph or C-11), 119.9 (C-12), 113.7 (C-6), 102.0 (C-13), 56.4 (C-2), 54.3 (C-17), 53.6 (C-9), 44.1 (C-8), 43.6 (C-1), 39.6 (C-10), 37.7 (C-3), 28.8 (C-19), 27.1 (C-15), 24.8 (C-16), 24.7 (C-20), -5.7 (C-18); HRMS (ESI) calculated for $C_{37}H_{48}N_2O_6NaS_2Si$ $[M+Na]^+$ 731.2621, found 731.2612.

Preparation of piperazine **331**

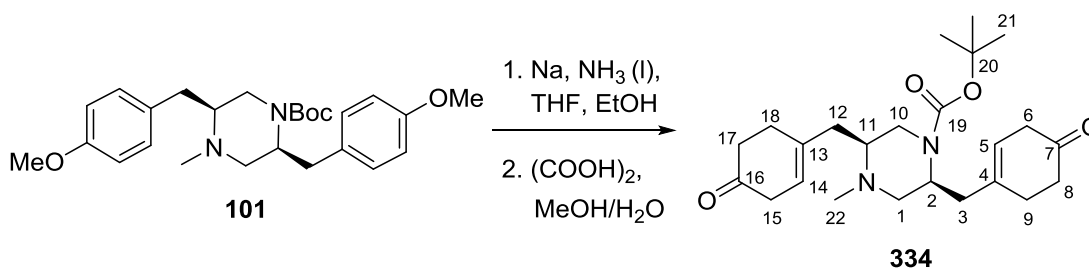
Piperazine **331** was obtained from the Birch reduction of **159** (0.33 g, 0.63 mmol) as a white solid (0.23 g, 0.43 mmol, 68% yield) and tended to rearomatise upon heating or standing in the air. M.p. 148-149 °C; $R_f = 0.60$ (EtOAc/petroleum ether 1:3); $[\alpha]_D^{20} = +6.8$ ($c = 1.0$, CHCl_3); FTIR (film) ν_{max} 2972, 2926, 2831, 1690, 1415, 1170, 1106; $^1\text{H NMR}$ (CDCl_3 , 400 MHz) δ 5.43 (br s, H-5, 2H), 4.61 (br s, H-8, 2H), 4.14-3.97 (br m, H-2 and H-1a, 4H), 3.56 (s, H-13, 6H), 2.91-2.58 (m, H-1b and H-6 and H-9, 10H), 2.33 (dd, $J = 13.2, 2.9$ Hz, H-3a, 2H), 2.02 (dd, $J = 13.2, 8.6$ Hz, H-3b, 2H), 1.46 (s, H-12, 18H); $^{13}\text{C NMR}$ (CDCl_3 , 100 MHz) δ 155.2 (C-10), 152.7 (C-7), 131.3 (C-4), 120.6 (C-5), 90.4 (C-8), 80.0 (C-11), 53.9 (C-13), 51.6 (C-2), 41.4 (C-1), 39.5 (C-3), 29.4 (C-9), 29.2 (C-6), 28.4 (C-12); HRMS (ESI) calculated for $\text{C}_{30}\text{H}_{46}\text{N}_2\text{O}_6\text{Na}$ $[\text{M}+\text{Na}]^+$ 553.3254, found 553.3258.

Preparation of bis-ketone **333**

Bis-ketone **333** was prepared from the hydrolysis of **331** (0.18 g, 0.34 mmol) with aqueous oxalic acid and was obtained as a colourless oil (88 mg, 0.18 mmol, 52% yield). $R_f = 0.65$

(EtOAc); $[\alpha]_{\text{D}}^{20} = +21.6$ ($c = 1.0$, CHCl_3); FTIR (film) ν_{max} 2973, 2925, 1689, 1417, 1366, 1168; ^1H NMR (CDCl_3 , 300 MHz) δ 5.53 (t, $J = 3.3$ Hz, H-5, 2H), 4.20-3.93 (br m, H-1a and H-2, 4H), 2.86 (br s, H-6, 4H), 2.70 (dd, $J = 14.0, 10.4$ Hz, H-1b, 2H), 2.56-2.45 (br m, H-8 and H-9, 8H), 2.42 (dd, $J = 14.0, 4.3$ Hz, H-3a, 2H), 2.12 (dd, $J = 13.2, 8.3$ Hz, H-3b, 2H), 1.47 (s, H-12, 18H); ^{13}C NMR (CDCl_3 , 100 MHz) δ 238.1 (C-7), 155.0 (C-10), 134.8 (C-4), 121.2 (C-5), 80.3 (C-11), 51.6 (C-2), 41.7 (C-1), 41.2 (C-6), 39.6 (C-3), 38.6 (C-8), 28.4 (C-12), 28.3 (C-9); HRMS (ESI) calculated for $\text{C}_{28}\text{H}_{42}\text{N}_2\text{O}_6\text{Na}$ $[\text{M}+\text{Na}]^+$ 525.2941, found 525.2944.

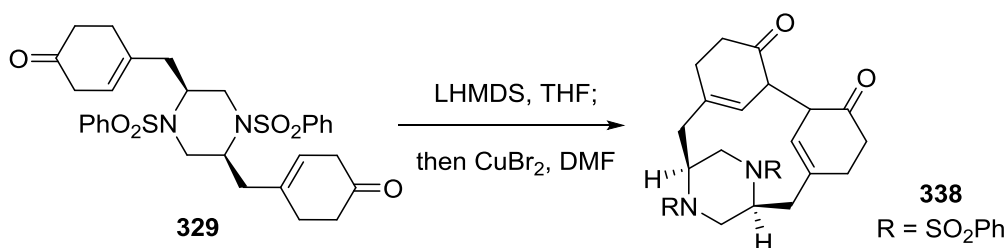
Preparation of bis-ketone **334**



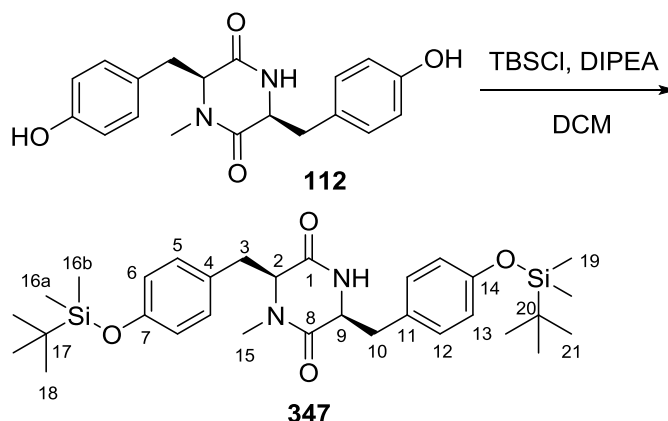
Bis-ketone **334** was prepared from the Birch reduction of **101** (0.48 g, 1.09 mmol) followed by hydrolysis of the crude bis-diene intermediate with aqueous oxalic acid and was obtained as a colourless oil (0.11 g, 0.27 mmol, 25% yield over two steps). $R_f = 0.45$ (MeOH:EtOAc = 1:3); $[\alpha]_{\text{D}}^{20} = -32$ ($c = 0.3$, CHCl_3); FTIR (film) ν_{max} 2976, 2925, 1687, 1417, 1166; ^1H NMR (CDCl_3 , 300 MHz) δ 5.59 (br s, H-5 and H-14, 2H), 4.42-4.23 (br m, H-2, 1H), 4.17-3.99 (br m, H-10a, 1H), 3.95-3.70 (br m, H-1a and H-10b, 2H), 3.02-2.78 (m, H-6 and H-15, 4H), 2.79-2.34 (m, H-1b and H-3a and H-8 and H-9 and H-11 and H-12a and H-17 and H-18, 12H), 2.28 (s, H-22, 3H), 2.09-1.95 (m, H-3b and H-12b, 2H), 1.45 (s, H-21, 9H); ^{13}C NMR (CDCl_3 , 100 MHz) δ 211.1 (C-7 or C-16), 210.0 (C-16 or C-7), 154.2 (C-19), 135.9 (C-4 or C-13), 135.4 (C-13 or C-4), 121.4 (C-5 or C-14), 120.2 (C-14 or C-5), 79.7 (C-20), 60.8 (C-11), 59.3

(C-1), 50.0 (C-2), 44.0 (C-10), 43.0 (C-22), 40.8 (C-6 or C-15), 40.6 (C-15 or C-6), 39.7 (C-3 or C-12), 39.6 (C-12 or C-3), 38.7 (C-8 or C-17), 38.6 (C-17 or C-8), 28.6 (C-9 and C-18), 28.4 (C-21); HRMS (ESI) calculated for $C_{28}H_{42}N_2O_6Na$ $[M+Na]^+$ 439.2573, found 439.2563.

Oxidative enolate coupling with bis-ketone **329**



To a solution of LHMDS (0.45 mL, 0.45 mmol, 1.0 M in THF) in anhydrous THF (15 mL) at -78 °C was added a solution of bis-ketone **329** (0.12 g, 0.21 mmol) in anhydrous THF (5 mL) over a period of 10 min. The resulting mixture was stirred at -78 °C for 30 min and then at -10 °C for 10 min. At -10 °C, to the enolate solution was added a solution of CuBr₂ (0.12 g, 0.53 mmol) in anhydrous DMF (2 mL) and the reaction system was warmed up to rt. After stirring for 3 h, saturated NH₄Cl solution (20 mL) was added to the reaction solution and the mixture was extracted with DCM (3×15 mL). The organic fractions were combined, washed with brine (15 mL), dried over MgSO₄ and concentrated under reduced pressure. The residue was purified by flash column chromatography eluting with 15% EtOAc in petroleum ether to afford a trace amount of **338** (4 mg, 3% yield) as a yellow oil. The molecular formula was determined by HRMS (ESI): calculated for $C_{30}H_{32}N_2O_6S_2Na$ $[M+Na]^+$ 603.1600, found 603.1597.

Preparation of DKP **347**

A mixture of DKP derivative **112** (0.29 g, 0.86 mmol), TBSCl (0.32 g, 2.16 mmol) and imidazole (0.15 g, 2.16 mmol) in DCM (20 mL) was stirred at rt for 8 h. Upon completion, the mixture was transferred to a separating funnel and partitioned between brine (20 mL) and DCM (15 mL). The aqueous phase was extracted with DCM (2×15 mL). The combined organic fractions were washed with brine (20 mL), dried over MgSO₄, filtered and concentrated under reduced pressure. The crude product was purified by flash column chromatography eluting with EtOAc to afford **347** as a colourless wax (0.37 g, 76% yield). $R_f = 0.30$ (EtOAc/MeOH 6:1); $[\alpha]_D^{24} = -77$ ($c = 1.0$, CHCl₃); FTIR (film) ν_{\max} 2957, 2930, 2861, 1682, 1661, 1511, 1263, 916; ¹H NMR (CDCl₃, 300 MHz) δ 7.05 (d, $J = 8.6$ Hz, H-5 or H-12, 2H), 6.85 (d, $J = 8.4$ Hz, H-12 or H-5, 2H), 6.82 (d, $J = 8.4$ Hz, H-6 or H-13, 2H), 6.74 (d, $J = 8.6$ Hz, H-13 or H-6, 2H), 5.72 (d, $J = 1.9$ Hz, NH, 1H), 4.17 (t, $J = 3.9$ Hz, H-2, 1H), 3.84 (dt, $J = 11.4, 2.4$ Hz, H-9, 1H), 3.22 (dd, $J = 14.2, 3.9$ Hz, H-3a, 1H), 3.11 (s, H-15, 3H), 3.10 (dd, $J = 14.2, 3.9$ Hz, H-3b, 1H), 2.89 (dd, $J = 13.6, 2.4$ Hz, H-10a, 1H), 0.97 (s, H-18 or H-21, 9H), 0.92 (dd, $J = 13.6, 11.4$ Hz, H-10b, 1H), 0.91 (s, H-21 or H-18, 9H), 0.18 (s, H-19, 6H), 0.09 (s, H-16a, 3H), 0.06 (s, H-16b, 3H); ¹³C NMR (CDCl₃, 100 MHz) δ 165.9 (C-1 or C-8), 165.5 (C-8 or C-1), 155.4 (C-7 or C-14), 154.8 (C-14 or C-7), 131.4 (C-5 or C-12), 130.3 (C-12 or C-5), 128.6 (C-4 or C-11), 127.3 (C-11 or C-4), 120.5 (C-6 and C-13), 63.2 (C-2), 56.9

(C-9), 40.1 (C-10), 35.9 (C-3), 33.1 (C-15), 25.7 (C-18 or C-21), 25.6 (C-21 or C-18), 18.2 (C-17 or C-20), 18.1 (C-20 or C-17), -4.4 (C-19), -4.5 (C-16a and C-16b); HRMS (ESI) calculated for $C_{19}H_{20}N_2O_4Na$ $[M+Na]^+$ 363.1321, found 363.1324.

Appendix A - X-ray Crystal Structure Data for Compound **108**.

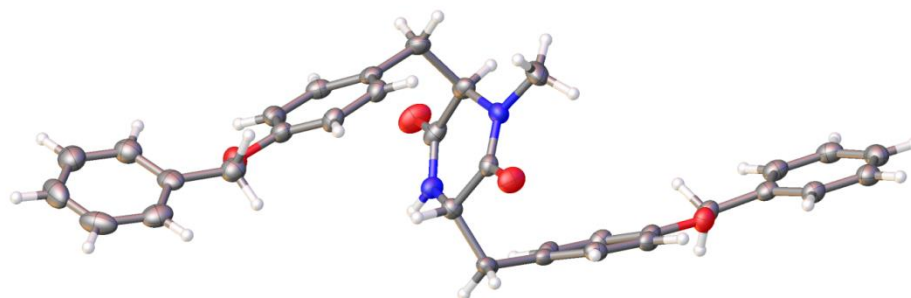


Table 1: Crystal data and structure refinement.

Empirical formula	$C_{33}H_{32}N_2O_4$	
Formula weight	520.61	
Temperature	120(2) K	
Wavelength	1.54184 Å	
Crystal system	Monoclinic	
Space group	P 2 ₁	
Unit cell dimensions	$a = 15.1004(4)$ Å	$\alpha = 90^\circ$.
	$b = 10.4371(3)$ Å	$\beta = 103.269(2)^\circ$.
	$c = 17.2617(5)$ Å	$\gamma = 90^\circ$.
Volume	$2647.89(13)$ Å ³	
Z	4	
Density (calculated)	1.306 Mg/m ³	
Absorption coefficient	0.687 mm ⁻¹	
F(000)	1104	
Crystal size	0.29 x 0.11 x 0.02 mm ³	
Theta range for data collection	2.63 to 71.01°.	
Index ranges	$-18 \leq h \leq 18$, $-12 \leq k \leq 12$, $-20 \leq l \leq 21$	
Reflections collected	25298	
Independent reflections	9750 [R(int) = 0.0308]	

Completeness to theta = 71.01°	98.7 %
Absorption correction	Semi-empirical from equivalents
Max. and min. transmission	0.9864 and 0.8256
Refinement method	Full-matrix least-squares on F ²
Data / restraints / parameters	9750/13/713
Goodness-of-fit on F ²	1.041
Final R indices [I>2sigma(I)]	R1 = 0.0380, wR2 = 0.0933
R indices (all data)	R1 = 0.0439, wR2 = 0.0982
Absolute structure parameter	0.04(14)
Largest diff. peak and hole	0.436 and -0.210 e.Å ⁻³

Appendix B - X-ray Crystal Structure Data for Compound 102.

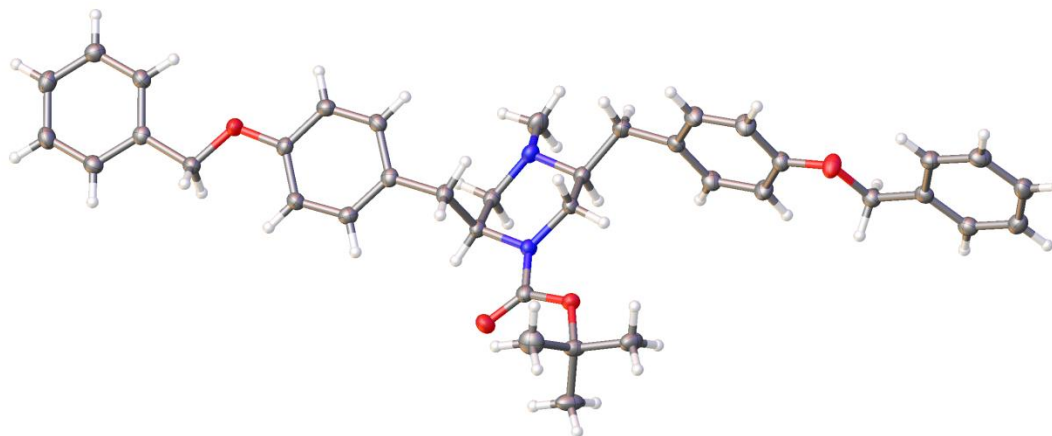


Table 1: Crystal data and structure refinement.

Empirical formula	$C_{38}H_{44}N_2O_4$	
Formula weight	592.75	
Temperature	100.01(10) K	
Wavelength	1.54184 Å	
Crystal system	Orthorhombic	
Space group	$P2_12_12_1$	
Unit cell dimensions	$a = 5.68231(6)$ Å	$\alpha = 90^\circ$.
	$b = 15.67459(18)$ Å	$\beta = 90^\circ$.
	$c = 36.2806(4)$ Å	$\gamma = 90^\circ$.
Volume	$3231.44(6)$ Å ³	
Z	4	
Density (calculated)	1.218 Mg/m ³	
Absorption coefficient	0.620 mm ⁻¹	
F(000)	1272.0	
Crystal size	0.187 × 0.1404 × 0.0836 mm ³	
Theta range for data collection	13.446 to 148.97°.	
Index ranges	-6 ≤ h ≤ 7, -18 ≤ k ≤ 19, -41 ≤ l ≤ 45	

Reflections collected	30250
Independent reflections	6488 [$R_{\text{int}} = 0.0246$, $R_{\text{sigma}} = 0.0169$]
Completeness to $\theta = 66.97^\circ$	99.94 %
Absorption correction	Semi-empirical from equivalents
Refinement method	Full-matrix least-squares on F^2
Data / restraints / parameters	6488/0/401
Goodness-of-fit on F^2	1.037
Final R indices [$I > 2\sigma(I)$]	$R_1 = 0.0282$, $wR_2 = 0.0701$
R indices (all data)	$R_1 = 0.0298$, $wR_2 = 0.0714$
Largest diff. peak and hole	0.28/-0.15 e. \AA^{-3}

Appendix C - X-ray Crystal Structure Data for Compound **160**.

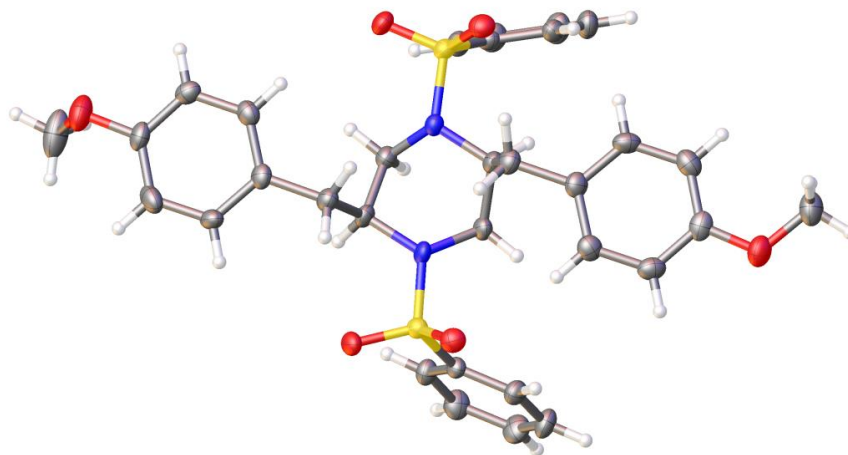
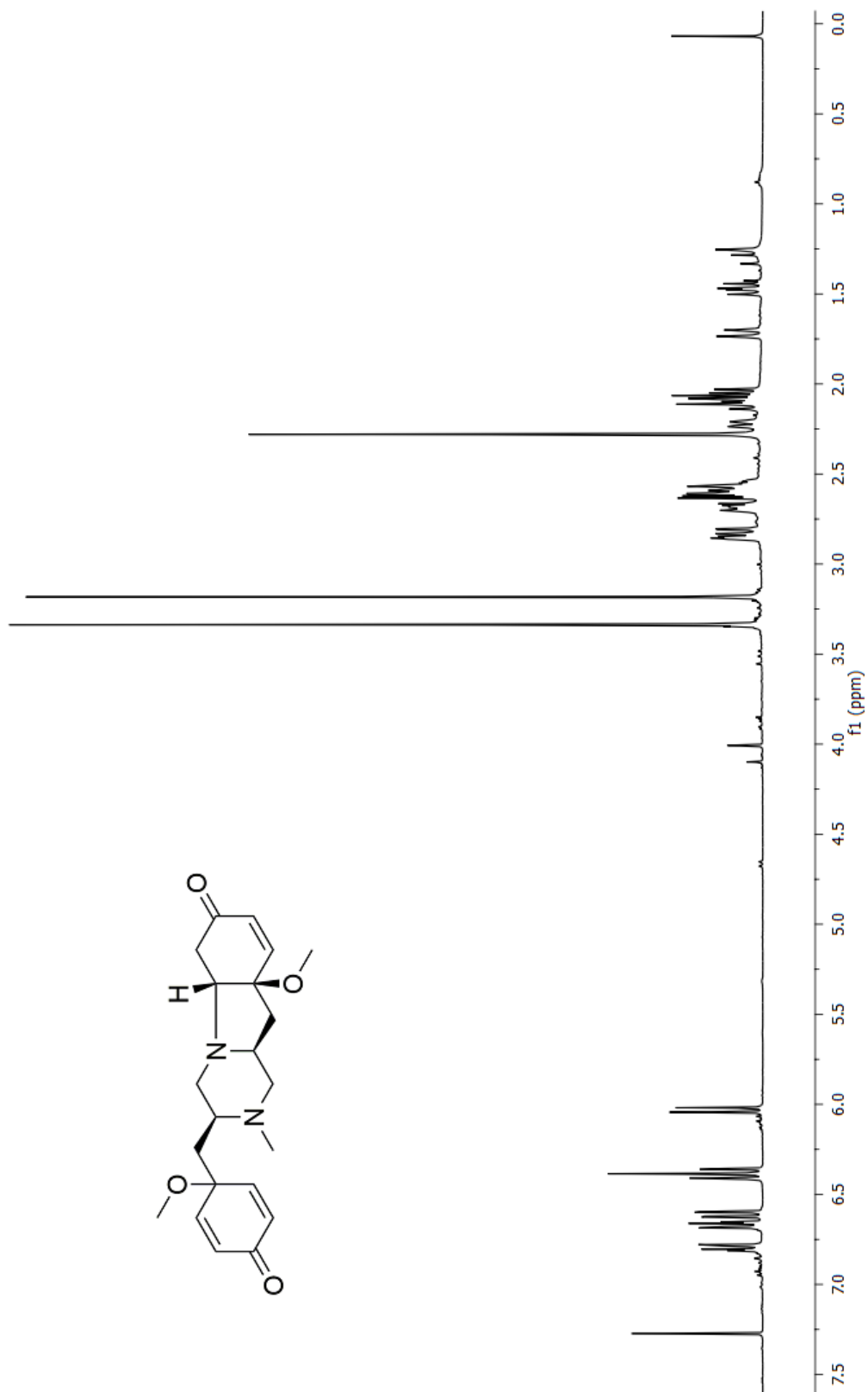


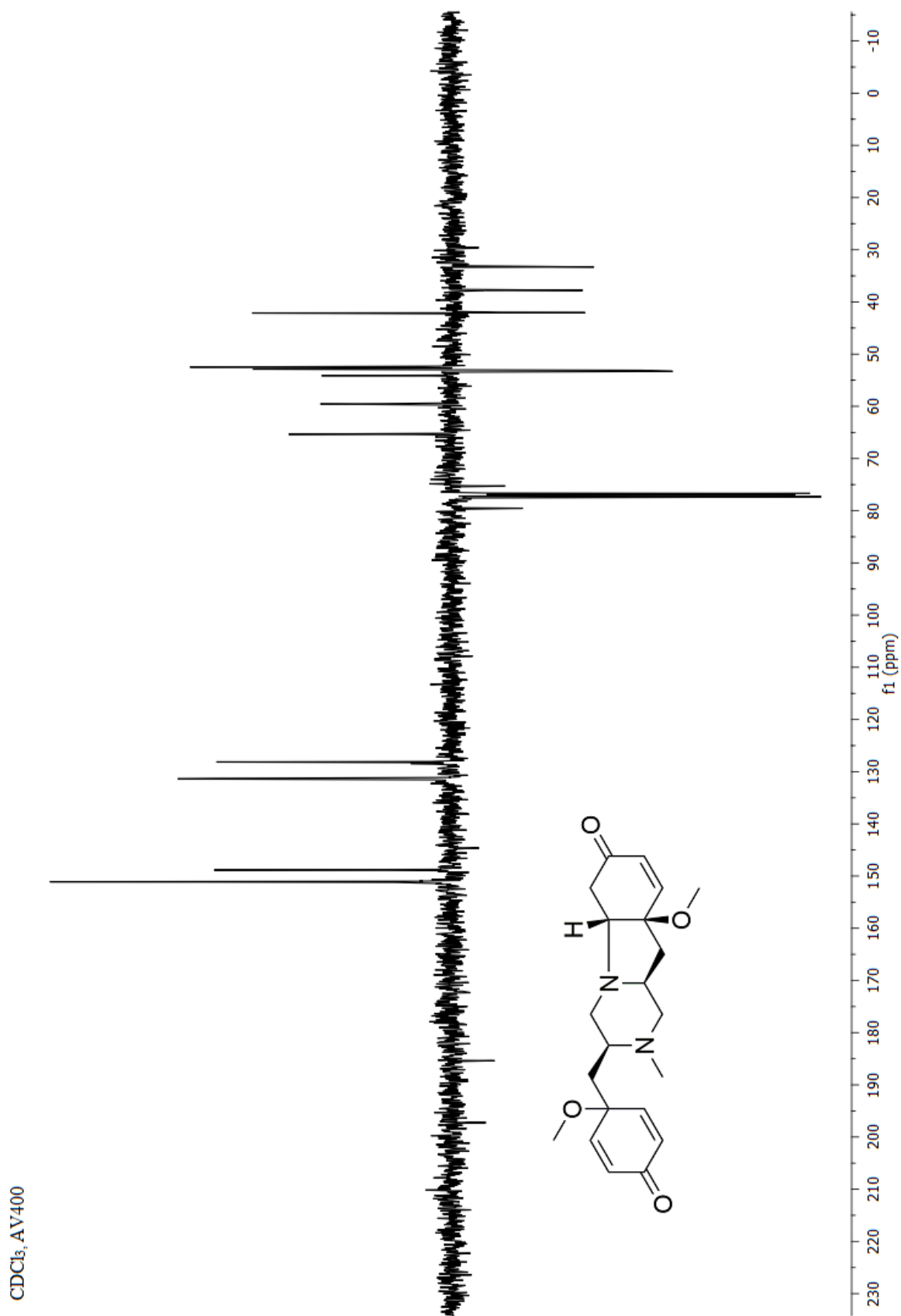
Table 1: Crystal data and structure refinement.

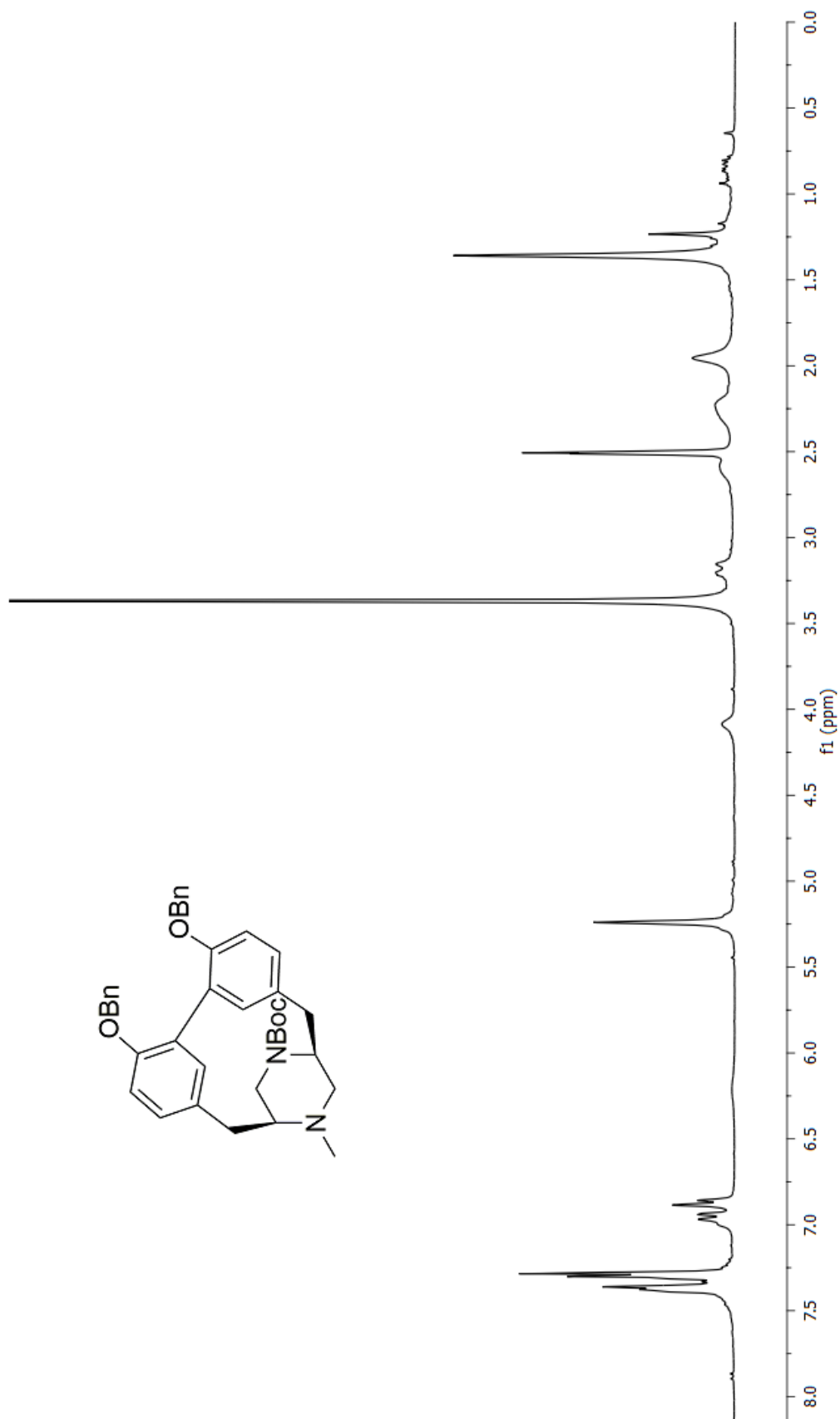
Empirical formula	$C_{32}H_{34}N_2O_6S_2$	
Formula weight	606.73	
Temperature	99.95(19) K	
Wavelength	1.54184 Å	
Crystal system	Monoclinic	
Space group	$P2_1$	
Unit cell dimensions	$a = 15.5497(2)$ Å	$\alpha = 90^\circ$.
	$b = 11.38339(15)$ Å	$\beta = 91.5569(13)^\circ$.
	$c = 16.2563(2)$ Å	$\gamma = 90^\circ$.
Volume	$2876.43(7)$ Å ³	
Z	4	
Density (calculated)	1.401 Mg/m ³	
Absorption coefficient	2.087 mm ⁻¹	
F(000)	1280.0	
Crystal size	$0.2094 \times 0.1624 \times 0.0455$ mm ³	
Theta range for data collection	5.438 to 138.262°.	
Index ranges	$-18 \leq h \leq 18$, $-13 \leq k \leq 13$, $-19 \leq l \leq 19$	

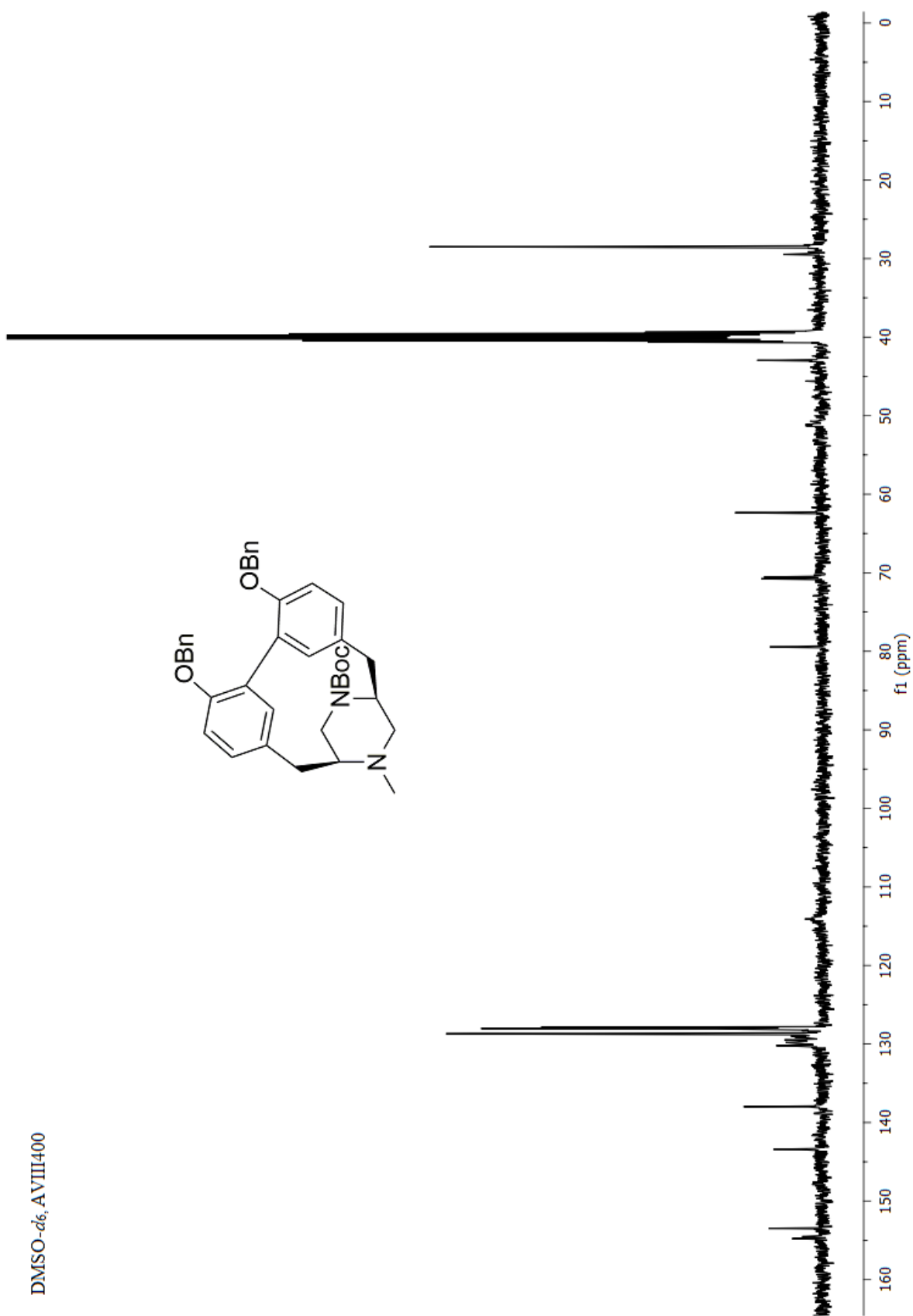
Reflections collected	27559
Independent reflections	10440 [$R_{\text{int}} = 0.0372$, $R_{\text{sigma}} = 0.0374$]
Absorption correction	Semi-empirical from equivalents
Refinement method	Full-matrix least-squares on F^2
Data / restraints / parameters	10440/1/761
Goodness-of-fit on F^2	1.060
Final R indices [$I > 2\sigma(I)$]	$R_1 = 0.0534$, $wR_2 = 0.1424$
R indices (all data)	$R_1 = 0.0560$, $wR_2 = 0.1454$
Largest diff. peak and hole	1.17/-0.40 e. \AA^{-3}

Appendix D - Selected NMR Spectra.

¹H NMR spectrum of compound **130a**CDCl₃, AV400

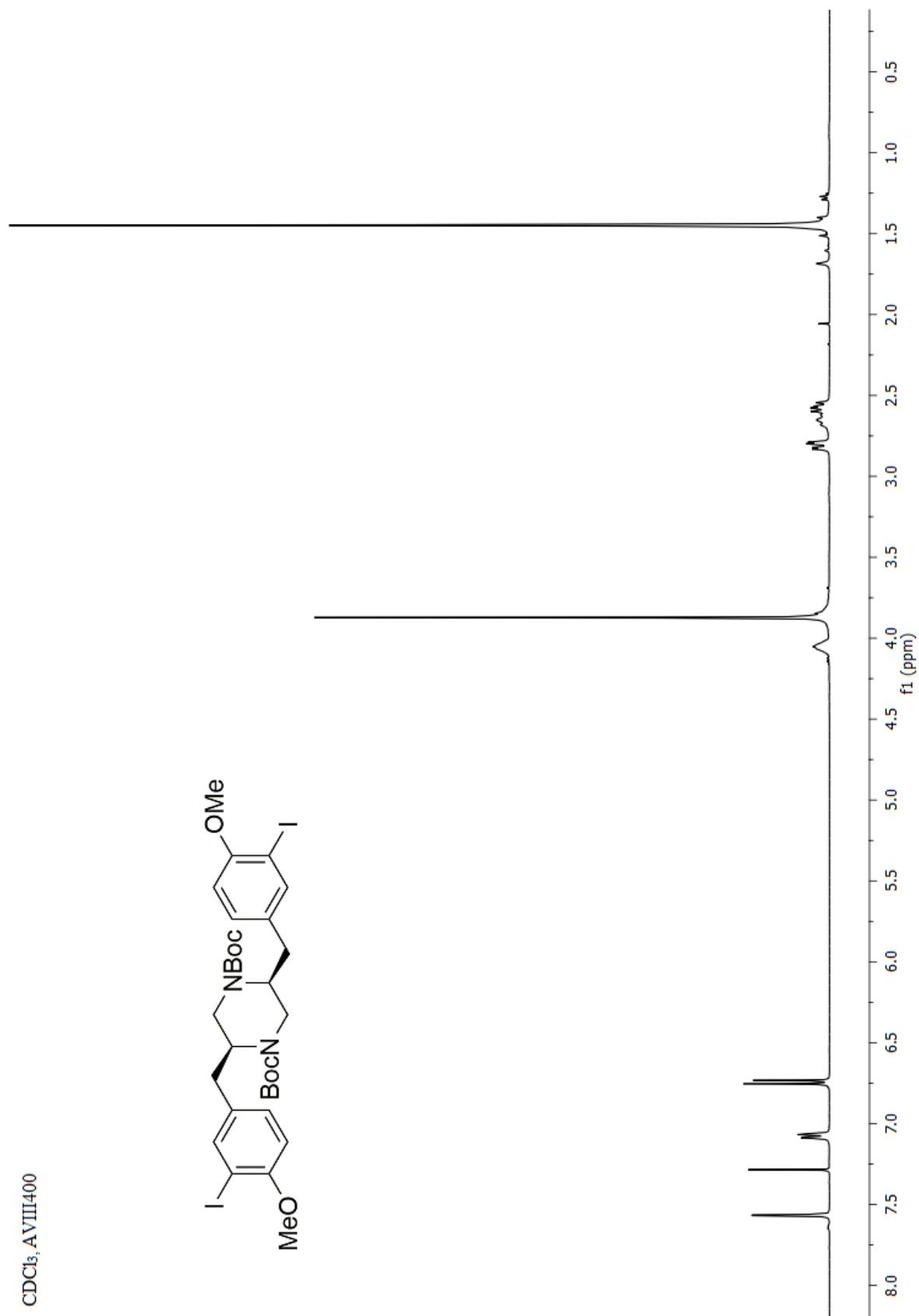
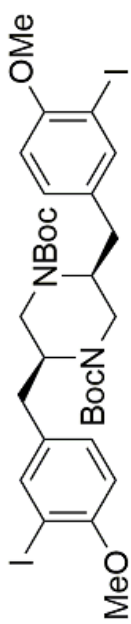
^{13}C NMR spectrum of compound **130a**

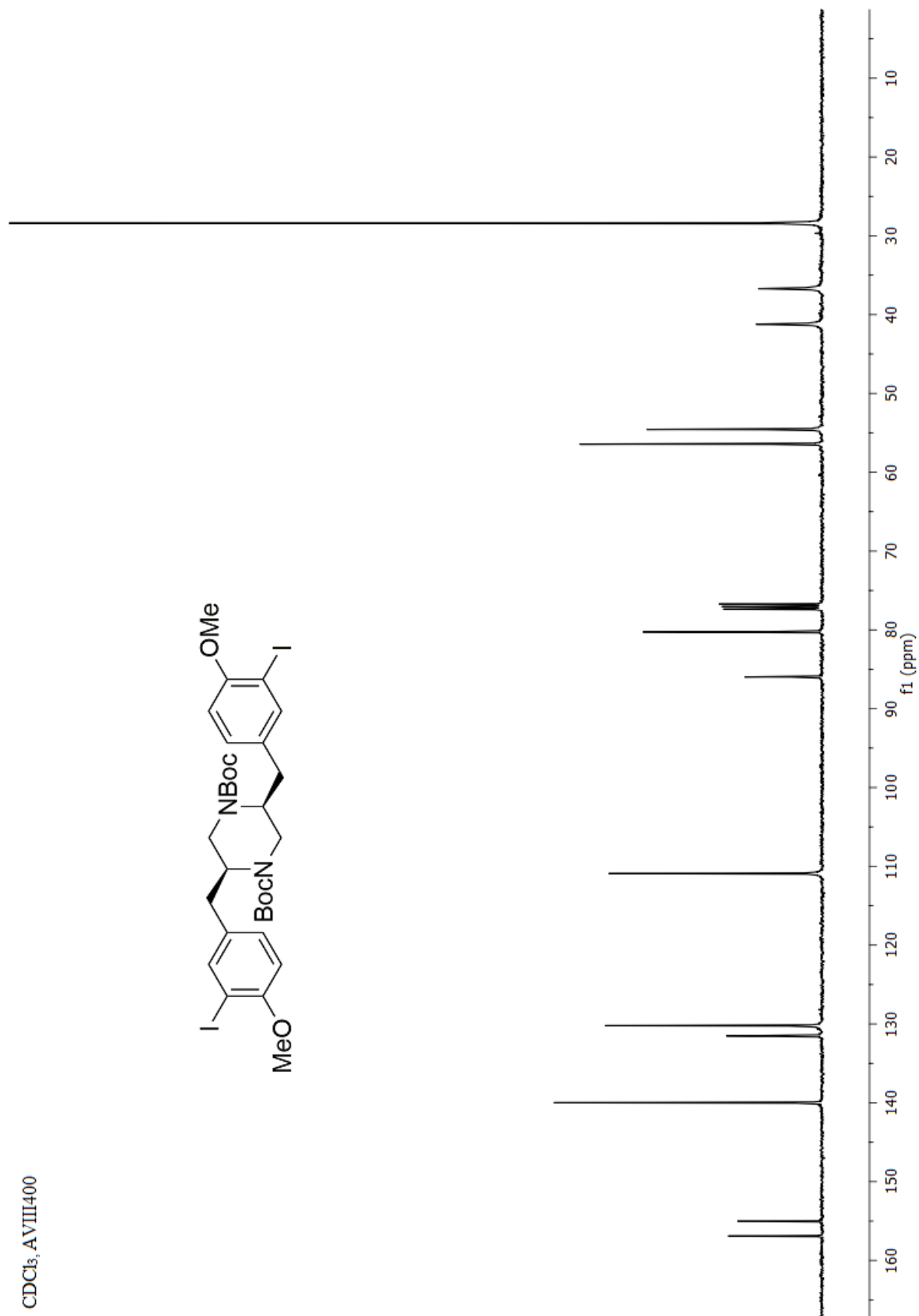
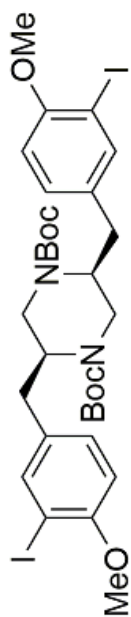
¹H NMR spectrum of compound **214**DMSO-*d*₆, AVIII300

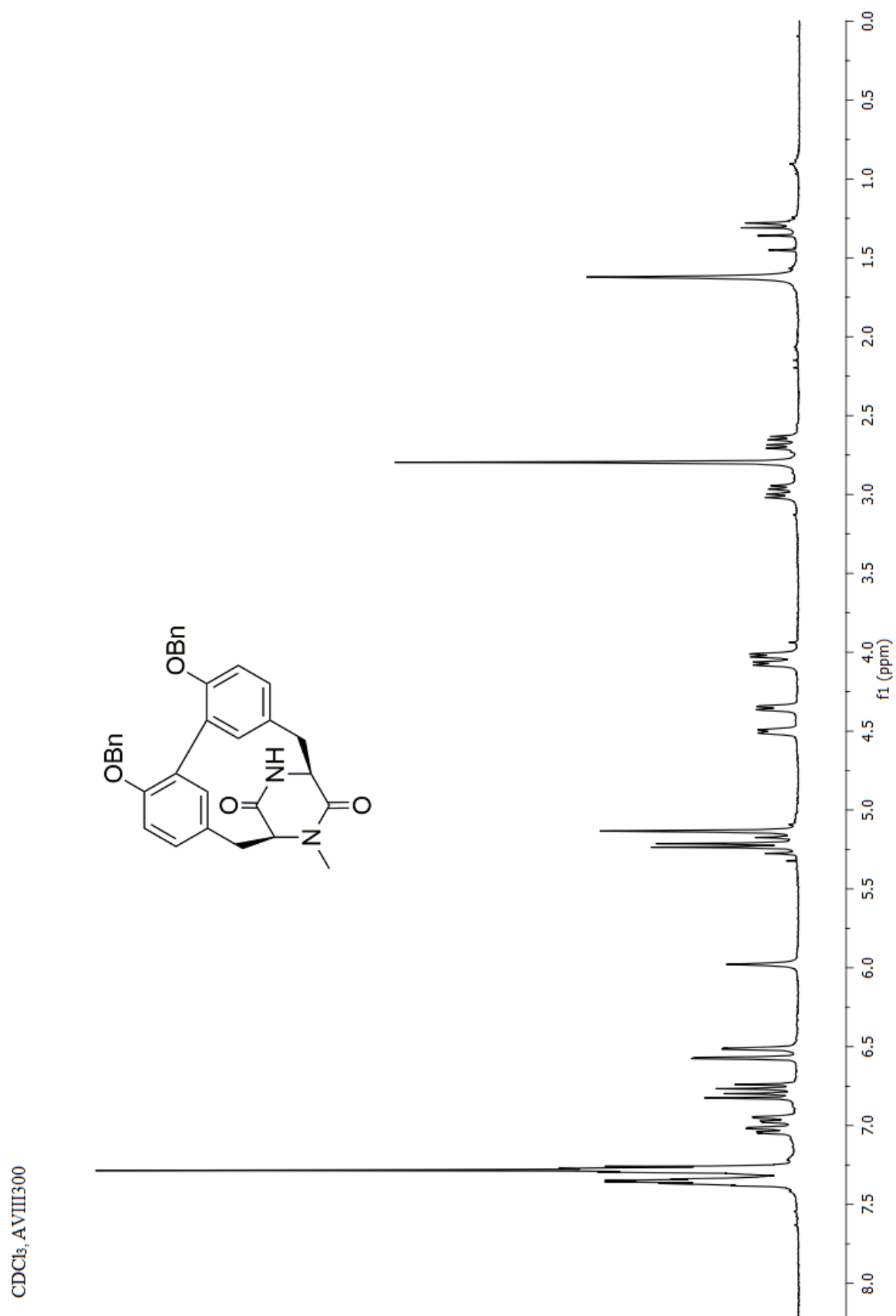
^{13}C NMR spectrum of compound **214**

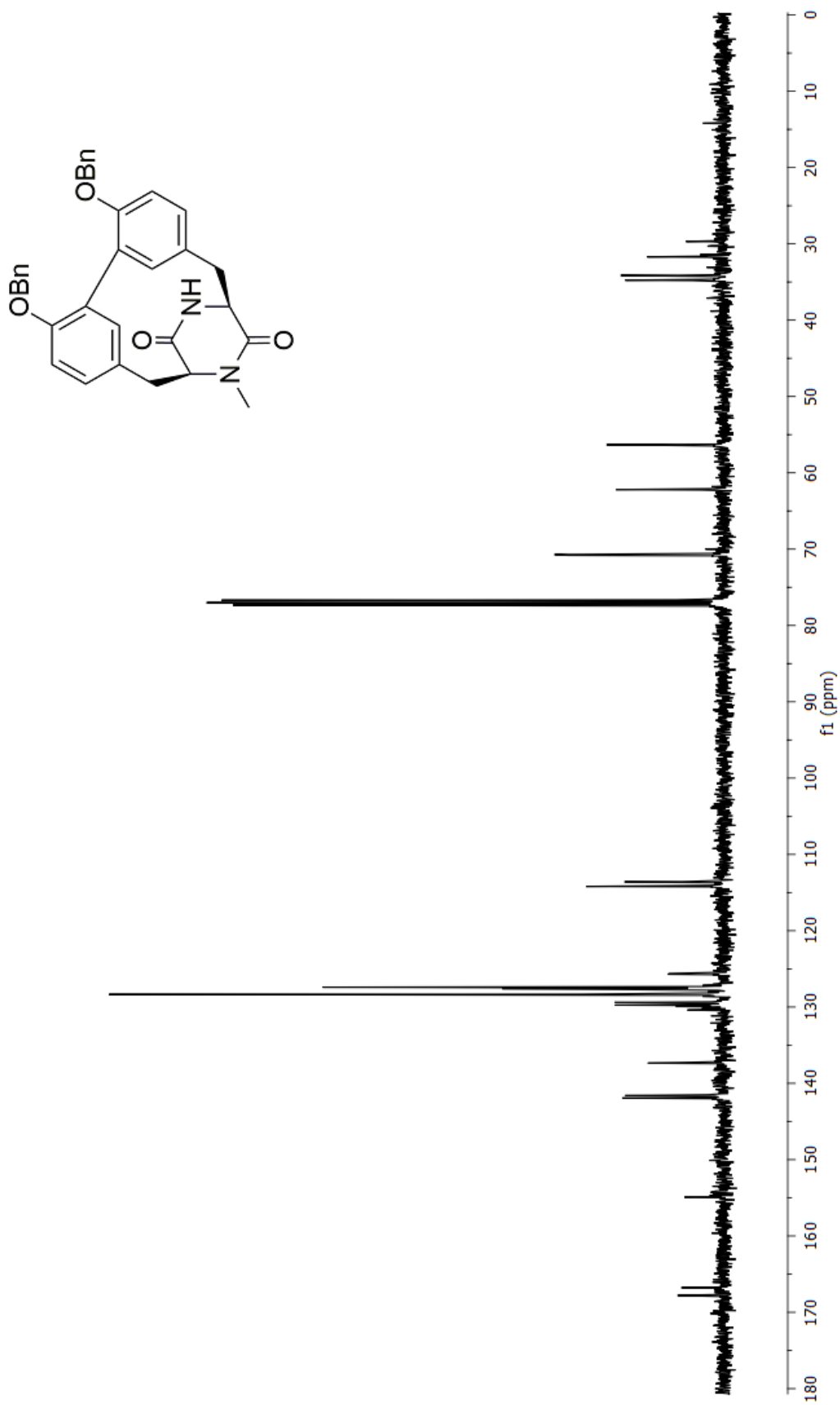
^1H NMR spectrum of compound **169**

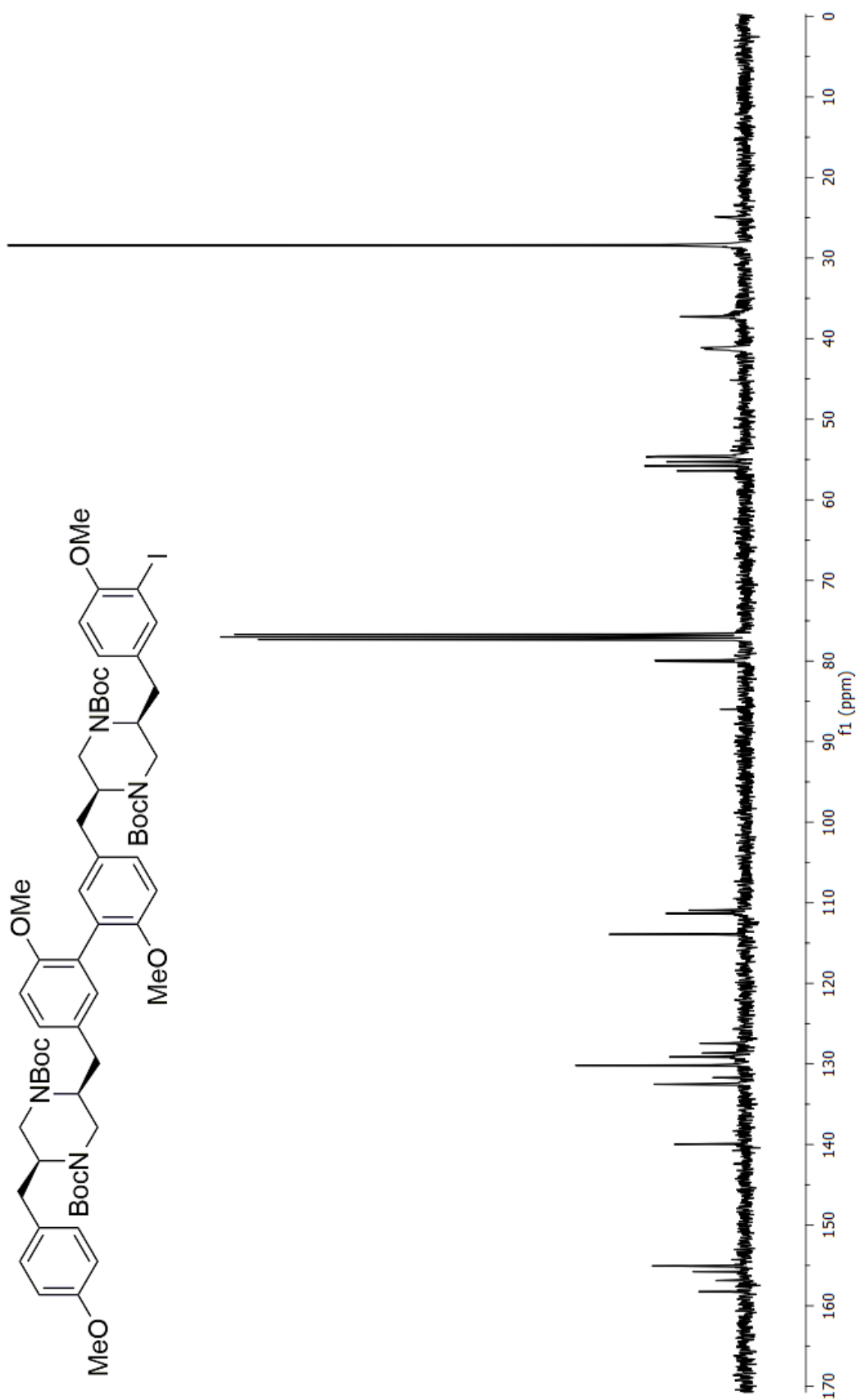
CDCl_3 , AVIII400



^{13}C NMR spectrum of compound **169**CDCl₃, AVIII400

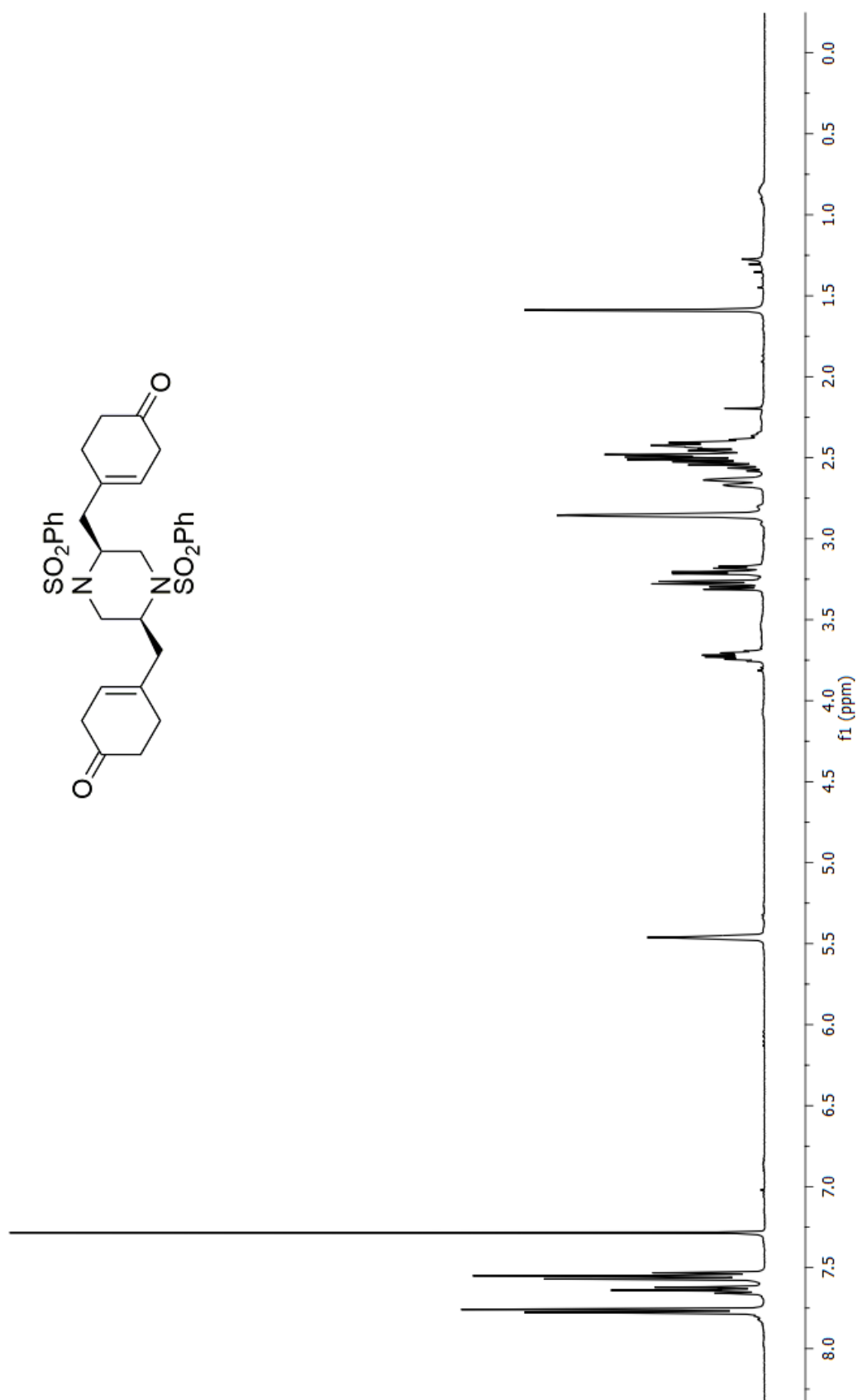
¹H NMR spectrum of compound **220**

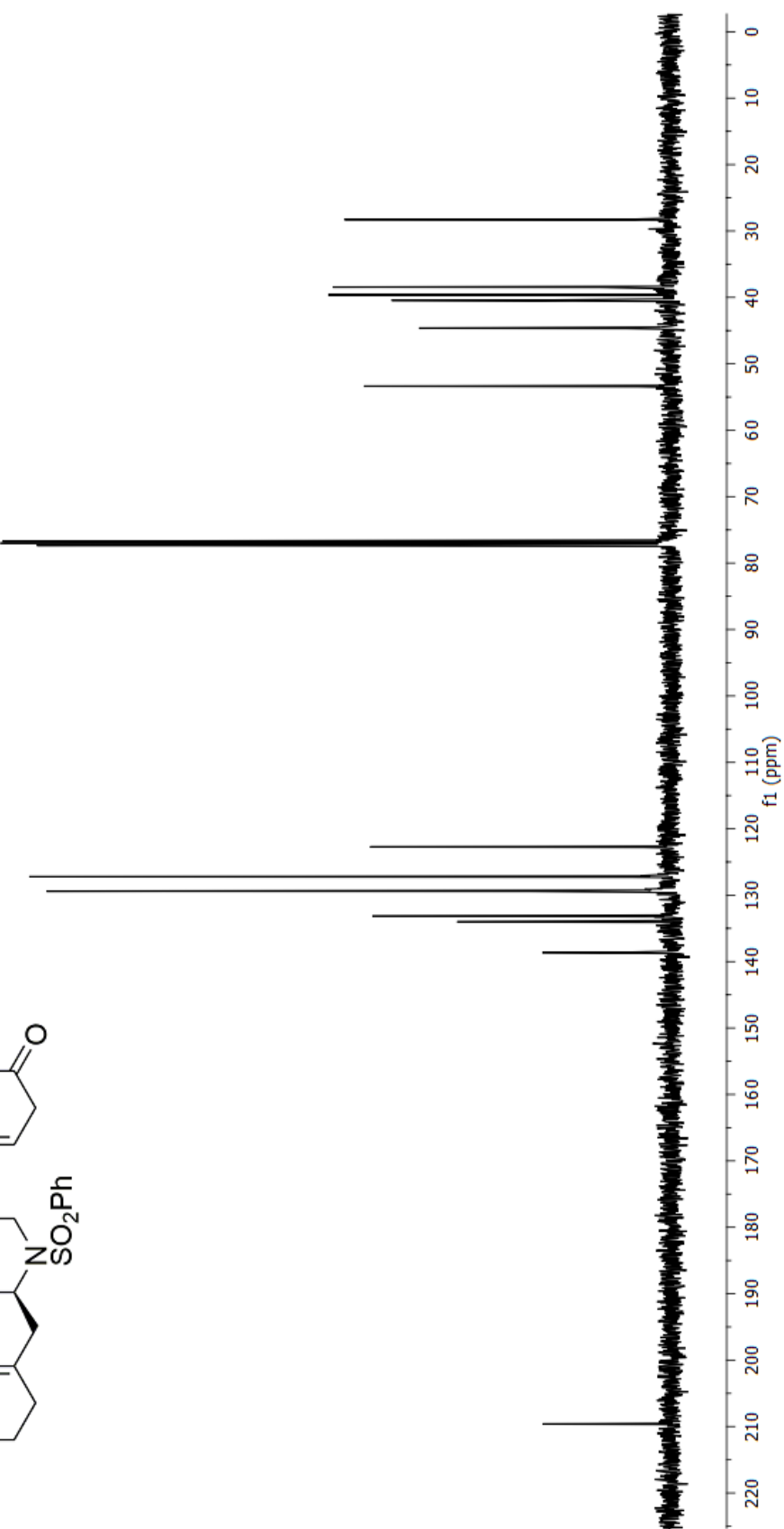
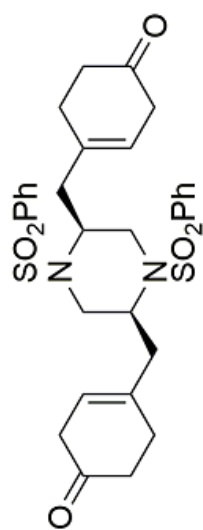
^{13}C NMR spectrum of compound **220**CDCl₃, AVIII400

^{13}C NMR spectrum of compound **206** CDCl_3 , AVIII400

¹H NMR spectrum of compound **329**

CDCl₃, AVIII400



^{13}C NMR spectrum of compound **329**CDCl₃, AVIII400

References

1. Ōmura, S.; Hirano, A.; Iwai, Y.; Masuma, R. *J. Antibiot.* **1979**, *32*, 786.
2. Kagata, T.; Shigemori, H.; Mikami, Y.; Kobayashi, J. *J. Nat. Prod.* **2000**, *63*, 886.
3. Furusaki, A.; Matsumoto, T.; Ogura, H.; Takayanagi, H.; Hirano, A.; Ōmura, S. *J. Chem. Soc. Chem. Comm.* **1980**, 698.
4. Enomoto, Y.; Shiomi, K.; Hayashi, M.; Masuma, R.; Kawakubo, T.; Tomosawa, K.; Iwai, Y.; Ōmura, S. *J. Antibiot.* **1996**, *49*, 50.
5. Hartwig, J. H.; DeSisto, M. *J. Cell Biol.* **1991**, *112*, 407.
6. Gibbins, J. M. *J. Cell Sci.* **2004**, *117*, 3415.
7. Ahmad, S. S.; London, F. S.; Walsh, P. N. *J. Thromb. Haemost.* **2003**, *1*, 48.
8. Singh, P.; Singh, I. N.; Mondal, S. C.; Singh, L.; Garg, V. K. *Fitoterapia* **2013**, *84*, 180.
9. Rozalski, M.; Nocun, M.; Watala, C. *Acta Biochim. Pol.* **2005**, *52*, 411.
10. Andre, P.; Delaney, S. M.; LaRocca, T.; Vincent, D.; DeGuzman, F.; Jurek, M.; Koller, B.; Phillips, D. R.; Conley, P. B. *J. Clin. Invest.* **2003**, *112*, 398.
11. Gachet, C. *Pharmacol. Therapeut.* **2005**, *108*, 180.
12. Fontana, P.; Dupont, A.; Gandrille, S.; Bachelot-Loza, C.; Reny, J. L.; Aiach, M.; Gaussem, P. *Circulation* **2003**, *108*, 989.
13. Zhang, D.; Gao, Z. G.; Zhang, K.; Kiselev, E.; Crane, S.; Wang, J.; Paoletta, S.; Yi,

- C.; Ma, L.; Zhang, W.; Han, G. W.; Liu, H.; Cherezov, V.; Katritch, V.; Jiang, H.; Stevens, R. C.; Jacobson, K. A.; Zhao, Q.; Wu, B. *Nature* **2015**, *520*, 317.
14. Kim, G. T. Ph.D. thesis, Korea Advanced Institute of Science and Technology, 1997. Retrieved from http://library.kaist.ac.kr/thesis01/1998/1998D000945041_S1Ver2.pdf
 15. Hart, J. M. Ph.D. thesis, The University of Leeds, 2004. Retrieved from <http://ethos.bl.uk/OrderDetails.do?uin=uk.bl.ethos.411144>
 16. Stawski, P. S. Ph.D. thesis, Ludwig-Maximilians-Universität München, 2012. Retrieved from <http://edoc.ub.uni-muenchen.de/15523/>
 17. Tamai, S.; Kaneda, M.; Nakamura, S. *J. Antibiot.* **1982**, *35*, 1130.
 18. Kaneda, M.; Tamai, S.; Nakamura, S.; Hirata, T.; Kushi, Y.; Suga, T. *J. Antibiot.* **1982**, *35*, 1137.
 19. Boger, D. L.; Zhou, J. *J. Am. Chem. Soc.* **1993**, *115*, 11426.
 20. Ghosh, S.; Kumar, A. S.; Mehta, G. N.; Soundararajan, R.; Sen, S. *Arkivoc* **2009**, 72.
 21. Nishiyama, S.; Nakamura, K.; Suzuki, Y.; Yamamura, S. *Tetrahedron Lett.* **1986**, *27*, 4481.
 22. Atsumi, T.; Noriyoshi, K. *Nippon Kagakkai Koen Yokoshu* **2003**, *83*, 777.
 23. Cochrane, J. R.; White, J. M.; Wille, U.; Hutton, C. A. *Org. Lett.* **2012**, *14*, 2402.
 24. Vetting, M. W.; Hegde, S. S.; Blanchard, J. S. *Nat. Chem. Biol.* **2010**, *6*, 797.

25. Belin, P.; Le Du, M. H.; Fielding, A.; Lequin, O.; Jacquet, M.; Charbonnier, J. B.; Lecoq, A.; Thai, R.; Courçon, M.; Masson, C.; Dugave, C.; Genet, R.; Pernodet, J. L.; Gondry, M. *Proc. Natl. Acad. Sci. USA* **2009**, *106*, 7426.
26. Hubbard, B. K.; Walsh, C. T. *Angew. Chem. Int. Ed.* **2003**, *42*, 730.
27. Pylypenko, O.; Vitali, F.; Zerbe, K.; Robinson, J. A.; Schlichting, I. *J. Biol. Chem.* **2003**, *278*, 46727.
28. Woithe, K.; Geib, N.; Zerbe, K.; Li, D. B.; Heck, M.; Fournier-Rousset, S.; Meyer, O.; Vitali, F.; Matoba, N.; Abou-Hadeed, K.; Robinson, J. A. *J. Am. Chem. Soc.* **2007**, *129*, 6887.
29. Ikezawa, N.; Iwasa, K.; Sato, F. *J. Biol. Chem.* **2008**, *283*, 8810.
30. Gesell, A.; Rolf, M.; Ziegler, J.; Chávez, M. L. D.; Huang, F. C.; Kutchan, T. M. *J. Biol. Chem.* **2009**, *284*, 24432.
31. McLean, K. J.; Carroll, P.; Lewis, D. G.; Dunford, A. J.; Seward, H. E.; Neeli, R.; Cheesman, M. R.; Marsollier, L.; Douglas, P.; Smith, W. E.; Rosenkrands, I.; Cole, S. T.; Leys, D.; Parish, T.; Munro, A. W. *J. Biol. Chem.* **2008**, *283*, 33406.
32. Momoi, Y.; Okuyama, K.; Toya, H.; Sugimoto, K.; Okano, K.; Tokuyama, H. *Angew. Chem. Int. Ed.* **2014**, *53*, 13215.
33. Matveenko, M.; Liang, G.; Lauterwasser, E. M. W.; Zubía, E.; Trauner, D. *J. Am. Chem. Soc.* **2012**, *134*, 9291.
34. Baran, P. S.; Burns, N. Z. *J. Am. Chem. Soc.* **2006**, *128*, 3908.

35. Chausset-Boissarie, L.; Àrvai, R.; Cumming, G. R.; Guénée, L.; Kündig, E. P. *Org. Biomol. Chem.* **2012**, *10*, 6473.
36. Shan, Z. H.; Liu, J.; Xu, L. M.; Tang, Y. F.; Chen, J. H.; Yang, Z. *Org. Lett.* **2012**, *14*, 3712.
37. Carrick, W. L.; Karapinka, G. L.; Kwiatkowski, G. T. *J. Org. Chem.* **1969**, *34*, 2388.
38. Kupchan, S. M.; Dhingra, O. P.; Kim, C. K. *J. Org. Chem.* **1978**, *43*, 4076.
39. Evans, D. A.; Dinsmore, C. J.; Evrard, D. A.; DeVries, K. M. *J. Am. Chem. Soc.* **1993**, *115*, 6426.
40. Evans, D. A.; Wood, M. R.; Trotter, B. W.; Richardson, T. I.; Barrow, J. C.; Katz, J. L. *Angew. Chem. Int. Ed.* **1998**, *37*, 2700.
41. Kita, Y.; Takada, T.; Gyoten, M.; Tohma, H.; Zenk, M. H.; Eichhorn, J. *J. Org. Chem.* **1996**, *61*, 5857.
42. Tohma, H.; Morioka, H.; Takizawa, S.; Arisawa, M.; Kita, Y. *Tetrahedron* **2001**, *57*, 345.
43. Burgett, A. W. G.; Li, Q. Y.; Wei, Q.; Harran, P. G. *Angew. Chem. Int. Ed.* **2003**, *42*, 4961.
44. Kita, Y.; Gyoten, M.; Ohtsubo, M.; Tohma, H.; Takada, T. *Chem. Commun.* **1996**, 1481.
45. Hamamoto, H.; Anilkumar, G.; Tohma, H.; Kita, Y. *Chem. Eur. J.* **2002**, *8*, 5377.

46. Kita, Y.; Tohma, H.; Hatanaka, K.; Takada, T.; Fujita, S.; Mitoh, S.; Sakurai, H.; Oka, S. *J. Am. Chem. Soc.* **1994**, *116*, 3684.
47. Sarhan, A. A. O.; Bolm, C. *Chem. Soc. Rev.* **2009**, *38*, 2730.
48. Herbert, R. B.; Kattah, A. E.; Murtagh, A. J.; Sheldrake, P. W. *Tetrahedron Lett.* **1995**, *36*, 5649.
49. Tobinaga, S.; Kotani, E. *J. Am. Chem. Soc.* **1972**, *94*, 309.
50. Bringmann, G.; Saeb, W.; Mies, J.; Messer, K.; Wohlfarth, M.; Brun, R. *Synthesis* **2000**, 1843.
51. Bringmann, G.; Götz, R.; François, G. *Tetrahedron* **1996**, *52*, 13419.
52. Yamada, H.; Nagao, K.; Dokei, K.; Kasai, Y.; Michihata, N. *J. Am. Chem. Soc.* **2008**, *130*, 7566.
53. Edwankar, C. R.; Edwankar, R. V.; Deschamps, J. R.; Cook, J. M. *Angew. Chem. Int. Ed.* **2012**, *51*, 11762.
54. Mirk, D.; Wibbeling, B.; Fröhlich, R.; Waldvogel, S. R. *Synlett* **2004**, 1970.
55. Ma, Y. A.; Guo, Z. W.; Sih, C. J. *Tetrahedron Lett.* **1998**, *39*, 9357.
56. Kirste, A.; Schnakenburg, G.; Stecker, F.; Fischer, A.; Waldvogel, S. R. *Angew. Chem. Int. Ed.* **2010**, *49*, 971.
57. Qiu, L. H.; Shen, Z. X.; Chen, W. H.; Zhang, Y.; Zhang, Y. W. *Chin. J. Chem.* **2003**, *21*, 1098.

58. Guo, Y.; Cao, S.; Wei, D.; Zong, X.; Yuan, X.; Tang, M.; Zhao, Y. *J. Mass Spectrom.* **2009**, *44*, 1188.
59. Nonappa; Ahonen, K.; Lahtinen, M.; Kolehmainen, E. *Green Chem.* **2011**, *13*, 1203.
60. Boger, D. L.; Yohannes, D. *J. Org. Chem.* **1988**, *53*, 487.
61. Han, S. Y.; Kim, Y. A. *Tetrahedron* **2004**, *60*, 2447.
62. Nishiyama, S.; Nakamura, K.; Suzuki, Y.; Yamamura, S. *Tetrahedron Lett.* **1986**, *27*, 4481.
63. Jung, M. E.; Rohloff, J. C. *J. Org. Chem.* **1985**, *50*, 4909.
64. Kawasaki, T.; Ohno, K.; Enoki, H.; Umemoto, Y.; Sakamoto, M. *Tetrahedron Lett.* **2002**, *43*, 4245.
65. Grina, J. A.; Stermitz, F. R. *Tetrahedron Lett.* **1981**, *22*, 5257.
66. Selvakumar, S.; Sivasankaran, D.; Singh, V. K. *Org. Biomol. Chem.* **2009**, *7*, 3156.
67. Soai, K.; Hayashi, H.; Shinozaki, A.; Umebayashi, H.; Yamada, Y. *Bull. Chem. Soc. Jpn.* **1987**, *60*, 3450.
68. Aurelio, L.; Brownlee, R. T. C.; Hughes, A. B. *Chem. Rev.* **2004**, *104*, 5823.
69. Malkov, A. V.; Vranková, K.; Černý, M.; Kočovský, P. *J. Org. Chem.* **2009**, *74*, 8425.
70. Wen, S. J.; Hu, T. S.; Yao, Z. J. *Tetrahedron* **2005**, *61*, 4931.
71. Ressurreição, A. S. M.; Bordessa, A.; Civera, M.; Belvisi, L.; Gennari, C.; Piarulli, U. *J. Org. Chem.* **2008**, *73*, 652.

72. Misicka, A.; Verheyden, P. M. F.; Van Binst, G. *Lett. Pept. Sci.* **1998**, *5*, 375.
73. Kopple, K. D.; Marr, D. H. *J. Am. Chem. Soc.* **1967**, *89*, 6193.
74. Hong, Y. P.; Lee, S. H.; Choi, J. H.; Kashima, A.; Nakamura, G.; Suzuki, T. *Bull. Korean Chem. Soc.* **2014**, *35*, 2299.
75. Gdaniec, M.; Liberek, B. *Acta Crystallogr. Sect. C* **1986**, *42*, 1343.
76. Sheinblatt, M. *J. Chem. Soc. Perkin Trans. 2* **1990**, 127.
77. Brown, A. G.; Edwards, P. D. *Tetrahedron Lett.* **1990**, *31*, 6581.
78. Nicolaou, K. C.; Snyder, S. A.; Huang, X.; Simonsen, K. B.; Koumbis, A. E.; Bigot, A. *J. Am. Chem. Soc.* **2004**, *126*, 10162.
79. Bates, R. B.; Gin, S. L.; Hassen, M. A.; Hruby, V. J.; Janda, K. D.; Kriek, G. R.; Michaud, J. P.; Vine, D. B. *Heterocycles* **1984**, *22*, 785.
80. Boger, D. L.; Yohannes, D.; Zhou, J.; Patane, M. A. *J. Am. Chem. Soc.* **1993**, *115*, 3420.
81. Wipf, P.; Furegati, M. *Org. Lett.* **2006**, *8*, 1901.
82. Wipf, P.; Kim, Y. T. *Tetrahedron Lett.* **1992**, *33*, 5477.
83. Pierce, J. G.; Kasi, D.; Fushimi, M.; Cuzzupe, A.; Wipf, P. *J. Org. Chem.* **2008**, *73*, 7807.
84. Whitesides, G. M.; San Filippo, J.; Casey, C. P.; Panek, E. J. *J. Am. Chem. Soc.* **1967**, *89*, 5302.
85. Lipshutz, B. H.; Siegmann, K.; Garcia, E. *J. Am. Chem. Soc.* **1991**, *113*, 8161.

86. Surry, D. S.; Fox, D. J.; Macdonald, S. J. F.; Spring, D. R. *Chem. Commun.* **2005**, 2589.
87. Su, X.; Surry, D. S.; Spandl, R. J.; Spring, D. R. *Org. Lett.* **2008**, *10*, 2593.
88. Usui, S.; Hashimoto, Y.; Morey, J. V.; Wheatley, A. E. H.; Uchiyama, M. *J. Am. Chem. Soc.* **2007**, *129*, 15102.
89. Haywood, J.; Morey, J. V.; Wheatley, A. E. H.; Liu, C. Y.; Yasuike, S.; Kurita, J.; Uchiyama, M.; Raithby, P. R. *Organometallics* **2009**, *28*, 38.
90. Surry, D. S.; Spring, D. R. *Chem. Soc. Rev.* **2006**, *35*, 218.
91. Tsuboyama, S.; Tsuboyama, K.; Uzawa, J.; Koda, R.; Nakamaru, M.; Kobayashi, K.; Sakurai, T. *Tetrahedron Lett.* **1977**, *18*, 2895.
92. Shainyan, B. A.; Moskalik, M. Y.; Starke, I.; Schilde, U. *Tetrahedron* **2010**, *66*, 8383.
93. Slocum, D. W.; Moon, R.; Thompson, J.; Coffey, D. S.; Li, J. D.; Slocum, M. G.; Siegel, A.; Gayton-Garcia, R. *Tetrahedron Lett.* **1994**, *35*, 385.
94. Slocum, D. W.; Thompson, J.; Friesen, C. *Tetrahedron Lett.* **1995**, *36*, 8171.
95. Crowther, G. P.; Sundberg, R. J.; Sarpeshkar, A. M. *J. Org. Chem.* **1984**, *49*, 4657.
96. Snieckus, V. *Chem. Rev.* **1990**, *90*, 879.
97. Parker, K. A.; Koziski, K. A. *J. Org. Chem.* **1987**, *52*, 674.
98. Nguyen, T. T.; Marquise, N.; Chevallier, F.; Mongin, F. *Chem. Eur. J.* **2011**, *17*, 10405.

99. Liao, B. B.; Milgram, B. C.; Shair, M. D. *J. Am. Chem. Soc.* **2012**, *134*, 16765.
100. Facchetti, S.; Losi, D.; Iuliano, A. *Tetrahedron Asymm.* **2006**, *17*, 2993.
101. Hitotsuyanagi, Y.; Odagiri, M.; Kato, S.; Kusano, J.; Hasuda, T.; Fukaya, H.; Takeya, K. *Chem. Eur. J.* **2012**, *18*, 2839.
102. Carbonnelle, A. C.; Zhu, J. *Org. Lett.* **2000**, *2*, 3477.
103. Fukuyama, Y.; Yaso, H.; Nakamura, K.; Kodama, M. *Tetrahedron Lett.* **1999**, *40*, 105.
104. Grigg, R.; Teasdale, A.; Sridharan, V. *Tetrahedron Lett.* **1991**, *32*, 3859.
105. Wang, L.; Lu, W. *Org. Lett.* **2009**, *11*, 1079.
106. Venkatraman, S.; Li, C. J. *Org. Lett.* **1999**, *1*, 1133.
107. Lee, P. H.; Seomoon, D.; Lee, K. *Org. Lett.* **2005**, *7*, 343.
108. Ishiyama, T.; Murata, M.; Miyaura, N. *J. Org. Chem.* **1995**, *60*, 7508.
109. Bergman, J.; Carlsson, R.; Sjöberg, B. *Org. Syn.* **1977**, *57*, 18.
110. Barton, D. H. R.; Ozbalik, N.; Ramesh, M. *Tetrahedron Lett.* **1988**, *29*, 3533.
111. Hauptmann, H.; Walter, W. F.; Marino, C. *J. Am. Chem. Soc.* **1958**, *80*, 5832.
112. Uemura, S.; Wakasugi, M.; Okano, M. *J. Organomet. Chem.* **1980**, *194*, 277.
113. Stefani, H. A.; Pena, J. M.; Zukerman-Schpector, J.; Tiekink, E. R. T. *J. Braz. Chem. Soc.* **2011**, *22*, 1439.
114. Nishibayashi, Y.; Cho, C. S.; Ohe, K.; Uemura, S. *J. Organomet. Chem.* **1996**, *526*, 335.

115. Zhang, S.; Karra, K.; Koe, A.; Jin, J. *Tetrahedron Lett.* **2013**, *54*, 2452.
116. Suzuki, H.; Inouye, M. *Chem. Lett.* **1985**, 389.
117. Li, Y.; Nie, C.; Wang, H.; Li, X.; Verpoort, F.; Duan, C. *Eur. J. Org. Chem.* **2011**, 7331.
118. Hartman, W. W.; Smith, L. A.; Dickey, J. B. *Org. Syn.* **1934**, *14*, 36.
119. Jung, M. E.; Jachiet, D.; Khan, S. I.; Kim, C. *Tetrahedron Lett.* **1995**, *36*, 361.
120. Jang, Y.; Kim, K. T.; Jeon, H. B. *J. Org. Chem.* **2013**, *78*, 6328.
121. Borthwick, A. D. *Chem. Rev.* **2012**, *112*, 3641.
122. Hirst, J. D.; Persson, B. J. *J. Phys. Chem. A* **1998**, *102*, 7519.
123. Hückel, W.; Schwen, R. *Chem. Ber.* **1956**, *89*, 150.
124. Birch, A. J.; Nadamuni, G. *J. Chem. Soc. Perkin Trans. 1* **1974**, 545.
125. Miyashita, M.; Yanami, T.; Yoshikoshi, A. *J. Am. Chem. Soc.* **1976**, *98*, 4679.
126. Read de Alaniz, J.; Rovis, T. *J. Am. Chem. Soc.* **2005**, *127*, 6284.
127. Fürstner, A.; Krause, H.; Lehmann, C. W. *Angew. Chem. Int. Ed.* **2006**, *45*, 440.
128. Krafft, M. E.; Holton, R. A. *J. Am. Chem. Soc.* **1984**, *106*, 7619.
129. Simpkins, N. S.; Weller, M. D. *Topics Stereochem.* **2010**, *26*, 1.
130. O'Brien, P. *J. Chem. Soc. Perkin Trans. 1* **1998**, 1439.
131. Cain, C. M.; Cousins, R. P. C.; Coumbarides, G.; Simpkins, N. S. *Tetrahedron* **1990**, *46*, 523.

132. Wild, H. *J. Org. Chem.* **1994**, *59*, 2748.
133. Wild, H.; Born, L. *Angew. Chem. Int. Ed.* **1991**, *30*, 1685.
134. Simpkins, N. S.; Gill, C. D. *Org. Lett.* **2003**, *5*, 535.
135. Ito, Y.; Konoike, T.; Saegusa, T. *J. Am. Chem. Soc.* **1975**, *97*, 649.
136. Fujii, T.; Hirao, T.; Ohshiro, Y. *Tetrahedron Lett.* **1992**, *33*, 5823.
137. Paolobelli, A. B.; Latini, D.; Ruzziconi, R. *Tetrahedron Lett.* **1993**, *34*, 721.
138. Baciocchi, E.; Casu, A.; Ruzziconi, R. *Tetrahedron Lett.* **1989**, *30*, 3707.
139. Woo, C. M.; Gholap, S. L.; Lu, L.; Kaneko, M.; Li, Z. W.; Ravikumar, P. C.; Herzon, S. B. *J. Am. Chem. Soc.* **2012**, *134*, 17262.
140. Herzon, S. B.; Lu, L.; Woo, C. M.; Gholap, S. L. *J. Am. Chem. Soc.* **2011**, *133*, 7260.
141. Ito, Y.; Konoike, T.; Harada, T.; Saegusa, T. *J. Am. Chem. Soc.* **1977**, *99*, 1487.
142. Baran, P. S.; DeMartino, M. P. *Angew. Chem. Int. Ed.* **2006**, *45*, 7083.
143. DeMartino, M. P.; Chen, K.; Baran, P. S. *J. Am. Chem. Soc.* **2008**, *130*, 11546.
144. Martin, C. L.; Overman, L. E.; Rohde, J. M. *J. Am. Chem. Soc.* **2008**, *130*, 7568.
145. Martin, C. L.; Overman, L. E.; Rohde, J. M. *J. Am. Chem. Soc.* **2010**, *132*, 4894.
146. Baran, P. S.; Guerrero, C. A.; Ambhaikar, N. B.; Hafensteiner, B. D. *Angew. Chem. Int. Ed.* **2005**, *44*, 606.
147. Baran, P. S.; Hafensteiner, B. D.; Ambhaikar, N. B.; Guerrero, C. A.; Gallagher, J. D. *J. Am. Chem. Soc.* **2006**, *128*, 8678.

148. Wang, Y.; Yao, J.; Li, H.; Su, D.; Antonietti, M. *J. Am. Chem. Soc.* **2011**, *133*, 2362.
149. Neri, G.; Visco, A. M.; Donato, A.; Milone, C.; Malentacchi, M.; Gubitosa, G. *Appl. Catal. A: Gen.* **1994**, *110*, 49.
150. Cheng, H.; Liu, R.; Wang, Q.; Wu, C.; Yu, Y.; Zhao, F. *New J. Chem.* **2012**, *36*, 1085.
151. Maegawa, T.; Akashi, A.; Yaguchi, K.; Iwasaki, Y.; Shigetsura, M.; Monguchi, Y.; Sajiki, H. *Chem. Eur. J.* **2009**, *15*, 6953.
152. Rylander, P. N. *Catalytic Hydrogenation in Organic Syntheses*, Academic Press, San Diego, California, **1979**, p175.
153. Nishimura, S. *Handbook of Heterogeneous Catalytic Hydrogenation for Organic Synthesis*, Wiley-VCH: Weinheim, **2001**, p414.
154. Hegedűs, L.; Háda, V.; Tungler, A.; Máthé, T.; Szepesy, L. *Appl. Catal. A: Gen.* **2000**, *201*, 107.
155. Bachiller-Baeza, B.; Guerrero-Ruíz, A.; Rodríguez-Ramos, I. *J. Catal.* **2005**, *229*, 439.
156. Tobičik, J.; Červený, L. *J. Mol. Catal. A: Chem.* **2003**, *194*, 249.
157. Bartholomew, C. H. *Appl. Catal. A: Gen.* **2001**, *212*, 17.
158. Freifelder, M. *J. Org. Chem.* **1961**, *26*, 1835.
159. Lautens, M.; Fagnou, K.; Yang, D. *J. Am. Chem. Soc.* **2003**, *125*, 14884.
160. Avetta, C. T.; Konkol, L. C.; Taylor, C. N.; Dugan, K. C.; Stern, C. L.; Thomson, R. J. *Org. Lett.* **2008**, *10*, 5621.
161. Denmark, S. E.; Cramer, C. J.; Sternberg, J. A. *Tetrahedron Lett.* **1986**, *27*, 3693.

162. Donaldson, R. E.; Fuchs, P. L. *J. Org. Chem.* **1977**, *42*, 2032.
163. Saito, Y.; Ouchi, H.; Takahata, H. *Tetrahedron* **2006**, *62*, 11599.
164. Chalker, J. M.; Wood, C. S. C.; Davis, B. G. *J. Am. Chem. Soc.* **2009**, *131*, 16346.
165. Scott, W. L.; Martynow, J. G.; Huffman, J. C.; O'Donnell, M. J. *J. Am. Chem. Soc.* **2007**, *129*, 7077.
166. Page, P. C. B.; Buckley, B. R.; Rassias, G. A.; Blacker, A. J. *Eur. J. Org. Chem.* **2006**, 803.
167. Oswald, C. L.; Carrillo-Márquez, T.; Caggiano, L.; Jackson, R. F. W. *Tetrahedron* **2008**, *64*, 681.
168. Belagali, S. L.; Mathew, T.; Himaja, M.; Kocienski, P. *Indian J. Chem. B* **1995**, *34*, 45.
169. Jouin, P.; Poncet, J.; Dufour, M. N.; Pantaloni, A.; Castro, B. *J. Org. Chem.* **1989**, *54*, 617.
170. Chen, Y.; Bilban, M.; Foster, C. A.; Boger, D. L. *J. Am. Chem. Soc.* **2002**, *124*, 5431.
171. Boger, D. L.; Zhou, J. *J. Am. Chem. Soc.* **1995**, *117*, 7364.
172. Čaplar, V.; Raza, Z.; Katalenić, D.; Žinić, M. *Croat. Chem. Acta* **2003**, *76*, 23.
173. Brunel, F. M.; Spatola, A. F. *J. Pept. Res.* **2004**, *63*, 213.
174. Gros, G.; Martinez, L.; Gimenez, A. S.; Adler, P.; Maurin, P.; Wolkowicz, R.; Falson, P.; Hasserodt, J. *Bioorg. Med. Chem.* **2013**, *21*, 5407.
175. Lin, S.; Yang, Z. Q.; Kwok, B. H. B.; Koldobskiy, M.; Crews, C. M.; Danishefsky, S. *J. Am. Chem. Soc.* **2004**, *126*, 6347.

176. Bosch, M. P.; Campos, F.; Niubó, I.; Rosell, G.; Díaz, J. L.; Brea, J.; Loza, M. I.; Guerrero, A. *J. Med. Chem.* **2004**, *47*, 4041.
177. Donkor, I. O.; Sanders, M. L. *Bioorg. Med. Chem. Lett.* **2001**, *11*, 2647.
178. Forseth, R. R.; Amaike, S.; Schwenk, D.; Affeldt, K. J.; Hoffmeister, D.; Schroeder, F. C.; Keller, N. P. *Angew. Chem. Int. Ed.* **2013**, *52*, 1590.
179. Dufour, J.; Neuville, L.; Zhu, J. *Chem. Eur. J.* **2010**, *16*, 10523.
180. Liu, N. N.; Zhao, S. M.; Zhao, J. F.; Zeng, G. Z.; Tan, N. H.; Liu, J. P. *Tetrahedron* **2014**, *70*, 6630.
181. Reboud-Ravaux, M. C. Y.; Vidal, J.; Piguel, S.; Basse, N.; Ferrier-Berthelot, A.; Pagano, M. WO Patent 2006/105811 A1, October 12, 2006.
182. Cahiez, G.; Chaboche, C.; Mahuteau-Betzer, F.; Ahr, M. *Org. Lett.* **2005**, *7*, 1943.
183. McNeill, E.; Barder, T. E.; Buchwald, S. L. *Org. Lett.* **2007**, *9*, 3785.
184. Dayaker, G.; Chevallier, F.; Gros, P. C.; Mongin, F. *Tetrahedron* **2010**, *66*, 8904.
185. Pflieger, R.; Waldmann, K. *Chem. Ber.* **1957**, *90*, 2395.
186. Baldwin, J. J.; Claremon, D. A.; Tice, C.; Cacatian, S.; Dillard, L. W.; Ishchenko, A. V.; Yuan, J.; Xu, Z.; McGeehan, G.; Simpson, R. D.; Singh, S. B.; Zhao, W.; Flaherty, P. T. US Patent 8487108B2, July 16, 2013.
187. Carrillo-Marquez, T.; Caggiano, L.; Jackson, R. F. W.; Grabowska, U.; Rae, A.; Tozer, M. J. *Org. Biomol. Chem.* **2005**, *3*, 4117.
188. Lim, S. M.; Hill, N.; Myers, A. G. *J. Am. Chem. Soc.* **2009**, *131*, 5763.